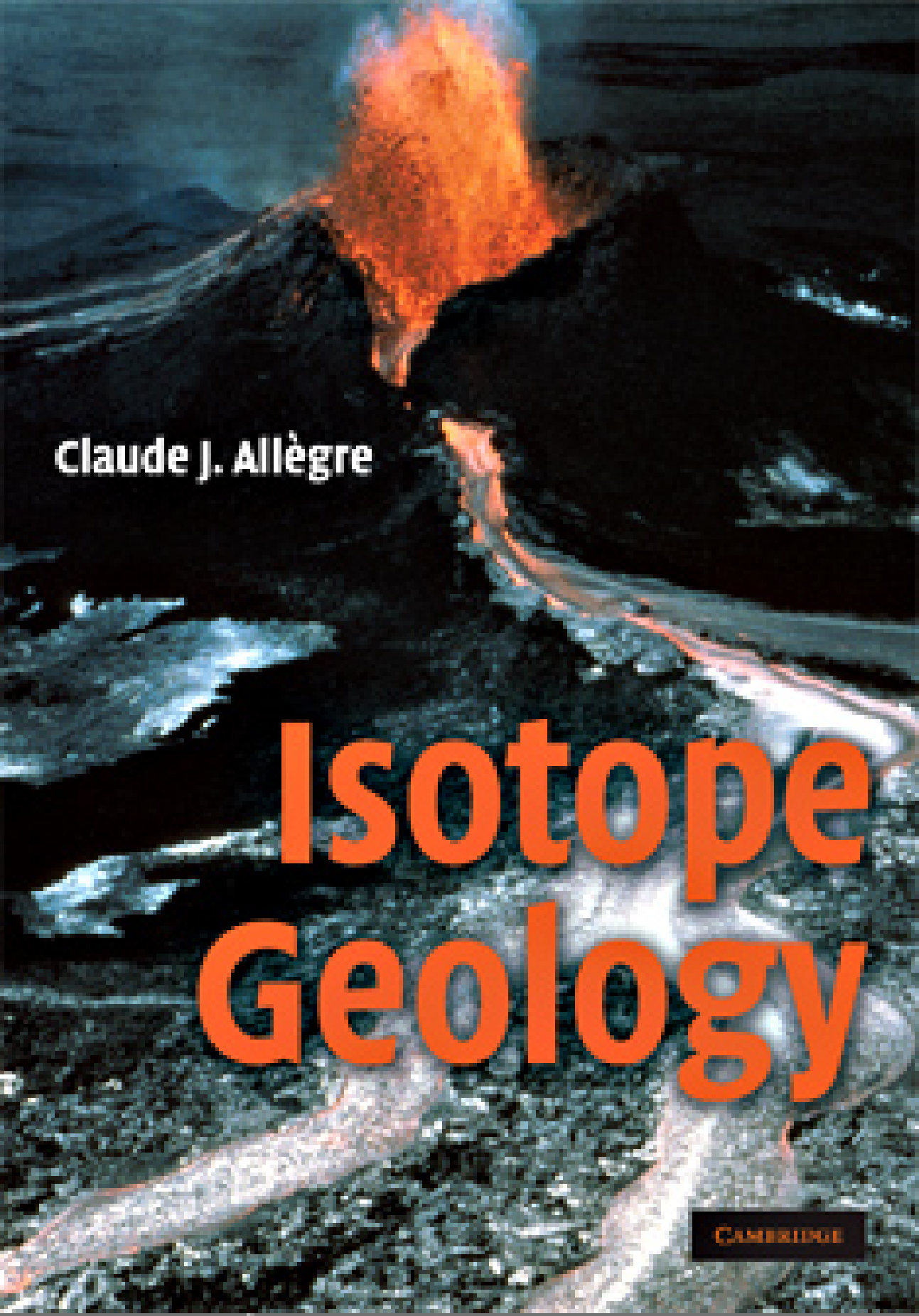


CAMBRIDGE www.cambridge.org/9780521862288

# ISOTOPE GEOLOGY

Radiogenic and stable isotopes are used widely in the Earth sciences to determine the ages of rocks, meteorites, and archeological objects, and as tracers to understand geological and environmental processes. Isotope methods determine the age of the Earth, help reconstruct the climate of the past, and explain the formation of the chemical elements in the Universe. This textbook provides a comprehensive introduction to both radiogenic and stable isotope techniques. An understanding of the basic principles of isotope geology is important in a wide range of the sciences: geology, astronomy, paleontology, geophysics, climatology, archeology, and others.

Claude Allègre is one of the world's most respected and best-known geochemists, and this textbook has been developed from his many years of teaching and research experience.

*Isotope Geology* is tailored for all undergraduate and graduate courses on the topic, and is also an excellent reference text for all Earth scientists.

CLAUDE ALLÈGRE is extremely well known globally in the Earth science research and teaching community. He is currently an Emeritus Professor at the Institut Universitaire de France, Université Denis Diderot, and the Institut de Physique du Globe de Paris, and has had a long and illustrious career in science. He is a former Director of the Department of Earth Sciences, Université Paris VII, former Director of the Institut de Physique du Globe de Paris, past President of the French Bureau of Geological and Mining Research (BRGM), and former National Education Minister for Research and Technology for the French government. In his career he has won most of the available honours and awards in the geosciences, including the Crafoord Prize from the Swedish Royal Academy of Sciences, the Goldschmidt Medal from the Geochemical Society of America, the Wollaston Medal from the Geological Society of London, the Arthur Day Gold Medal from the Geological Society of America, the Médaille d'Or du CNRS, the Holmes Medal from the European Union Geosciences, and the Bowie Medal from the American Geophysical Union. He is member of several academics: Foreign Associate of the National Academy of Sciences (USA), Foreign Member of the Academy of Art and Science, Foreign Member of the Philosophical Society, Foreign Member of the Royal Society, Foreign Member of the National Academy of India, and Membre de l'Académie des Sciences de Paris. He is also a Commandeur de la Légion d'Honneur, a past President of the European Union of Geosciences, past President of the NATO Earth Sciences Committee, and former editor of the journals *Physics of the Earth and Planetary Interiors* and *Chemical Geology*. He has written hundreds of research articles, and 25 books in French.

# Isotope Geology

CLAUDE J. ALLÈGRE

*Institut de Physique du Globe de Paris*
*and*
*Université Denis Diderot*

CAMBRIDGE
UNIVERSITY PRESS

CAMBRIDGE UNIVERSITY PRESS
Cambridge, New York, Melbourne, Madrid, Cape Town, Singapore, São Paulo

Cambridge University Press
The Edinburgh Building, Cambridge CB2 8RU, UK
Published in the United States of America by Cambridge University Press, New York

www.cambridge.org
Information on this title: www.cambridge.org/9780521862288



First published in print format 2008

ISBN-13 978-0-511-45524-7 eBook (EBL)

ISBN-13 978-0-521-86228-8 hardback

# Dedication

I dedicate this book to all those who have helped me to take part in the extraordinary adventure of developing isotope geology.

To my family, who have probably suffered from my scientific hyperactivity.

To those who were paragons for me and have become very dear friends: Jerry Wasserburg, Paul Gast, George Wetherill, Al Nier, John Reynolds, Mitsunobu Tatsumoto, Clair Patterson, George Tilton, Harmon Craig, Samuel Epstein, Karl Turekian, Paul Damon, Pat Hurley, Edgar Picciotto, Wally Broecker, and Devendra Lal. I have tried to stand on their shoulders.

To my colleagues and friends with whom I have shared the intense joy of international scientific competition: Stan Hart, Keith O'Nions, Al Hofmann, Marc Javoy, Don DePaolo, Charles Langmuir, Jean Guy Schilling, Chris Hawkesworth, and many others.

To my undergraduate and graduate students, and postdoctoral fellows, to my laboratory staff and first and foremost to those who have participated in almost all of this adventure: Jean-Louis Birck, Gérard Manhès, Françoise Capmas, Lydia Zerbib, and the sorely missed Dominique Rousseau. Without them, none of this would have been possible, because modern research is primarily teamwork in the full sense of the word.

# CONTENTS

# PREFACE

Isotope geology is the offspring of geology on one hand and of the concepts and methods of nuclear physics on the other. It was initially known as "nuclear geology" and then as "isotope geochemistry" before its current name of isotope geology came to be preferred because it is based on the measurement and interpretation of the isotopic compositions of chemical elements making up the various natural systems. Variations in these isotope compositions yield useful information for the geological sciences (in the broad sense). The first breakthrough for isotope geology was the age determination of rocks and minerals, which at a stroke transformed geology into a quantitative science. Next came the measurement of past temperatures and the birth of paleoclimatology. Then horizons broadened with the emergence of the concept of isotopic tracers to encompass not only questions of the Earth's structures and internal dynamics, of erosion, and of the transport of material, but also problems of cosmochemistry, including those relating to the origins of the chemical elements. And so isotope geology has not only extended across the entire domain of the earth sciences but has also expanded that domain, opening up many new areas, from astrophysics to environmental studies.

This book is designed to provide an introduction to the methods, techniques, and main findings of isotope geology. The general character of the subject defines its potential readership: final-year undergraduates and postgraduates in the earth sciences (or environmental sciences), geologists, geophysicists, or climatologists wanting an overview of the field.

This is an educational textbook. To my mind, an educational textbook must set out its subject matter and explain it, but it must also involve readers in the various stages in the reasoning. One cannot understand the development and the spirit of a science passively. The reader must be active. This book therefore makes constant use of questions, exercises, and problems. I have sought to write a book on isotope geology in the vein of Turcotte and Schubert's *Geodynamics* (Cambridge University Press) or Arthur Beiser's *Concepts of Modern Physics* (McGraw-Hill), which to my mind are exemplary.

As it is an educational textbook, information is sometimes repeated in different places. As modern research in the neurosciences shows, learning is based on repetition, and so I have adopted this approach. This is why, for example, although numerical constants are often given in the main text, many of them are listed again in tables at the end. In other cases, I have deliberately not given values so that readers will have to look them up for themselves, because information one has to seek out is remembered better than information served up on a plate.

Readers must therefore work through the exercises, failing which they may not fully understand how the ideas follow on from one another. I have given solutions as we go along,

sometimes in detail, sometimes more summarily. At the end of each chapter, I have set a number of problems whose solutions can be found at the end of the book.

Another message I want to get across to students of isotope geology is that this is not an isolated discipline. It is immersed both in the physical sciences and in the earth sciences. Hence the deliberate use here and there of concepts from physics, from chemistry (Boltzmann distribution, Arrhenius equation, etc.), or from geology (plate tectonics, petrography, etc.) to encourage study of these essential disciplines and, where need be, to make readers look up information in basic textbooks. Isotope geology is the outcome of an encounter between nuclear physics and geology; this multidisciplinary outlook must be maintained.

This book does not set out to review all the results of isotope geology but to bring readers to a point where they can consult the original literature directly and without difficulty. Among current literature on the same topics, this book could be placed in the same category as Gunter Faure's *Isotope Geology* (Wiley), to be read in preparation for Alan Dickin's excellent *Radiogenic Isotope Geology* (Cambridge University Press).

The guideline I have opted to follow has been to leave aside axiomatic exposition and to take instead a didactic, stepwise approach. The final chapter alone takes a more synthetic perspective, while giving pointers for future developments.

I have to give a warning about the references. Since this is a book primarily directed towards teaching I have not given a full set of references for each topic. I have endeavored to give due credit to the significant contributors with the proper order of priority (which is not always the case in modern scientific journals). Because it is what I am most familiar with, I have made extensive use of work done in my laboratory. This leads to excessive emphasis on my own laboratory's contributions in some chapters. I feel sure my colleagues will forgive me for this. The references at the end of each chapter are supplemented by a list of suggestions for further reading at the end of the book.

# ACKNOWLEDGMENTS

I would like to thank all those who have helped me in writing this book.

My colleagues Bernard Dupré, Bruno Hamelin, Éric Lewin, Gérard Manhès, and Laure Meynadier made many suggestions and remarks right from the outset. Didier Bourles, Serge Fourcade, Claude Jaupart, and Manuel Moreira actively reread parts of the manuscript.

I am grateful too to those who helped in producing the book: Sandra Jeunet, who word-processed a difficult manuscript, Les Éditions Belin, and above all Joël Dyon, who did the graphics. Christopher Sutcliffe has been a most co-operative translator.

My very sincere thanks to all.

CHAPTER SEVEN

# Stable isotope geochemistry

When defining the properties of isotopes we invariably say that the isotopes of an element have the same chemical properties, because they have the same electron shell, but different physical properties, because they have different masses. However, if the behavior of isotopes of any chemical element is scrutinized very closely, small differences are noticeable: in the course of a chemical reaction as in the course of a physical process, isotope ratios vary and isotopic fractionation occurs. Such fractionation is very small, a few tenths or hundredths of 1%, and is only well marked for the light elements, let us say those whose atomic mass is less than 40. However, thanks to the extreme precision of modern measurement techniques, values can be measured for almost all of the chemical elements, even if they are extremely small for the heavy ones.

When we spoke of isotope geochemistry in the first part of this book, we voluntarily omitted such phenomena and concentrated on isotope variations related to radioactivity, which are preponderant. We now need to look into the subtle physical and chemical fractionation of stable isotopes, the use of which is extremely important in the earth sciences.

## 7.1 Identifying natural isotopic fractionation of light elements

The systematic study of the isotopic composition of light elements in the various naturally occurring compounds brings out variations which seem to comply with a purely naturalistic logic. These variations in isotope composition are extremely slight, and are generally expressed in a specific unit, **the δ unit**.

$$\delta = \left( \frac{\text{sample isotope ratio} - \text{standard isotope ratio}}{\text{standard isotope ratio}} \right) \times 10^3.$$

Ultimately, $\delta$ is a relative deviation from a standard, expressed as the number of parts per mil (‰). Isotope ratios are expressed with the heavier isotope in the numerator.

If $\delta$ is positive then the sample is richer in the heavy isotope than the standard. If $\delta$ is negative then the sample is poorer in the heavy isotope than the standard. The terms "rich" and "poor" are understood as relative to the isotope in the numerator of the isotope ratio in the formula above: by convention it is always the heavy isotope. Thus we speak of the $^{18}O/^{16}O$, D/H, $^{13}C/^{12}C$ ratio, etc. The standard is chosen for convenience and may be naturally

abundant such as sea water for $^{18}O/^{16}O$ and D/H, a given carbonate for $^{13}C/^{12}C$, or even a commercial chemical (Craig, 1965).

## Exercise

Oxygen has three stable isotopes, $^{16}O$, $^{17}O$, and $^{18}O$, with average abundances of 99.756%, 0.039%, and 0.205%, respectively. The $^{16}O/^{18}O$ ratio in a Jurassic limestone is 472.4335. In average sea water, this same ratio is $^{16}O/^{18}O = 486.594$. If average sea water is taken as the standard, what is the $\delta$ of the limestone in question?

### Answer

By convention, $\delta$ is always expressed relative to the heavy isotope. We must therefore invert the ratios stated in the question, giving 0.002 116 7 and 0.002 055 1, respectively. Applying the formula defining $\delta^{18}O$ gives $\delta^{18}O = +30$.

## Exercise

The four naturally occurring, stable isotopes of sulfur are $^{32}S$, $^{33}S$, $^{34}S$, and $^{36}S$. Their average abundances are 95.02%, 0.75%, 4.21%, and 0.017%, respectively. Generally, we are interested in the ratio of the two most abundant isotopes, $^{34}S$ and $^{32}S$. The standard for sulfur is the sulfide of the famous Canyon Diablo meteorite[1] with a $^{32}S/^{34}S$ value of 22.22. We express $\delta$ relative to the heavy isotope, therefore:

$$\delta = \left( \frac{(^{34}S/^{32}S)_{\text{sample}}}{(^{34}S/^{32}S)_{\text{standard}}} - 1 \right) \times 10^3.$$

If we have a sample of sulfur from a natural sulfide, for example, with $^{32}S/^{34}S = 23.20$, what is its $\delta^{34}S$?

### Answer

Given that the standard has a $^{34}S/^{32}S$ ratio of 0.0450 and the sample a ratio of 0.0431, $\delta^{34}S = -42.22$. Notice here that the sign is negative, which is important. By definition, the standard has a value $\delta = 0$.

## 7.1.1 The double-collection mass spectrometer

Variations in the isotope composition of light elements are small, even very small. A precise instrument is required to detect them (and a fast one, if we want enough results to represent natural situations). We have already seen the principle of how a mass spectrometer works. Remember that in a scanning spectrometer, the magnetic field is varied and the ion beams corresponding to the different masses (or different isotopes) are picked up in turn in a collector. The collector picks up the ions and provides an electric current which is fed through a resistor to give a voltage read-out.

As we have already said, in multicollector mass spectrometers, the collectors are fixed and the beams of the various isotopes are received simultaneously. In this way we get around

[1] Canyon Diablo is the meteorite that dug Meteor Crater in the Arizona desert.

the temporary fluctuations that may occur during ionization. However, the recording circuits for the various collectors must be identical.

Since 1948, the double-collection mass spectrometer invented by **Nier** has been used for measuring slight isotopic differences for elements which can be measured in the gaseous state and which are ionized by electron bombardment (Nier, 1947; Nier *et al.*, 1947).[2] The two electrical currents, picked up by two Faraday cups, are computed using a Wheatstone bridge arrangement, which we balance (we measure the resistance values required to balance the bridge). The ratio of electrical currents $I_{a/b}$ is therefore directly related to the isotope ratio $R_{a/b}$ by the equation:

$$I_{a/b} = K R_{a/b}$$

where $K$ is a fractionation factor and reflects bias that may occur during measurement. It is evaluated with an instantaneous calibration system using a standard. The standard sample is measured immediately after the unknown sample $x$. This gives:

$$I_s = K R_s.$$

Eliminating $K$ from the two equations gives:

$$\frac{I_x}{I_s} = \frac{R_x}{R_s}.$$

The measurement of the relative deviation is then introduced quite naturally:

$$\Delta_x = \frac{R_x - R_s}{R_s} = \left(\frac{R_x}{R_s} - 1\right)\left(\frac{I_x}{I_s} - 1\right).$$

As we are handling small numbers, this number is multiplied by 1000 for the sake of convenience. This is where the definition of the $\delta$ unit comes from, which is therefore provided directly by the mass spectrometer measurement, since $\delta = \Delta_x \cdot 10^3$.

This gas-source, double-collection mass spectrometer automatically corrects two types of effect. First, it eliminates time fluctuations which mean that when we "scan" by varying the magnetic field (see Chapter 1), the emission at time $t$ when isotope 1 is recorded may be different from emission at time $(t + \Delta t)$ when isotope 2 is recorded. Second, it corrects errors generated by the appliance by the sample–standard switching technique.

The measurement sequence is straightforward: sample measurement, standard measurement, sample measurement, etc. The operation is repeated several times to ensure measurement reproducibility. Fortunately, many light elements can enter gas compounds. This is the case of hydrogen in the form $H_2$ (or $H_2O$), of carbon and oxygen as $CO_2$, of sulfur ($SO_2$) or ($SF_6$), of nitrogen ($N_2$), of chlorine ($Cl_2$), and so on. For other elements such as boron, lithium, magnesium, calcium, and iron, it was not until advances were made in solid-source mass spectrometry or the emergence of inductively coupled plasma mass spectrometry (ICPMS), originally developed for radiogenic isotope studies, that an

[2] Multicollector mass spectrometers for thermo-ionization or plasma sources have been routinely used only since the year 2000 because of electronic calibration difficulties.

effective multicollection technique could be used. This domain is booming today and we shall touch upon it at the end of this chapter.[3]

## 7.1.2 Some isotope variations and identifying coherence

### Oxygen

This is the most abundant chemical element on Earth, not only in the ocean but also in the silicate Earth (Figure 7.1). Its isotope composition varies clearly, which is a godsend!

Oxygen has three isotopes: $^{18}O$, $^{17}O$, and $^{16}O$ (the most abundant). We generally study variations in the $^{18}O/^{16}O$ ratio expressed, of course, in $\delta$ units, taking ordinary sea water as the benchmark (with $\delta = 0$ by definition).[4] Systematic measurement of various naturally occurring compounds (molecules, minerals, rocks, water vapor, etc.) reveals that they have characteristic isotope compositions that are peculiar to their chemical natures and their geochemical origins, whatever their geological ages or their geographical origins. For igneous or metamorphic silicate rocks $\delta$ is positive, ranging from +5 to +13. Such rocks are therefore enriched in $^{18}O$ (relative to sea water). Limestones are even more enriched since their $\delta$ values vary from +25 to +34. Of course, we may ask what "offsets" such enrichment in $^{18}O$.

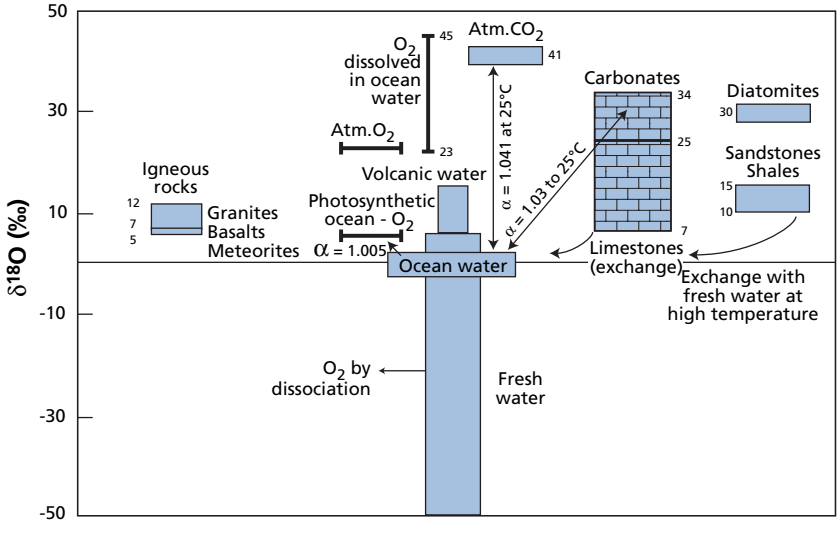


**Figure 7.1** Distribution of oxygen isotope compositions in the main terrestrial reservoirs expressed in $\delta^{18}O$. The isotope fractionation factors are shown for various important reservoirs. The smaller numbers indicate extreme values. Values are of $\delta^{18}O$ expressed relative to standard mean ocean water (SMOW). After Craig and Boato (1955).

[3] The technique of alternating sample and standard used with electron bombardment of gas sources is difficult to implement whether with sources working by thermo-ionic emission or by ICPMS because of the possible memory effects or cross-contamination.

[4] It is called standard mean ocean water (SMOW).

Which compounds have negative $\delta$ values? We observe that those of fresh water are negative, ranging from $-10$ to $-50$. A few useful but merely empirical observations can be inferred from this. As we know that limestones precipitate from sea water, enrichment in $^{18}O$ suggests that limestone precipitates with enrichment in the heavy isotope. Conversely, we know that fresh water comes from evaporation and then condensation of a universal source, the ocean. It can therefore be deduced that there is depletion in $^{18}O$ during the hydrological cycle (evaporation–condensation). These observations suggest there is a connection between certain natural phenomena, their physical and chemical mechanisms, the origin of the products, and isotope fractionation.

## Hydrogen

Let us now look at the natural isotopic variations of hydrogen, that is, variations in the (D/H) ratio (D is the symbol for deuterium). Taking mean ocean water as the standard, it is observed that organic products, trees, petroleum, etc. and rocks are enriched in deuterium whereas fresh water contains less of it (Figure 7.2).

We find similar behavior to that observed for oxygen, namely depletion of the heavy isotope in fresh water and enrichment in rocks and organic products. The product in which hydrogen and oxygen are associated is water ($H_2O$). It is important therefore to know whether the variations observed for D/H and $^{18}O/^{16}O$ in natural water are "coherent" or not. Coherence in geochemistry is first reflected by correlation. **Epstein** and **Mayeda** (1953) from Chicago and then **Harmon Craig** (1961) of the Scripps Institution of Oceanography at the University of California observed excellent correlation for rainwater between D/H and $^{18}O/^{16}O$, which shows that there is "coherence" in isotopic fractionation related to the water cycle (Figure 7.3). This invites us therefore to look more closely at any quantitative relations between isotope fractionation and the major natural phenomena.

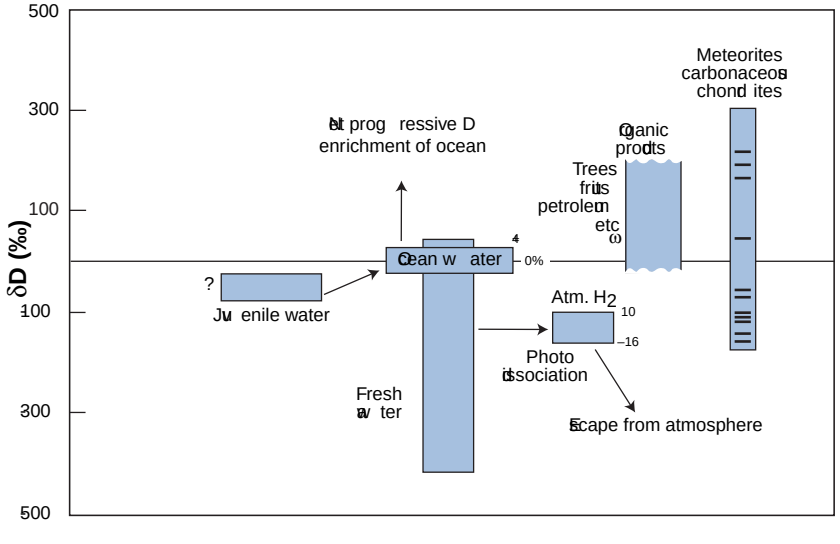


**Figure 7.2** Distribution of isotope compositions of hydrogen expressed in $\delta$D in the main terrestrial reservoirs. After Craig and Boato (1955).

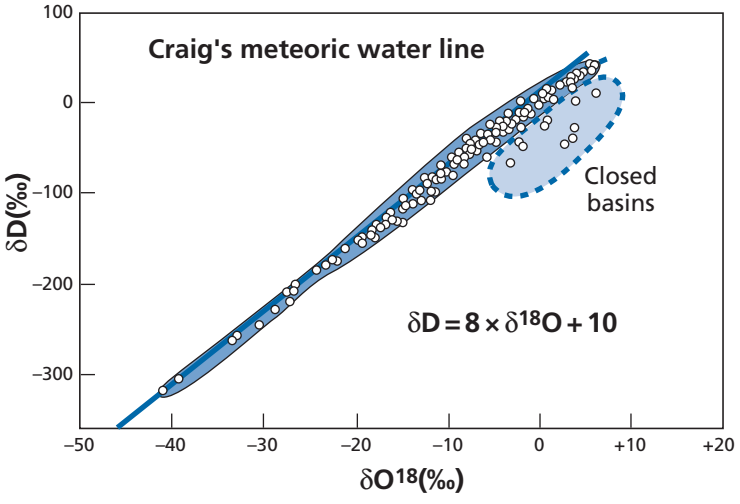


**Figure 7.3** Correlation between (D/H, $^{18}O/^{16}O$) of rainwater. After Craig (1961).

## 7.1.3 Characterization of isotope variations

Between two geological products A and B, related by a natural process, and whose isotope ratios are notated $R_A$ and $R_B$, we can write:

$$\theta_{AB} = \frac{R_A}{R_B}$$

where $\theta_{AB}$ is the overall fractionation factor between A and B. With $\boldsymbol{\delta}_A$ and $\boldsymbol{\delta}_B$ being defined as previously, we can write:

$$\theta_{AB} = \frac{1 + \frac{\delta_A}{1000}}{1 + \frac{\delta_B}{1000}} \approx 1 + \frac{(\boldsymbol{\delta}_A - \boldsymbol{\delta}_B)}{1000}$$

following the approximation $(1 + \varepsilon)/(1 + \varepsilon') \approx 1 + (\varepsilon - \varepsilon')$.

We note $\Delta_{AB} = \boldsymbol{\delta}_A - \boldsymbol{\delta}_B$. This yields a fundamental formula for all stable isotope geochemistry:

$$1000(\theta_{AB} - 1) \approx \Delta_{AB}.$$

### Exercise

Given that the $\boldsymbol{\delta}^{18}O$ value of a limestone is +24 and that the limestone formed by precipitation from sea water, calculate the overall limestone–sea water fractionation factor $\theta$.

**Answer**

$\Delta_{Lim-H_2O} = \boldsymbol{\delta}_{Ca} - \boldsymbol{\delta}_{H_2O} = 24 - 0$. We deduce that $\theta = 1.024$.

It is possible, then, to calculate the overall fractionation factors for various geological processes: the transition from granite to clay by weathering, the evaporation of water between ocean and clouds, the exchange of $CO_2$ in the atmosphere with that dissolved in the ocean or with carbon of plants, and so on.

This is a descriptive approach, not an explanatory one. Various chemical reactions and physical processes have been studied in the laboratory to determine the variations in their associated isotope compositions. Thus, for instance, it has been observed that when water evaporates, the vapor is enriched in light isotopes for both hydrogen and oxygen. Fractionation factors have been defined for each process from careful measurements made in the laboratory. These elementary fractionation factors will be denoted $\alpha$.

Geochemists have endeavored to synthesize these two types of information, that is, **to connect $\theta$ and $\alpha$**, in other words, to break down natural phenomena into a series of elementary physical and chemical processes whose isotope fractionations are measured experimentally. This approach involves making models of natural processes. We then calculate $\theta$ from measurements of $\alpha$ made in the laboratory. When the agreement between $\theta$ so calculated and $\theta$ observed in nature is "good," the model proposed can be considered a "satisfactory" image of reality. Thus, while the study of the isotopic compositions of natural compounds is interesting in itself, it also provides insight into the underlying mechanisms of natural phenomena. Hence the role of tracers of physical–chemical mechanisms in geological processes that are associated with studies of light-isotope fractionation.

In attempting to expose matters logically, we shall not trace its historical development. We shall endeavor first to present isotope fractionation associated with various types of physical and chemical phenomena and then to look at some examples of natural isotope fractionation.

## 7.2 Modes of isotope fractionation

### 7.2.1 Equilibrium fractionation

As a consequence of elements having several isotopes, combinations between chemical elements, that is molecules and crystals, have many isotopic varieties. Let us take the molecule $H_2O$ by way of illustration. There are different isotopic varieties: $H_2{}^{18}O$, $H_2{}^{17}O$, $H_2{}^{16}O$, $D_2{}^{18}O$, $D_2{}^{17}O$, $D_2{}^{16}O$, $DH^{18}O$, $DH^{17}O$, $DH^{16}O$ (omitting combinations with tritium, T). These different molecules are known as **isotopologs**. Of these, $H_2{}^{16}O$ accounts for 97%, $H_2{}^{18}O$ for 2.2%, $H_2{}^{17}O$ for about 0.5%, and $DH^{16}O$ for about 0.3%. When the molecule $H_2O$ is involved in a chemical process, all of its varieties contribute and we should write the various equilibrium equations not just for $H_2O$ alone but for all the corresponding isotopic molecules.

#### Chemical equilibria

Let us consider, for example, the reaction

$$Si^{18}O_2 + 2H_2^{16}O \rightleftarrows Si^{16}O_2 + 2H^{18}O,$$

which corresponds to a mass action law:

$$\frac{(H_2{}^{18}O)^2(Si^{16}O_2)}{(H_2{}^{16}O)^2(Si^{18}O_2)} = K(T).$$

**Harold Urey** (1947), and independently **Bigeleisen** and **Mayer** (1947), showed using statistical quantum mechanics that this kind of equilibrium constant, although close to 1, is different from 1.

More generally, for an isotope exchange reaction $aA_1 + bB_2 \rightleftarrows aA_2 + bB_1$, where $B$ and $A$ are compounds and the subscripts 1 and 2 indicate the existence of two isotopes of an element common to both compounds, we can write in statistical thermodynamics, following Urey (1947) and Bigeleisen and Mayer (1947):

$$K = \left[\frac{Q(A_2)}{Q(A_1)}\right]^a \cdot \left[\frac{Q(B_1)}{Q(B_2)}\right]^b.$$

Functions $Q$ are termed partition functions of the molecule and are such that for a given single chemical species we can write:

$$\frac{Q_2}{Q_1} = \frac{\sigma_1}{\sigma_2}\left(\frac{M_2}{M_1}\right)^{3/2} \frac{\sum \exp\left(\frac{-E_{2i}}{kT}\right)}{\sum \exp\left(\frac{-E_{1i}}{kT}\right)} \cdot \frac{I_1}{I_2}.$$

In this equation $\sigma_1$ and $\sigma_2$ are the symmetry numbers of molecules 1 and 2, $E_{2i}$ and $E_{1i}$ are the different rotational or vibrational energy levels of the molecules, $M_1$ and $M_2$ are their masses, and $I_1$ and $I_2$ are their moments of inertia.

The greater the ratio $M_1/M_2$ the greater the fractionation between isotope species, all else being equal. It can also be shown that ln $K$, as for any equilibrium constant, can be put in the form $\boldsymbol{a' + b'/T + c'/T^2}$, which induces the principle of the isotopic thermometer. It can be deduced from the formula that as $T$ increases $K$ tends towards 1. At very high temperatures, isotope fractionation tends to become zero and at low temperature it is much greater.[5] If we define the isotope fractionation factor $\alpha$ associated with a process by the ratio $(A_2/A_1)/(B_2/B_1) = \alpha_{AB}$, $\alpha$ and $K$ are related by the equation $\alpha = K^{1/n}$, where $n$ is the number of exchangeable atoms. Thus, in the previous example, $n = 2$ as there are two oxygen atoms to be exchanged, but usually $\alpha = K$.

Let us now write the fractionation factor $\alpha_{AB}$ in $\boldsymbol{\delta}$ notation, noting each isotope ratio $R_A$ and $R_B$:

$$\boldsymbol{\delta}_A = \left(\frac{R_A}{R_S} - 1\right)10^3 \qquad \boldsymbol{\delta}_B = \left(\frac{R_B}{R_S} - 1\right)10^3,$$

$R_S$ being the standard.

$$\alpha = \left(\frac{1 + \frac{\delta_A}{1000}}{1 + \frac{\delta_B}{1000}}\right) \approx 1 + \frac{(\boldsymbol{\delta}_A - \boldsymbol{\delta}_B)}{1000},$$

since $\boldsymbol{\delta}_A$ and $\boldsymbol{\delta}_B$ are small.

[5] Remember that isotope geology studies phenomena from −80 °C (polar ice caps) to 1500 °C (magmas) and in the cosmic domain the differences are even higher.

We come back to the equation $(\alpha_{AB} - 1)\ 1000 = \boldsymbol{\delta}_A - \boldsymbol{\delta}_B = \Delta_{AB}$, which we met for the factor $\theta$.

## Exercise

We measure the $\boldsymbol{\delta}\,^{18}O$ of calcite and water with which we have tried to establish equilibrium. We find $\boldsymbol{\delta}_{cal} = 18.9$ and $\boldsymbol{\delta}_{H_2O} = -5$. What is the calcite–water partition coefficient at 50 °C? Calculate it without and with the approximation $(1 + \boldsymbol{\delta}_1)/(1 + \boldsymbol{\delta}_2) \approx 1 + (\boldsymbol{\delta}_1 - \boldsymbol{\delta}_2)$.

### Answer

(1) Without approximation: $\alpha_{cal-H_2O} = 1.024\,02$.
(2) With approximation: $\alpha_{cal-H_2O} = 1.0239$.

## Physical equilibria

Such equilibrium fractionation is not reserved for the sole case where chemical species are different, but also applies when a phase change is observed, for instance. The partial pressure of a gas is $Pg = P_{total} \cdot Xg$, where $Xg$ is the molar fraction. Moreover, the gas–liquid equilibrium obeys Henry's law. Thus, when water evaporates, the vapor is enriched in the light isotope. If the mixture $H_2{}^{18}O$ and $H_2{}^{16}O$ is considered perfect, and if the water vapor is a perfect gas, we can write:

$$P(H_2{}^{16}O) = X^e_{H_2{}^{16}O} \cdot P^0(H_2{}^{16}O)$$

$$P(H_2{}^{18}O) = X^e_{H_2{}^{18}O} \cdot P^0(H_2{}^{18}O)$$

where $P$ is the total pressure, $X$ designates the molar fractions in the liquid, and $P^0(H_2O)$ the saturated vapor pressure. Then (prove it as an exercise):

$$\alpha(\text{vapor} - \text{liquid}) = \frac{P^0(H_2{}^{18}O)}{P^0(H_2{}^{16}O)},$$

the denser liquid being the less volatile $P^0(H_2{}^{18}O) < P^0(H_2{}^{16}O)$ and $\alpha < 1$. Like all fractionation factors, $\alpha$ is dependent on temperature. Using Clapeyron's equation, it can be shown that $\ln \alpha$ can be written in the form $\ln\ \alpha = (a/T) + b$. For water at 20 °C (this is the vapor–liquid coefficient, not the opposite!), $\alpha_{^{18}O} = 0.991$ and $\alpha_D = 0.918$. At 20 °C fractionation is therefore about eight times greater for deuterium than for $^{18}O$. (Remember this factor of 8 for later.)

## Exercise

What is the law of variation of $\alpha$ with temperature in a process of gas–liquid phase change? We are given that $\alpha = P^0(X_1)/P^0(X_2)$, where $X_1$ and $X_2$ are the two isotopes.

### Answer

Let us begin from Clapeyron's equation:

$$\frac{dP}{dT} = \frac{L_{vapor}}{TV_{vapor}}$$

where $T$ is the temperature, $V$ the volume, and $L_{vapor}$ the latent heat of vaporization.

$$\frac{1}{P}\frac{dP}{dT} = \frac{L}{TVP}.$$

Since $PV = nRT$ (Mariotte's law):

$$\frac{1}{P}\frac{dP}{dT} = \frac{L}{RT^2} \text{ hence } \frac{dP}{P} = \frac{L}{RT^2}dT.$$

Integrating both terms gives $\ln P = \frac{L}{RT} + C$.

Since $\alpha = P^0(X_1)/P^0(X_2)$, we have:

$$\ln \alpha = \ln P^0(X_1) - \ln P^0(X_2) = \frac{L_{X_1} - L_{X_2}}{RT} + C.$$

## Exercise

The liquid–vapor isotope fractionation is measured for oxygen and hydrogen of water at three temperatures (see table below):

| Temperature (°C) | $\alpha_D$ | $\alpha_{^{18}O}$ |
|---|---|---|
| +20 | 1.0850 | 1.0098 |
| 0 | 1.1123 | 1.0117 |
| −20 | 1.1492 | 1.0141 |

(1) Draw the curve of variation of $\alpha$ with temperature in ($\alpha$, $T$), [ln($\alpha$), 1/$T$], and [ln($\alpha$), 1/$T^2$].
(2) What is the $\delta$ value of water vapor in deuterium and $^{18}O$ at 20 °C and at 0 °C, given that water has $\delta = 0$ for (H) and (O)?
(3) Let us imagine a simple process whereby water evaporates at 20 °C in the temperate zone and then precipitates anew at 0 °C. What is the slope of the precipitation diagram ($\delta$ D, $\delta$ $^{18}O$)?

**Answer**

(1) The answer is left for readers to find (it will be given in the main text).
(2) At +20 °C, $\delta$ D = −85 and $\delta$ $^{18}O$ = −9.8, and at 0 °C, $\delta$ D = −112.3 and $\delta$ $^{18}O$ = −11.7.
(3) The slope is 14.3. In nature it is 8, proving that we need to refine the model somewhat (the liquids have as starting values at 20 °C, $\delta$ D = 0 and $\delta$ $^{18}O$ = 0 and at 0 °C, $\delta$ D = −27.3 and $\delta$ $^{18}O$ = −1.9).

### 7.2.2 Kinetic fractionation

For a general account of kinetic fractionation see **Bigeleisen** (1965).

#### Transport phenomena

During transport, as isotopic species have different masses, they move at different speeds. The fastest isotopes are the lightest ones. Isotopic fractionation may result from these

differences in speed. Suppose we have molecules or atoms with the same kinetic energy $E = \frac{1}{2}mv^2$. For two isotopic molecules 1 and 2 of masses $m_1$ and $m_2$, we can write $v_1$, $v_2$ being the velocities:

$$\frac{v_1}{v_2} = \left(\frac{m_2}{m_1}\right)^{1/2}.$$

The ratio of the speed of two "isotopic molecules" is proportional to the square root of the inverse ratio of their mass. This law corresponds, for example, to the isotopic fractionation that occurs during gaseous diffusion for which the fractionation factor between two isotopes of $^{16}O$ and $^{18}O$ for the molecule $O_2$ is written:

$$\alpha = \left(\frac{32}{34}\right)^{1/2} = 1.030.$$

Note in passing that such fractionation is of the same order as the fractionation we encountered during equilibrium processes! Such fractionation is commonplace during physical transport phenomena. For example, when water evaporates, vapor is enriched in molecules containing light isotopes (H rather than D, $^{16}O$ rather than $^{18}O$). In the temperate zone ($T = 20\ ^\circ C$), for water vapor over the ocean $\delta^{18}O = -13$, whereas for vapor in equilibrium the value is closer to $\delta^{18}O = -9$, as seen.

## Chemical reactions

Isotopically different molecules react chemically at different rates. Generally, the lighter molecules react more quickly. Lighter molecules are therefore at a kinetic advantage. This is due to two combined causes. First, as we have just seen, light molecules move faster than heavy molecules. Therefore light molecules will collide more. Second, heavy molecules are more stable than light ones. During collisions, they will be dissociated less often and will be less chemically reactive. The details of the mechanisms are more complex. During a chemical reaction, there is a variation in isotopic composition between the initial product and the end product. Let us consider, for example, the reaction:

$$C + O_2 \rightarrow CO_2.$$

In terms of oxygen isotopes, there are two main reactions:

$$C + {}^{16}O\,{}^{18}O \rightarrow C\,{}^{16}O\,{}^{18}O$$

$$C + {}^{16}O\,{}^{16}O \rightarrow C\,{}^{16}O_2.$$

### Remark

The other possible reactions are not important. The reaction $C + {}^{18}O\,{}^{16}O \rightarrow C\,{}^{16}O\,{}^{18}O$ is identical to the first in terms of its result. The reaction $C + {}^{18}O\,{}^{18}O \rightarrow C\,{}^{18}O_2$ yields a molecule of very low abundance as $^{18}O$ is much rarer than $^{16}O$.

These two reactions occur at different speeds, with two kinetic constants, $K_{18}$ and $K_{16}$. Let us note the initial concentrations of the product containing the isotopes 18 and 16 as $U_{18}$ and

$U_{16}$, giving $^{16}O^{16}O$, and note as $Y_{18}$ and $Y_{16}$ the concentrations of $C^{18}O^{16}O$ and $C^{16}O_2$. We can write:

$$-\frac{dU_{18}}{dt} = K_{18} \qquad U_{18} = \frac{dY_{18}}{dt}$$

and

$$-\frac{dU_{16}}{dt} = K_{16} \qquad U_{16} = \frac{dY_{16}}{dt}.$$

If the concentration of initial products is kept constant

$$\frac{Y_{18}}{Y_{16}} = \frac{K_{18}}{K_{16}}\frac{U_{18}}{U_{16}}.$$

Therefore

$$\left(\frac{^{18}O}{^{16}O}\right)_{CO_2} = \alpha\left(\frac{^{18}O}{^{16}O}\right)_{O_2},$$

or:

$$\alpha = \frac{K_{18}}{K_{16}}.$$

The isotopic fractionation factor is equal to the ratio of the kinetic constants for each isotope.

A fuller expression of this ratio may be obtained by statistical mechanics by using the fact that the kinetic process consists of two transitions, one towards the activated complex and the other towards the stable compound. Naturally, we usually have very few data on this activated complex which is very short-lived. Two reactions with two different isotopes (see Lasaga, 1997) are written:

$$A + BC \xrightarrow{K_1} AB + C \text{ and } A + BC' \xrightarrow{K_2} AB + C'.$$

It can be shown that

$$\frac{K_1}{K_2} = \frac{Q_{ABC'}\, Q_{BC}}{Q_{ABC}\, Q_{BC'}},$$

$Q$ being partition functions corresponding to the activated complex and to the molecules. It should be possible to determine the parameters by spectrometry and so check the precision of this theory but in fact the problem is so complex that we are far from having resolved the theoretical approach and having determined the necessary spectroscopic parameters. But we do understand the general sense of the mechanisms, which is the most important thing. Experimental data are therefore used to model natural phenomena.

## The temperature effect

During transport, isotopic fractionation is insensitive to temperature as it is in $(m_1/m_2)^{1/2}$. However, collisions and molecular recombinations are a function of energy and therefore of temperature and are theoretically activated. It is understandable, then, that isotopic fractionation varies with temperature during kinetic processes.

Roughly speaking, temperature should promote kinetic fractionation. Having made this simple observation, things become more complicated. Isotopic exchange, the process by which equilibrium is attained, is itself a kinetic process and is therefore activated by temperature, so much so that the increased fractionation because of kinetic effects is progressively cancelled because the equilibrium processes become dominant and therefore fractionation will diminish with the increase in temperature.

This double general process will thus lead to a law of kinetic fractionation represented by a bell-shaped curve: fractionation increasing with temperature at first, and then declining beyond a certain temperature. This rule is modulated by specific kinetic mechanisms. This is why, despite many attempts, we have never managed to give a general expression for kinetic isotopic fractionation based on statistical mechanics.

## Biological effects

Many (if not all) biochemical reactions involve isotopic fractionation. A number of these fractionation phenomena have been studied in vitro and in vivo, elucidating the intimate mechanisms of certain important biochemical reactions. It is understandable, then, that some biological mechanisms, formed by the combination or the succession of biochemical reactions, produce isotopic effects some of which are particularly important in geochemistry and so deserve our attention. Let us discuss two of them: sulfate–sulfide reduction by *Desulfovibrio desulfuricans* bacteria and chlorophyll photosynthesis (Harrison and Thode, 1957, 1958).

**Sulfate–sulfide reduction by *Desulfovibrio desulfuricans* bacteria** The reaction for the reduction of sulfate to sulfide is written $SO_4^{2-} \Rightarrow S^{2-}$. It involves a big change in the degree of oxidation of sulfur (+6) to (−2), which is made possible at low temperature only by the intervention of the bacteria in question (conversely, the reaction $S^{2-} \rightarrow SO_4^{2-}$ is easy). This bacterial reduction goes along with isotopic fractionation favoring the light isotope of sulfur but whose amplitude is well below that of the sulfide ⇔ sulfate equilibrium process, governed by the mass action law ($\alpha = 1.025$ at 25 °C versus $\alpha = 1.075$ for the equilibrium process). This means the sulfate is enriched in the heavy isotope ($^{34}S$) when there is fractionation with the sulfide. This fractionation plays a role in nature and helps to fix the isotopic composition of low-temperature naturally occurring sulfides (see the end of this chapter).

**Chlorophyll photosynthesis** During this process atmospheric $CO_2$ is fixed and the reduced carbon is incorporated into organic molecules. An enrichment in $^{12}C$ compared with $^{13}C$ is observed. The $\delta^{13}C$ value of atmospheric $CO_2$ is −8‰. For carbonate sediments, $\delta^{13}C$ varies from +5 to −5‰. However, plants have $\delta^{13}C$ values ranging, depending on varieties, from −15 to −35‰. **Park** and **Epstein** (1960) of the California

Institute of Technology showed that an important step in $^{12}C$ enrichment occurred in the process of photosynthesis. They were even able to attribute partition coefficients to the different photosynthetic mechanisms (this is outside our field but is important in biochemistry).

In short, let us say that the biochemical effects are important. They are even fundamental in some instances in geochemistry for understanding a whole series of phenomena such as those related to the $CO_2$ cycle or the sulfur cycle. But need they be considered as specific effects of living organisms that are not bound by ordinary physical and chemical laws? Various studies have shown on the contrary that biological processes involving enzymes are in fact a series of chemical reactions. These reactions are associated with isotopic fractionation, generally of the kinetic type. There do not seem to be certain specific mechanisms (such as the spin effect) for biological reactions. These biological fractionations of isotopes have been discussed in detail by **Eric Galimov** (1985).

### 7.2.3 The effects of molecular symmetry: mass-independent fractionation

All the effects we have examined so far fractionate isotopes according to laws proportional to the difference in mass of the isotopes. Thus, in carbonate precipitation, $^{18}O/^{16}O$ fractionation is twice $^{17}O/^{16}O$ fractionation. In bacterial reduction of sulfate, $^{34}S/^{32}S$ fractionation is half $^{36}S/^{32}S$ fractionation. However, kinetic fractionation has been discovered where differences do not depend on the mass difference but on the symmetry of the molecule. Thus, $^{18}O/^{16}O$ and $^{17}O/^{16}O$ fractionation is the same. **Mark Thiemens** of the University of California at San Diego has referred to these phenomena explaining some fractionation observed by **Robert Clayton** in meteorites (Figure 7.4). He has proved the reality of this phenomenon in the laboratory (Thiemens and Heidenreich, 1983). These effects also occur in nature, for instance, with ozone ($O_3$) in the atmosphere and for sulfides in meteorites and also in Precambrian rocks. Although their theoretical explanation is complex,[6] it does seem that the decisive parameter in such fractionation is molecular symmetry.

In this sense, two molecules $^{16}O-^{18}O$ or $^{16}O-^{17}O$, both equally asymmetrical, should have similar degrees of fractionation. During the ozone-forming reaction in the high atmosphere (at an altitude of 50 km),which reaction is extremely important as ozone not only absorbs ultraviolet radiation and protects the Earth,

$$O + O_2 \rightarrow O_3^*$$

and then

$$O_3^* + M \rightarrow O_3 + M$$

in which $O_3^*$ is the excited molecule, and M is the molecule with which $O_3^*$ collides and becomes de-excited.

[6] This explanation was given by **Rudy Marcus**'s team at the California Institute of Technology chemistry department, but is quite complicated. See Gao and Marcus (2001) for an example.

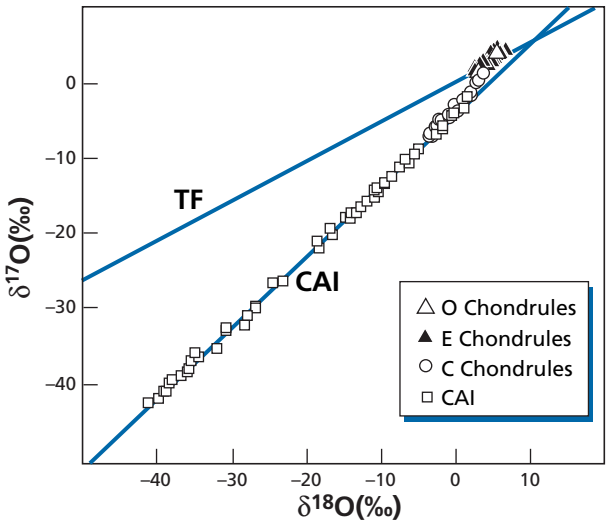


**Figure 7.4** The $\delta^{17}O$, $\delta^{18}O$ relation in chondrules and refractory inclusions of various meteorites (CAI, calcium–aluminum inclusions). For these objects the correlation is of slope 1 whereas the usual terrestrial fractionation (TF) correlation observed is of slope $\frac{1}{2}$, in line with the mass difference between $^{17}O$ and $^{16}O$ and $^{18}O$ and $^{16}O$. This discovery made by Robert Clayton *et al.* (1973) is interpreted by Thiemens (1999) as mass-independent fractionation, unlike Clayton who interpreted it as a nucleosynthetic effect, and later as a photochemical effect (Clayton, 2002).

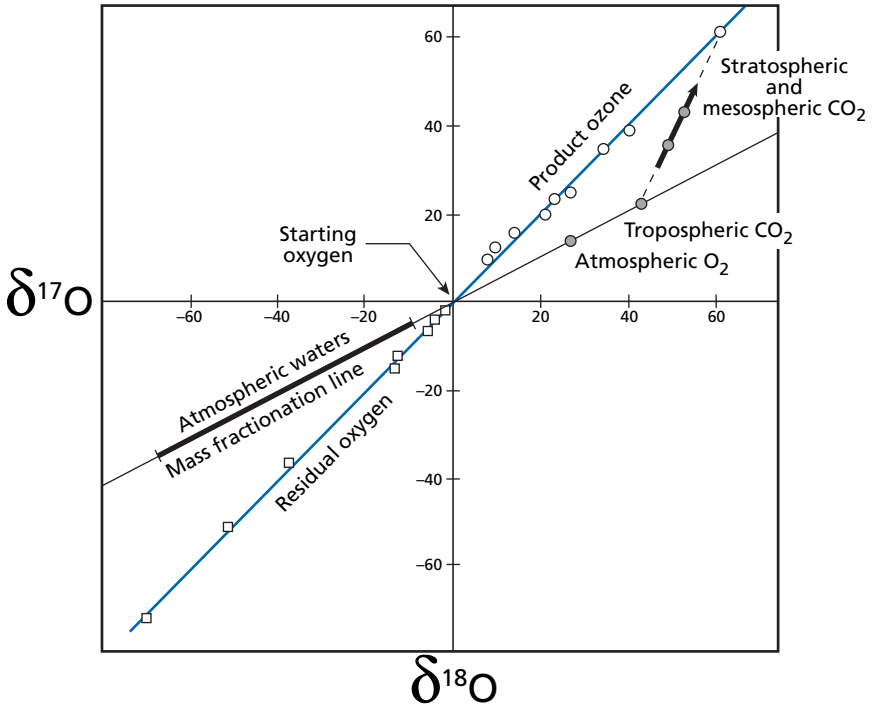


**Figure 7.5** Mass-independent fractionation (MIF) for oxygen isotopes in atmospheric material compared with classical mass-dependent fractionation. The line of slope 1 is MIF; the line of slope $\frac{1}{2}$ is mass-dependent fractionation.

It has been shown that ozone of mass 54 ($^{18}O^{18}O^{18}O$) is not enriched relative to $^{16}O^{16}O^{16}O$ ozone of mass 48, whereas the asymmetrical molecule $^{16}O^{17}O^{18}O$ of mass 51 is enriched by 200%. It has also been shown that symmetrical ozone molecules $^{17}O^{17}O^{17}O$ or $^{18}O^{18}O^{18}O$ are depleted, whereas all the asymmetrical molecules $^{16}O^{17}O^{17}O$ or $^{17}O^{18}O^{18}O$, etc. are enriched. This effect, which is called **mass-independent fractionation** and might be more appropriately termed the molecular symmetry effect, seems to act with reactions such as $O + CO \rightarrow CO_2$, $O + SiO \rightarrow SiO_2$, etc.

This is an important process in the atmosphere and seems to have played a role in the presolar primitive nebula as a linear relation of slope 1 is found in carbonaceous meteorites between $\delta^{17}O$ and $\delta^{18}O$ (Figure 7.5). This is an important effect but highly specific to certain processes. It is just beginning to be exploited but already very successfully (see below).

## 7.3 The modalities of isotope fractionation

### 7.3.1 Kinetic effects or equilibrium effects? Isotopic exchange

We have already spoken of this in the earlier chapters. Let us recall a few facts here, as it is a very important but often neglected phenomenon. Let us bring into contact two chemical compounds, AO and BO, with at least one element in common, for example, both having oxygen in their formulas. One of these species has been prepared with $^{18}O$ exclusively, the other with $^{16}O$. After a certain time in contact it can be seen that the $^{18}O/^{16}O$ composition of the two compounds is such that:

$$\frac{(^{18}O/^{16}O)_{AO}}{(^{18}O/^{16}O)_{BO}} = K(T)$$

where $K(T)$ is the equilibrium constant. In other words, the isotopes $^{18}O$ and $^{16}O$ have exchanged such that equilibrium has been attained. The rate of this isotope exchange can be measured and several phenomena observed:

(1) It is faster at higher temperatures.
(2) It is faster in gases or liquids than solids. If one of the compounds is a solid it becomes very slow (in this case the rate of diffusion in the solid limits the kinetics of the process).
(3) It depends largely on the position oxygen occupies in the steric configuration of compounds AO and BO,[7] that is, the nearer oxygen is to the outside of the molecular structure, the faster the kinetics[8] – this isotope exchange is essential in geochemistry as it provides understanding of various fundamental observations (Figure 7.6).

[7] Which relates to the spatial arrangement of the atoms composing the molecule.
[8] For example, in the complex ion $SO_4$, oxygen exchanges much faster than sulfur. This is why in sulfate water S retains the memory of its source but O does not.

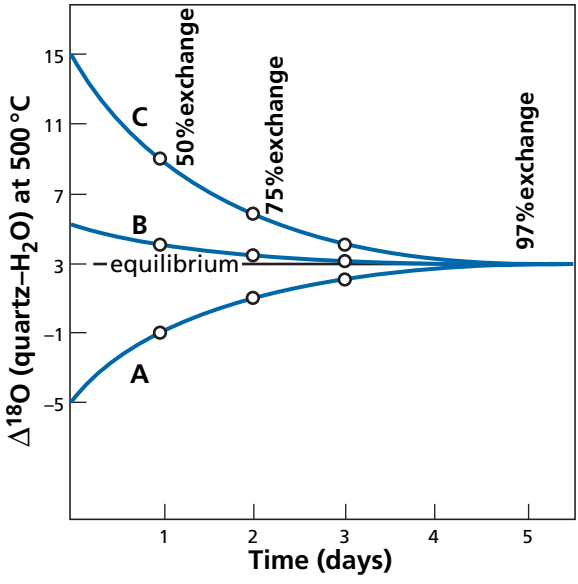


**Figure 7.6** Kinetic curve showing the speed of equilibration by water–quartz exchange. The quartz has a $\delta^{18}O$ value of 10. Three types of water with different compositions are brought into contact with the quartz at 500 °C. The initial isotope compositions of the waters are expressed in $\delta$: A (−5), B (+5), and C (+15). The equilibrium value is 3. It can be seen that the three equilibration curves converge towards the equilibrium value in a matter of days. After O'Neil (1986).

Let us suppose we have a reaction A → B together with kinetic isotope fractionation. If A and B are left in contact for long enough, the isotopes of A and B swap over, and eventually the fractionation between A and B is of the equilibrium fractionation type. To maintain kinetic fractionation, the initial product and the end product must not be left in contact. An example of this is the reduction of the sulfate ion $SO_4^{2-}$ to the sulfide $S^{2-}$ (by bacteria) which goes along with an out-of-equilibrium isotope effect. If, after partial reduction, the sulfate ion remains in contact with the sulfide ion, the system tends to establish sulfate–sulfide isotopic equilibrium. Conversely, if the sulfide ion $S^{2-}$ is in the presence of a ferrous ion $Fe^{2+}$, the following reaction occurs: $2S^{2-} + Fe^{2+} \rightarrow FeS_2$. This iron sulfide crystallizes and "isolates" the sulfide from any further isotopic exchange which would cancel out the kinetic effect. This is why a number of naturally occurring sulfides have isotope compositions reflecting the kinetic effect (bacterial) related to sulfate reduction.

Isotope exchange is activated by temperature; therefore, at high temperatures, only swift and complete isolation of the resulting product can prevent equilibrium fractionation from taking over. In practice, except for the case of gases that escape and become isolated, such as gases from volcanoes, it is generally difficult to observe kinetic effects at high temperatures. In these circumstances, equilibrium effects are mostly preponderant.

## 7.3.2 A consequence: isotopic memory

As we have already said when discussing radiogenic isotopes, it is fundamental to understand that all isotope geochemistry, including that of stable light isotopes, is based on the fact that isotope exchange in the solid phase at low temperatures is very slow and the system is not constantly re-equilibrated, otherwise there would be no isotopic memory. This derives from the issues of diffusion covered previously.

Let us take the example of calcareous fossil shells. A shell records the $^{18}O/^{16}O$ isotope composition of the sea water it was formed in and also the ambient temperature. Once formed, the shell moves around with the animal that carries it and when the animal dies the shell falls to the sea floor. There it is incorporated into sediments and with them will be petrified in a certain proportion and possibly, much later, will be brought to the surface on the continents by tectonic processes. It will remain there for millions of years before a geologist comes along and collects it for analysis. During this time, the fossil shell is in contact with the groundwater that circulates in the outer layer of the Earth. How does the shell behave in contact with this new water? If it is isotopically re-equilibrated with the fresh water whose $\delta$ value is very different from zero, it loses its former isotopic composition and so its paleothermal memory. Its isotopic composition no longer reflects the conditions of the old ocean but the conditions of recent aqueous circulation. In fact, in most (but not all!) cases, the shell remains compact and no isotope exchange occurs. The low rate of diffusion of oxygen in calcite at low or moderate temperatures limits the mechanism. And all the better for geologists! They can determine the past temperature of the ocean where the animal whose shell it was lived.

An important phenomenon is cooling. Isotopic equilibrium among minerals is established at high temperature. The mineral assemblage cools and so follows a decreasing thermal trajectory. The isotope equilibrium constant is dependent on temperature, and isotope reactions should continue to take place constantly matching temperature and isotope composition. If this were so, the system would lose all memory of its past at high temperature and isotope analysis would merely reflect the low-temperature equilibrium. In fact, as isotope exchange at low temperatures occurs very slowly, if cooling is rapid, the minerals often retain the composition acquired at high temperature. But this is not always so. Cooling is not always rapid. In metamorphism especially, exchanges are sometimes accelerated by certain factors and "initial" isotope compositions are not always maintained. But as the oxygen diffusion constants of the various silicate minerals are different, the temperatures indicated by the various minerals also differ. There is a sort of disequilibrium allowing us to detect the occurrence of any secondary effect.

All of this means that when measuring a compound's isotopic composition we must question the meaning of the message it carries and the time it was encoded. Does it correspond to the period when the object formed? Is it the outcome of secondary phenomena? If so, what phenomena? Once again, everything is dominated by isotope exchange mechanisms. The importance of these effects is attested by the answer to the following general observation. Why is sulfur isotope geochemistry not used more often, since it has substantial natural variations (from +60 to −40)? Because in

many compounds, and particularly in sulfides, secondary isotope exchange occurs very rapidly. Through this exchange, the compounds lose much of the isotope memory of their origins. Another reason is the fact that sulfur geochemistry is highly complex with many degrees of oxidation, etc. However, interesting results have been obtained with sulfur isotopes.

## 7.3.3 Open system or closed system

### The open system or infinite reservoir

When one of the reservoirs present is of infinite size (or is in direct contact with a boundless reservoir) the modalities of isotope fractionation are governed by the initial fractionation conditions and by conditions related to subsequent isotope exchange. No mass balance effect disturbs the relation between $\theta$ and $\alpha$:

$$\theta = \alpha_{\text{equilibrium}}, \theta = \alpha_{\text{kinetic}}, \text{ or } \theta = \alpha_{\text{mixed}},$$

depending on the nature of the initial fractionation and the subsequent isotope exchange. If the isotope composition of the infinite reservoir is $R_0$, the "large" reservoir imposes its isotope composition through the fractionation factor:

$$R = \alpha R_0 \text{ and } \delta \approx \delta_0 + (\alpha - 1)\, 1000.$$

**Exercise**

Sea water has a $\delta^{18}O$ value of 0. Liquid–vapor fractionation at equilibrium at 20 °C is $\alpha = 1.0098$. What is the composition of the water vapor evaporating if it is in equilibrium with the water?

**Answer**

The fractionation factor $(^{18}O/^{16}O)_{\text{vapor}}/\left(^{18}O/^{16}O\right)_{\text{liquid}} = 1/\alpha = 0.990\,29$. Therefore $(\alpha - 1) = -0.0097$, or $\delta^{18}O = -9.7‰$.

### The closed system

Where the system is closed, a balance effect is superimposed on the modalities described. We note the isotope composition of the initial system $R_0$ and assume that from there two compounds, A and B, are produced with isotopic ratios $R_A$ and $R_B$. We can write an isotope fractionation law (without specifying whether it is for equilibrium or not) characterized by $\Delta_{AB}$, and an atom conservation equation. This gives: $R_0 = R_A x + R_B (1 - x)$, where $x$ is the molar fraction of the element. In $\delta$ notation, this gives:

$$\boldsymbol{\delta}_0 = \boldsymbol{\delta}_A x + \boldsymbol{\delta}_B (1 - x) \text{ or } \boldsymbol{\delta}_0 = (\boldsymbol{\delta}_A - \boldsymbol{\delta}_B) x + \boldsymbol{\delta}_B \text{ or } \boldsymbol{\delta}_0 = \Delta_{AB} x + \boldsymbol{\delta}_B.$$

**Exercise**

Let us consider bacterial reduction $SO_4^{2-} \rightarrow S^{2-}$ by *Desulfovibrio desulfuricans*. The kinetic fractionation factor $^{34}S/^{32}S$ between sulfate and sulfide at 25 °C is 1.025 (Harrison and

Thode, 1958). Let us suppose that bacterial reduction occurred in oceanic sediment that was continually supplied with sulfate ions. The sulfate stock can therefore be considered infinite. What is the composition of the $S^{2-}$ on the ocean floor if the $\delta^{34}S$ of the sulfate is +24?

**Answer**

Applying the equation $\Delta_{AB} = 10^3 \ln \alpha$ gives $\Delta = +24.6$.

$\delta_{sulfate} - \delta_{sulfide} = +24.6$ hence it can be deduced that $\delta_{sulfide} = -0.6$.

## Exercise

Let us suppose now that the sediment becomes isolated from the ocean and is no longer supplied with sulfate ions and that the same phenomenon occurs. The quantity of organic matter is such that the proportion of sulfur in the state of sulfate is 1/3. Suppose that, in the initial state, all of the sulfur was in the sulfate state at $\delta^{34}S = +24$. What is the isotope composition of $S^{2-}$? What is the isotope composition of the sulfate?

**Answer**

We apply the equation:

$\delta_0 = \Delta_{AB} x + \delta_B$, or $\delta_B = \delta_0 - \Delta_{AB} x$.

From this we obtain $\delta_{S^{2-}} = 15.8, \delta_{SO_4} = 40.4$.

As seen in the previous exercise, the result is markedly different for an open system, as the $\delta$ value is then positive. The effect of the closed system has shifted the isotope values of the sulfate and sulfide, but not the fractionation factor, of course! (The limiting cases where $x = 0$ and $x = 1$ should be examined.)

However, a flaw can be found in the foregoing reasoning. If the sulfides remained in a closed system as ions long enough, it might be that there was some isotopic exchange and that the sulfate and sulfide attained thermodynamic equilibrium. In this case $\alpha = 1.075$ at 25 °C (Tudge and Thode, 1950). Repeating the calculation with this value gives $\delta^{34}_{sulfide} = 0.14$ and $\delta^{34}_{sulfate} = 72.4$.

Intermediate scenarios can be imagined and therefore, in nature, the values will probably be intermediate ones.

As just seen, then, widely different isotope values are obtained for the same phenomenon but different modalities. It is probably the diversity of modalities that accounts for the great isotopic variation in sulfides of sedimentary origin (Figure 7.7).

## Distillation

Here we look at a rather special (but widely applicable!) case where the system is closed but where the product is isolated as it forms. Let $X_2$ and $X_1$ represent the number of atoms of the two isotopes. At each moment in time, we have:

$$\frac{dX_2/dX_1}{(X_2/X_1)_A} = \alpha$$

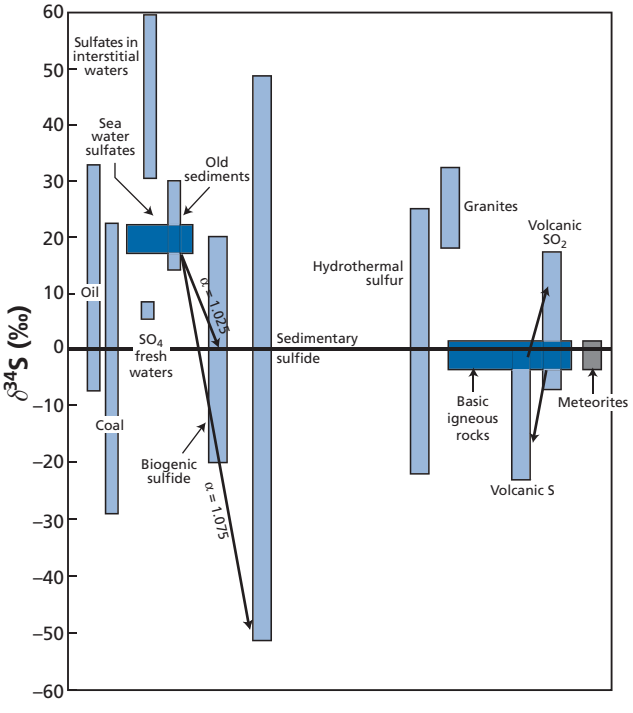


**Figure 7.7** Analysis of $^{34}S/^{32}S$ isotope composition in the main terrestrial reservoirs. Notice that the domains are very extensive for all reservoirs. This corresponds to highly variable reducing conditions to which sulfur is subjected.

where $\alpha$ may be an equilibrium or kinetic value, $dX_2$ is the quantity of isotope 2 of A which is transformed into B, and $dX_1$ is the quantity of isotope 1 of A which is transformed into B. By separating the variables and integrating, we get:

$$X_2^{\mathrm{A}} = cX_1^{\alpha}$$

therefore:

$$(X_2/X_1)_{\mathrm{A}} = c\,X_1^{\alpha-1}.$$

At time $t = 0$ $(X_2/X_1)_{\mathrm{A}} = (X_2/X_1)_0$ and $X_1 = X_{1,0}$, therefore: $c = (X_2/X_1)\,\frac{1}{X_{1,0}^{\alpha-1}}$.
Hence:

$$(X_2/X_1)^{\mathrm{A}} = (X_2/X_1)_0\left(X_1/X_{1,0}\right)^{\alpha-1}.$$

If the transformed remaining fraction of $X_1$ is called $f$, we get the famous **Rayleigh distillation law**:

$$R_{\mathrm{A}} = R_0 f^{\alpha-1}.$$

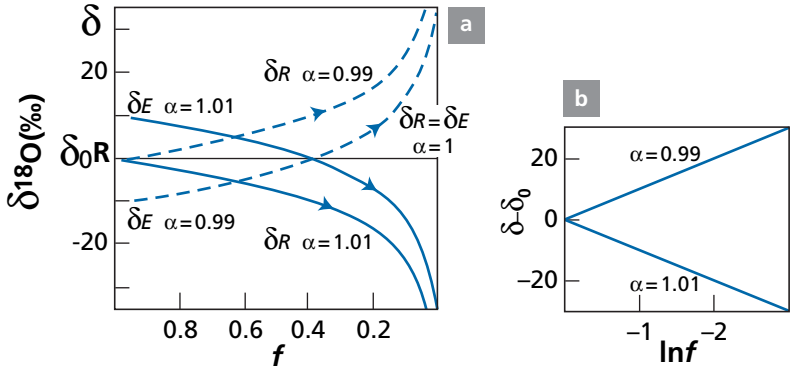


**Figure 7.8** Changes in the instantaneous isotopic composition of a reservoir ($\delta$**R**) and an extract ($\delta$**E**) during a Rayleigh distillation process as a function of the partition coefficient (1.01 and 0.99 respectively). We have $\alpha_{\text{ext-res}} > 1$, $\alpha_{\text{ext-res}} = 1$, and $\alpha_{\text{ext-res}} < 1$ and an initial isotopic composition of the reservoir $\delta_{0R} = 0$; $f$ is the remaining fraction of the reservoir and $(1 - f)$ the extent to which the reaction has progressed. After Fourcade (1998).

Figure 7.8 shows the Rayleigh law as a function of $f$ where $\alpha > 1$ and $\alpha < 1$. We shall see that the effects are opposite but are only extreme when $f$ is very small. We see how A evolves, and also B, for which, of course, we have

$$R_B = \alpha R_0 f^{\alpha-1}.$$

The mean composition of A is written:

$$\overline{R}_A = R_{\text{A},0}\left(\frac{f^{\alpha} - 1}{f - 1}\right).$$

It can be seen that when $f$ is small, the compositions of the two compounds seem to converge. And yet their partition coefficient remains constant! But it is clear that as small variations in $f$ lead to large variations in $\delta$, the optical illusion gives the impression of convergence. Notice too that when $f = 0$, $R = R_{\text{A},0}$, because of course "matter is neither created or destroyed" as Lavoisier said (except in nuclear reactions at high energy!).

## Exercise

Find the Rayleigh formula expressed in $\delta$.

**Answer**

$\delta = \delta_0 + 10^3\ (\alpha - 1)$ ln $f$. See the next exercise.

## Exercise

Let us go back to our example of the formation of sedimentary sulfides. For the time being, we assume that as soon as the sulfide is formed, it reacts with iron dissolved in solution and

forms $FeS_2$, without isotope fractionation (in fact, things are more complex than this). Being heavy in its solid state, the iron sulfide settles out and is removed from contact with the sulfates. This is a distillation effect. Given that in the end sulfates make up only one-third, what are the sulfide compositions?

### Answer

The initial $\delta\ ^{34}S$ is still $+24$. The kinetic coefficient $\alpha$ is 1.025. Let us first apply the Rayleigh equation, which we can use in a handier form with $\delta$. Its mathematical form invites us to shift to logarithms. The formula becomes:

$$\ln R = \ln R_0 + (\alpha - 1) \ln f.$$

Given that $R = R_S\,(1 + \delta/1000)$ with the logarithmic approximations $\ln(1 + \varepsilon) \approx \varepsilon$, and approximating the two terms $\ln R_S$, we get:

$$\delta = \delta_0 + 10^3\,(\alpha - 1) \ln f.$$

This is the form we shall use. The final composition of the sulfates is $\delta = 24 + 25 \ln(1/3) = 24 + 27.7 = 51.7$.

The sulfides precipitating in the end have a $\delta$ value of $+27.1$. The average sulfide is obtained by the balance equation $\delta_{S\ \text{average}} = +10.4$.

## Exercise

In the first quantitative studies to estimate the degassing rate of magmas, **Françoise Pineau** and **Marc Javoy** (1983) of the Institut de Physique du Globe in Paris measured the $^{13}C/^{12}C$ partition coefficient of $CO_2$ in a magma at 1200 °C and found 4.5‰ ($CO_2$ being enriched in $^{13}C$). Let us take a basalt with an initial $\delta^{13}C$ value of $-7$. After degassing we find $\delta^{13}C = -26$‰, with a carbon content of 100–150 ppm. If we assume a Rayleigh distillation, what is the extent of degassing of the magma? What was the initial carbon content of the magma?

### Answer

We apply the Rayleigh law in $\delta$:

$$\delta - \delta_0 = 1000\,(\alpha - 1) \ln f.$$

Hence: $-20 = 4.5 \ln f$ and $f = 0.011$, therefore the magma was degassed to 98.8%. Its initial carbon content was therefore 9000–13 000 ppm.

## EXAMPLE

### Isotopic evolution of a cloud shedding rain

A cloud forms over the sea. It then migrates over a landmass or migrates to higher latitudes and loses rain. It is assumed that the cloud formed by the evaporation of sea water and that the fractionation factor for the oxygen isotopes remains constant at $\alpha = 1.008$. Figure 7.9 summarizes the isotope evolution of the cloud and of the rain that falls as it evolves. It is described by a simple Rayleigh distillation.

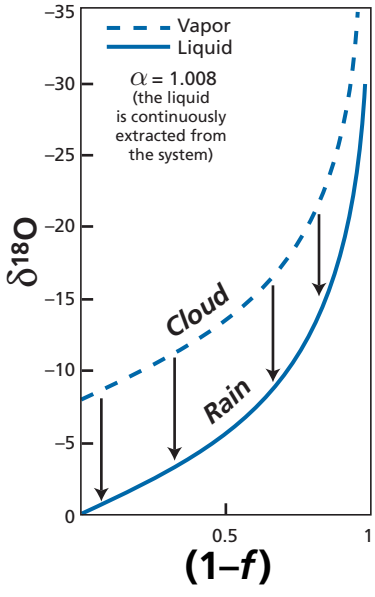


**Figure 7.9** Rayleigh distillation between a cloud and rain for $\delta^{18}O$. The liquid (rain) is continuously removed. The vapor fraction is $1 - f$. After Dansgaard (1953).

## 7.3.4 Mixing

As we have already seen several times, mixing of two sources is an extremely important phenomenon in geochemistry. For example, sea water is a mixture of the various inputs of rivers, submarine volcanoes, rain, and atmospheric dust. We have a mixture of two components $A_1$ and $A_2$ with isotopic compositions:

$$\left(\frac{{}^{x}A}{{}^{y}A}\right)_1 \text{ and } \left(\frac{{}^{x}B}{{}^{y}B}\right)_2.$$

The isotope composition of the mixture is:

$$\left(\frac{{}^{x}A}{{}^{y}A}\right)_m = \frac{{}^{x}A_1 + {}^{x}A_2}{{}^{y}A_1 + {}^{y}A_2} = \frac{\left(\frac{{}^{x}A}{{}^{y}A}\right)_1 {}^{y}A_1 + \left(\frac{{}^{y}A}{{}^{y}A}\right)_2 {}^{y}A_2}{{}^{y}A_1 + {}^{y}A_2}.$$

If we posit:

$$\frac{{}^{y}A_1}{{}^{y}A_1 + {}^{y}A_2} = x_1 \text{ and } \frac{{}^{y}A_2}{{}^{y}A_1 + {}^{y}A_2} = 1 - x_1,$$

and if we write the ratios

$${}^{x/y}R : {}^{x/y}R_m = {}^{x/y}R_1 x_1 + {}^{x/y}R_2(1 - x_1),$$

then replacing $R$ by the $\delta$ notation gives:

$$\delta_m = \delta_1 x_1 + \delta_2 (1 - x_1).$$

We find a familiar old formula!

**Exercise**

Carbonates have a $^{13}C/^{12}C$ isotope composition expressed in $\delta^{13}C$ of 0‰. Organic products precipitating on the sea floor have a $\delta^{13}C$ value of −25‰. What is the mean value of $\delta^{13}C$ of the sediments, given that 80% of the sedimentary carbon is in the carbonates and 20% in the organic products?

**Answer**

The main isotopic component of carbon is $^{12}C$. Therefore $x$ and $(1 - x)$ are 0.2 and 0.8, respectively. This gives $0.2 \times (-25‰) + 0.8 \times 0‰ = -5‰$. The average composition of the sediments is therefore −5‰.

Mixing in a correlation diagram of two isotope ratios obeys the equations already developed for radiogenic isotopes. Let the two elements whose isotopes are under study be A and B. Remember that if the $(C_A/C_B)$ ratio is constant for the two components of the mixture, the mixture is represented by a straight line. If the two ratios are different, the mixture is represented by a hyperbola whose direction of concavity is determined by the concentration ratios of A and B.

## 7.4 The paleothermometer

In some sense, paleothermometry is to stable isotopes what geochronometry is to radiogenic isotopes, both an example and a symbol.

### 7.4.1 The carbonate thermometer

An example of this field of research has become a legend of sorts. In 1947, **Harold Urey** (1934 Nobel Prize winner for his discovery of deuterium, the hydrogen isotope $^2H$) and **Bigeleisen** and **Mayer** published two theoretical papers in which they calculated isotope fractionation occurring in a series of chemical equilibria. In 1951, while professor at Chicago University, Urey and his co-workers used his method of calculation to determine the isotope equilibrium of carbonate ions $CO_3^{2-}$ and water ($H_2O$) and calculated the isotopic fractionation that must affect the $^{18}O$ and $^{16}O$ oxygen isotopes whose common natural abundances are 0.205% and 99.756%, respectively. The $(^{18}O/^{16}O)_{carbonate}/(^{18}O/^{16}O)_{water}$ ratio must be a function of the temperature at which the two species are in equilibrium. The variations Urey predicted were small but could be measured, after converting the $CO_3^{2-}$ into $CO_2$ gas, on the double-collection mass spectrometer already developed by **Alfred Nier** and his students at the University of Minnesota at the time. This fractionation was measured experimentally by Urey's team with the special involvement of **Samuel Epstein**, who was to become one of the big names in the speciality. Together, they developed the simple thermometric equation (in fact, the original coefficients were slightly different):

$$T_{°C} = 16.5 - 4.3\left(\delta^{18}_{CO_3} - \delta^{18}_{H_2O}\right) + 0.13\left(\delta^{18}_{CO_3} - \delta^{18}_{H_2O}\right)^2$$

where $T_{°C}$ is the temperature in degrees centigrade, and $\delta^{18}_{CO_3}$ the isotope composition of the $CO_2$ extracted from the carbonate, which is expressed by a deviation from the reference carbonate sample:[9]

$$\delta^{18}_{CO_3} = \left[ \frac{\left(^{18}O/^{16}O\right)_{CO_2,\,carbonateX} - \left(^{18}O/^{16}O\right)_{CO_2,\,standard}}{\left(^{18}O/^{16}O\right)_{CO_2,\,standard}} \right] \cdot 10^3.$$

The standard chosen is a reference limestone known as PDB. The Chicago team decided to use its carbonate thermometer to measure geological temperatures. To do this, they chose a common, robust fossil, the rostrum (the front spike on the shell) of a cephalopod known as a belemnite that lived in the Jurassic (−150 Ma) and was similar to present-day squids. Suppose that in the course of geological time, the isotopic composition of oxygen in sea water had remained constant at $\delta^{18}O = 0$. Then the $^{18}O/^{16}O$ oxygen isotopic composition of the carbonate of the fossils reflects the temperature of the sea water in which the shell formed. This isotope composition became fixed when the carbonate was incorporated as calcite crystals in the fossil shells (as solid-phase reactions at low temperature are very slow, there is little chance that the composition was altered by secondary processes). By measuring the isotope composition of fossils, it is possible to determine the temperature of the ancient seas. To confirm this idea, the Chicago team therefore measured a series of belemnite rostra from various geographic areas and of different stratigraphic ages (Figure 7.10).

The results, first announced in preliminary form at the 1950 annual meeting of the Geological Society of America were spectacular and immediately claimed the attention of the entire geological community. Let us summarize them.

At the scale of the planet, for the Jurassic, when belemnites lived, isotope temperature obtained varied from 12 to 18 °C. These are likely and coherent temperatures; likely because other paleoecological indicators are in agreement with them, coherent because variations over time in various measurements in various parts of the world concord. Thus it has been determined that the maximum temperature was in the Late Cretaceous, using samples from a single area (Sweden, Britain) or samples including fossils collected from North America and Europe.

Encouraged by these worldwide results, the Chicago scientists set about dissecting individual rostra. Each rostrum is made up of concentric layers which are evidence of belemnite annual growth. Layer-by-layer analysis revealed regularly alternating temperatures. There were therefore summers and winters at the time! They even managed to show that one particular individual was born in the fall and died in springtime!

## Exercise

The standard chosen for oxygen is SMOW ($\delta^{18}O = 0$). McCrea and Epstein's simplified thermometric equation is:

$T_{°C} = 16.5 - 4.3\,\delta^{18O}_{CO_3}$.

[9] This is an important detail. It is not the isotopic composition of the $CO_3^{2-}$ that is measured but that of the $CO_2$ in equilibrium with the carbonate!

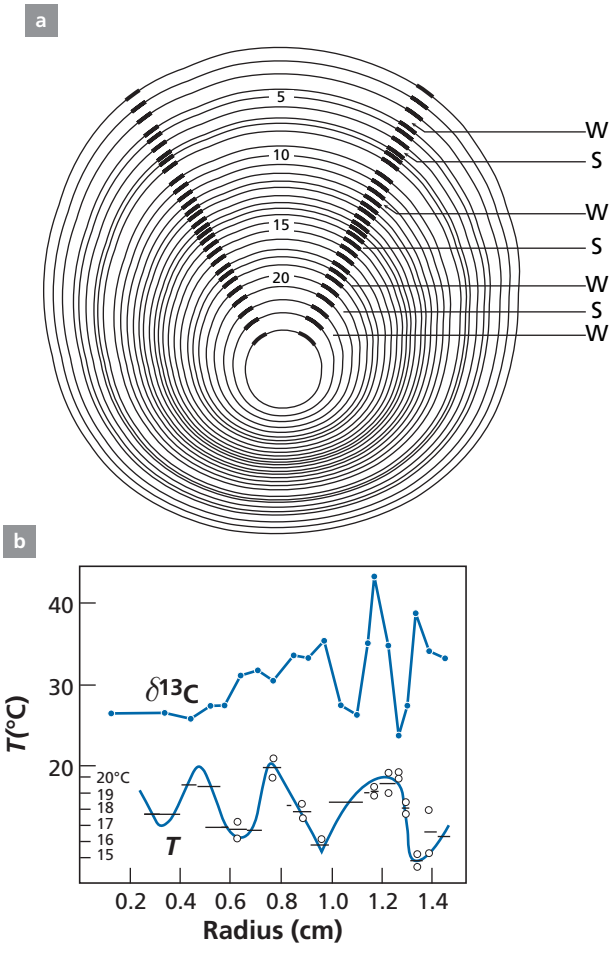


**Figure 7.10** Study of a Jurassic belemnite rostrum. (a) A famous figure of a cross-section through a Jurassic belemnite rostrum. Samples were taken a different radial distances (S, summer; W, winter; numbers of rings are counted from the outside). (b) Values of $\delta^{13}C$ and below $\delta^{18}O$ converted directly into temperature. The curve shows that the belemnite was born in the fall and died in spring! After Urey *et al.* (1951).

The precision of measurement of oxygen isotope composition is 0.1 in $\delta$ units. What is the power of resolution in temperature of the isotope method defined by Urey?

## Answer

Differentiating the formula above gives $\Delta T = 4.3\ \Delta\delta$. So the precision is 0.43 °C. One might envisage further increasing the precision when making measurements with the mass spectrometer to attain 0.01%, but this raises a geochemical problem: what do the tiny differences revealed signify? We shall get some inkling of an answer in what follows.

This exceptional scientific success story opened the way to a new geological discipline, **paleothermometry**, or the study of past temperatures on a precise scientific basis, which gave tremendous impetus to paleoclimatology. It also encouraged researchers to forge ahead. If stable isotopes of oxygen had yielded such significant results in their first application in geology, it could be hoped that the examination of other problems, other properties, and other elements would be equally successful. This hope gave rise to the work that founded **stable isotope geochemistry**. However, the Chicago team's paleothermometer was based on the assumption that $\delta_{\text{sea water}} = 0$ has been constant throughout geological times. As we shall see, this hypothesis probably holds over the average for millions of years but not on the scale of thousands of years which is the timescale of the Quaternary era (Epstein *et al.*, 1953; Epstein, 1959).

## 7.4.2 The $^{18}O/^{16}O$ isotope composition of silicates and high-temperature thermometry

It is relatively easy to measure the isotopic composition of oxygen in carbonates since $CO_3^{2-}$ reacts with phosphoric acid to transform into $CO_2$, which can be measured directly in double-collector mass spectrometers. It is far more difficult to extract oxygen from silicate minerals. This means using fluorine gas or even the gas $BrF_5$ and then transforming the oxygen into $CO_2$ by burning. Of course, all such processes should be performed with no isotopic fractionation or well-controlled fractionation! These techniques were developed at the California Institute of Technology by **Hugh Taylor** and **Sam Epstein** in the late 1960s (Epstein and Taylor, 1967).

Measuring the oxygen isotope composition of silicate minerals reveals systematic variations with the type of mineral and the type of rock to which the mineral belongs. These compositions can be characterized by measuring isotope fractionation between minerals. Now, one of the great features of isotopes is that isotope fractionation is very largely independent of pressure and dependent mainly on temperature. Variations in volume associated with exchange reactions are virtually zero. Therefore isotope equilibrium reactions are very useful for determining the temperatures at which natural mineral associations formed. Indeed $\alpha$ varies with temperature and tends towards unity at very high temperatures. As we have said, the variation of $\alpha$ with $T$ takes the form:

$$\ln \alpha = B + \frac{C}{T} + \frac{A}{T^2}.$$

The form of this equation is preserved for $\alpha$ and $\delta$. Between two minerals $m_1$ and $m_2$ in equilibrium:[10]

$$\Delta_{m_1 m_2} = \delta_{m_1} - \delta_{m_2} \approx A\left(10^6\, T^{-2}\right) + B = 1000 \ln \alpha.$$

The term $1/T$ is generally negligible. Oxygen isotopes are especially useful here. Oxygen is the most abundant element in silicates and the $^{18}O$ and $^{16}O$ isotopes fractionate in nature in proportions that can be easily measured by mass spectrometry. Experimental studies conducted mostly by the Chicago University group under **Robert Clayton** and

[10] Tables usually give absolute temperatures so degrees must be converted from Celsius to Kelvin.

**Table 7.1** Isotope fractionation for mineral–water pairs

| Mineral | Temperature (°C) | $A$ | $B$ |
|---|---|---|---|
| Calcite ($CO_3Ca$) | 0–500 | 2.78 | − 2.89 |
| Dolomite | 300–500 | 3.20 | − 1.5 |
| Quartz | 200–500 | 3.38 | − 2.90 |
| Quartz | 500–800 | 4.10 | − 3.7 |
| Alkali feldspar | 350–800 | 3.13 | − 3.7 |
| Plagioclase | 500–800 | 3.13 | − 3.7 |
| Anorthite | 500–800 | 2.09 | − 3.7 |
| Muscovite | 500–800 | 1.9 | − 3.10 |
| Magnetite | (reversed slope) 0–500 | − 1.47 | − 3.70 |

**Table 7.2** Results of $^{18}O$ isotope thermometry based on $^{18}O/^{16}O$ fractionation of mineral pairs

| Pair | $A$ | $B$ |
|---|---|---|
| Quartz–albite | 0.97 | 0 |
| Quartz–anorthite | 2.01 | 0 |
| Quartz–diopside | 2.08 | 0 |
| Quartz–magnetite | 5.57 | 0 |
| Quartz–muscovite | 2.20 | − 0.6 |
| Diopside–magnetite | 5.57 | 0 |

*Source:* After O'Neil (1986) modified by Bottinga and Javoy (1975).

**Jim O'Neil** and supplemented by theoretical work of **Yan Bottinga** and **Marc Javoy** at the Institut de Physique du Globe in Paris have provided a series of reliable values for coefficients $A$ and $B$ (see O'Neil and Clayton, 1964; Bottinga and Javoy, 1975; Javoy, 1977).

In the experimental procedure, the isotope fractionation between minerals and water is measured first. This is a convenient method as isotope equilibration is attained quite rapidly at about 80–100 °C. The fractionation between minerals is then calculated.

Tables 7.1 and 7.2 show the values of coefficients $A$ and $B$ for various mineral–water equilibria (we shall see the intrinsic importance of such fractionation later) and then for fractionation between pairs of minerals.

## Exercise

What is the $\delta^{18}O$ composition of a muscovite in equilibrium with water at 600 °C whose $\delta = -10$?

### Answer

The $\Delta$ is written:

$$1.9\left(10^6 \times \frac{1}{(873)^2}\right) - 3.1 = -0.6$$

where $\Delta = \delta_{musc} - \delta_{water}$.
From this we obtain $\delta_{musc} = -10.6$.

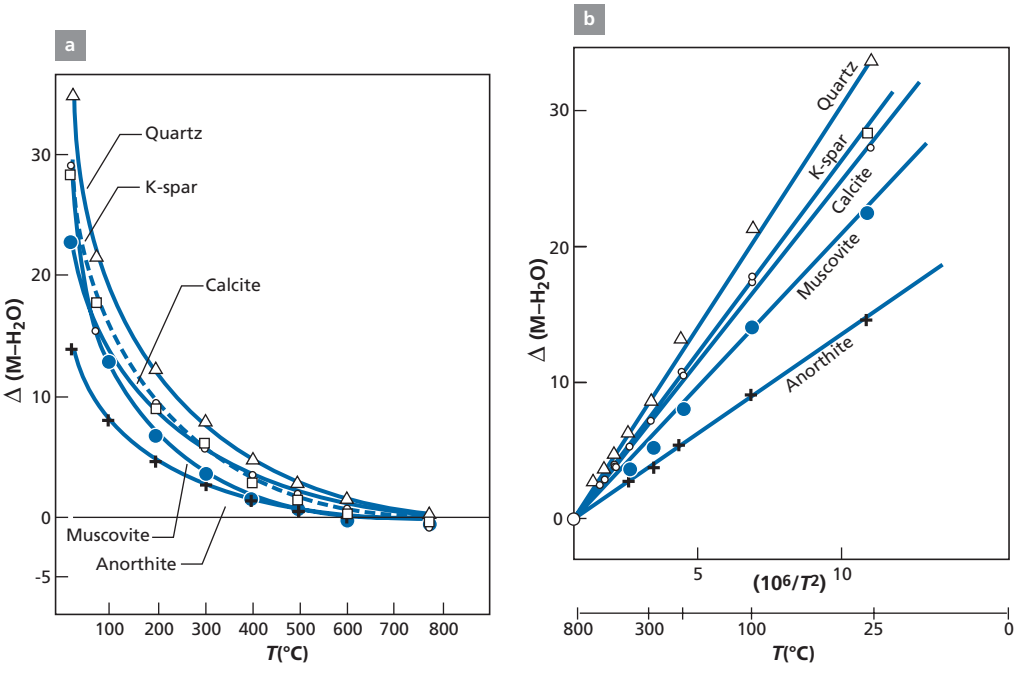


**Figure 7.11** Isotope fractionation curves for water and some minerals as a function of temperature ($T$, or $10^6/T^2$). Notice that the curve should theoretically converge to zero. The error is the result of experimental uncertainty. After O'Neil (1986).

These are shown in Figure 7.11 in two ways: as a function of temperature (°C) and as a function of $10^6/T^2$ because the fractionations are linear. We plot 1000 ln$\alpha$, that is $\Delta$, on the ordinates, which means we can calculate $\Delta_{water} = \delta_{mineral} - \delta_{water}$ directly. Notice that fractionation cancels itself out at high temperatures. On the experimental curves, this convergence seems to occur at less than $\Delta = 0$, but this effect is probably due to experimental errors. That would mean that minerals and water were of the same composition at high temperatures.

## Exercise

Water with $\delta_{water} = -10$ and rock (composed of several minerals) with an initial $\delta$ value of $\delta_{(0)rock} = +6$ are put together. If we mix 100 g of rock and 110 g of water and heat them to high temperature (500 °C in an autoclave) for which we take a zero overall $\Delta$ value, what will be the composition of the rock and water after the experiment, given that the rock contains 50% oxygen and 90% water?

### Answer

$\delta_{water} = \delta_{rock} = -4.29$.

So having the values $A$ and $B$ for several minerals, we can calculate fractionation between mineral pairs for each temperature:

$$\Delta_{m_1-m_2} = \Delta_{m_1-\text{water}} - \Delta_{m_2-\text{water}}.$$

Let us take the case of quartz–muscovite between 500 and 800 °C:

$$\Delta_{\text{quartz–musc}} = 2.20 \cdot 10^6/T^2 - 0.6.$$

We can set about geological thermometry using these various pairs of minerals. Having measured $\Delta_{m_1-m_2}$, we return to the established formula and calculate $T$.

In this way, the temperatures of various metamorphic zones have been determined. But, of course, much as with concordance of ages by various methods, we must make sure the various pairs of minerals yield the same temperature.

**Marc Javoy**, **Serge Fourcade**, and **the present author**, at the Institut de Physique du Globe in Paris, came up with a graphical discussion method: after choosing a reference mineral, we write for each mineral:

$$\Delta_{\text{quartz–mineral}} - B = A/T^2.$$

In a plot of $\Delta - B$ against $A$, the various minerals of a rock in isotopic equilibrium are aligned on a straight line through the origin whose slope $(1/T^2)$ gives the temperature at which they formed (Figure 7.12). If the points are not aligned, the rock is not in equilibrium and the temperature cannot be determined. It was thus possible to draw up a table of the thermal domains where the main rocks were formed (Figure 7.13). These findings are consistent with indirect evidence from mineral synthesis experiments and metamorphic zoneography.

## Exercise

The $\delta^{18}O$ values of the minerals of a metamorphic rock are: quartz +14.8, magnetite +5.

(1) Calculate the equilibrium temperature of quartz–magnetite.
(2) Calculate the $\delta^{18}O$ of an aqueous fluid in equilibrium with the rock.

### Answer

(1) 481 °C.
(2) +11.3.

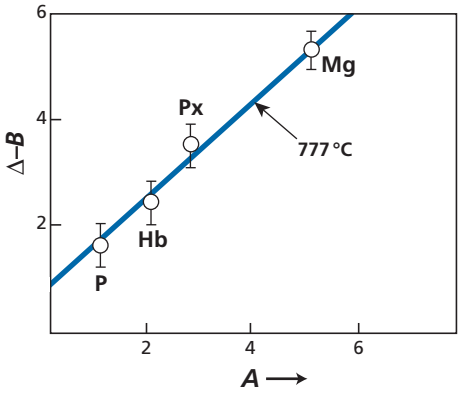


**Figure 7.12** Javoy's method of determining paleotemperatures, used here for San Marcos gabbro. P, plagioclase; Hb, hornblende; Px, pyroxene; Mg, magnetite; *A* and *B* are defined in the text.

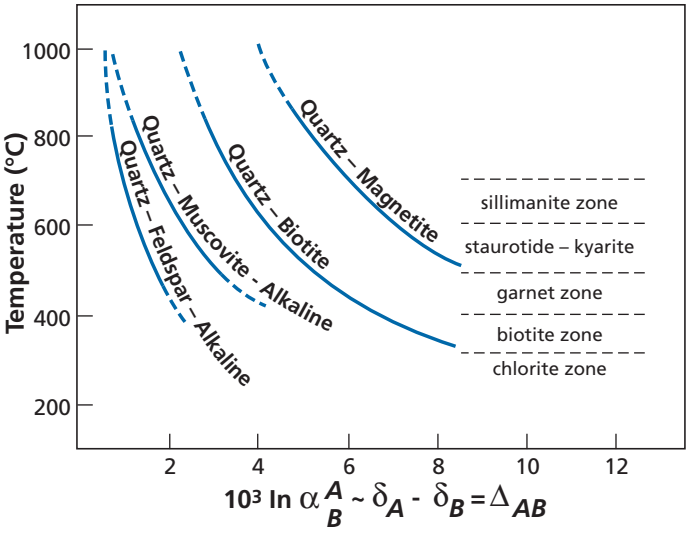


**Figure 7.13** Isotope temperature of different metamorphic grades determined from pairs of minerals. After Garlick and Epstein (1967).

## 7.4.3 Paleothermometry of intracrystalline isotopic order/disorder

After the paleothermometry of silicate rocks, one might legitimately ask with hindsight why the same approach was not adopted for low-temperature paleothermometry and why several minerals were not used instead of calcite alone to break free of the hypothesis of a constant $\delta$ value for sea water? In fact, research was conducted along these lines and, for this, the isotopic fractionation between water and calcium phosphate and water and silica was measured since these minerals are commonplace in marine sediments and in particular in fish teeth for phosphates and diatoms for silica. Unfortunately, as Figure 7.14 shows, while the fractionations are different for the three minerals ($CaCO_3$, $CaPO_4$, and $SiO_2$), their variations with temperature are parallel. They may therefore not be used two-by-two to eliminate the unknown factor which is the isotopic composition of sea water!

A new method has very recently emerged to eliminate the unknown quantity of the isotopic composition of ancient water. It was developed by the new team around **John Eiler** at the California Institute of Technology. It is based on isotopic fractionations existing within a single molecular species among the different varieties of isotope (see Ghosh *et al.*, 2006b). Let us take the carbonate ion $CO_3^{2-}$ as an example. This ion comprises numerous isotopic varieties: $^{12}C^{16}O^{16}O^{16}O$, $^{12}C^{16}O^{16}O^{18}O$, $^{12}C^{16}O^{18}O^{18}O$, . . ., $^{13}C^{16}O^{16}O^{16}O$, $^{13}C^{16}O^{16}O^{18}O$, . . ., etc. These are what are called **isotopologs** (see Section 7.2.1). Table 7.3 provides an inventory and gives their mean proportions in the "ordinary" carbonate ion. Each is characterized by a different molecular mass.

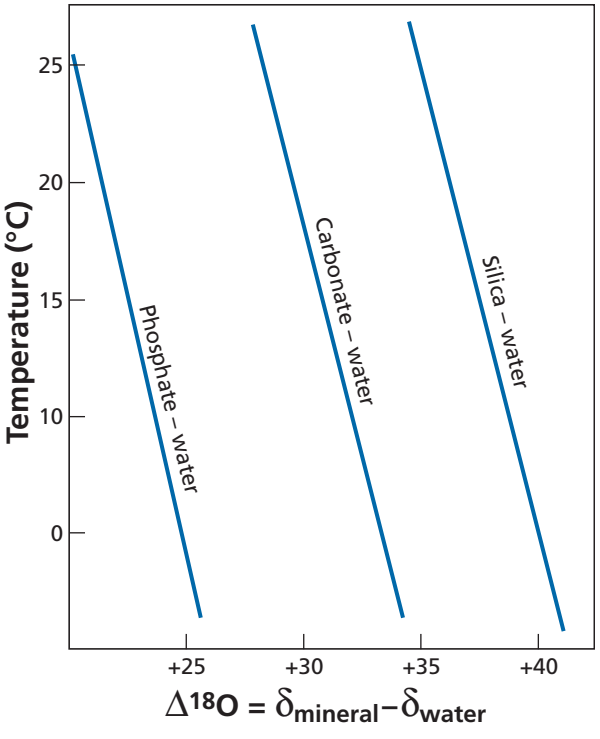


**Figure 7.14** Fractionation for $^{18}O/^{16}O$ for various minerals with water. The curve shows clearly that they are parallel. After Longinelli and Nutti (1973); Labeyrie (1974).

In a calcium carbonate crystal, thermodynamic equilibria in the sense of Urey occur among the various isotopic species. Keeping to the most abundant varieties, we can write the equilibrium:

$$^{13}C^{16}O_3^{2-} + {}^{12}C^{18}O^{16}O_2^{2-} \Leftrightarrow {}^{13}C^{18}O^{16}O_2^{2-} + {}^{12}C^{16}O_2^{2-}.$$

masses: (61) (62) (63) (60).

The equilibrium constant depends on temperature. The lower the temperature, the more the reaction favors the right-hand members, that is the members with the heavy isotopes of carbon and oxygen (the most advantaged would be $^{13}C^{18}O^{18}O^{18}O$, but as its abundance is 94 ppt, it can barely be measured). In fact, this reaction may be considered an order/disorder reaction. The lower the temperature, the greater the ordering (light species with light, heavy species with heavy). The higher the temperature, the more disordered the assembly and the equilibrium constant tends towards unity.

It is a smart idea to use these equilibria within the calcite crystal, but there is a major difficulty in practice. Calcium carbonate isotopic compositions cannot be measured directly in the laboratory (they may be measurable one day with instruments for *in situ* isotope analysis, but for the time being they are not precise enough). To measure the isotopic

**Table 7.3** Isotopologs

| | Mass | Abundance |
|---|---|---|
| $CO_2$ | | |
| $^{16}O^{12}C^{16}O$ | 44 | 98.40% |
| $^{16}O^{13}C^{16}O$ | 45 | 1.10% |
| $^{17}O^{12}C^{16}O$ | 45 | 730 ppm |
| $^{18}O^{12}C^{16}O$ | 46 | 0.40% |
| $^{17}O^{13}C^{16}O$ | 46 | 8.19 ppm |
| $^{17}O^{12}C^{17}O$ | 46 | 135 ppm |
| $^{18}O^{13}C^{16}O$ | 47 | 45 ppm |
| $^{17}O^{12}C^{18}O$ | 47 | 1.5 ppm |
| $^{17}O^{13}C^{17}O$ | 47 | 1.5 ppm |
| $^{18}O^{12}C^{18}O$ | 48 | 4.1 ppm |
| $^{17}O^{13}C^{18}O$ | 48 | 16.7 ppm |
| $^{18}O^{13}C^{18}O$ | 49 | 46 ppb |
| $CO_3$ | | |
| $^{12}C^{16}O^{16}O^{16}O$ | 60 | 98.20% |
| $^{13}C^{16}O^{16}O^{16}O$ | 61 | 1.10% |
| $^{12}C^{17}O^{16}O^{16}O$ | 61 | 0.11% |
| $^{12}C^{18}O^{16}O^{16}O$ | 62 | 0.60% |
| $^{13}C^{17}O^{16}O^{16}O$ | 62 | 12 ppm |
| $^{12}C^{17}O^{17}O^{16}O$ | 62 | 405 ppb |
| $^{13}C^{18}O^{16}O^{16}O$ | 63 | 67 ppm |
| $^{12}C^{17}O^{18}O^{16}O$ | 63 | 4.4 ppm |
| $^{13}C^{17}O^{17}O^{16}O$ | 63 | 4.54 ppb |
| $^{12}C^{17}O^{17}O^{17}O$ | 63 | 50 ppt |
| $^{12}C^{18}O^{18}O^{16}O$ | 64 | 12 ppm |
| $^{13}C^{17}O^{18}O^{16}O$ | 64 | 50 ppb |
| $^{12}C^{17}O^{17}O^{18}O$ | 64 | 828 ppt |
| $^{13}C^{17}O^{17}O^{17}O$ | 64 | 0.5 ppt |
| $^{13}C^{18}O^{18}O^{16}O$ | 65 | 138 ppb |
| $^{12}C^{17}O^{18}O^{18}O$ | 65 | 4.5 ppb |
| $^{13}C^{17}O^{17}O^{18}O$ | 65 | 9 ppt |
| $^{12}C^{18}O^{18}O^{18}O$ | 66 | 8 ppb |
| $^{13}C^{17}O^{18}O^{18}O$ | 66 | 51 ppt |
| $^{13}C^{18}O^{18}O^{18}O$ | 67 | 94 ppt |

composition of $CO_3^{2-}$ radicals they are transformed into $CO_2$ molecules by a reaction with phosphoric acid.

The breakthrough by the Caltech team was to have developed a technique for extracting carbonate isotope varieties and transforming them into clearly identifiable $CO_2$ molecules and in particular for distinguishing $^{13}C^{18}O^{16}O$ (mass = 47), $^{12}C^{16}O^{16}O$ (mass = 44), $^{12}C^{18}O^{16}O$ (mass = 46), and $^{13}C^{16}O^{16}O$ (mass = 45) and showing they reflect the proportions of $CO_3^{2-}$ molecules (by adding $^{16}O$ to each). To do this, they defined the unit $\Delta_{47}$ between the ratios measured for masses 47 and 44:

$$\Delta_{47} = \left[(47/44)_{\text{sample}} - (47/44)_{\text{reference}}\right] \times 10^3.$$

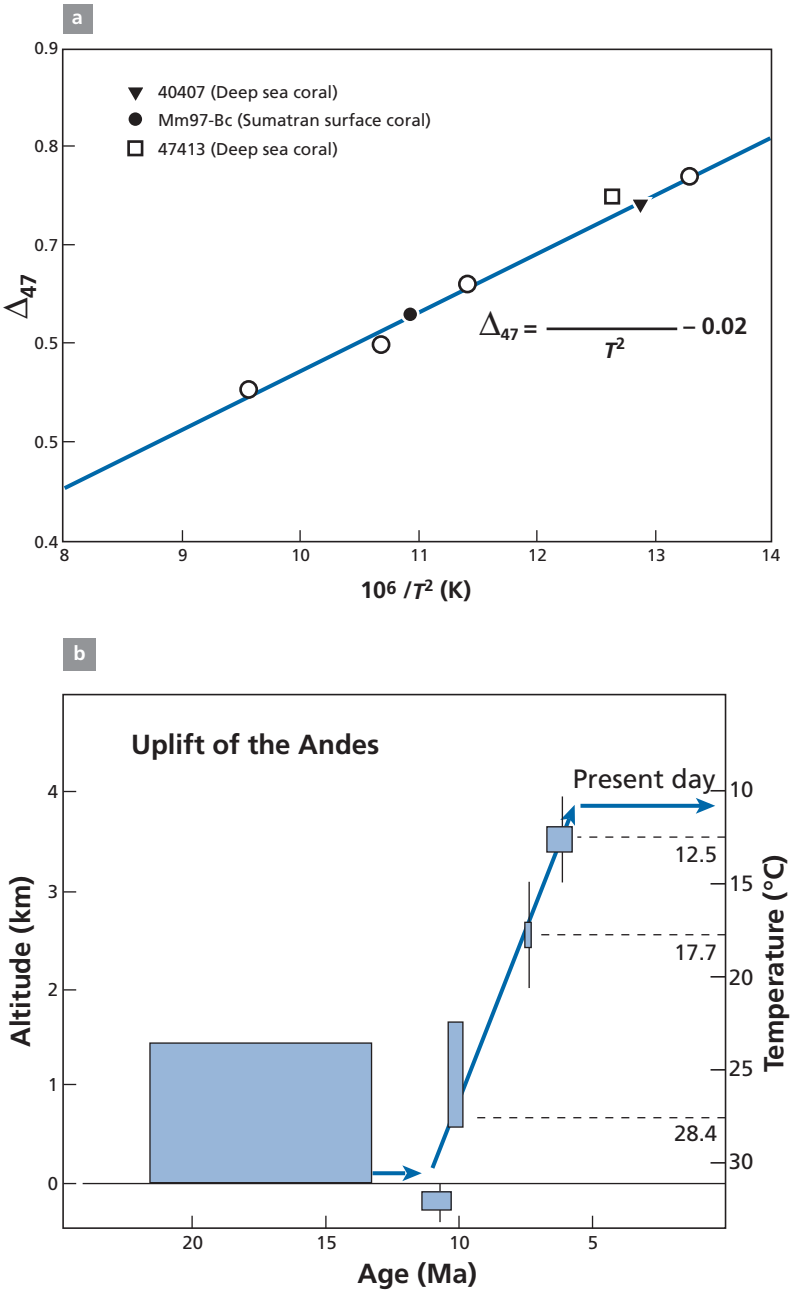


**Figure 7.15** (a) Calibration of the isotopic order/disorder thermometer with the corresponding formula. (b) Uplift of the Andes reconstructed by the isotopic order/disorder chemometer. After Ghosh *et al.* (2006).

The reference (47/44) is the ratio that would pertain if the isotopic distribution among the varieties of isotopes were purely random. They established the fractionation curve ($\Delta_{47}$, as a function of temperature).

The temperature can therefore be determined from a measurement of $\Delta_{47}$. The exact formula (between 0 and 50 °C) is:

$$\Delta_{47} = 0.0592 \cdot 10^6 T^{-2} - 0.02.$$

Precision is estimated to be ±2 °C.

An interesting application of this method has been to determine the rate of uplift of the Bolivian Altiplano. Samples of carbonates contained in soil were taken from the plateau but of different ages and dated by other methods. The temperature at which these carbonates formed was then calculated. As the curve of temperature variation with altitude in the Andes is known, the curve of altitude versus time could be determined (Figure 7.15).

### Exercise

Do you think this isotopic order/disorder method could apply to $SiO_2$ at low temperature (diatoms)? Write the equivalent equation to that written for carbonate. What would the isotopic parameter be? Do you see any practical difficulty in this?

**Answer**

Yes, in principle. The order/disorder equilibrium equation would be:

$$^{30}Si^{16}O_2 + {}^{28}Si^{18}O^{16}O \Leftrightarrow {}^{30}Si^{18}O^{16}O + {}^{28}Si^{16}O_2$$

mass : (62) (62) (64) (60)

$$\Delta_{64} = \left[(64/60)_{\text{sample}} - (64/60)_{\text{reference}}\right] \times 10^3 \text{ (or } 10^4 \text{ as necessary).}$$

The difficulty is that with the present-day method, Si is measured in the form of $SiF_4$ on the one hand, oxygen being extracted on the other hand. To apply the method, direct measurement by an *in situ* method in the form of $SiO_2$ would be required. This will probably be feasible in the future with ion probes or laser beam ionization.

## 7.5 The isotope cycle of water

Let us return to the water cycle mentioned at the beginning of this chapter. On Earth, it is dominated by the following factors.

(1) *The existence of four reservoirs.* A series of exchanges among the ocean, the ice caps, fresh water, and the atmosphere make up the water cycle. It is another dynamic system. The reservoirs are of very different dimensions: the ocean (1370 million $km^3$), the ice caps (29 million $km^3$), river water and lakes (0.002 12 million $km^3$). The transit time of water in each reservoir varies roughly inversely with its size, each reservoir playing an important geochemical role. Thus the quantity of water that evaporates and precipitates

is 500 million km$^3$ per thousand years, or more than one-quarter of the volume of the oceans.[11]

(2) *The ocean–atmosphere hydrological cycle.* Water evaporates from the ocean and atmospheric water vapor forms clouds that migrate and may occasionally produce rain. Thus salt water is changed into fresh water and transferred from tropical to polar regions and from the ocean to the landmasses. The hydrological cycle has a double effect. Clouds move from low to high latitudes and also from the ocean to the continents. The fresh water that falls as rain over the landmasses re-evaporates in part, runs off or seeps in, thus forming the freshwater reservoir which ultimately flows back to the ocean.

(3) *The polar regions.* When precipitation from clouds occurs in polar regions, we no longer have rain but snow. The snow accumulates and changes into ice forming the polar ice caps. These ice caps flow (like mountain glaciers, but more slowly) and eventually break up in the ocean as icebergs and mix with the ocean.

The whole of water circulation on the planet and the various stages of the cycle have been studied in terms of isotopes. We have seen, when examining theoretical aspects, that when water and water vapor are in equilibrium, oxygen and hydrogen isotope fractionation are associated. This double pair of isotopes has allowed us to construct quantitative models of water circulation. However, the problems raised by these studies are not as simple as the theoretical study suggested.

## 7.5.1 Isotope fractionation of clouds and precipitation

A cloud is composed of water droplets in equilibrium with water vapor. Water vapor and droplets are in isotopic equilibrium. All of this comes, of course, from water which initially evaporated.

Let us take a cloud near the equator and follow it as it moves to higher latitudes. The cloud is enriched as a whole in $^{16}O$ relative to sea water, as we have seen, and so has a negative $\delta$ value. As it moves it discharges some of its water as rainfall. The rainwater is enriched in the heavy isotope, and so the cloud becomes increasingly enriched in the light isotope. The precipitation is increasingly rich in light isotopes, which effect is offset in part by the fact that the fractionation factor varies with $1/T$. As we move away from the equator, it can be seen statistically that the precipitation has increasingly negative $\delta^{18}O$ values (Figure 7.16).

As clouds undergo genuine distillation, by progressively losing their substance, their isotope composition obeys a Rayleigh law, but a "super law" because as they move polewards, the temperature falls, the fractionation factor also increases and distillation becomes increasingly effective (Figure 7.17), so much so that at the poles the $\delta^{18}O$ values are extremely negative.

We observe geographical zoning for which the $\delta^{18}O$ value and mean air temperature can be related (Epstein *et al.*, 1965; Dansgaard and Tauber, 1969) (Figure 7.18).

The general cycle of clouds is repeated at local scale, when clouds move over landmasses and progressively shed their water. Thus, fresh water has negative $\delta$ values. This phenomenon has been studied using the paired tracers $^{18}O/^{16}O$ and D/H. **Harmon Craig** of the Scripps Institution of the University of California showed that rain and snow precipitation and the

[11] 1 km$^3 \approx 10^{12}$ kg.

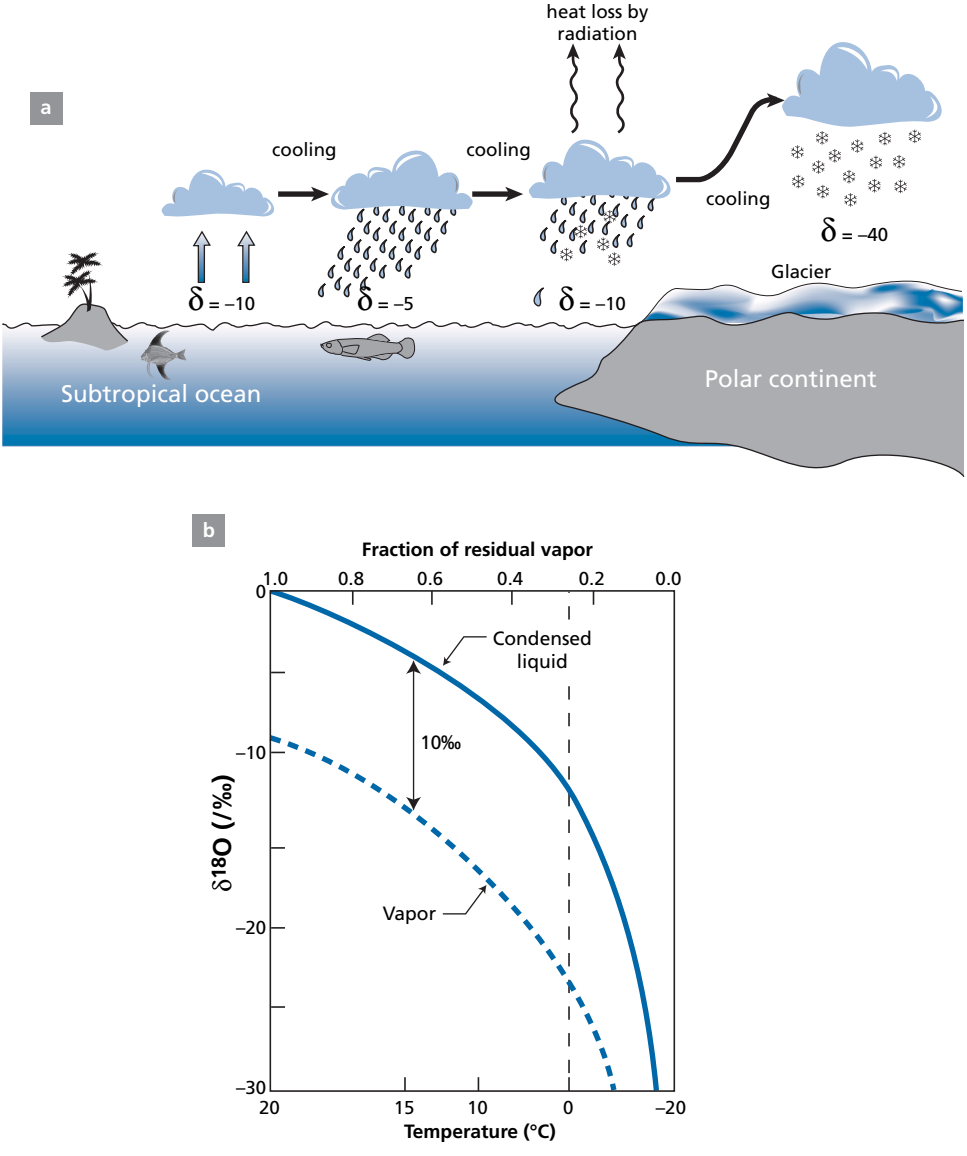


**Figure 7.16** Fractionation of $\delta^{18}O$ in a cloud as a function of Rayleigh distillation. The cloud forms at the equator and moves to higher latitudes, losing water. The fractionation factor varies with temperature. Modified after Dansgaard (1964).

composition of glaciers lie on what is known as the meteoric water line: $\delta D = 8 \times \delta^{18}O + 10$ in the ($\delta D$, $\delta^{18}O$) diagram (Figure 7.3). The slope of value 8 corresponds to an equilibrium fractionation between the water and its vapor at around 20 °C. We have good grounds to think, then, that precipitation occurs in conditions of equilibrium. It was thought in early studies of the water cycle that evaporation was also statistically an equilibrium phenomenon. In fact, this is not so. Evaporation, which is a **kinetic phenomenon** in isotopic terms, leads to

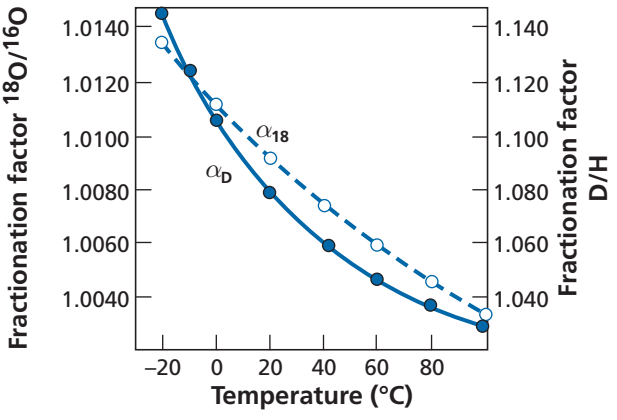


**Figure 7.17** Study of $^{18}O/^{16}O$ fractionation. Liquid–vapor fractionation of $H_2O$ for $^{18}O/^{16}O$ and D/H as a function of temperature. Notice that the scales are different. After Jouzel (1986).

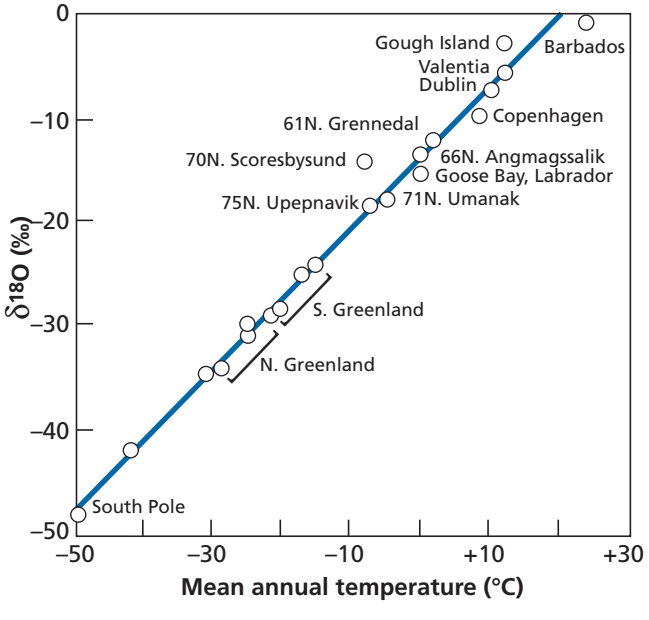


**Figure 7.18** Variation of the $^{18}O/^{16}O$ ratio in rainwater and snow with latitude and so with temperature. After Dansgaard (1964).

$^{18}O$ contents of vapor that are much lower than they would be in equilibrium. But depending on the climate, kinetic evaporation may or may not be followed by partial isotope re-equilibration which means the vapor composition does not lie on the straight line of precipitation. The same is true, of course, of surface sea water, which forms the residue of evaporation. Its $^{18}O$ composition is variable and depends on the relative extent of

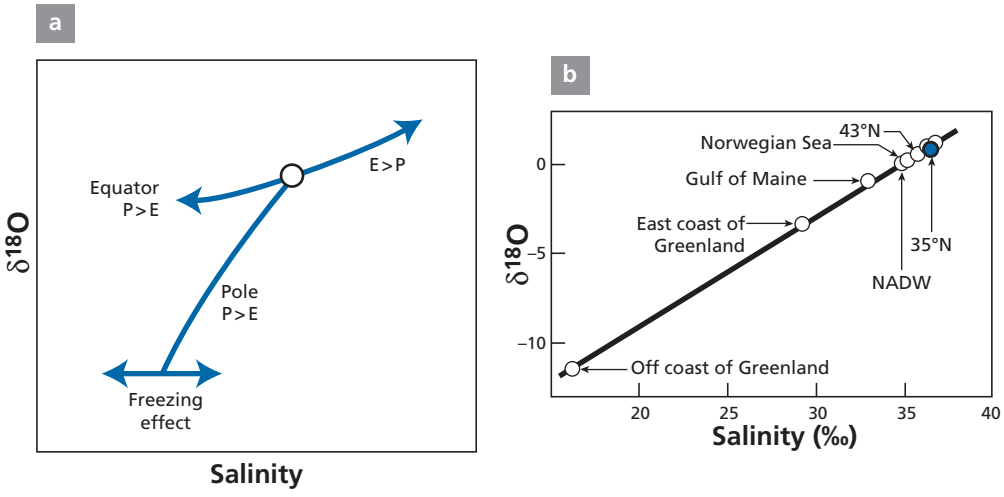


**Figure 7.19** Relations between $\delta^{18}O$ and salinity. (a) Theoretical relation. P, precipitation; E, evaporation. (b) Various measurements for the North Atlantic. NADW, North Atlantic Deep Water. After Craig (1965).

evaporation and of precipitation (which are substantial over the ocean) and of the input of fresh water. These variations are particularly sensitive in the North Atlantic (Epstein and Mayeda, 1953). We visualize the variations and the influence of the various phenomena that causes them in a ($\delta^{18}O$, S‰) plot, where S‰ is the salinity of sea water (Figure 7.19). As can be seen, there is a very close correlation between the two. All of this shows that this is a well-understood field of research.

## EXAMPLE

### Precipitation in North America

This is a map of $\delta D$ and $\delta^{18}O$ for precipitation in North America (Figure 7.20). From what has just been said about the effect of isotope distillation of clouds, the pattern of rainfall over North America is described. The main source of rainfall comes from the Gulf of Mexico with clouds moving northwards and becoming distilled. This distribution is modified by several factors. First, the relief, which means the clouds penetrate further up the Mississippi valley but discharge sooner over the Appalachian Mountains in the east and the Rocky Mountains in the west. Other rain comes in from the Atlantic, of course, so the distribution is asymmetrical. Conversely rain from the Pacific is confined to the coast and moves inland little, so the lines are more tightly packed to the west.

## Exercise

From the information given since the beginning of this chapter, use theoretical considerations to establish Craig's equation:

$\delta_{^{18}O} = +8, \delta_D + 10.$

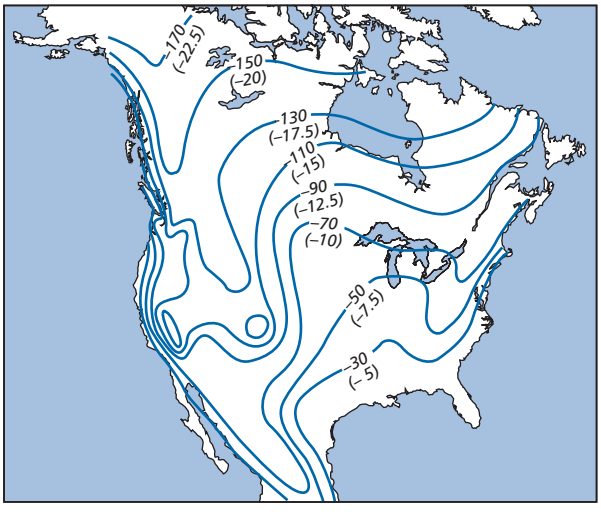


**Figure 7.20** Distribution of $^{18}O/^{16}O$ and D/H in rainfall in North America. The $^{18}O/^{16}O$ ratios are in brackets. After Taylor (1974).

**Answer**

Clouds obey a Rayleigh law:

$$\delta_D \approx \delta_{D,O} + 10^3(\alpha_D - 1)\ln f$$

$$\delta_O \approx \delta_{18_{O,O}} + 10^3(\alpha_O - 1)\ln f.$$

This simplifies to:

$$\frac{\delta_D - \delta_{D,O}}{\delta_{18_O} - \delta_{18_{O,O}}} \approx \left(\frac{\alpha_D - 1}{\alpha_O - 1}\right).$$

At 20 °C, as seen in the previous problem, $\alpha_D = 1.0850$ and $\alpha_{^{18}O} \approx 1.0098$, hence:

$$\frac{\alpha_D - 1}{\alpha_{18_O} - 1} \approx 8.$$

We therefore have the slope. The ordinate at the origin seems more difficult to model because for vapor formed at 20 °C, $\delta_{D,O} - 8\delta_{^{18}O,O} = -6.8$ whereas we should find 10. We shall not go into the explanation of this difference, which is a highly complex problem, as shown by **Jean Jouzel** of the French Atomic Energy Commission. The different aspects of the hydrological cycle, including kinetic effects during evaporation, play a part.

## 7.5.2 Juvenile water

It is well known that in the water cycle, there is an input from hot water from the depths of the Earth. It was long thought that this hot water was the gradual degassing of water trapped by the Earth when it first formed, as with the primitive ocean. If this were so, this water would progressively increase the volume of the hydrosphere. Water from deep beneath the surface

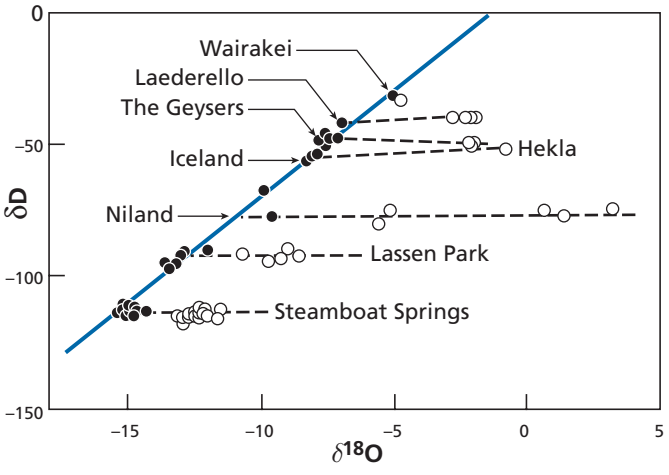


**Figure 7.21** Correlation diagram for ($^{18}O/^{16}O$, D/H) in geothermal waters. They form horizontal lines cutting the meteoric straight line at the point corresponding to local rainwater. This is interpreted by saying that water has exchanged its oxygen isotopically with the rock but the hydrogen of water does not change because it is an infinite hydrogen isotope reservoir compared with rocks that are relatively poor in hydrogen. After Craig (1963).

is still referred to as juvenile water. **Harmon Craig** (he again) studied geothermal water to determine the isotope composition of any juvenile water. He showed that the $\delta$ values of geothermal waters from the same source can be plotted on a ($\delta$D, $\delta^{18}$O) diagram on straight lines pretty well parallel to the $\delta^{18}$O axis and which cut the straight line of precipitation corresponding to the composition of rainwater for the region. And so the composition of geothermal water can be explained by the evolution of meteoric water via isotope exchange of oxygen with the country rock. There is no need to invoke juvenile water from the mantle to explain these isotope compositions (Figure 7.21).

As these relations are systematic for all the geothermal regions studied, Craig concluded that the input of juvenile water into the current water cycle is negligible and that geothermal waters are only recycled surface water. The same goes for water from volcanoes. This hypothesis has been confirmed by more elaborate studies of variations in the isotope composition of geothermal water over time. In many cases, it has been shown that variations tracked those observed in the same place for rainwater, with a time lag corresponding to the transit time which varied from months to years.[12]

EXAMPLE

## Iceland's geysers

In some instances, such as the geysers of Iceland, the straight line of ($\delta$D, $\delta^{18}$O) correlation is not horizontal but has a positive slope (Figure 7.22).

[12] A spa water company signed a research contract with a Parisian professor to study the isotopic composition of the water it sold to prove it was "juvenile" water, a name whose advertising value can be well imagined. As the studies showed the water was not juvenile, the company terminated the contract and demanded that the results should not be published!

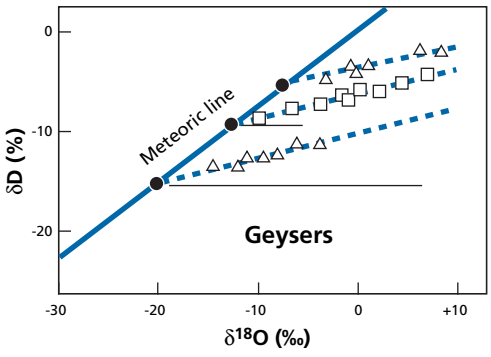


**Figure 7.22** Correlation diagram for ($^{18}O/^{16}O$, D/H) in acidic geothermal waters and geysers. The diagram is identical to the previous one except that these are acidic geothermal waters with a high sulfate content whose pH is close to 3 and for which the correlated enrichment in D and $^{18}O$ results mostly from more rapid evaporation of light molecules with kinetic fractionation into the bargain. After Craig (1963).

Suppose we begin with rainwater of local composition and that this water undergoes distillation by evaporating. Then:

$$\delta_D \approx \delta_{O,D} + 10^3(\alpha_D - 1)\ln f.$$

$$\delta^{18}O \approx \delta^{18}O,O + 10^3(\alpha^{18}O - 1)\ln f.$$

Eliminating ln $f$ gives:

$$\frac{\delta_D - \delta_{O,D}}{\delta_{18}O - \delta_{18}O,O} \approx \left(\frac{\alpha_D - 1}{\alpha_O - 1}\right).$$

We know that at 100 °C, for water–vapor fractionation, $\alpha_D = 1.028$ and $\delta^{18}O = 1.005$. The slope corresponds to 5.6, a lower value than that of equilibrium fractionation (8). The effect is therefore a combination between exchange and distillation.

In fact, in nature, isotopic compositions of geothermal water or vapor are combinations between Rayleigh distillation and the water–rock oxygen isotope exchange, between kinetic fractionation and equilibrium fractionation. A horizontal slope indicates that isotope exchange has been possible and so the transit time is long. When the slope is identical to that of the Rayleigh law, the transit time has been short.

## 7.6 Oxygen isotopes in igneous processes

Examination shows that the $^{18}O/^{16}O$ isotope composition of unaltered rock of deep origin, whether ocean basalts or ultrabasic rocks, is extraordinarily constant at $\delta^{18}O = +5.5$ (Figure 7.23). This value is analogous to the mean value of meteorites. It has therefore been agreed that this value is the reference value for the mantle. When taking stock of measurements on basic or acid, volcanic or plutonic igneous rocks, the results are found to divide between:

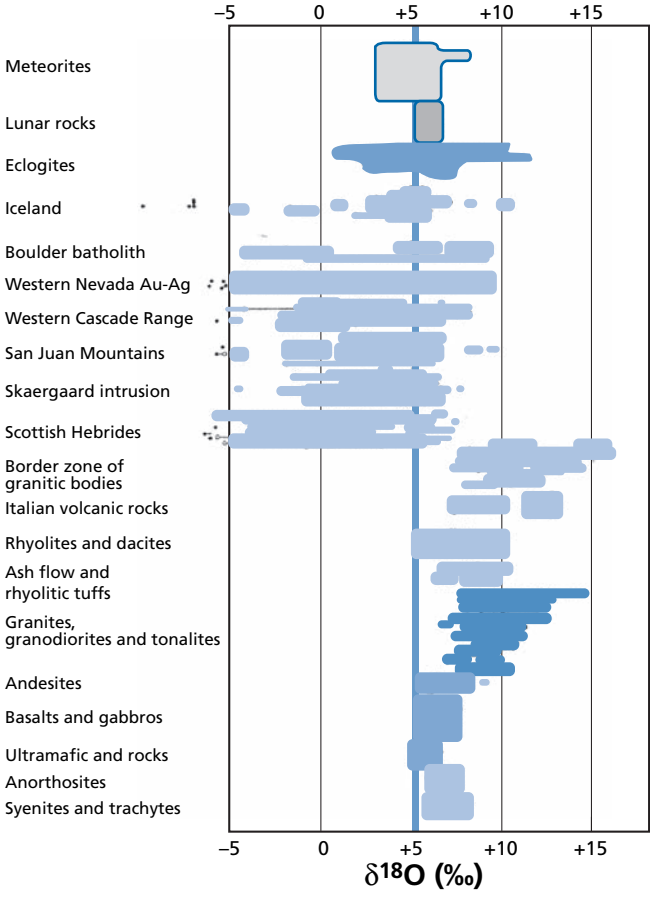


**Figure 7.23** Values of $\delta^{18}O$ in rocks and minerals. After Taylor (1974).

- igneous rocks with a $\delta^{18}O$ value greater than 5.5;
- igneous rocks with a $\delta^{18}O$ value less than 5.5, and some with negative values.

These two trends correspond to two types of phenomena affecting igneous rocks: contamination by crustal rocks and *post solidus* exchanges with hydrothermal fluids.

## 7.6.1 Contamination phenomena

These phenomena are classified under two types: those involving mixing at the magma source where melting affected both acidic and basic metamorphic rocks, and those where contamination occurred when the magma was emplaced. The latter process, known as assimilation, obeys a mechanism already accounted for by **Bowen** (1928). Mineral crystallization in a magma chamber releases **latent heat** of crystallization. This latent heat melts rock around the edges of the magma chamber leading to their assimilation.

$$m\downarrow L = m\uparrow C_P\,\Delta T,$$

where $L$ is the latent heat, $m\downarrow$ the mass of crystals precipitating per unit time, $m\uparrow$ the mass of rock assimilated, $C_P$ the specific heat of the surrounding rocks, and $\Delta T$ the temperature difference between the wall rock and the magma. If we can write $m\downarrow = kM$, then $kML = m\downarrow C_P\,\Delta T$, therefore:

$$\left(\frac{m\uparrow}{M}\right) = \left(\frac{kL}{C_P\,\Delta T}\right).$$

The magma is contaminated isotopically too by the mixing law:

$$(\delta^{18}O)_{Hy} = (\delta^{18}O)_{magma}(1-x) + (\delta^{18}O)_{country\ rock}(x)$$

with $x = (m\downarrow/M)$, because the oxygen contents of the country rock and the magma are almost identical. This was shown by **Hugh Taylor** (1968) of the California Institute of Technology (see also Taylor, 1979).

## Exercise

What is the $\delta^{18}O$ value of a basaltic magma whose $\delta^{18}O = 0$ and which assimilates 1%, 5%, and 10% of the country rock whose $\delta^{18}O = +20$?

### Answer

| | Assimilation | | |
|---|---|---|---|
| | 1% | 5% | 10% |
| $\delta^{18}O$ | 5.64 | 6.22 | 6.95 |

The contamination effect therefore increases the $\delta^{18}O$ value because sedimentary and metamorphic rocks have positive $\delta^{18}O$ values. An interesting approach to studying the contamination of magmas by continental crust is to cross the studies of oxygen isotopes with those of strontium isotopes. The (O–Sr) isotope diagram can be calculated quite simply because it is assumed that the oxygen content is analogous in the different rocks. The mixing diagram depends only on the Sr contents of the two components of the mixture. Figure 7.24 is the theoretical mixing diagram.

Such combined studies have been made of volcanic rocks of the Japan arcs and the Peninsular Range batholith in California (Figure 7.25).

## Exercise

A basaltic magma is emplaced and assimilates 1%, 5%, and 10% of the country rock. The $\delta^{18}O$ values are those of the previous exercise. The $^{87}Sr/^{86}Sr$ values are 0.703 for the magma and 0.730 for the country rock. The Sr content of the magma is 350 ppm and that of the country rock is 100 ppm. Calculate the isotopic compositions of the mixture and plot the ($\delta^{18}O$, $^{87}Sr/^{86}Sr$) diagram.

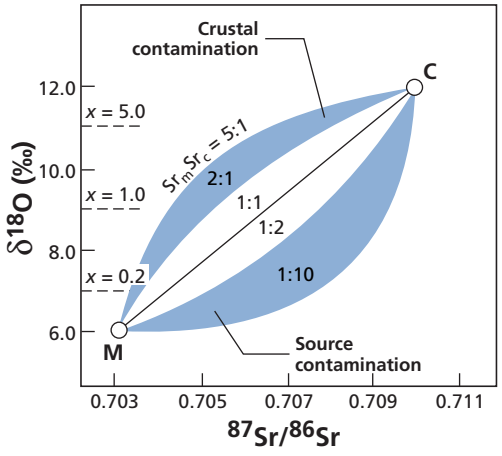


**Figure 7.24** Theoretical O–Sr isotope mixing plots. The *x* values show the proportion of country rock relative to the magma. The $Sr_{magma}/Sr_{country\ rock}$ parameter varies from 5 to 0.1. M, magma; C, crust. After James (1981).

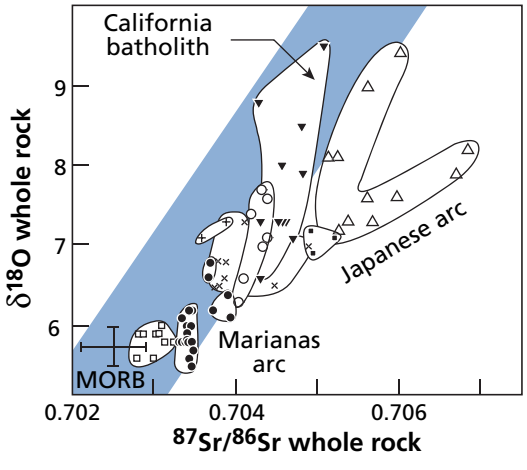


**Figure 7.25** Example of an O–Sr isotope correlation diagram showing the Japan arcs and batholith granites in California. After Ito and Stern (1985).

## Answer

The $\delta^{18}O$ values have already been given.

| | Assimilation | | |
|---|---|---|---|
| | 1% | 5% | 10% |
| $^{87}Sr/^{86}Sr$ | 0.703 08 | 0.7034 | 0.703 94 |

It is left to the reader to plot the diagram.

### 7.6.2 Water–rock interaction

As we have said, isotope memory is retained if no exchange occurs after crystallization. When this is not the case, secondary isotopic disturbances can be turned to account. **Hugh Taylor** and his students observed when examining various granite massifs or hydrothermal mineral deposits that the $^{18}O/^{16}O$ isotope compositions had been disrupted after their initial crystallization by water–rock exchanges. The calibration made on water–mineral fractionation was therefore turned directly to account.

Whereas the $\delta^{18}O$ values of minerals and rocks of deep origin are generally positive (between +5 and +8), these rocks had negative $\delta^{18}O$ values of −6 to −7. In the same cases, relative fractionation as can be observed between minerals, such as quartz–potassium feldspar fractionation, was reversed. Taylor remembered Craig's results on thermal waters and postulated that, rather than observing the waters, he was observing rock with which the waters had swapped isotopes. From that point, he was able to show that the emplacement of granite plutons, especially those with associated mineral deposits, involves intense fluid circulation in the surrounding rock. Of course, the existence of such fluids was already known because they give rise to veins of aplite and quartz pegmatite and they engender certain forms of mineralization around granites, but their full importance was not understood.

In a closed system, we can write the mass balance equation:

$$W g_w \delta_{0,W} + R g_r \delta_{0,R} = W g_w \delta_W + R g_r \delta_R$$

where $W$ is the mass of water and $R$ the mass of rock, $g_w$ is the proportion of oxygen in the water and $g_r$ the proportion of oxygen in the rock, $\delta_{0,W}$ and $\delta_{0,R}$ are the initial compositions of water and rock, and $\delta_W$ and $\delta_R$ are the final compositions thereof.

$$\frac{W}{R} = \left(\frac{g_r}{g_w}\right)\left(\frac{\delta_R - \delta_{0,R}}{\delta_{0,W} - \delta_W}\right),$$

since $\delta_W$ and $\delta_R$ are related by fractionation reactions $\delta_W = \delta_R - \Delta$. This gives:

$$\frac{W}{R} = \left(\frac{g_r}{g_w}\right)\left(\frac{\delta_R - \delta_{0,R}}{\delta_{0,W} - (\delta_R - \Delta)}\right) \qquad \frac{g_r}{g_w} \approx 0.5.$$

Indeed, $g_r = 0.45$ and $g_w = 0.89$. We estimate $\delta_{0,R}$ from the nature of the rock and the catalog of sound rock (close to +5), and we estimate $\Delta$ by calibrating and estimating temperature by fractionation among minerals. This temperature can be compared with the temperature obtained by the heat budget.

A calculation may be made, for example, for a feldspar with $\delta^{18}O = +8$ and $\delta_{W,^{18}O} = -16$ at various temperatures (Figure 7.26a). It shows that in a closed system, the $W/R$ ratios may be extremely variable.

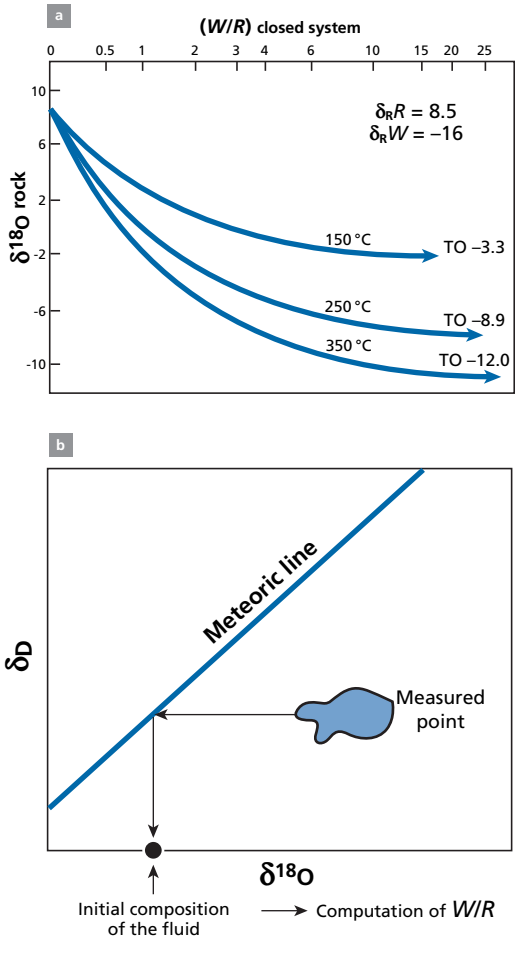


**Figure 7.26** Variation in $\delta^{18}$O composition and ($\delta$D, $\delta^{18}$O) correlation diagram. (a) The variation in the $\delta^{18}$O composition of a feldspar with an initial composition $\delta = +18$ is calculated as a function of (W/R) for various temperatures, with the initial composition of water being $\delta = -16$. (b) It is assumed the altered rocks are represented by the blue area in the ($\delta$D, $\delta^{18}$O) diagram. We can try to determine the initial composition of the fluid by assuming, as a first approximation, that the $\delta$D values of the rock and water are almost identical. The intersection between the horizontal and the ($\delta$D, $\delta^{18}$O) correlation diagram of rainwater gives the value of water involved in alteration. Reconstructed from several of Taylor's papers.

## Exercise

What is the W/R ratio of a hydrothermal system supposedly working in a closed system at 400 °C?

The initial $\delta^{18}$O value of feldspar is +8, that of the water determined by the meteoric straight line is $\delta_{0,W} = -20$. The $\Delta_{\text{feldspar–water}}$ fractionation factor is $3.13 \times 10^6\ T^{-2} - 3.7$. The $\delta^{18}$O of feldspar is measured as $\delta_R = -2$.

### Answer

The fractionation factor $\Delta = 3.13 \cdot 10^6/(673)^2 - 3.7 = 3.21 = \delta_R - \delta_W(W/R) = 0.34$.

### Exercise

Let us now suppose the $W/R$ ratio $= 5$, that is, there is much more water. All else being equal, what will be the $\delta^{18}O$ value of the feldspar measured?

**Answer**
$\delta^{18}O = -14.54$.

The process described in the previous exercise involves a double exchange and it is either the water or the rock that influences the isotopic composition of the other depending on the $W/R$ ratio.

Allowing for the point that $\Delta$ varies with temperature, a whole range of scenarios can be generated.

### Exercise

Let us pick up from where we left off in the previous exercise. Imagine an exchange between sea water and oceanic crust whose $\delta_{0,R} = +5.5$. The exchange occurs at $W/R = 0.2$. What will the isotope composition of the water and rock be?

**Answer**
At high temperature $\Delta = 0$; maintaining $g_r/g_w = 0.5$ gives $\delta_{rock} = +3.64$ and $\delta_{water} = +3.64$.

### Exercise

Let us imagine now that the water is driven out of the deep rock and rises to the surface and cools to, say, 200 °C. It attains equilibrium with the country rock and its minerals. If the rock contains feldspar, what will the isotope composition of the feldspar be?

**Answer**
At 100 °C, $\Delta_{feldspar-water} = 10$. Therefore the feldspar of the rock will have a $\delta$ value of $13.92 \approx +14$.

It can be seen from the water cycle in the previous exercise that hydrothermal circulation reduces the $\delta$ value of deep rocks and increases the $\delta$ value of surface rocks. (This is what is observed in ophiolite massifs.)

## 7.7 Paleothermometry and the water cycle: paleoclimatology

We have just seen how hydrothermalism can be studied by combining information on the isotope cycle of water and that of isotope fractionation. We are going to see how these two effects combine to give fundamental information on the evolution of our planet and its climate. After the initial impetus from **Cesare Emiliani** at Miami University and **Sam Epstein** at the California Institute of Technology, European teams have been the more active

ones in this field: for sediment paleothermometry, the teams from Cambridge and Gif-sur-Yvette; for glacial records, those from Copenhagen, Berne, Grenoble, and Saclay.

## 7.7.1 The two paleoclimatic records: sediments and polar ice

### Carbonate paleoclimatology

In order to use oxygen isotopes as a thermometer, we must, strictly, know the $\delta^{18}O$ values of two compounds in equilibrium: water and carbonate. The formula established by **Urey** and his team for the carbonate thermometer draws on $\delta^{18}O_{CaCO_3}$ and $\delta^{18}O_{H_2O}$. In a first approach, the Chicago team had considered that $\delta H_2O$, that is the $\delta$ of sea water, was constant over geological time and therefore that the $\delta^{18}O_{CaCO_3}$ measurement gave paleotemperatures directly. The discovery of extreme $\delta^{18}O$ values for Antarctic ice challenged this postulate. If the amount of Antarctic ice lost every year into the ocean varies, the $\delta^{18}O$ value of the ocean must vary too, since this ice may have $\delta^{18}O$ values as low as $-50$. In this case, the hypothesis of constant $\delta H_2O$ is untenable and it seems that temperatures cannot be calculated simply. On the other hand, if the dissolution of Antarctic ice in the ocean varies in volume, this phenomenon must be related to climate and therefore, to some extent, must reflect the average global temperature.

The first idea developed by **Emiliani** in 1955 was therefore to measure the $\delta^{18}O$ values of carbonate foraminifera in Quaternary sediment cores for which (glacial and interglacial) climatic fluctuations have long been known. Variations in isotope composition are observed (Figure 7.27) and seem to be modulated by glacial and interglacial cycles and more

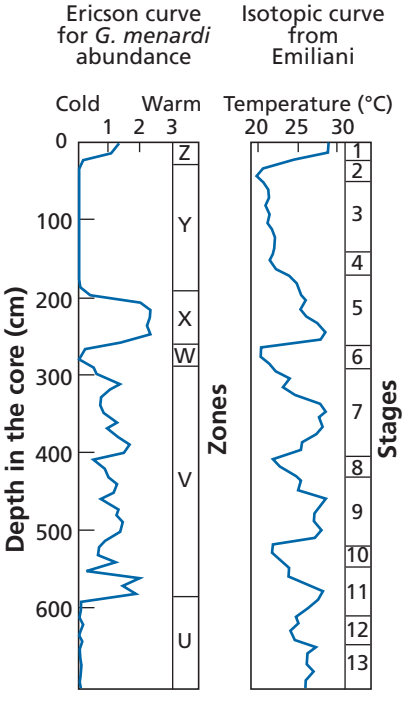


**Figure 7.27** The first isotope determination using $\delta^{18}O$ of Quaternary paleotemperatures by Emiliani (1955) compared with glacial–interglacial divisions by **Ericson**. (*Globorotalia menardi* is a foraminifer.)

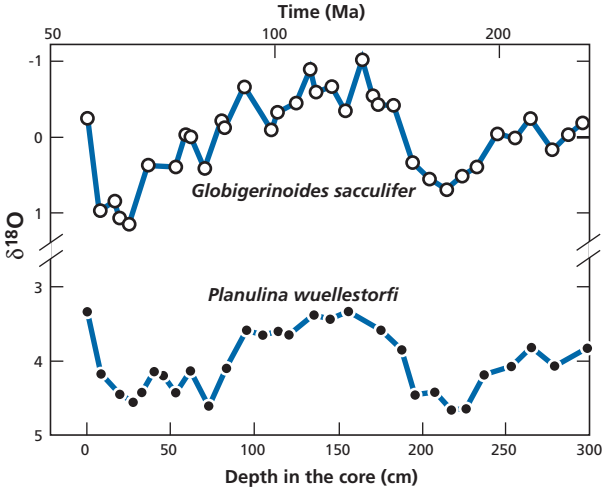


**Figure 7.28** Variation in $\delta^{18}O$ in samples of two species of foraminifer. Top: a pelagic (ocean surface) species. Bottom: a benthic (ocean floor) species. Modified after Duplessy *et al.* (1970).

specifically to follow the theoretical predictions of the Yugoslav astronomer **Milankovitch**. Are these variations a direct effect of temperature on (carbonate–water) fractionation or are they the effect of $^{18}O$ dilution by polar ice? The question remained unanswered. The formula:

$$T_{\circ C} = 16.9 - 4.2\left(\delta^{18}_{CaCO_3} - \delta^{18}_{H_2O}\right) + 0.13\left(\delta^{18}_{CaCO_3} - \delta^{18}_{H_2O}\right)^2$$

shows us that that two effects work in the same direction. When $T$ increases, ($\delta CaCO_3 - \delta H_2O$) fractionation decreases and so $\delta CaCO_3$ decreases if $\delta H_2O$ remains constant. If, with constant local $\Delta$ fractionation, $\delta^{18}_{H_2O}$ decreases for want of polar ice then $\delta^{18}_{CaCO_3}$ also declines. **Nick Shackleton** of the University of Cambridge suggested that the $^{18}O/^{16}O$ variations measured in forams were the result of fluctuations in the volume of polar ice, a climate-related phenomenon.

**Jean-Claude Duplessy** and his colleagues in the Centre National de la Recherche Scientifique (CNRS) at Gif-sur-Yvette had the idea of comparing $\delta^{18}O$ fluctuations of surface-living (pelagic) foraminifera and bottom-dwelling (benthic) foraminifera. It is known that the temperature of the deep ocean varies little around +4 °C.

In conducting their study they realized that $\delta^{18}O$ fluctuations of pelagic and benthic species were very similar (Figure 7.28). At most, extremely close scrutiny reveals an additional fluctuation of 2‰ in the $\delta^{18}O$ of pelagic species, whereas no great difference appears for the same comparison with $\delta^{13}C$. This means, then, that the $\delta^{18}O$ variations in foraminifera reflect just as much variation in the $\delta$ value of sea water as variations in local temperature. The signal recorded is therefore meaningful for the global climate (Emiliani, 1972).

In fact, more recent studies have confirmed that, for pelagic species, some 50% of the signal reflects a Urey-type local temperature effect (remember that when temperature rises $\delta^{18}O$ falls), above all in the temperate zones, and 50% the effect of melting of the polar ice

caps. For benthic species, the dominant factor is the isotopic fluctuation of the ocean as **Shackleton** (1967b) had surmised. In addition, **Duplessy**'s group and **Shackleton** established that an additional isotope fractionation occurred which was characteristic of each species of foraminifera studied. But those "vital effects" were calibrated and so isotopic measurements on different species could be made consistent with each other.

## Exercise

We have just seen that the $\delta^{18}O$ variation of foraminifera was mostly due to $\delta^{16}O$ variation because of melting ice. Let us look more closely at the quantitative influence of melting polar ice on $\delta^{18}O$. Imagine an intense glacial period when the sea level falls by 120 m. What would be the volume of polar ice and the $\delta^{18}O$ value of sea water?

### Answer

The ocean surface area is $3.61 \cdot 10^8$ km$^2$. The volume of the ocean is $1370 \cdot 10^6$ km$^3$. The volume of present-day polar ice is $29 \cdot 10^6$ km$^3$. If the sea level is 120 m lower, $46 \cdot 10^6$ km$^3$ has been stored in the ice caps, corresponding to a mass fraction of the hydrosphere of 3.3%. The polar ice caps were 1.6–2 times larger than today.

If we take the $\delta^{18}O$ value of ice as $-50‰$, then $-50‰ \times 0.033 = -1.65‰$. There is indeed a difference in $\delta^{18}O$ of this order of magnitude between glacial and interglacial periods. Notice that, as with radiogenic isotopes, these effects could not be detected if we did not have a very precise method for measuring $\delta^{18}O$.

## Glaciers

Another interesting application of this fractionation was begun on glaciers independently by **Samuel Epstein** of the California Institute of Technology and (more systematically and continuously) by **Willi Dansgaard** of Copenhagen University. When a core of polar glacier ice is taken, it has layers of stratified ice which can be dated by patient stratigraphy and various radiochronological methods. Now, the study of these ice strata reveals variations in $\delta^{18}O$ and $\delta D$ (Dansgaard, 1964; Epstein *et al.*, 1965; Dansgaard and Tanber, 1969) (Figures 7.29 and 7.30).

For a single region such variations are analogous and mean the sequence of one glacier can be matched with the sequence of a neighboring glacier. An isotope stratigraphy of glaciers can be defined. We can venture an interpretation of these facts in two ways. Either we accept that the origin of precipitation has varied over recent geological time and we then have a way of determining variations in the meteorological cycle of the past. Or we consider that the fractionation factor has varied and therefore the temperature has varied.

Research by **Dansgaard** and his team on the ice first of Greenland and then of Antarctica showed that **the temperature effect is predominant**. By simultaneously measuring isotope composition and temperature, he showed that the $\delta^{18}O$ and $\delta D$ correlation did indeed correspond to this effect. Moreover, the qualitative rule is the reverse of the carbonate rule: when the temperature rises, both $\delta^{18}O$ and $\delta D$ increase, because fractionation diminishes with temperature; but the $\delta$ values are negative and so move closer to zero (Figure 7.31). A simple empirical rule is that whenever the temperature rises by 1 °C, $\delta^{18}O$ increases by 0.7‰.

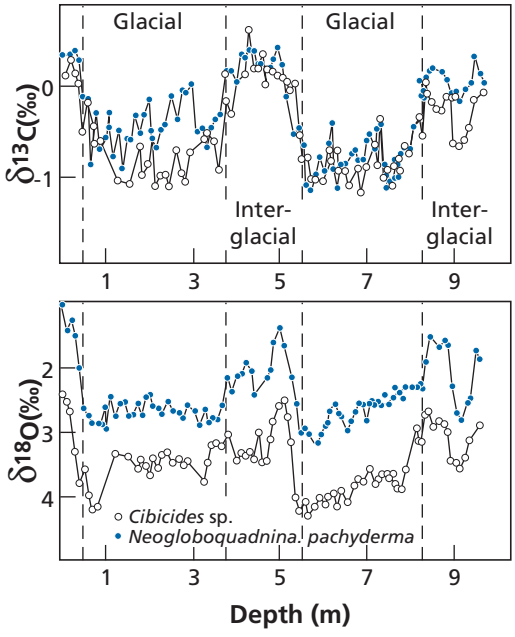


**Figure 7.29** Comparison of $\delta^{13}C$ and $\delta^{18}O$ fluctuations in a pelagic (blue circles) and a benthic (white circles) species of foraminifer from the Antarctic Ocean. The $\delta^{13}C$ variation (above) is represented to show there is a shift for $\delta^{18}O$ (below) but not for $\delta^{13}C$.

We can investigate why $\delta^{18}_{H_2O}$ fluctuation is very important for foraminifera and why it is the local temperature effect that dominates with ice. Because isotope fractionation at very low temperatures becomes very large and dominates isotope fluctuation related to the water cycle. But we shall see that this assertion must be qualified. Modern studies of isotope fluctuations of glaciers use a combination of both effects, local temperatures and isotopic changes in the water cycle, as for foraminifera, but with different relative weightings.

## 7.7.2 Systematic isotope paleoclimatology of the Quaternary

We have just seen there are two ways of recording past temperatures.

(1) One is based on $\delta^{18}O$ analysis of fossil shells in sedimentary series (marine and continental cores).
(2) The other uses $\delta^{18}O$ analysis of accumulated layers of ice in the ice caps.

Both these methods have progressively converged to allow very precise studies of climatic fluctuations in the Quaternary and more especially for the last million years. **Nick Shackleton** and **Willi Dansgaard** shared the Crafoord Prize in recognition of their complementary achievement. Each method has its limits, and it is only gradually that we have been able to compare and use both types of records in a complementary way to decipher climatic variations that have affected our planet over the last million years and which consist in alternating glacial and warmer interglacial periods.

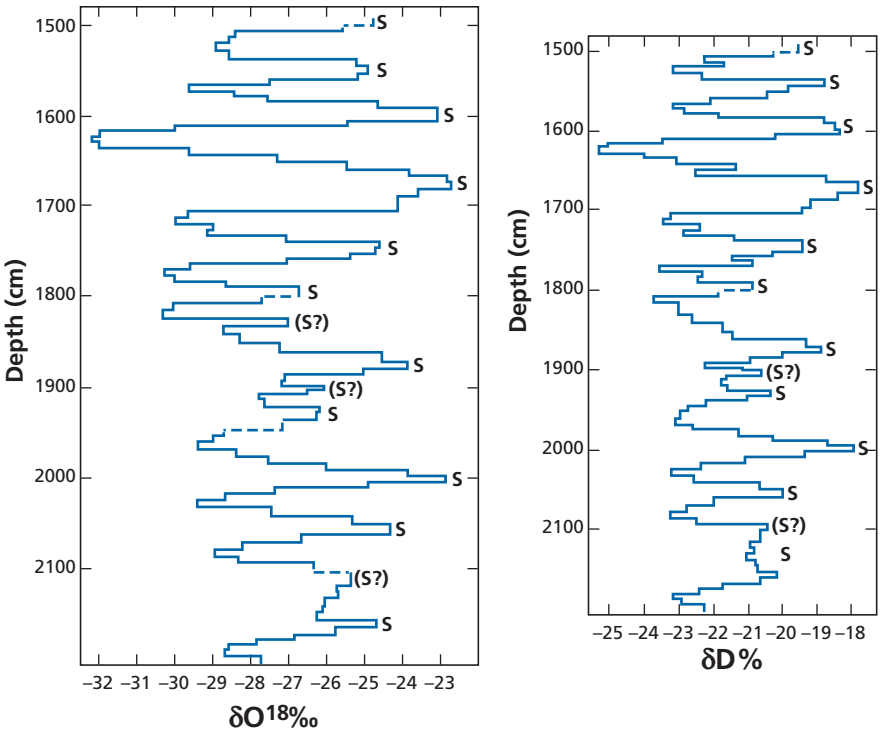


**Figure 7.30** Variations in $\delta^{18}O$ and $\delta D$ with depth in an Antarctic glacier. Summers (S) can be distinguished from winters. (Caution! $\delta D$ is in percent!) After Epstein and Sharp (1967).

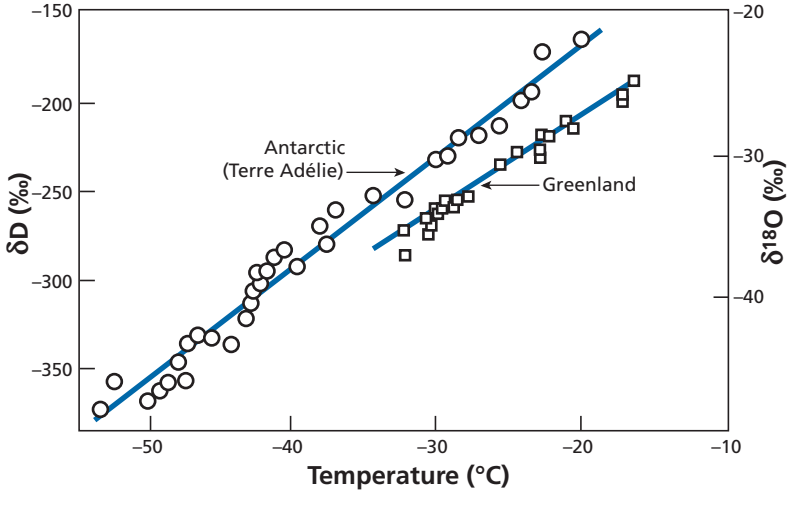


**Figure 7.31** Relationship between temperature, $\delta^{18}O$, and $\delta D$ in snowfall at the poles. After Lorius and Merlivat (1977) and Johnsen *et al.* (1989).

## Core sampling (sequential records)

Cores of marine sediments can be taken from all latitudes and longitudes (in the ocean and from continents and lakes); however, two conditions restrict their use. First, sedimentation must have occurred above the "carbonate compensation depth" for there to be any measurable fossil tests left. And second, sedimentation must have been very rapid to provide a record with good time resolution. Sedimentary cores have no time limits other than the lifespan of the ocean floor. Quaternary, Tertiary, and Secondary cores can be studied up to 120 Ma, which is the age of the oldest remnants of oceanic crust that have not been swallowed up by subduction (ancient cores are compacted and transformed into hard rocks and so time resolution is not as good).

For ice caps, the first problem is, of course, their limited geographical and temporal extent. Geographically, records are primarily from the glaciers of Antarctica and Greenland. Mountain glaciers have also recorded climatic events but over much shorter time-spans.[13]

Ice caps are limited in time. For a long time, the longest core was one from Vostok in Antarctica covering 420 000 years. A new core of EPICA has been drilled and covers 700 000 years. Cores from the big mountain glaciers go back a mere 2000 years or so. For both types of record – sediments and ice – precise, absolute dating is essential, but here again many difficulties arise. Especially because as research advances and as studies become ever more refined for ever smaller time-spans, the need for precision increases constantly. There is scope for $^{14}C$ dating and radioactive disequilibrium methods on sedimentary cores, but their precision leaves something to be desired. Useful cross-checking can be done with paleomagnetism and well-calibrated paleontological methods. In turn, the oxygen isotopes of a well-dated core can be used to date the levels of other cores. Thus, gradually, a more or less reliable chronology is established, which must be constantly improved. Dating is difficult on ice caps except for the most recent periods where annual layers can be counted. Methods based on radioactive isotopes such as $^{14}C$, $^{10}Be$, $^{36}Cl$, $^{87}Kr$, and $^{37}Ar$ are used, but they are extremely difficult to implement both analytically (ice is a very pure material!) and in terms of reliability. Switzerland's **Hans Oeschger** (and his team) is associated with the development of these intricate techniques for dating ice, which, despite their limitations, have brought about decisive advances in deciphering the ice record (Oeschger, 1982).

These clarifications should make it understandable that establishing time sequences of records is a difficult and lengthy job that is constantly being improved. All reasoning should make allowance for this.

## Deciphering sedimentary series and the triumph of Milankovitch's theory

Between 1920 and 1930, the Yugoslav mathematician and astronomer **Milutin Milankovitch** developed a theory to account for the ice ages that had already been identified by Quaternary geologists (see Milankovitch, 1941). These periods were thought to be colder. The polar ice extended far to the south and mountain glaciers were more extensive too (Figure 7.32). Alpine glaciers stretched down as far as Lyon in France. These glacial traces can be identified from striated rock blocks forming what are known as moraines.

[13] They have been used by **Lony Thompson** of Ohio State University for careful study of recent temperature fluctuations (see his 1991 review paper).

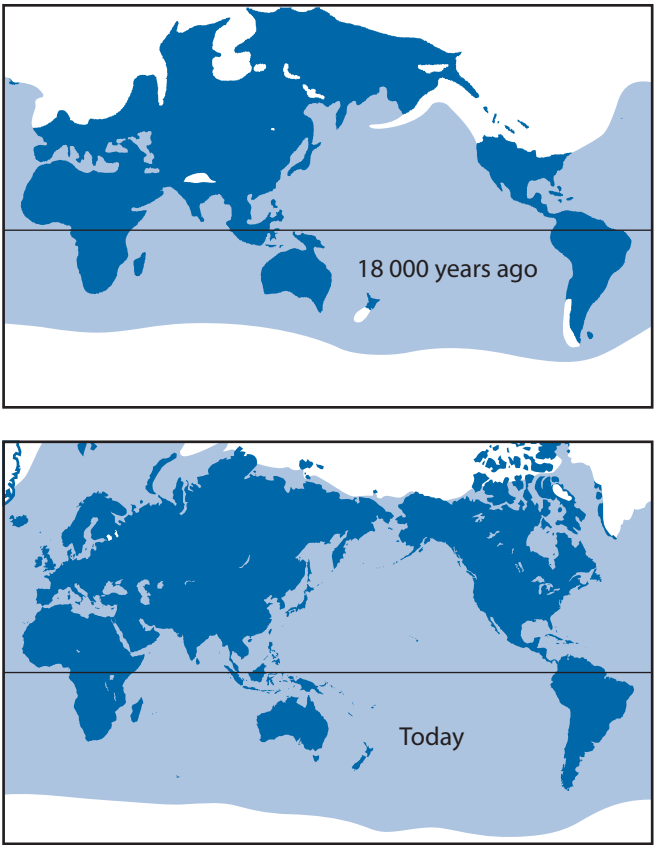


**Figure 7.32** Worldwide distribution of ice in glacial and interglacial times.

Milankovitch's theory gave rise to vehement controversy (as vehement as that over **Wegener**'s theory of continental drift[14]). And yet this vision of the pioneers of the 1920s was largely accurate. This is not the place to set out this theory in full. It can be found in textbooks on paleoclimatology, for example, Bradley (1999). However, we shall outline the main principles and the terms to clarify what we have to say about it.

The Earth's axis of rotation is not perpendicular to its plane of rotation around the Sun. It deviates from it by 23° on average. But the axis of this deviation rotates around the vertical over a period of 23 000 years. A further movement is superimposed on these, which is the fluctuation of the angle of deviation between 21.8° and 24.4°. The period of this fluctuation is 41 000 years. The first of these phenomena is termed **precession**, the second is **obliquity**. A third phenomenon is the variation in the **ellipiticity of the Earth's orbit**, with a period of 95 000 years. These three phenomena arise from the influence on the Earth of the Sun, Jupiter, and the other planets and the tides. They not only combine but are

[14] Wegener had been the first, with his father-in-law Köppen, to suggest an astronomical explanation for the ice ages before becoming an ardent defender of Milankovitch.

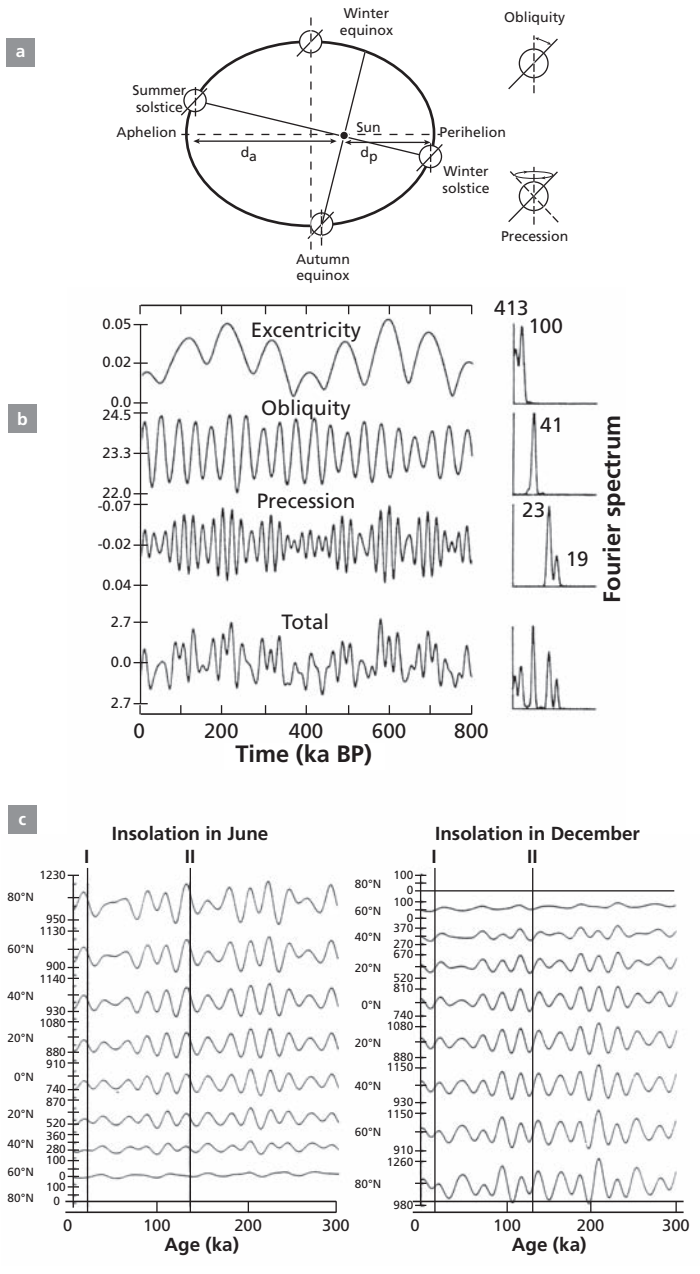


**Figure 7.33** The principle of Milankovitch's theory. (a) The three parameters that change: eccentricity of the orbit, obliquity, and precession. (b) Variations in the three parameters calculated by astronomical methods with their Fourier spectrum on the right. (c) Variation in the sunlight curves in June and December with latitude, calculated by the theory.

superimposed, leading to complex phenomena. Thus, at present, the Earth is closest to the Sun on 21 December, but the Earth's axis is aligned away from the Sun, and so, in all, the northern hemisphere receives little sunlight. It is winter there, but other conjunctions also occur. Thus we can calculate the sunshine received during the year at various latitudes. Celestial mechanics mean such calculations can be made precisely (see Figure 7.33 for a simplified summary). As Milankovitch understood, if little sunshine reaches the Earth at high latitudes in summer the winter ice will remain, the white surface will reflect solar radiation, and the cooling effect will be amplified. This is a good starting point for climatic cooling.

What should be remembered is that when we break down the complex signal of sunlight received by the Earth using Fourier analysis methods (that is, when we identify the sine-wave frequencies that are superimposed to make up the signal) we find peaks at 21 000, 41 000, and 95 000 years. When we conduct a similar Fourier decomposition for $\delta^{18}O$ values recorded by foraminifera in sedimentary series, we find the same three frequencies (Figure 7.34).

The $\delta^{18}O$ variations reflect those of the Earth's temperatures. This finding confirms Milankovitch's theory (at least as a first approximation) and so fully bears out the early studies of Emiliani. In complete agreement with the theory, the sedimentary series also showed that climatic variations were very marked at the poles (several tens of degrees), very low in the intertropical zone, and intermediate in the temperate zones (of the order of $\pm 5\,^{\circ}C$).

Figures 7.35 and 7.36 give a fairly complete summary of the essential isotopic observations made from sedimentary cores.

The sedimentary core record (Figure 7.35) also shows in detail how the temperature variations evolved. Cooling is slow, followed by sudden warming. Finer fluctuations are superimposed on these trends but their frequencies match those of the Milankovitch cycles.

## Confirmation of Milankovitch cycles by Antarctic isotope records

It was some considerable time before Milankovitch cycles were confirmed in the ice records, for two reasons. There were no ice cores long enough and so covering a long enough timespan and the dating methods were too imprecise.

It was only after the famous Vostok core from Antarctica was studied by the Franco-Russian team that evidence of Milankovitch cycles was found in the ice record. But the core yielded much more than that: it allowed climatic variations to be correlated with variations of other parameters:

- dust content: it was realized that during ice ages there was much more dust and therefore more wind than during interglacial periods.
- greenhouse gas ($CO_2$ and $CH_4$) content in air bubbles trapped in the ice – when the temperature increases there is an increase in $CO_2$ (in the absence of human activity!).

This last question on the debate about the influence of human activity on the greenhouse effect and so on climate is a fundamental one. Which increased first, temperature or $CO_2$ levels? It is a difficult problem to solve because temperature is measured by $\delta D$ in ice

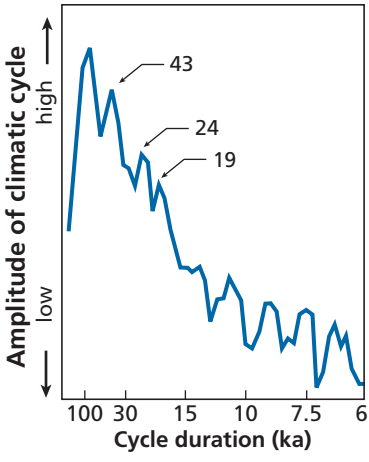


**Figure 7.34** Fourier spectrum of paleotemperatures using oxygen isotopes.

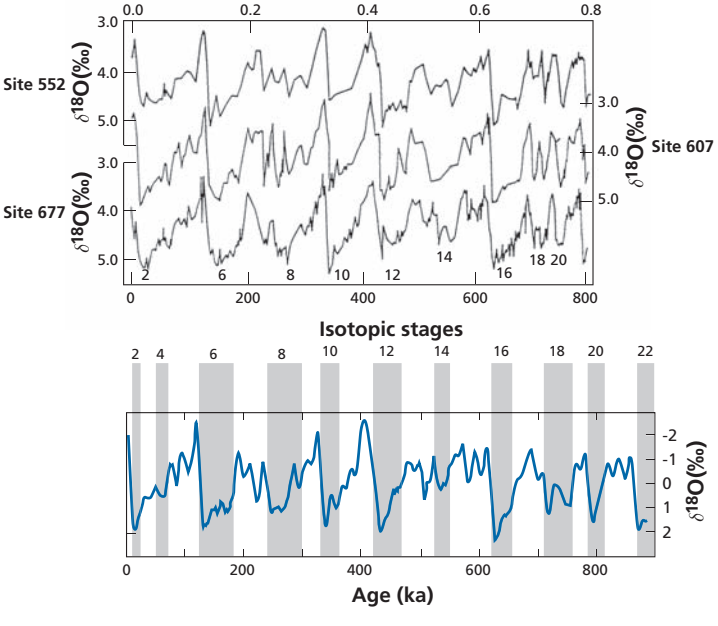


**Figure 7.35** Records of $\delta^{18}O$ in foraminifera and the synthetic reference curve. (a) Record of $\delta^{18}O$ for benthic foraminifera at three sites: site 552 – 56° N, 23° W in the North Atlantic; site 607 – 41° N, 33° W in the mid Atlantic; site 667 – 1° N, 84° W in the equatorial Pacific. Correlation between the three cores is excellent. (b) Synthetic reference curve produced by tuning, which consists in defining the timescale so that the Fourier decomposition frequencies of the $\delta^{18}O$ values of the cores match the astronomical frequencies from Milankovitch's theory. The period is then subdivided into isotopic stages. The odd stages are warm periods and the even stages (shaded) glacial periods. (Notice that the interglacials correspond to increased $\delta^{18}O$ values and fluctuations are just a few per mill.) After various compilations from Bradley (1999).

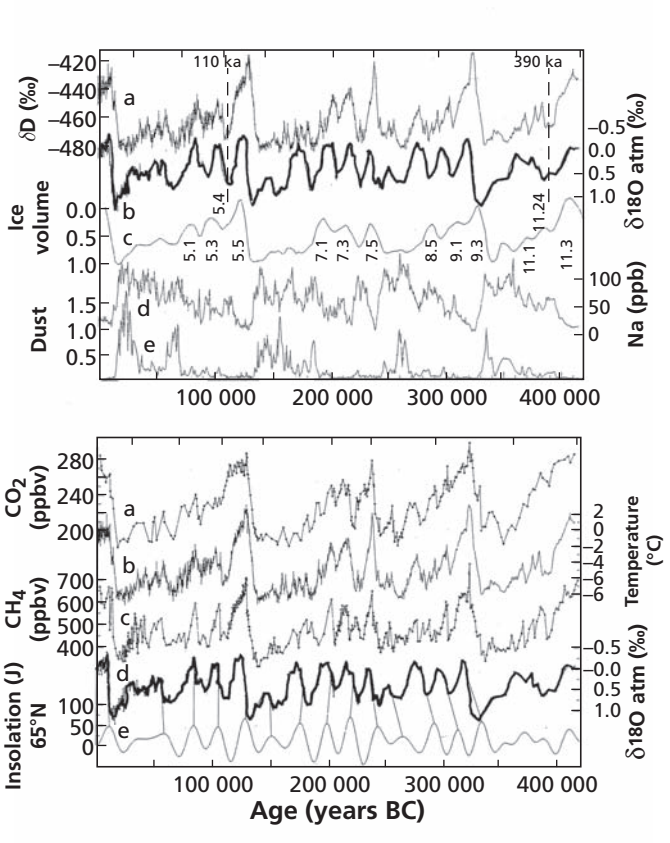


**Figure 7.36** Various parameters recorded in the Vostok ice core. After Jouzel *et al.* (1987) and Petit *et al.* (1999).

whereas $CO_2$ is measured from its inclusion in ice. Now, gaseous inclusions are formed by the compacting of ice and continue to equilibrate with the atmosphere, that is, the air samples are younger than the ice that entraps them (Figure 7.37).

We need, then, to be able to measure the temperature of inclusions directly and compare it with the temperature measured from the $\delta$D value of the ice. A method has been developed by **Severinghaus** *et al.* (2003) for measuring the temperature of fluid inclusions using $^{40}Ar/^{36}Ar$ and $^{15}N/^{14}N$ isotope fractionation. After stringent calibration, the teams at the Institut Simon-Laplace at Versailles University and at the Scripps Institution of Oceanography (La Jolla, California) managed to show that the increase in $CO_2$ lags behind the increase in temperature by 800 years (Figure 7.38) and not the other way round as asserted by the traditional greenhouse-effect model (Severinghaus *et al.*, 1999; Caillon *et al.*, 2003). Now, we know that $CO_2$ solubility in sea water declines as temperature rises and that the characteristic time for renewal of the ocean water is 1000 years. The first phase of temperature increase followed by the increase in $CO_2$, with a lag of 800 years, can be readily understood, then, if we invoke the lag because of the thermal inertia of the ocean. There may also be some feedback of the $CO_2$ effect on temperature.

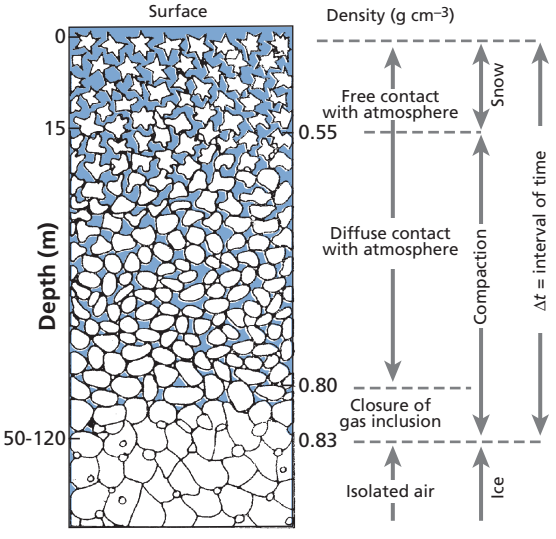


**Figure 7.37** As ice is compacted, the air trapped is younger than the snow.

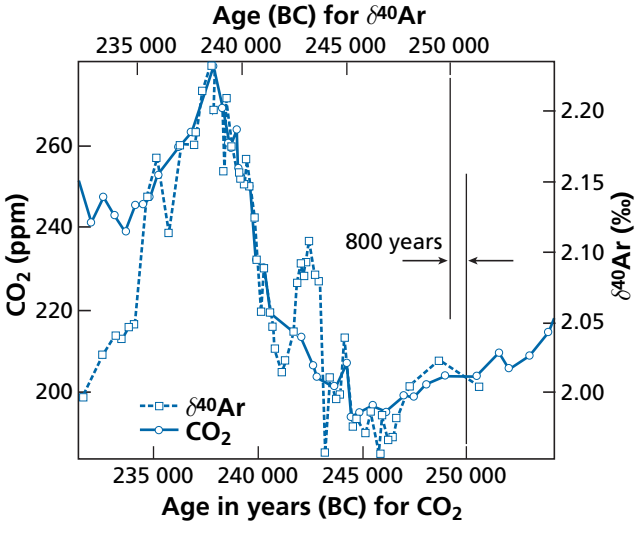


**Figure 7.38** Records of $\delta^{40}$Ar and $CO_2$ from the Vostok core after shifting the $CO_2$ curve 800 years backwards. After Caillon *et al.* (2003).

## Exercise

Argon and nitrogen isotope fractionations are caused by gravitational fractionation in the ice over the poles. Using what has been shown for liquid–vapor isotope fractionation, find the formula explaining this new isotope thermometer.

### Answer

If we write the fractionation:

$$\alpha = \frac{C_{m_1}\, P(1)}{C_{m_2}\, P(2)}$$

$$\ln \alpha = \ln P_{m_1} - \ln P_{m_2} = \Delta m \frac{gz}{RT}.$$

From the approximation formulae we have already met:

$$\frac{\Delta\delta}{1000} \approx \left(\Delta m \frac{gz}{RT}\right)$$

with $g = 10\ \text{m s}^{-1}$, $T = 200\ \text{K}$, for $z = 10\ \text{m}$, and $R = 2$.

This gives $\Delta\delta = 0.25$ for nitrogen and $\Delta\delta = 1.1$ for argon. Once again, extremely precise methods for measuring isotope ratios had to be developed.

## Greenland and Antarctica records compared and the complexity of climatic determinants

Although studies of Greenland ice cores pre-dated that of the Vostok core by far, it was only after the Vostok core had been deciphered that the signification of the Greenland cores was fully understood by contrast (Figure 7.39). It was observed that the record of the oxygen and hydrogen isotopes at Vostok was much simpler than in Greenland and that the Milankovitch cycles were clearly recorded.

Things are more complex in Greenland because sudden climatic events are superimposed on the Milankovitch cycles. The first well-documented event is a recurrent cold period at the time of transition from the last ice age to the Holocene reported by **Dansgaard**'s team in 1989. While some 12 800 years ago a climate comparable to that of today set in, it was interrupted 11 000 years ago by a cold episode that was to last about 1000 years and which is known as the Younger Dryas. This event was found some years later in the sedimentary record of the North Atlantic.

Generalizing on this discovery, Dansgaard used oxygen isotopes to show that the glacial period was interrupted by warm periods that began suddenly and ended more gradually. These events, of the order of a few thousand years, correspond to a 4–5‰ change in the $\delta^{18}O$ value of the ice and so to a temperature variation of about 7 °C. Dansgaard's team reported 24 instances of this type of D–O episode, as they are called (D is for Dansgaard and O is for Oeschger), between 12 000 and 110 000 years ago. They have been detected in the sedimentary records of the North Atlantic and as far south as the intertropical zone. Cross-referencing between sedimentary cores and polar ice cores has proved so instructive that both types of record continue to be used to analyze one and the same event.

A second series of events was read this time from the sedimentary records. These were brief events characterized by the discharge of glaciers as far as the Azores. There are 34 of these H events (see Heinrich, 1988) during the last glacial period and nothing comparable has been identified in the ice of Greenland. The relationship between D–O and H events is unclear, but what is clear is that they are not identical happenings.

What compounds the mystery is that these brief events are recorded very faintly in Antarctica, with a time lag. There are therefore one or more mechanisms governing climate

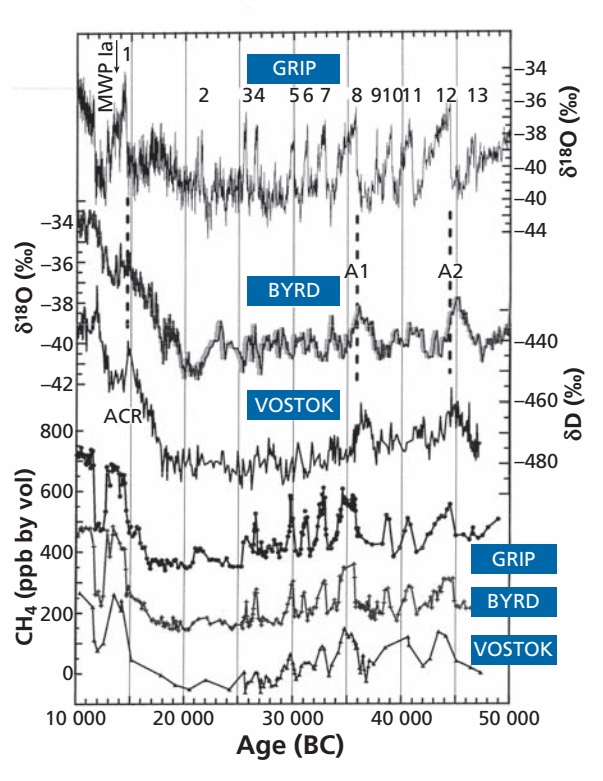


**Figure 7.39** Comparison of records from the Antarctic and Greenland. Vostok and Byrd are two stations in the Antarctic; Grip is a borehole in Greenland. Notice that the two $CH_4$ (methane) peaks are quite comparable in both hemispheres, which is evidence that chemically the atmosphere is broadly homogeneous. By contrast, the $\delta^{18}O$ (and $\delta D$) records are very different. Greenland is the site of many sudden climatic events that have been numbered, which events are not seen in Antarctica. After Petit *et al.* (1999).

that are superimposed on the Milankovitch cycles. Why are these events more readily detectable in the northern hemisphere? One of the big differences between the two hemispheres is the asymmetrical distribution of landmasses and oceans (Figure 7.40). This is probably an important factor, but how does it operate? We don't know. This qualitative asymmetry is compounded by a further asymmetry. It seems that the transitions between glacial and interglacial periods occur 400–500 years earlier in the Antarctic. Once again, there is as yet no clear and definite explanation for this.

## Exercise

When the $\delta^{18}O$ values of foraminiferan shells are analyzed for glacial and interglacial periods, variations are of 1.5‰ for cores from the intertropical zone but of 3‰ for cores from the temperate zones. How can you account for this phenomenon?

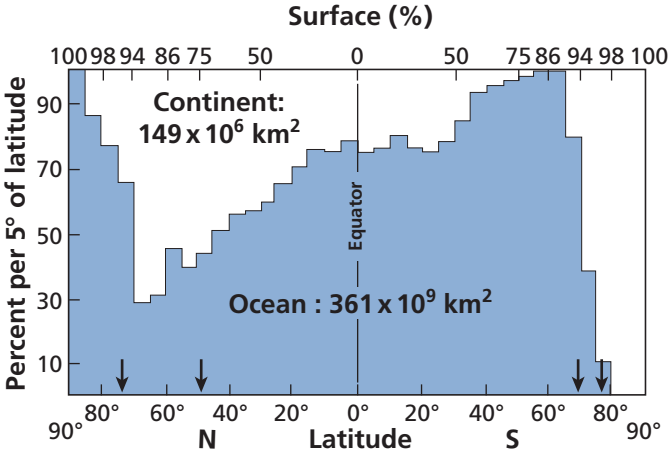


**Figure 7.40** Distribution of landmasses and continents by latitude. The difference between northern and southern hemispheres is clearly visible.

**Answer**

Temperature variations between glacial and interglacial periods are very large at the poles, very low in the intertropical zone, and intermediate in the temperate zones. The variation of 1.5‰ for the intertropical zone is caused by the melting of ice. It must therefore be considered that the additional variation of 1.5‰ of the temperate zones is due to a local temperature effect. Applying the Urey–Epstein formula of the carbonate thermometer

$$T_{°C} = 16.3 - 4.3(\Delta\delta)/0.13(\Delta\delta)^2$$

gives $\Delta T \approx 4.3\ \Delta\delta$. This corresponds to 5–6 °C, the type of temperature difference one would expect in the temperate zone between a glacial and interglacial period.

Very recently, the ice record has been extended to 700 000 years thanks to the core drilled by an international consortium in Antarctica at the EPICA site. As Figure 7.41 shows, this facilitates comparison between sedimentary and ice records. New data can be expected shortly.

## 7.8 The combined use of stable isotopes and radiogenic isotopes and the construction of a global geodynamic system

Climate is a complex phenomenon with multiple parameters. Temperature, of course, is a cardinal parameter, but the distribution of rainfall, vegetation, mountain glaciers, and winds are essential factors too. Oxygen and deuterium isotopes provide vital information about temperatures and the volume of the polar ice caps. The $^{13}C/^{12}C$ isotopes are more difficult to

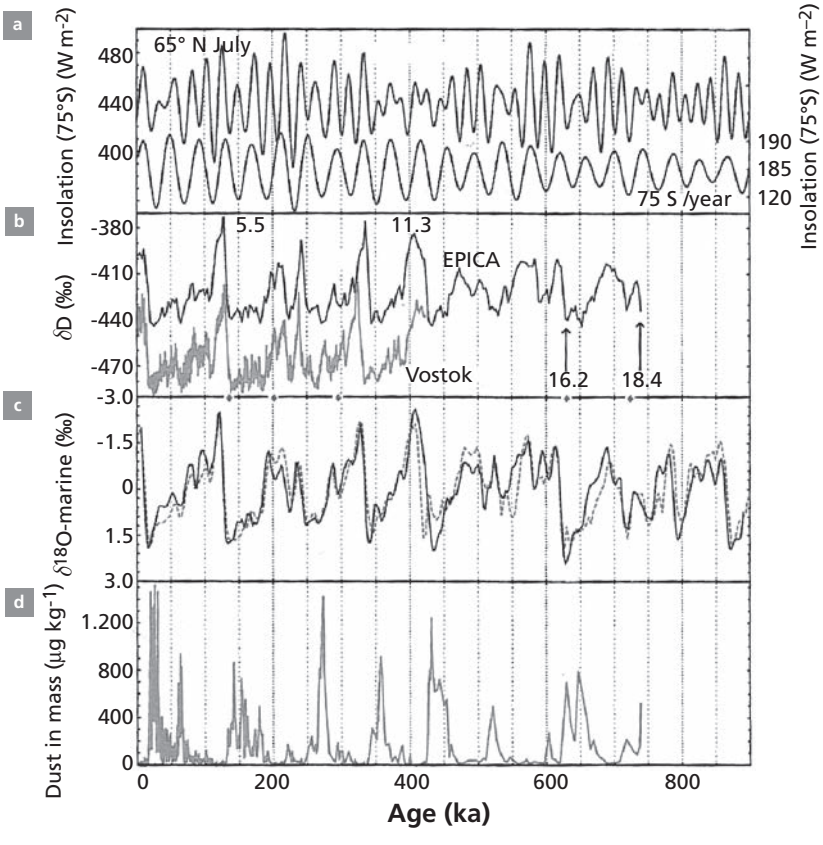


**Figure 7.41** Comparisons of (a) insolation and sedimentary (c) and glacial (b, d) records at the EPICA site. After the EPICA Community (2004).

interpret but yield useful pointers, for example, about the type of vegetation ($C_3/C_4$ plants) and its extent. But such information, which should in principle enable us to construct a biogeochemical picture, is still very difficult to decipher and has been oversimplified in the past.

The use of long-lived radiogenic isotopes has a similar objective, namely to determine how climatic fluctuations are reflected in the planet's erosional system. Erosion is a fundamental surface process. It is what changes volcanoes or mountain ranges into plains and peneplains. The end products of erosion are of two types. Some chemical elements are dissolved as simple or complex ions, while others remain in the solid state. The former are transported in solution, the latter as particles. Whichever state they are in, they are carried by rivers down to the oceans where they form sea water in one case and sediments in the other. The radiogenic isotope ratios are preserved throughout these erosion and transport processes. They are then mixed in the ocean, either as solutions in sea water or as particles in sediments. The erosion sites have characteristic radiogenic isotope signatures which distinguish old landmasses, young continents, and volcanic products of mantle origin. The isotopic compositions of the mixture that makes up sea water thus reflect the proportion of the various sources involved in the erosion processes.

## 7.8.1 Strontium in the ocean

A first example is the $^{87}Sr/^{86}Sr$ isotopic composition of present-day sea water. The $^{87}Sr/^{86}Sr$ ratio is 0.709 17 and is identical whichever ocean is considered. Where does the Sr come from? Obviously from the erosion of landmasses and subaerial or submarine volcanic activity. Measurement of the isotopic composition of Sr dissolved in rivers yields a mean value of $0.712 \pm 0.001$. The mean isotopic composition of the various volcanic sources (mid-ocean ridges, island volcanoes, and subduction zones) lies between 0.7030 and 0.7035 (depending on the relative importance attributed to the various sources). From the mass balance equation:

$$\left(\frac{^{87}Sr}{^{86}Sr}\right)_{\text{sea water}} = \left(\frac{^{87}Sr}{^{86}Sr}\right)_{\text{continental rivers}} x + \left(\frac{^{87}Sr}{^{86}Sr}\right)_{\text{volcanic input}} (1 - x).$$

The fraction from continental rivers corresponds to $66\% \pm 2\%$ of the Sr in sea water. (Notice this fraction $x$ reflects the mass of chemically eroded continent modulated by the corresponding absolute concentration of Sr.)

$$x = \frac{\dot{m}_c\, C_c}{\dot{m}_c\, C_c + \dot{m}_v\, C_v}$$

where $\dot{m}_c$ is the mass of continent eroded chemically per unit time, $\dot{m}_v$ is the mass of volcanoes eroded chemically per unit time, and $C_c$ and $C_v$ are the Sr contents of rivers flowing from continents and of volcanoes, respectively.

We can go a little further in this breakdown. The isotopic composition of Sr in rivers is itself a mixture of the erosion of silicates of the continental crust, whose mean isotopic composition we have seen is $^{87}Sr/^{86}Sr \approx 0.724 \pm 0.003$,[15] and the erosion of limestones, which are very rich in Sr and are the isotopic record of the Sr of ancient oceans. For reasons we shall be in a better position to understand a little later on, the mean composition of these ancient limestones is $^{87}Sr/^{86}Sr = 0.708 \pm 0.001$. The mass balance can be written:

$$\left(\frac{^{87}Sr}{^{86}Sr}\right)_{\text{rivers}} = \left(\frac{^{87}Sr}{^{86}Sr}\right)_{\text{limestones}} y + \left(\frac{^{87}Sr}{^{86}Sr}\right)_{\text{silicates}} (1 - y),$$

which means that limestones make up 71% of the Sr carried to the ocean in solution from the continents. Therefore, all told, the Sr of sea water is made up of 49.5% from reworked limestone, of 16.5% from the silicate fraction of landmasses, and of 34% from volcanic rock of mantle origin. Of course, these figures must not be taken too strictly. The true values may vary a little from these, but not the relative orders of magnitude.

The $^{87}Sr/^{86}Sr$ isotopic composition of present-day marine carbonates is identical to that of sea water in all the oceans. It is assumed, then, that the $^{87}Sr/^{86}Sr$ isotopic compositions measured on more ancient limestones were identical to those of the oceans from which they precipitated (Figure 7.42).

[15] Corresponding to the mean value of detrital particles transported by rivers.

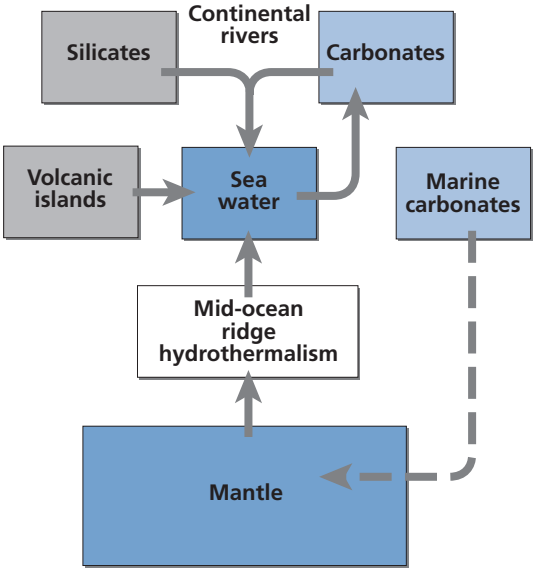


**Figure 7.42** The determining factors of the isotope composition of strontium in sea water. The strontium in the ocean comes from alteration of the continents and volcanic arcs. Hydrothermal circulation along the ridges also injects strontium into sea water. Limestones reflect the isotopic composition of the ocean at the time they formed. They are recycled either by erosion or by inclusion in the mantle.

These isotopic compositions have been studied and are found to have varied in the past. The curve of variation of strontium in the course of the Cenozoic has been drawn up with particular care (Figure 7.43).

It shows that the $^{87}Sr/^{86}Sr$ ratio was lower 65 Ma ago than it is today and remained roughly constant from 65 Ma to 40 Ma, from which date it began to rise, at varying rates, up to the present-day value. Why did these variations occur?

Returning to our fundamental mass balance equation, we must conclude that the growth in the ocean's $^{87}Sr/^{86}Sr$ ratio since 40 Ma can be attributed to a variation in the relative input of erosion from the landmasses or the input from the mantle, or both. Initially, a fierce conflict opposed proponents of the growth of continental input with mantle input supposedly remaining constant and their adversaries who thought that it was the mantle input that had varied along with the intensity of erosion. For the former, the predominant phenomenon was the uplift of the Himalayas after India collided with Asia 40 Ma ago (Raymo and Ruddiman, 1992). For the latter, the essential variation was in the activity of mid-ocean ridges in the form of the hydrothermal circulation occurring there (Berner *et al.*, 1983). Now, it was once thought that the total activity of the mid-ocean ridges had varied over geological time and in particular had declined since 40 Ma ago. We no longer think this. The idea today is that both changes are concomitant. The increased erosion because of the uplift of the Himalayas is consistent with reduced input from the mantle, which derives mostly from erosion of subduction zone volcanoes. Such erosion has been partially slowed by the disappearance of a significant source which was swallowed up in the Himalayan collision. All in all, then, it is the formation of the Himalayas that explains the $^{87}Sr/^{86}Sr$ curve as

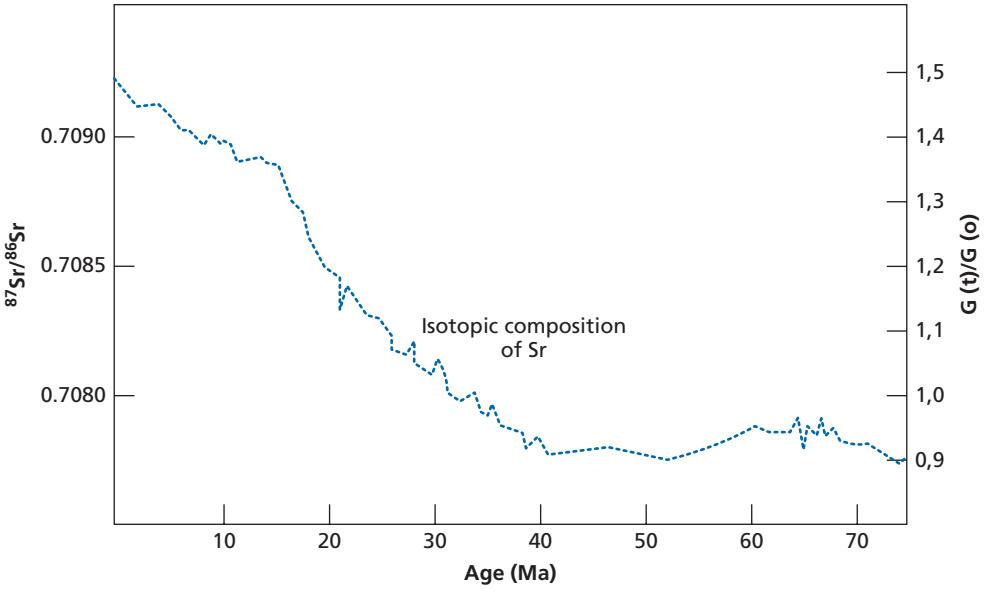


**Figure 7.43** Curve of evolution of the $^{87}Sr/^{86}Sr$ ratio in sea water in Tertiary times (Cenozoic).

suggested by the former Columbia team (Raymo and Ruddiman, 1992) and John Edmond (1992) from MIT independently.

Regardless of any causal explanations, the curve is nowadays used to date Cenozoic limestones. This is known as Sr stratigraphic dating. The idea is straightforward enough. Since the curve is identical for all the oceans, it is an absolute marker. As the variation in the $^{87}Sr/^{86}Sr$ curve is all one way, the measurement of an $^{87}Sr/^{86}Sr$ ratio for any limestone can be used to determine its age from the curve. As can be seen, this clock is effective from 0 to 40 Ma, but barely beyond that as the curve flattens out. The precision achieved for an age is $\pm 1$ Ma. This is a useful coupling with micropaleontological techniques.

But, of course, what everyone wants to know is why the $^{87}Sr/^{86}Sr$ ratio curve in limestones is identical whichever the ocean? The answer is that the residence time of Sr in the ocean is very much greater than its mixing time and so it has time to homogenize on a global scale. This will be explained in the next chapter.

The second question relates to climate. As it is observed that $\delta^{18}O$ increased throughout the Cenozoic, corresponding to a general cooling, what relation is there between tectonic activity and climate? This is a fundamental question to which there is as yet no clear answer.

## Exercise

There are two inputs to the isotope composition of continental rivers: one from silicates and one from carbonates, in the proportions of 75% from carbonates and 25% from silicates, with average isotope ratios of $(^{87}Sr/^{86}Sr)_{silicates} = 0.708$ for carbonates and $(^{87}Sr/^{86}Sr)_{limestone} = 0.724$ for

silicates. Suppose that carbonate recycling falls to 70%. How much will the Sr content of sea water vary assuming that the Sr content of rivers remains the same (which is unrealistic, of course)?

**Answer**

In the current situation, the Sr isotope ratio of rivers is 0.712 with 75% carbonate and 25% silicate. Recycled limestone has a Sr isotope composition of about 0.708 while that of silicates is 0.724. The composition for rivers with the new proportions becomes 0.7128, which gives a value of 0.709 52 for sea water. The recycling of limestone is clearly an important parameter, then.

## Exercise

Assuming the isotope different compositions and inputs remain constant and the flow from volcanic sources remains the same, by how much does the Sr flow from rivers have to vary to change the ocean values from 0.708 to 0.709?

**Answer**

The calculation is the same as before:

$$\frac{\Delta R}{R} = \frac{\Delta x}{(1-x)x}.$$

Therefore $\Delta F/F = +0.49$. So the flow from rivers must increase by 50%.

### 7.8.2 Isotopic variations of neodymium in the course of glacial–interglacial cycles

As with Sr, the isotopic variations of Nd are related to long-period radioactivity. When isotopic variations are measured in Quaternary sedimentary cores, these variations can be attributed to differences in origin alone. The *in situ* decay of $^{147}$Sm in the core has virtually no influence. The fundamental difference between the behavior of Sr and of Nd in the ocean is that Sr, having a long residence time (1 or 2 Ma), is isotopically homogeneous on the scale of the world's oceans whereas Nd, having a shorter residence time (500–2000 years), varies isotopically between oceans and even within oceans. For example, the $\varepsilon_{Nd}$ value today averages $-12$ for the Atlantic Ocean, $-3$ for the Pacific, and $-7$ for the Indian Ocean. These variations are interpreted by admitting that the Nd of sea water is a mixture between a volcanic source coming from subduction zones ($\varepsilon \approx 0$ to $+6$) and a continental source ($\varepsilon \approx -12 \pm 2$). The $\varepsilon_{Nd}$ value varies depending on the degree of volcanic activity in the region relative to continental input (see Goldstein and Hemming, 2003).

Study of a Quaternary core from the Indian Ocean, south of the Himalayas, has allowed the Paris laboratory (Gourlan *et al.*, 2007) to highlight an interesting phenomenon. The sedimentary core is mostly carbonated (more than 70% carbonate). By appropriate chemical treatment, it is possible to extract the Nd of ancient sea water trapped in the small coatings of Mn surrounding foraminifers. Isotopic analysis of the Nd shows that $\varepsilon_{Nd}$ varies from $-7.5$ to $-10.5$ and that the variations follow the pattern of $^{18}O/^{16}O$ fluctuation

corresponding to the glacial–interglacial pattern. There is an excellent (inverse) correlation between $\delta^{18}O$ and $\varepsilon_{Nd}$ (Figure 7.44).

South of the Bay of Bengal, the mixture of outflow from Indonesia and the input from the Rivers Ganga–Brahmaputra (but also the Irrawaddy and the Salween rivers) homogenizes the values of sea water of about $\varepsilon \approx -6 \pm 1$.

So we can suppose that in the Bay of Bengal the fluctuation during glacial–interglacial alternation corresponds to the fluctuation in the impact from the Ganga–Brahmaputra Rivers from the Himalayas. Those variations are linked with variations in intensity of the

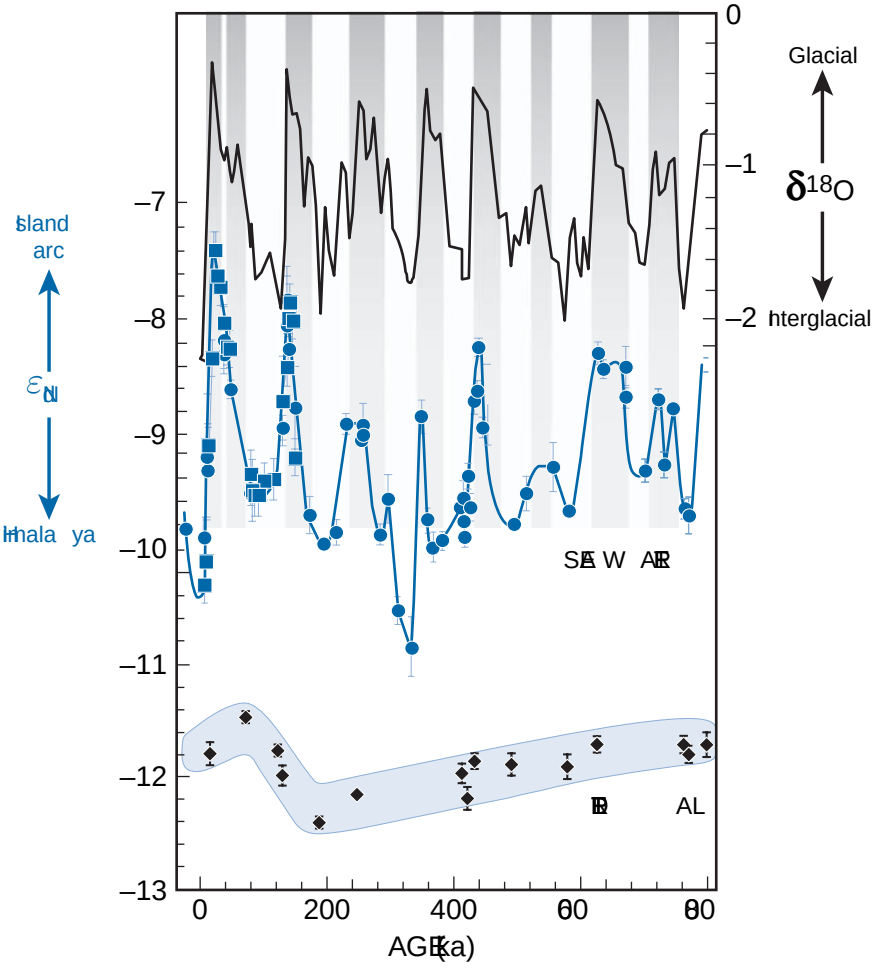


**Figure 7.44** Variation in the isotopic composition of neodymium in sea water expressed as $\varepsilon_{Nd}$ in a predominantly calcareous marine sedimentary core from the Ninety East Ridge in the Indian Ocean, representing the last 800 ka. Top: the curve of $\delta^{18}O$ variations allowing comparison of climatic fluctuations. Bottom: isotopic composition of the detrital fraction. (a) Oxygen isotopes compared with $\varepsilon_{Nd}$ variations. (b) Enlargement before 2 Ma. (c) Oxygen-neodymium maxima and minima correlations.

monsoon and the existence of large glaciers during glacial periods in the high Himalayas. Monsoons are weaker during glacial times and glaciers accumulate snow and then stop (or strongly reduce) the river runoff.

## Exercise

Calculate the relative input of the Ganges–Brahmaputra (GB) Rivers between interglacial and glacial if we suppose that $\varepsilon_{ND}^{GB} = -12$ and $\varepsilon_{Nd}^{ocean} = -6$. The measured ratios of concentration are $\varepsilon_{Nd} = -10$ during interglacials and $\varepsilon_{Nd} = -7.5$ during glacials, the concentration of Nd in river and ocean staying the same during all periods.

### Answer

We applied the mixing formula. Notating concentration as $C_{Nd}$ and the masses as $m$, we have:

$$\varepsilon_{Nd}^{measured} = \varepsilon_{Nd}^{GB} x + \varepsilon_{Nd}^{ocean}(1 - x)$$

$$x = \frac{\text{mass of fresh water} \cdot C_{Nd}^{river}}{\text{mass ocean} \cdot C_{Nd}^{ocean} + \text{mass of fresh water} \cdot C_{Nd}^{river}}.$$

With a little manipulation

$$\frac{m_{river}}{m_{ocean}} = \frac{C_{Nd}^{ocean}}{C_{Nd}^{river}} \left( \frac{1}{x^{-1} - 1} \right).$$

So for the ratios between interglacial (i) and glacial (g):

$$\frac{m_{river}^{i}}{m_{river}^{g}} = \left( \frac{x_g^{-1} - 1}{x_i^{-1} - 1} \right) = \frac{3}{0.5} = 6.$$

The river flux from the Himalayas was 6 times higher in interglacial than in glacial times.

This is a simple example in a work in progress in author's laboratory to illustrate the power of investigation of combining O and Nd isotopes.

# 7.9 Sulfur, carbon, and nitrogen isotopes and biological fractionation

We give two examples of how stable isotope geochemistry can be used in various types of study.

## 7.9.1 A few ideas on sulfur isotope fractionation

When we examine the $^{34}S/^{32}S$ composition of naturally occurring sulfur isotopes as a function of their geological characteristics, several features stand out. All sulfides associated with basic or ultrabasic rocks have extremely constant compositions close to

$^{34}S/^{32}S = 0.045$ ($\delta = 0$), that is, largely analogous to that of sulfur in meteorites (Nielsen, 1979).

Sulfur mineralization in veins crossing geological structures, with a gangue of quartz, fluorite, or barite, have $\delta$ values of about 0 which are very constant. It is therefore legitimate to attribute a deep origin to them or at least an origin related to deep-lying rocks. Cluster mineralization exhibits much more variable compositions, particularly mineralization related to sedimentary strata. Its composition may range from $\delta = +22$ to $\delta = -52$. This observation is tied in with the point that oxidation–reduction reactions $S^{2-} \Leftrightarrow SO_4^{2-}$ are accompanied by equilibrium isotope fractionation which, at low temperatures, is substantial (1.075 at 25 °C) (Tudge and Thode, 1950). Moreover, $S^{2-} \rightarrow SO_4^{2-}$ is an easy reaction at low temperature. However, reduction can only occur through *Desulfovibrio desulfuricans* bacteria. This bacterial reduction is accompanied by an isotopic effect that is weaker than the equilibrium reaction ($\alpha = 1.025$ at 25 °C) (Harrison and Thode, 1958). Remembering that sulfates of sea water and fresh water have $\delta^{34}S$ values that range from +26 to +4, we can explain the dispersion observed by assuming that the sulfides related to strata derive from bacterial reduction of sulfates, but that such reduction exhibits a number of variations. Sometimes reduction may involve sea water, sometimes groundwater circulation. Sometimes it occurs in replenished systems, sometimes in bounded reservoirs (Rayleigh distillation). Sometimes it is followed by isotope exchange leading to equilibrium fractionation, sometimes not. Here we find, but in a different context, variations in scenarios similar to what was calculated for bacterial reduction in sediments.

In any event, case by case, the sulfur isotope composition, associated with metallogenic and geological observations, allows distinctions to be drawn between the various types of deposits (Figure 7.45) and then allows the potential mechanism for the origin of mineralization to be limited. Generally, these data have made it possible to assert the occurrence of sulfur mineralization of exogenous origin, which many workers had contested before, claiming that all mineralization derived from the depths of the planet through mineralizing fluids (Ohmoto and Rye, 1979).

One particularly fascinating observation with sulfur isotope geochemistry relates to mass-independent fractionation (MIF). Such fractionation has been mentioned for oxygen, but it exists for sulfur too. Sulfur has four isotopes: $^{32}S$, $^{33}S$, $^{34}S$, and $^{36}S$. In terrestrial sulfur compounds variations in $^{33}S/^{32}S$ ratios account for about half of $^{34}S/^{32}S$ fractionations (0.515 to be precise). If we define $\Delta^{33}S = (\delta^{33}S) - 0.515\,(\delta^{34}S)$, this difference is generally zero. When measuring the isotopic composition of sulfides and sulfates of geologically varied ages, we obtain an unusual result. Between 2.30 Ga and the present day, $\Delta^{33}S = 0$. For samples of 2.30–2.60 Ga, $\Delta^{33}S$ varies with an amplitude of 12‰. For older samples, fluctuations are smaller but around 4‰. Samples of barium sulfate are depleted in $^{33}S$ (compared with "normal" fractionation, their $\Delta^{33}S$ is negative). Sulfide samples are enriched in $^{33}S$ (their $\Delta^{33}S$ is positive). This observation cannot be easily interpreted. **James Farquhar** and his team think that there was little oxygen in the atmosphere in ancient periods. The ozone layer surrounding the Earth at an altitude of 30 km and which now filters the Sun's ultraviolet rays did not exist. Sulfur reduction phenomena shifted sulfur from the degree of oxidation −2 (sulfide) to +6 (sulfate) via a cycle of photochemical reactions involving these ultraviolet rays. Now, laboratory experiments show that photochemical reactions (that

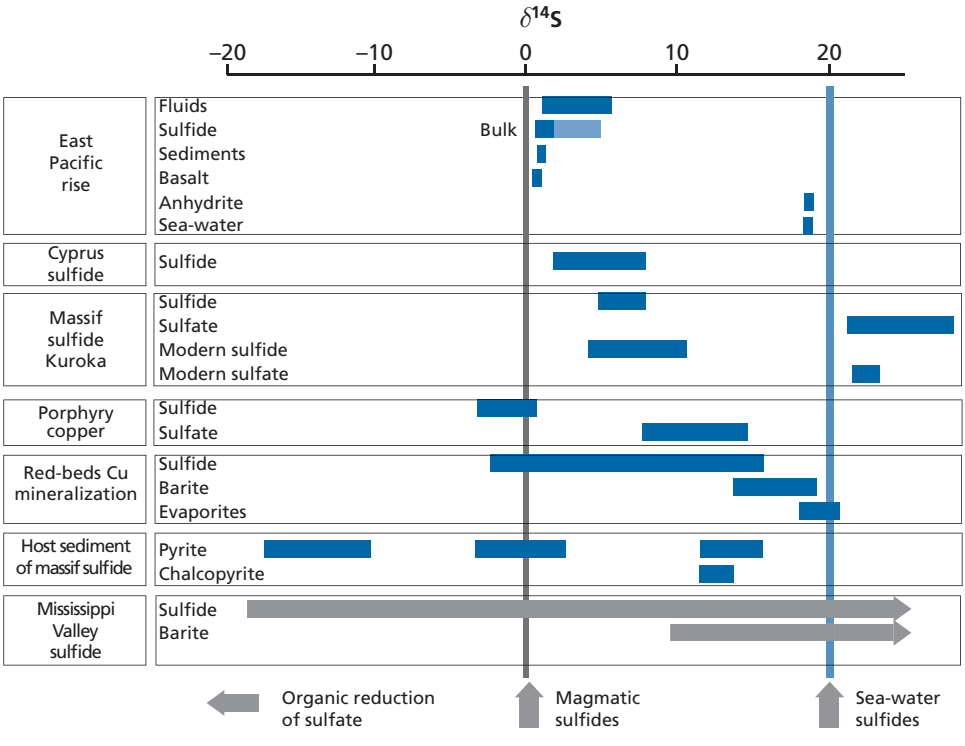


**Figure 7.45** Distribution of sulfur isotopes in the main sulfur-bearing deposits.

is, reactions taking place under the influence of light) produce important non-mass-dependent fractionations (Farquhar *et al.*, 2007).

This idea of oxygen being absent from the ancient atmosphere is consistent with many geochemical observations: the presence of detrital uranium in the form of $UO_2$ in ancient sedimentary series and particularly in the famous Witwatersrand deposits of South Africa. Uranium in its degree of oxidation +4 is insoluble whereas in the +6 form, it forms soluble complex ions. Today uranium is mostly in the +6 state (in solution), but in the Archean it was in the +4 state (as detrital minerals) . Until 2 Ga, very special rich iron deposits are found, known as banded hematite quartzite or banded iron formation (BIF). These are evidence that at that time rivers carried soluble iron in the +2 oxidation state and that it precipitated in the +3 oxidation state on reaching the ocean. Nowadays, surface iron is in the +3 oxidation state and forms insoluble compounds in soils. These iron compounds give tropical soils their characteristic red coloring.

**Dick Holland** (1984) has long used these observations to argue that the ancient atmosphere was rich in $CO_2$ and $N_2$ (as are the atmospheres of Mars and Venus today) and that oxygen, which makes up 20% of our atmosphere today, appeared only 2 Ga ago as a consequence of the superactivity of bacteria or of photosynthetic algae. The appearance of oxygen meant the end of both detrital uranium and chemical iron deposits, which, in fact, are not found after that period. Observations of sulfur isotope

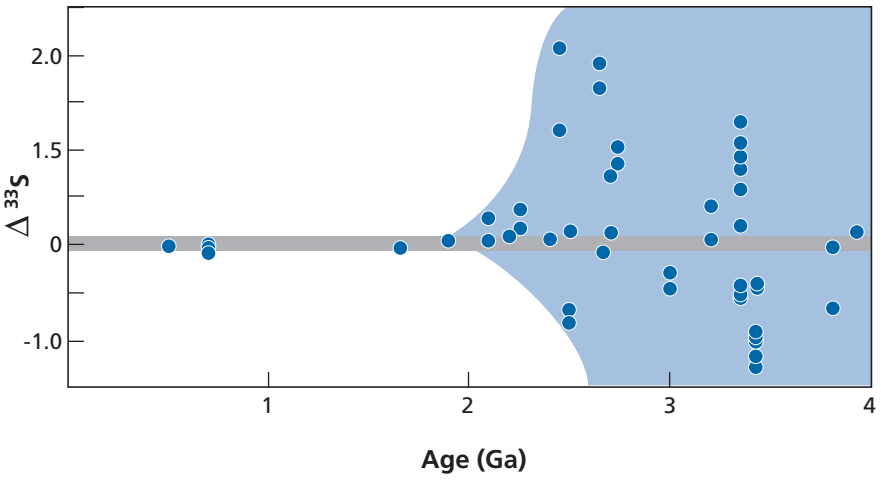


**Figure 7.46** $\Delta^{33}S = (\delta^{33}S) - 0.515\ (\delta^{34}S)$. The figure shows $^{33}S$ variation in $\Delta^{33}S$ of sulfides and sulfates of various ages.

fractionations by **Thiemens**'s team refine this model. They seem to indicate that the growth of oxygen in the atmosphere occurred very quickly, almost suddenly, between 2.5 and 2.1 Ga and that this growth was accompanied by the progressive formation of the ozone layer protecting the Earth's surface from excessive solar ultraviolet radiation (Figure 7.46).

## 7.9.2 Carbon–nitrogen fractionation and the diet of early humans

Biochemical operators fractionate carbon and nitrogen isotopes. Gradually the mechanisms and the practical rules such fractionation obeys have been determined. Thus, it was correctly predicted that $C_3$ plants (the first product of photosynthesis with three carbon atoms) (trees, wheat, and rice) fractionate differently from $C_4$ plants (corn, grass, sugar cane). It has also been shown that marine plants are different again. From these observations **Michael DeNiro** of the University of California at Los Angeles studied the isotope composition of herbivores (eating the various types of plant) and of carnivores eating those herbivores. Oddly enough, a number of regularities were preserved and turned up in the isotope composition of bone (in the mineral matter and also in collagen which withstood decay quite well). He was thus able to determine what early humans ate (Figure 7.47). Those of the Neolithic ate $C_3$ plant leaves and then people later certainly began to eat corn ($C_4$). Wheat does not seem to have been grown until much later. This is an example of isotope tracing which is developing in biology and archeology. Stable isotopes measured on bone and tooth remains of extinct animals can be used to answer questions about the type of metabolism of certain dinosaurs (hot or cold blooded), the diet of extinct animals, or the effect of paleoclimate on the cellulose of tree rings. Once again this discipline offers considerable prospects.

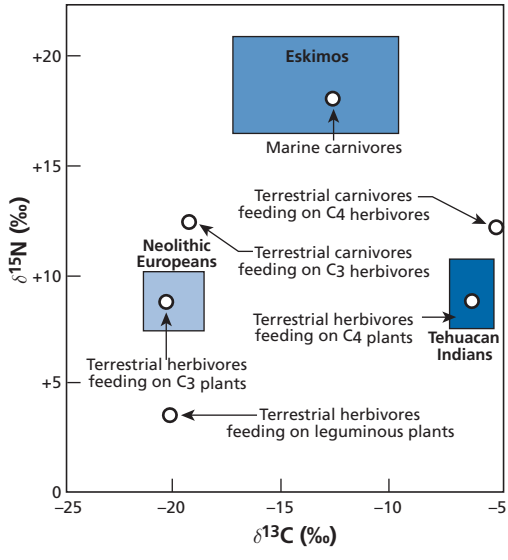


**Figure 7.47** Isotopic composition of fossil plants, animals, and humans in the $\delta^{15}$N and $\delta^{13}$C diagram. After DeNiro (1987).

## 7.10 The current state of stable isotope geochemistry and its future prospects

As has been repeated incessantly throughout this book, developments in isotope geology have always tracked advances in measurement methods, which themselves are often the consequence of technological progress. The development of the double-collection mass spectrometer by **Nier** and his collaborators (Nier, 1947; Nier *et al.*, 1947) made it possible to study the effects of very weak isotopic fractionation (oxygen, hydrogen, carbon, and sulfur) in carbonates, water, rock, and living matter.

Since then technical advances have moved in three directions. The first was that of sensitivity. It has become possible to analyze isotopic fractionation on small quantities of material. **Hugh Taylor** managed to analyze D/H in rocks while **Françoise Pineau** and **Marc Javoy** have analyzed $^{13}C/^{12}C$ and $^{15}N/^{14}N$ in basalts.

The second direction was that of precision. In 1950, ratios could be measured to 0.5‰. Now the figure is 0.05‰. This has made it possible to analyze sedimentary cores with precision and to highlight Milankovitch cycles. **Robert Clayton** was able to discover paired $^{17}O/^{16}O$ and $^{18}O/^{16}O$ fractionations of meteorites, which had many consequences for the study of meteorites even if the initial interpretations have been modified. **Mark Thiemens** has been able to move on from there to open up the study of mass-independent fractionation.

The third advance has been the automation of analytical procedures which has enabled large numbers of samples to be studied both in sedimentary carbonates and in polar ice for O, C, and H isotopes. Climatology has gained enormously from this.

Today two new technical advances have occurred: multicollection ICPMS and the development of *in situ* probes, ion probes, or ICPMS laser ionization. In addition, advances

in computing and electronics have brought progressive gains in precision, sensitivity, and measurement time for all conventional techniques, TIMS, or double-collection gas spectrometry.

What will come of all this? It is probably too early to answer this question but the trends as perceived can be set out. The most spectacular trend is probably the rush to study isotopic fractionation of "non-classical" elements that are often present in terrestrial materials. These include some major elements (Si, Mg, Fe, or Ca) for which physicochemical fractionations have been identified and then minor light elements like B and Li and minor heavy elements like Cr, Cu, Zn, Cd, Se, Mo, or Tl (the list is not exhaustive) (see the review edited by Johnson *et al.*, 2004). It is undeniable that some interesting results have been obtained for the major elements Mg, Fe, Ca, and Si as well as for B, Li, Cu, Mo, Tl, and Cl. For trace elements, no result has as yet allowed new tracers of geological phenomena to be introduced, as is the case for the isotopes of the major elements H, O, C, and S. Analyses are difficult, the results are often uncertain, and approaches are not systematic enough. These attempts have not achieved the results expected. The present author thinks, but this is open to question, that the most interesting processes are:

- first in biogeochemistry. It seems that living organisms fractionate some isotopes: Ca for the food chain ending with shells, Si for the food chain ending with diatoms, Cu for cephalopods. This, combined with C, N, and S geochemistry, may be the advent of the famous biogeochemistry we have been waiting for since Vernadsky's 1929 book!
- then, for pH conditions boron is a hope, provided the hypothesis of constant $\delta^{11}B$ for the ocean over geological time is eliminated. The degree of oxidation–reduction with the use of iron isotopes and molybdenum isotopes is also relevant. We shall review this if this book runs to a new edition!

The other trend is illustrated by **John Eiler**'s program at the California Institute of Technology. He is trying to take advantage of the improvement in techniques of analysis of traditional elements to develop new and original methods, the most spectacular of which is intercrystalline order–disorder fractionation, which we have spoken of, but also for $^{18}O/^{16}O$ or D/H fractionations in high-temperature phenomena.

The study of non-mass-dependent fractionation by **Mark Thiemens**'s team has probably still not yielded all its results but perhaps requires a more structured approach.

## Problems

**1** Take a cloud that evaporates at the equator with a mass $M_0$ $\delta_{H_2O} = 0$ for D and $^{18}O$ (to simplify). It moves polewards and when the temperature is $+10\,^{\circ}C$ loses one-third of its mass as rain and continues in the same direction. In the cold zone, where the temperature is $0\,^{\circ}C$, it loses one-third of its remaining mass. It moves on and loses another one-third of its remaining mass at $-20\,^{\circ}C$. When it reaches temperatures of $-30\,^{\circ}C$ it loses a further one-third of its mass. The fractionation factors at three temperatures are given in Table 7.4 below.

**Table 7.4** Fractionation factors

| $T$ (°C) | $\alpha_D$ | $\alpha_{^{18}O}$ |
|---|---|---|
| +20 | 1.085 | 1.0098 |
| 0 | 1.1123 | 1.0117 |
| −20 | 1.1492 | 1.0411 |

(i) Calculate the $\delta$D and $\delta^{18}$O composition of the rain and snow.
(ii) Plot the ($\delta$D, $\delta^{18}$O) curve and calculate its slope.
(iii) Plot the $\delta$D and $\delta^{18}$O curves as a function of the remaining fraction of the cloud.

**2** Take a magma chamber whose magma has an initial $\delta^{18}$O isotope composition of +5.5. Some 30% of olivine $Mg_2SiO_4$ precipitates in the chamber. Then we precipitate a eutectic mixture with equal proportions of olivine–pyroxene. We precipitate 30% of the remaining melt and then the olivine, orthopyroxene, and plagioclase mixture in equal proportions for 20% of the remaining melt. Given the melt–silicate partition coefficients in Table 7.5 below, calculate the isotope evolution of the melt and the minerals.

**Table 7.5** Partition coefficients

| Plagioclase–melt | Olivine–melt | Pyroxene–melt |
|---|---|---|
| − 0.6‰ | − 0.2‰ | − 0.3‰ |
| $\alpha = 0.9994$ | $\alpha = 0.9998$ | $\alpha = 0.9997$ |

**3** Consider rainwater with $\delta_D = -70$‰. This water penetrates into the ground and finally reaches a metamorphic zone where it meets a schist whose proportion relative to water is 15% and whose composition is O = 53.8%, Si = 33.2%, Al = 7.8%, Fe = 2.8%, Ca = 7.1%, Na = 0.6%, K = 1.5%, and C = 1.8%. This schist contains the following minerals which equilibrate with water at 550 °C in a closed system. The composition of the rock is: 40% quartz, 4% magnetite, 16% plagioclase, 15% muscovite, 20% alkali feldspar, and 5% calcite. Calculate the oxygen isotope compositions of the minerals and the water in the end.

**4** The $CO_2$ content of the recent atmosphere is 320 ppm, its $\delta^{13}$C value is −7. As a result of burning of coal and oil the $\delta^{13}$C value has shifted from −7 to −10 in 20 years.
(i) Given that $\delta^{13}C_{oil} = -30$, what quantity of carbon has been burned?
(ii) However, a problem arises. The $CO_2$ content of the atmosphere is 330 ppm. How can you explain this?
(iii) Suppose the $\alpha_{calcite-CO_2}$ fractionation at 20% is 1.0102. What is the variation observed in the $\delta$ value in the calcites precipitating in sea water?
(iv) Does the $\delta^{13}$C isotope analysis of limestone seem to you a good way of testing $CO_2$ degassing in the atmosphere by human activity? Mass of the atmosphere: $5.1 \cdot 10^{21}$ g.

**5** Basalt magma contains sulfur in the form $S^{2-}$ (sulfide) and $SO_4^{2-}$ (sulfate), whose proportions vary with oxygen fugacity.

$$S^{2-} + 2\,O_2 \Leftrightarrow SO_4^{2-}$$

$$\frac{[S^{2-}][O_2]^2}{[SO_2]} = K(T).$$

Therefore:

$$\frac{S^{2-}}{SO_4^{2-}} = \frac{K(T)}{[O_2]^2}.$$

When the magma degasses, it loses almost exclusively its $SO_2$ and the $H_2S$ content is usually negligible (even if it smells). Determine the partition $\Delta_{gas-magma} = (\delta^{34}S)_g - (\delta^{34}S)_m$. Given that the magma contains $S^{2-}$ and $SO_4^{2-}$, show that degassing of the magma leads to an increase in the $\delta^{13}S$ value of the solidified magma or to a decrease depending on oxygen fugacity (after Sakaï *et al.*, 1982). (We know that $\Delta_{S^{2-}}^{SO_2} = +3$ and $\Delta_{S^{2-}}^{SO_4^{2-}} = +7$.)

**6** Various scenarios are imagined in which the temperature of the Earth reaches extremes. The first scenario, known as the snowball scenario, says that all the landmasses are covered by a layer of ice 100 m thick in addition to the present-day polar ice which has doubled in volume. The second, reverse, scenario says that the Earth has heated and the polar ice caps melted. In the first scenario the $\delta^{18}O$ of continental ice is supposed to reach $-30$, with the polar ice caps being like today at $-50$. The ocean is at $\delta = 0$.

(i) What is the $\delta$ value of sea water in the snowball scenario?
(ii) In the scorching Earth scenario, what is the $\delta$ value of sea water?
(iii) Examine each scenario. Calculate the rate of increase (or decrease) of $\delta^{18}O$ in meters above sea level.
(iv) Does this figure vary with the speed of the process?

CHAPTER EIGHT

# Isotope geology and dynamic systems analysis

We have seen that the Earth can be subdivided into five main reservoirs:

(1) the **continental crust**, where elements extracted from the mantle are stored (K, Rb, U, Th, rare earths, etc.) and which is made up of age provinces assembled like a mosaic;
(2) the **upper mantle**, the MORB source, which is mainly a residue of extraction of continental crust and the place where oceanic crust is formed and destroyed;
(3) the **lower mantle**, of which little is known by direct information other than that it is the source of the rare gas isotope signature in OIB;
(4) the **atmosphere**, which is the recipient of rare gases given out by the mantle and is not sealed for some gases (He, Ne); and
(5) the **hydrosphere**, which is the driving force and the potential vector of all transfers of material at the surface, through the cycle of erosion, transfer, and sedimentation.

These reservoirs exchange material with each other. Material is extracted from the upper mantle to form the continental crust, probably during subduction processes. Material from the landmasses is reinjected into the upper mantle, either during subduction or during episodes when the continental crust is delaminated and falls into the mantle (**Dupal province**).

Exchanges probably occur between the lower and upper mantle, as shown by mass balance calculations for the depleted mantle and the results for rare gases, implying the existence of two reservoirs in the mantle, with injection of the lower mantle into the upper mantle. But the exact processes are unknown even if it is obvious that mantle plumes and subduction are related in some way with these exchanges.

Exchanges with the atmosphere are by volcanic outgassing and, for the continental crust, erosion (which destroys rock and releases some of the rare gases in rock) or hydrothermal processes. It seems that gases are reinjected into the mantle through subduction phenomena as shown by **Marc Javoy** and colleagues of the Institut de Physique du Globe in Paris for $CO_2$ and $N_2$ (Javoy *et al.*, 1982) when these gases are transformed into chemical compounds. This does not seem to be so for rare gases, for which subduction is apparently a barrier, and which return to the atmosphere through volcanism in subduction zones.

There remain major questions that are the subject of fierce debate. Do subduction processes affect the lower mantle? Are plumes created in the upper mantle, the lower mantle, or both, and by what processes? Does the lower mantle exchange material with the upper mantle? All of these questions are suggested by the findings of seismic tomography

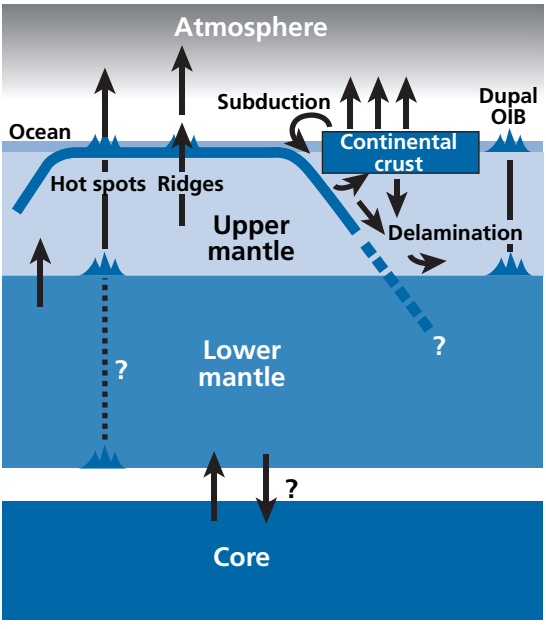


**Figure 8.1** The structure and dynamics of the mantle–landmass–atmosphere system. The Earth system is made up of reservoirs exchanging matter and energy with each other.

which provides spectacular color images but which cannot readily be interpreted because it is difficult to distinguish between heat and mass transfers. This is a reality that relates to the present day for geophysicists while isotope geochemistry includes the whole history of the Earth.

These exchanges of material between reservoirs have been modulated by the vagaries of geological history and, for the external reservoirs, by the vagaries of climate. All of this creates what is nowadays termed a dynamic system, or several interlocking dynamic systems if you prefer (Figure 8.1).

We have looked at the Earth's external system where the ocean exchanges with the atmosphere, is fed water charged with ions by the landmasses, precipitates some compounds, and stores water in ice and releases it under the influence of dynamic fluctuations (Figure 8.2). Once again, this is a huge dynamic system. The way in which the system receives energy from the Sun, distributes it, and modulates it triggers the water cycle, modifies the surface temperature and determines the climate.

Quite what the relative influence is of the greenhouse effect, caused by $CO_2$ or $CH_4$, and of the hydrological cycle, an extraordinary thermal machine, remains an unresolved issue. Geographical distribution is essential in this dynamic system and, as has been seen, the very different effects between the northern hemisphere with many landmasses and the southern hemisphere, which is largely ocean, are still poorly understood.

The evolution and determining factors of the chemical workings of the oceans and the question of the relative influence of chemical elements extracted from the mantle compared

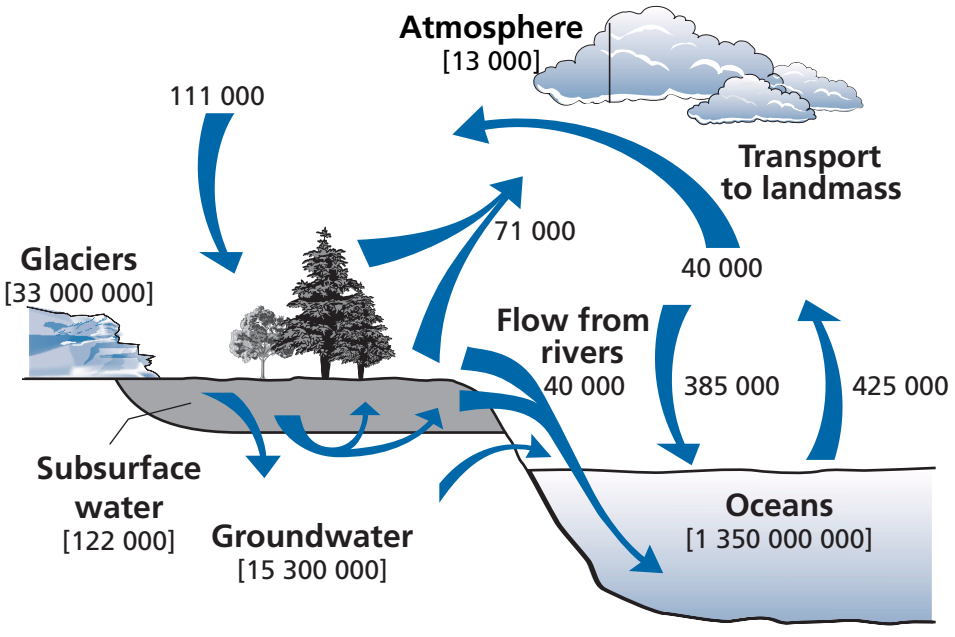


**Figure 8.2** The hydrological cycle considered as a system. The masses of the reservoirs are shown in brackets. Flows are marked by arrows. Units are $km^3$, corresponding to $10^{12}$ kg, and $km^3\ yr^{-1}$ for flows.

with those from the landmasses on the record of the past chemical or isotopic composition of the oceans depend largely on closely interconnected parameters. This is the example of vast dynamic systems with complex interactions whose determining factors we still do not understand properly.

Future developments of paleo-oceanography or paleoclimatology, like those of chemical geodynamics, are related to our understanding of such complex systems. Accordingly, at the end of this book, it has been thought useful to address, in an admittedly very elementary and succinct way, but prospectively, what is now a huge field of study in the earth sciences but whose formal features exceed our present framework and apply equally to biology and the chemical industry as well as to ecology or to physics. It is this methodology that we call **dynamic systems analysis**. When we say that the Earth is a "chemical plant" it is not just for the pleasure of a new image. The same methods of systems analysis apply to chemical plants as to the Earth and its component parts.

We shall give a few very elementary bases of these methods that we shall apply, of course, to the system that the Earth constitutes, looking at the questions specific to it, but, more than that, opening up future prospects. In this context, isotopes appear as tracers, indicators, like radioactive tracers in biology or industrial chemistry, but they contain a wealth of information as we shall see (for general references see: Jacobsen and Wasserburg, 1981; Beltrani, 1987; Jacobsen, 1988; Albarède, 1995; Haberman, 1997; Lasaga and Berner, 1998; Rodhe, 2000).

# 8.1 Basic reservoir analysis: steady states, residence time, and mean ages

## 8.1.1 Well-mixed, simple reservoirs

Let us consider a first simple example. A reservoir of mass $M$, in a steady state, into which a flow of matter $\dot{M}_{\downarrow}$ enters (and from which a quantity of matter $\dot{M}^{\uparrow}$ exits). The reservoir itself is well mixed and is assumed to be statistically homogeneous.[1] The reservoir might be the Earth's mantle, the ocean or the mass of sediments, etc. For the steady state $\dot{M}_{\downarrow} = \dot{M}^{\uparrow}$, we define the **residence time** as the average time matter spends in the reservoir. The residence time $R$ is defined by

$$R = \frac{M}{\dot{M}_{\uparrow}} = \frac{M}{\dot{M}_{\downarrow}}.$$

The dynamic equation is written $\mathrm{d}M/\mathrm{d}t = \dot{M}_{\downarrow} - \dot{M}^{\uparrow}$, with $\dot{M}_{\downarrow} = \dot{M}^{\uparrow}$ in the steady state. What goes into the reservoir equals what comes out of it, and so residence time can be calculated by considering either the input term or the output term.

To reason in terms of age, we must speak of the **mean age of material** leaving the reservoir and which entered at time $t = 0$. What is the mean age of material in the reservoir?

The output flow $\dot{M}^{\uparrow}$ may be written in the form: $\dot{M}^{\uparrow} = kM$, where $k$ is the fraction of the reservoir exiting per unit time. Then $\mathrm{d}M = kM\ \mathrm{d}t$, which may be written $\mathrm{d}M/\mathrm{d}t = kM$. Thus $k$ may be considered as the probability that an element of the reservoir will exit at a time $t$. As it is notated, $k = 1/R$ is the inverse of residence time. We can therefore write that the quantity of particles exiting the reservoir is:

$$\mathrm{d}M/\mathrm{d}t = -kM,$$

hence $M = M_0 \mathrm{e}^{-kt}$.

This equation translates the evolution at time $t$ of the number of particles that entered the reservoir at time $t = 0$. It is also the age distribution of the "particles" of matter present in the reservoir.

The proportion of particles of age $t$ still in the reservoir is written:

$$M(t)/M_0 = \mathrm{e}^{-kt}.$$

The mean age of particles in the reservoir is written:

$$\langle T \rangle = \int_0^{\infty} t\mathrm{e}^{-kt}\ \mathrm{d}t = \frac{1}{k}\int_0^{\infty} kt\ \mathrm{e}^{-kt}\ \mathrm{d}t.$$

Integrating by parts, $\int_0^{\infty} kt\ \mathrm{e}^{-kt}\ \mathrm{d}t = 1$, therefore $\langle T \rangle = 1/k = R$.

In this well-mixed reservoir, the **mean age** of particles is equal to the **residence time**. This is a fundamental result.

[1] We often refer to such reservoirs as **boxes** (a **single box** or **multiple boxes**).

## Exercise

The mantle may be thought of as a reservoir from which mantle escapes at the ocean ridges and which it enters at the subduction zones. Accepting that it operates in a steady state, what is the residence time of a lithospheric plate in the upper mantle? We ask the same question for the whole mantle.

It is taken that the rate of formation of ocean floor is 3 $km^2\ yr^{-1}$, the thickness of a plate is 8 km, and its mean density 3.5.

### Answer

The area subducted (swallowed up by the mantle) equals the area created, therefore the mass of the lithosphere subducted is $8.4 \cdot 10^{14}$ kg $yr^{-1}$.

The mass of the upper mantle is $1.05 \cdot 10^{24}$ kg, therefore the corresponding residence time is $R = 1.25$ Ga. The mass of the total mantle is $4.02 \cdot 14^{24}$ kg, therefore for the whole mantle $R = 4.78$ Ga.

## Exercise

Suppose we wish to calculate the residence time of the ocean crust alone, which would tend to suggest the ocean lithosphere is made up of oceanic crust and a piece of average mantle attached to it. What is the residence time of such an ocean crust in the upper mantle?

### Answer

Oceanic crust is 6 km thick, the mass of oceanic crust subducted is therefore $8.4 \cdot 10^{13}$ kg $yr^{-1}$. Hence $R = 12.4$ Ga for the upper mantle alone.

## Exercise

The quantity of $^3$He in the atmosphere is $1.26 \cdot 10^9$ moles. The degassing rate of $^3$He at the mid-ocean ridges is 1100 moles $yr^{-1}$. Atmospheric $^3$He is lost to space. Accepting that the atmosphere is in a steady state for helium, what is the residence time of $^3$He in the atmosphere?

### Answer

$R$ is about 1 million years, 1.18 Ma to be precise.

Let us now try to calculate the residence time of a chemical element $i$ in a well-mixed reservoir (**Galer** and **O'Nions**, 1985). We reason as before. Let $C^i_{\downarrow}$ be the chemical concentration of the element entering the reservoir and $C^i_M$ that present in the reservoir:

$$R^i = \frac{M\, C^i_M}{\dot{M}_{\downarrow}\, C^i_{\downarrow}} = R\,\frac{C^i_M}{C^i_{\downarrow}}$$

where $M$ and $\dot{M}_{\downarrow}$ are the overall mass and the mass of the flow entering the reservoir, respectively, and $R$ is the residence time of the material.

## Exercise

Suppose the ocean is a system in a steady state. The mass of the ocean is $M = 1.39 \cdot 10^{21}$ kg, and the mass of water entering from rivers $\dot{M}_{\downarrow} = 4.24 \cdot 10^{16}$ kg $yr^{-1}$.

Given the Sr and Nd concentrations in sea water and rivers in the table below, what is the residence time of these elements in sea water?

| | Sr (ppm) | Nd (ppt) |
|---|---|---|
| Sea water | 7.65 | 3.1 |
| Rivers | 0.06 | 40 |

**Answer**

For Sr, $R = 4 \cdot 10^6$ yr. For Nd, $R = 2500$ yr.

## Exercise

It is considered that most of the chemical elements in sea water disappear into pelagic sediments by various processes (absorption, precipitation, biochemical reaction, etc.), that the sedimentation rate for such sediments is $3 \cdot 10^{-3}$ kg m$^{-2}$, that the ocean area, excluding continental margins is $3.1 \cdot 10^{14}$ m$^2$, and that the average concentrations of Sr and Nd of these sediments are $C_{Sr} = 2000$ ppm and $C_{Nd} = 40$ ppm. Calculate the residence time of Sr and Nd in sea water and compare this result with the previous one.

**Answer**

For Sr, $R = 5.5 \cdot 10^6$ yr. For Nd, $R = 1162$ yr.

The figures are similar to the previous ones, which confirms the hypothesis that the ocean is in a steady state. (These values are controversial and not hard and fast, but they do give a good order of magnitude.)

## Exercise

What is the residence time of U and Ni in the upper mantle if we consider the ocean crust is "independent" of its underlying lithosphere? The enrichment of U in the oceanic crust is given as 10 and that of Ni as 0.1.

**Answer**

$R_U = 12.4/10 = 1.24$ Ga and $R_{Ni} = 12.4/0.1 = 124$ Ga. They differ by a factor of 100.

The average age is calculated using exactly the same process and leads to the various elements being differentiated by their geochemical properties. The ocean lithosphere structure is probably intermediate between the two extremes evoked. It is composed of an oceanic crust, a part of the depleted mantle, the residue of partial melting, and perhaps also a thermally added part which is just accreted averaged mantle.

## 8.1.2 Segmented reservoirs

Let us now look at a very different kind of reservoir formed by the juxtaposition of cells (or boxes) which do not mix but are adjacent and passed through in turn.

This reservoir is segmented. It takes a time $T$ to go from the first to the last segment. The maximum age of the reservoir is the exit age from the reservoir, which is the

residence time $R = T$. The mean age of the reservoir, supposing it is created in a uniform way, is:

$$\langle T \rangle = \frac{1}{M^{\uparrow} T} \int_0^T t \, \dot{M}^{\uparrow} \, \mathrm{d}t = \frac{T}{2}.$$

An example is that of the human population. The residence time is 80 years, the mean age 40 years. Of course, if $\dot{M}^{\uparrow}$ is not constant, $\langle T \rangle$ is different from $T/2$ and varies between 0 and $T$.

Reasoning like this can be applied to the continental crust, supposing the survival of a portion of the continent depends on its age and therefore that the pieces of continents are destroyed by the geodynamic processes (erosion, metamorphic recycling, etc.) and that their maximum age is 4.2 Ga and their mean age 2.2 Ga, as calculated for the (Sr, Nd) isotope balances. The relation between residence time and mean age of a reservoir reflects the internal dynamics of this reservoir and its internal structure.

## Exercise

Calculate the mean age of a continental reservoir made up of four segments aged 3.5, 2.5, 1.5, and 0.5 Ga whose masses in arbitrary units are in a first instance 10, 6, 3, and 1 and in a second instance 1, 3, 6, and 10.

### Answer

The proportions of the four segments are 0.5, 0.3, 0.15, and 0.05 respectively, and the inverse for the second case. The mean ages are $\overline{T} = 2.75$ Ga in the first case and $\overline{T} = 1.25$ Ga in the second.

## Exercise

Let us suppose regular mantle convection (without mixing with the environment) with, for example, subduction, a loop, and partial melting at a mid-ocean ridge (Figure 8.3). Suppose the subduction rate is 4 cm yr$^{-1}$, that the ridge is 20 000 km from the subduction zone (Pacific), and the depth is 400 km. What is the residence time of this portion of the mantle?

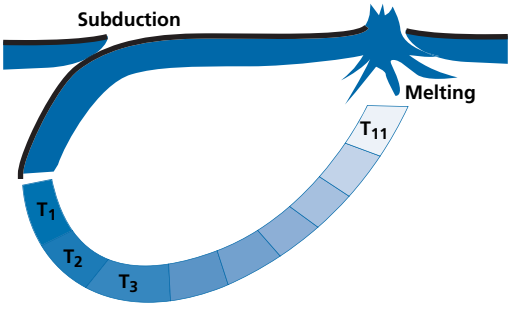


**Figure 8.3** Regular mantle convection. $T_1$, $T_2$, . . ., $T_{11}$ are a set of subduction dates with $T_{11}$ the earliest.

**Answer**

The length of time spent in the mantle is written:

$$T = \frac{\text{distance}}{\text{speed}} = \frac{400 \times 2 + 20\,000 \cdot 10^5}{4} = 502\ \text{Ma}.$$

This is just under half the residence time measured in the upper mantle. But such a process is very similar to that of a segmented reservoir!

## 8.2 Assemblages of reservoirs having reached the steady state

A whole series of complex (multi-box) systems can be imagined by combining the two types (well mixed or segmented) of simple system. We shall give a few examples which could apply to the upper mantle but also to the ocean, considered as a series of separate reservoirs (Atlantic, Indian, Pacific, surface water, deep water, etc.).

### 8.2.1 Model 1

Let us consider a mantle made up of two layers which exchange material (Figure 8.4). It may be the upper mantle–lower mantle system or even the upper mantle separated into two layers by the 400-km seismic discontinuity.

Let $M_1$ and $M_2$ be the masses of the two mantles. Let $\dot{S}$ and $\dot{D}$ be the flow of matter in the subduction zone and at the mid-ocean ridge. We have $\dot{S} = \dot{D}$. In addition, let $\dot{M}_{1-2}$ be the flow of material from mantle 1 to mantle 2 and $\dot{M}_{2-1}$ the flow from mantle 2 to mantle 1. Supposing a steady state (therefore $\dot{M}_{1-2} = \dot{M}_{2-1}$), what are the residence times (and therefore the mean ages)?

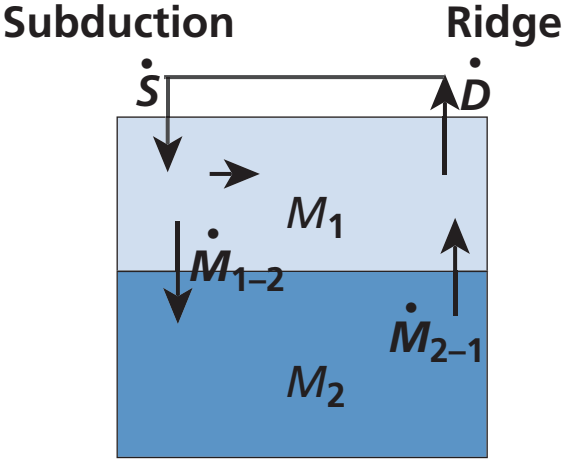


**Figure 8.4** Model of mantle with two layers exchanging matter (and energy). $M_1$ and $M_2$ are the reservoir masses; $\dot{M}_{1-2}$ and $\dot{M}_{2-1}$ are the mass fluxes.

$$R_1 = \frac{M_1}{\dot{S}} \text{ and } R_2 = \frac{M_2}{\dot{M}_{1-2}}.$$

The total residence time $\tau$ is such that:

$$R = \frac{M_1 + M_2}{\dot{S}} = \frac{M_1}{\dot{S}} + \frac{M_2}{\dot{S}} = \frac{M_1}{\dot{S}} + \frac{M_2}{\dot{M}_{1-2}} \cdot \frac{M_{1-2}}{\dot{S}}.$$

Positing $M_{1-2}/\dot{S} = f$, we get:

$$R = R_1 + R_2 f.$$

The mean ages are equal to the residence times.

## Exercise

Calculate $R$, $R_1$, and $R_2$ assuming a division between upper and lower mantle with $f = 0.1$.

**Answer**

$R = 4.75$ Ga; $R_1 = 1.28$ Ga; $R_2 = 34.7$ Ga.

## Exercise

Let us now suppose the upper mantle is divided in two by the 400-km discontinuity. Assuming $f = 0.3$, calculate $R$, $R_1$, and $R_2$.

**Answer**

Rounding the figures, the mass of the mantle above 400 km is $0.60 \cdot 10^{24}$ kg and from 400 to 670 km it is $0.4 \cdot 10^{24}$ kg.
$R = 1.28$ Ga; $R_1 = 0.769$ Ga; $R_2 = 1.7$ Ga.

### 8.2.2 Model 2

The upper mantle is assumed to be divided into two reservoirs: an upper layer (asthenosphere) and a lower layer (transition zone) of masses $M_1$ and $M_2$ (Figure 8.5). Subduction injects 50% into the upper layer and 50% into the lower layer. The upper layer is assumed to be well mixed, while the lower layer is segmented and matter advances horizontally in sequence and is then finally injected into the upper layer.

We have:

$$R_1 = \frac{M_1}{\dot{S}}$$

because the input is both direct and indirect, and

$$R_2 = \frac{M_2}{\dot{M}_{1\to 2}},$$

and $\langle T_1 \rangle = \tau_1$ and $\langle T_2 \rangle = \frac{\tau_2}{2}$.

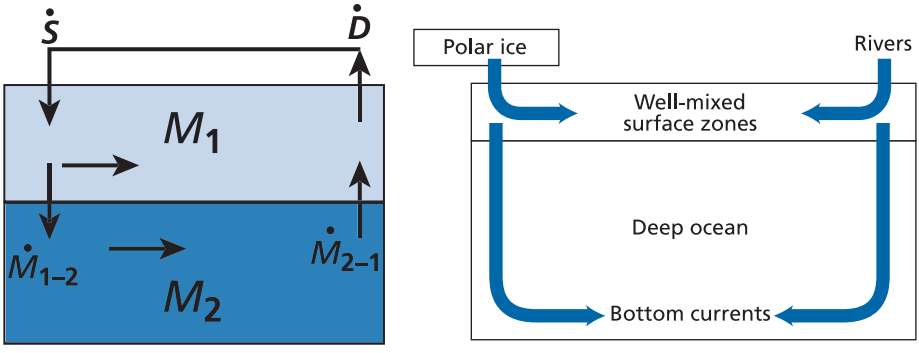


**Figure 8.5** Model 2 of the mantle (left) and ocean (right) showing the two layers that exchange material.

With $M_1 = 0.6 \cdot 10^{24}$ kg and $M_2 = 0.4 \cdot 10^{24}$ kg, we get: $R_1 = 0.714$ Ga, $R_2 = 0.952$ Ga, $\langle T_1 \rangle = 0.714$ Ga, and $\langle T_2 \rangle = 0.47$ Ga.

It can be seen that the mean age of the deep reservoir is less than that of the upper reservoir, while the opposite applies for residence time.

In these examples, information can be deduced about the convective structure of the reservoirs by juggling with **residence times** and **mean ages**. Such a model can be constructed for ocean dynamics with different time constants. The upper layer is the well-mixed surface layer, and the lower layer is traversed by slow moving, deep currents, similar to a segmented reservoir.

## 8.3 Non-steady states

### 8.3.1 Simple reservoirs

#### General equations

Let us go back to the simple case of a reservoir fed by an influx $J$, with an outflow considered proportional to the quantity of material $M$ in the reservoir. Let $k$ be the kinetic constant. The dynamic equation is written:

$$\frac{\mathrm{d}M}{\mathrm{d}t} = J - kM,$$

with at $t = 0, M = M_0 = 0$.

Integrating gives:

$$M = \frac{J}{k}\left(1 - \mathrm{e}^{-kt}\right).$$

It is confirmed that when $t \to 0$, $M \to 0$. When $t \to \infty$, $M$ tends towards $J/k$, that is, the steady state, since $J/k$ is the solution to the differential equation at equilibrium when $\mathrm{d}M/\mathrm{d}t = 0$.

But what is the significance of $k$? At equilibrium, the residence time is $R = M/kM = 1/k$, therefore $R = 1/k$. So $k$ is the inverse of residence time, as already said.

Let us rewrite the solution to the equation:

$$M = JR\left(1 - e^{t/R}\right).$$

The equilibrium solution for the full reservoir is therefore: $M =$ flow $\times$ residence time. The "speed" to attain equilibrium is proportional to $1/R = k$.

Suppose now that the reservoir is full, and so its mass is $M = JR$. We decide to empty it. What is the drainage law?

$$\frac{dM}{dt} = -kM$$

hence $M = JR\ e^{t/R}$.

The constant of the drainage time is the residence time. Likewise, $R$ controls the time the system takes to attain the state of equilibrium.

## Exercise

How long does the system take to attain 99% of its equilibrium mass?

**Answer**

$t = 4R$.

## Exercise

What is the mean age of the reservoir in this case? Remember that

$$T = \frac{1}{m}\int_0^\infty t\ \frac{dm}{dt}\ dt.$$

**Answer**

$$\frac{dM}{dt} = J - k\ \frac{J}{k}\left(1 - e^{-kT}\right).$$

Hence, as with the simple case of the well-mixed reservoir, $T = R$.

Such a model could apply to the growth of the continents where it is considered that at each period the same amount of material is formed and that the material is destroyed over time and reinjected into the mantle. As we shall see, this is a very general equation.

## The case of chemical elements

The problem of the evolution of concentrations of a chemical element in a reservoir is treated analogously following Galer and O'Nions (1985). Let us consider the evolution of the mass of an element $i$:

$$\frac{d(C^i M)}{dt} = C^i_{ex}\, J - k^i C^i M$$

where $C^i$ is the concentration in the reservoir, $C^i_{ex}$ the concentration in the flow of material entering from outside, $J$ the flux of incoming material, and $M$ the mass of the reservoir.

If the mass is constant, we can divide by $M$. This gives:

$$\frac{dC^i}{dt} = C^i_{ex}\left(\frac{J}{M}\right) - kC^i.$$

The residence time of the chemical element is written:

$$R = \frac{MC^i}{JC^i_{ex}} = R_M\,\frac{C^i}{C^i_{ex}} = \frac{1}{k},$$

where $R_M$ is the residence time of the mass making up the reservoir, a formula we have already established in the steady state.

### The case of a radioactive isotope

Let us write the equation for the evolution of the radioactive isotope:

$$\frac{dC^*}{dt} = Q^* - kC^* - \lambda C^*$$

with $Q^* = C^*_{ex}\,(J/M)$ ($\lambda$ is the radioactive constant). The constant $k$ is replaced in this equation by $(k+\lambda) = k^*$. The residence time is $R^* = 1/k^*$.

As can be seen, radioactivity is involved in residence time. If $\lambda$ is very large, it reduces the residence time.

**Exercise**

The residence time of carbon in the ocean is 350 years. What is the residence time of $^{14}C$?

**Answer**

About the same since for $^{14}C$, $\lambda = 1.209 \cdot 10^{-4}$ yr$^{-1}$.
$k^* = 1.2 \cdot 10^{-4} + 2.8 \cdot 10^{-3} = 2.92 \cdot 10^{-3}$.
$R_{14_c} = 342$ years.

## 8.3.2 Creation–destruction processes

The Earth is a living planet; all terrestrial structures are created by some processes and destroyed by others. What we observe is merely the outcome of antagonistic processes: birth and death. Thus, magmatic volcanic and metamorphic processes create portions of continents. These landmasses are then destroyed by erosion or by recycling of their materials in a new metamorphic cycle. The oceanic crust is formed at the mid-ocean ridges. It is swallowed up in the mantle in the subduction zones. There it is destroyed either by being thoroughly mixed with the middle mantle or by being fed back through an ocean ridge

where it is again melted and reformed. These problems are analogous to those of birth and death in demography, as can be seen by consulting books on the subject.

Let us first consider the question of the geodynamic cycle. Let $D$ be the quantity of mantle differentiated at the mid-ocean ridges. We have:

$$\frac{\mathrm{d}(D)}{\mathrm{d}t} = J - k(D)$$

where $J$ is the rate of formation at the ocean ridge, and $k(D)$ is the destruction of quantity $D$ which is fed back through an ocean ridge. But $J = kV$, if $V$ is the total volume of the mantle and if the residence time $R$ is such that $R = 1/k$.

$$\frac{\mathrm{d}D}{\mathrm{d}t} = k(V - D).$$

The solution of this differential equation where $V$ is constant is:

$$D = V\left(1 - \mathrm{e}^{-kt}\right).$$

Time is set to $t = 0$, 4.55 Ga ago. So $D/V = (1 - \mathrm{e}^{-kt})$ tends towards 1 when $t$ is large, and $D = 0$ when $t = 0$. The question is, of course, what value to take for $k$.

Let us take the value for the residence time of the upper mantle recycled by plate tectonics and assumed to be in a steady state: $R = 1.2 \cdot 10^9$ yr and $k = 0.83 \cdot 10^{-9}\ \mathrm{yr}^{-1}$ (Figure 8.6). It may also be that there was more recycling in the past because more heat was produced in the mantle and the time may have been 0.7 Ga, that is, $k = 1.4 \cdot 10^{-9}\ \mathrm{yr}^{-1}$.

On this basis then, let us look at two issues. The first is to determine the quantity of virgin upper mantle, that is, mantle that has not been melted at a mid-ocean ridge. This part of the virgin mantle is the complement of the mantle that has been recycled through ocean ridges:

$$1 = V\left(1 - \mathrm{e}^{-kt}\right) + \text{virgin mantle } (V_0)$$

$$\frac{V_0}{V} = \mathrm{e}^{-kt}.$$

It can be seen therefore that the mass of the virgin mantle decreases with time, of course. What of the upper mantle? For $k = 0.83 \cdot 10^{-9}\ \mathrm{yr}^{-1}$, it is 2.3‰. For $k = 1.4 \cdot 10^{-9}\ \mathrm{yr}^{-1}$ it is 1.8‰ (these are per mil values!).

## Exercise

What proportion of virgin mantle would be preserved if the flow at the ocean ridges were identical but the system were the entire mantle?

### Answer

Let us now try to calculate the age spectrum of this recycled mantle. It is the age distribution at the time the mantle went through the ridge-subduction cycle. It follows the law:

$$N(t_n) = kV\mathrm{e}^{-kt}.$$

As can be seen, the mathematical equations are analogous to those of the previous example, but their physical meaning is very different. It is an example to remember.

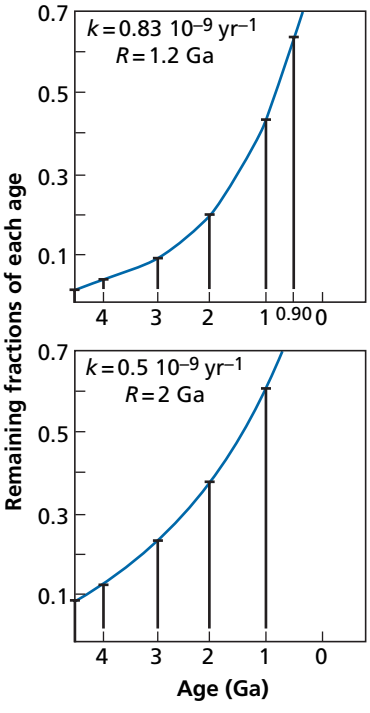


**Figure 8.6** Spectrum calculation for $k = 0.83 \cdot 10^{-9}\ \mathrm{yr}^{-1}$ and $0.5 \cdot 10^{-9}\ \mathrm{yr}^{-1}$. Notice the very rapid growth towards recent times. This is because the probability of double or triple recycling increases very rapidly with time.

### 8.3.3 Time-dependent formation

Let us now consider a slightly more complex case where the formation term decreases with time. This is geologically fairly logical as we know that the creation of radioactive energy has decreased with time. The equation becomes:

$$\frac{\mathrm{d}M}{\mathrm{d}t} = J_0\, \mathrm{e}^{-qt} - kM.$$

This is a very general equation found in many cases (Allègre and Jaupart, 1985). For example, for continental growth, where the equations found can be modified as a consequence or also for degassing of the mantle, which we have looked at.

Integrating gives:

$$M = \frac{J_0}{k - q}\left(\mathrm{e}^{-qt} - \mathrm{e}^{-kt}\right).$$

Therefore $M$ depends on the two constants $k$ and $q$.

To get our ideas straight, let us take the case of degassing of $^{40}\mathrm{Ar}$ from the upper mantle, and study the $^{40}\mathrm{Ar}$ content of the upper mantle:

$$\frac{\mathrm{d}\,^{40}\mathrm{Ar}}{\mathrm{d}t} = \lambda_{\mathrm{e}}\,{}^{40}\mathrm{K}_0\,\mathrm{e}^{-\lambda t} - G\,{}^{40}\mathrm{Ar}$$

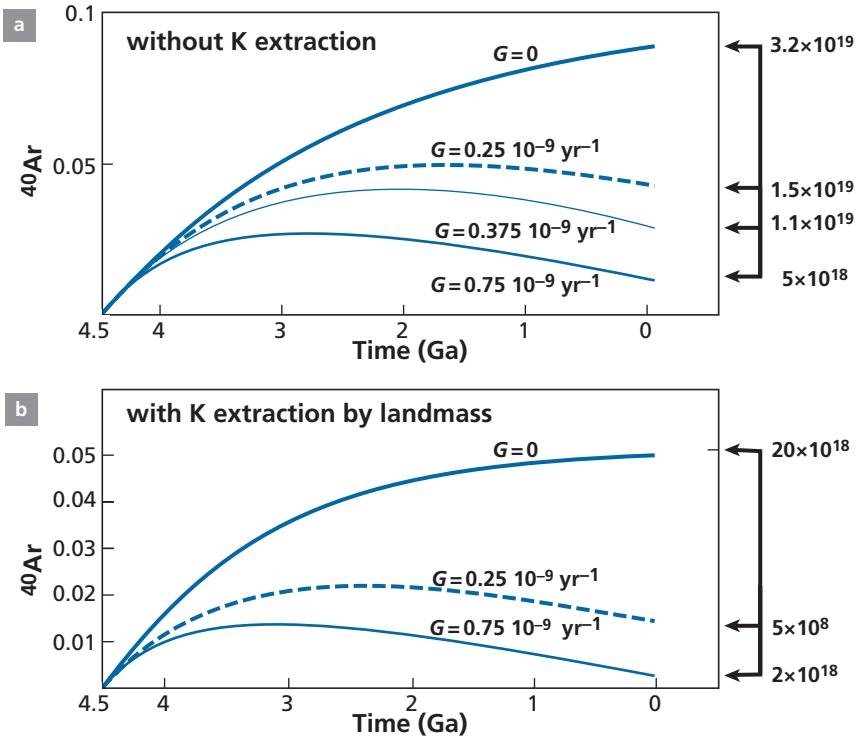


**Figure 8.7** Mantle degassing model. (a) Evolution of $^{40}$Ar in the mantle over time, assuming that $^{40}$K varies by radioactive decay alone. The scale on the right is drawn assuming $^{40}K_0 = 1$. The scale on the left is in $10^{19}$ g of $^{40}$Ar and corresponds to the total mass of $^{40}$Ar on the hypotheses made in the main text. (b) Evolution of $^{40}$Ar in the mantle assuming $^{40}$K decreases both by extraction from the continental crust and by radioactive decay. The scale on the left is in $10^{18}$ g of $^{40}$Ar. On the right, it is assumed that $^{40}K_0 = 1$.

where $\lambda_e$ is the fraction of $^{40}$K giving $^{40}$Ar; $\lambda$ is the total decay constant of $^{40}$K; G is the constant of outgassing (Figure 8.7). The equation can be easily integrated:

$$^{40}\mathrm{Ar} = \frac{\lambda_e \, {}^{40}\mathrm{K}_0}{G - \lambda} \left(\mathrm{e}^{-\lambda t} - \mathrm{e}^{-Gt}\right).$$

We are going to study the behavior of $^{40}$Ar for the different values of $G$, arbitrarily setting $G_0 = 1$.

The qualitative behavior is understandable. When $G$ is quite large, the quantity of $^{40}$Ar reaches a maximum and then declines. So let us try to apply this information to the actual upper mantle.

The present-day potassium level in the non-depleted mantle is K = 250 ppm, and $^{40}\mathrm{K} = 1.16 \cdot 10^{-4}$ or 116 ppm. The decay constant is $\lambda = 0.554 \cdot 10^{-9}$ yr$^{-1}$. Some $4.55 \cdot 10^9$ years ago, the $^{40}$K level was 12 times higher and so equal to 0.35 ppm.

Given that the mass of the upper mantle is $1 \cdot 10^{27}$ g, 4.55 Ga ago, there was therefore $0.35 \cdot 10^{21}$ g of $^{40}$K. From the previous calculation we obtain the following values of $^{40}$Ar today:

| | $G(10^{-9}\text{yr}^{-1})$ | | | |
|---|---|---|---|---|
| | 0.25 | 0.375 | 0.75 | 0 |
| $^{40}\text{Ar}(g)$ | $1.5 \cdot 10^{19}$ | $1.1 \cdot 10^{19}$ | $0.49 \cdot 10^{19}$ | $3.2 \cdot 10^{19}$ |

The present-day mass is estimated at $2–3 \cdot 10^{18}$ g, which is not bad!

There is one assumption in the model that is not very satisfactory because it was considered that $^{40}$K decreased in the upper mantle by radioactive decay alone. Now, we know that K has also decreased in the upper mantle because it has been extracted at the same time as continental crust in which it is enriched. Let us therefore consider that $^{40}$K decreases by the law:

$$^{40}\text{K} = {}^{40}\text{K}_0\, \text{e}^{-(\lambda+\beta)t}$$

where $\beta$ is the constant for extraction of K from the mantle to the continental crust. (Such extraction does not obey an exponential law exactly, but it is a first approximation.)

We take $\beta = 0.35 \cdot 10^{-9}\ \text{yr}^{-1}$ because, with this constant, total K evolves from 250 ppm to 50 ppm in $4.5 \cdot 10^9$ years, which is about the value estimated for the degree of depletion of the upper mantle in K. The change in $^{40}$Ar content of the mantle can therefore be calculated by replacing the value of $\lambda = 0.5 \cdot 10^{-9}\,\text{yr}^{-1}$ by $(\lambda + \beta) = 0.85 \cdot 10^{-9}\,\text{yr}^{-1}$.

$$^{40}\text{Ar} = \frac{\lambda_e}{G - (\lambda + \beta)} \left(\text{e}^{-(\lambda+\beta)t} - \text{e}^{-Gt}\right).$$

As can be seen from the curves, we obtain an acceptable value: $2.77 \cdot 10^{18}$ g of $^{40}$Ar in the upper mantle for $G = 0.75 \cdot 10^{-9}\ \text{yr}^{-1}$. Now, what does $0.75 \cdot 10^{-9}\ \text{yr}^{-1}$ represent? The value $1/G = 1.3 \cdot 10^9$ is about the residence time of plates subducting into the mantle. If it is taken that the oceanic lithosphere degasses entirely by being fed through the mid-ocean ridges, a plausible scenario can be reconstructed for degassing the upper mantle. Which is no guarantee at all that the model is a proper reflection of reality!

## 8.3.4 Effects of cyclic fluctuations

### General equations

We saw when examining climatic variations that the Earth's temperature varied cyclically (Milankovitch cycles). We can readily imagine that the Earth's tectonic activity varies cyclically (Wilson's plate tectonic cycles). How will such variations affect a dynamic system, a reservoir which receives and exchanges matter?[2]

Let us consider the equation for the dynamic evolution of a reservoir as we have already examined it:

$$\text{d}M/\text{d}t = J - kM,$$

but in which we write that the input flux varies periodically with the formula $J = J_0 + b \sin \omega t$, where $\omega = 2\pi/T$, $T$ being the oscillation period and $k = 1/R$, $R$ being the residence time.

[2] This problem has been addressed by Richter and Turekian (1993) and then by Lasaga and Berner (1998). The latter presentation has inspired the one given here.

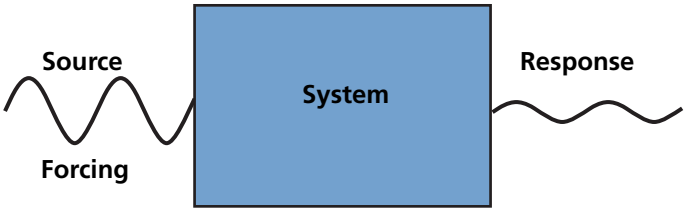


**Figure 8.8** Model of response of a system subjected to external action.

The equation for mass evolution $M$ (or concentration in an element) is therefore:

$$\frac{\mathrm{d}M}{\mathrm{d}t} = J_0 + b\ \sin\ \omega t - kM.$$

The equation can be written in the form:

$$kM\ +\ \frac{\mathrm{d}M}{\mathrm{d}t} = J_0 + b\ \sin\ \omega t.$$

The first term of this equation depends on $M$ alone, the second term being the forcing imposed on the system from outside (we shall also call this the source term). The question is, of course, how does the system react and what is its response to external stimulus (Figure 8.8).

We integrate this first-order differential equation with constant coefficients in the standard manner: integrate the equation without the second member dependent on $t$, then calculate the first integration "constant." In the course of calculation, we get on the integral:

$$\int \mathrm{e}^{kt} \sin \omega t\ \mathrm{d}t.$$

This is the only minor mathematical difficulty.

$$\int \mathrm{e}^{x} \sin x\ \mathrm{d}x$$

is integrated by parts, integrating twice. This leads to:

$$\int \mathrm{e}^{x} \sin x\ \mathrm{d}x = \mathrm{e}^{x} \sin x - \mathrm{e}^{x} \cos x - \int \mathrm{e}^{x} \sin x\ \mathrm{d}x,$$

hence the calculation of $\int \mathrm{e}^{x} \sin x\,\mathrm{d}x$. Integrating this general equation therefore gives:

$$M = M_0\ \mathrm{e}^{-kt}\ +\ \frac{J_0}{k}\ \left(1 - \mathrm{e}^{-kt}\right)\ +\ \frac{b\omega}{k^2 + \omega^2}\ \mathrm{e}^{-kt}\ +\ \left(\frac{bk}{k^2 + \omega^2}\ \sin\ \omega t\right)$$
$$-\ \left(\frac{b\omega}{k^2 + \omega^2}\ \cos\ \omega t\right).$$

It can be seen that if $M_0 = 0$ and $b = 0$, we find the equation in Section 8.3.1:

$$M = \frac{J_0}{k}\left(1 - e^{-kt}\right).$$

Whenever $t$ is quite large (say more than $3/k$), the equation is simplified and can be written:

$$M = \frac{J_0}{k} + \frac{bk}{k^2 + \omega^2} \sin \omega t - \frac{b\omega}{k^2 + \omega^2} \cos \omega t.$$

If $\omega \ll k$, that is, if $R \ll T$ (the residence time is very much less than the oscillation period), the cosine term is negligible. The equation can then be written:

$$M = \frac{J_0}{k} + \frac{b}{k} \sin \omega t$$

where $J_0/k$ is the equilibrium value around which oscillation occurs.

The system response is in phase with the source oscillation. The amplitude of fluctuation around equilibrium depends on the ratio $J_0/b$, that is, on the relative value between the equilibrium value and the pulse value, but if this ratio is not too large, the amplitude remains large.

Conversely, if $\omega \gg k$, that is, $R \gg T$ (the residence time is very much greater than oscillation period), the equation becomes:

$$M = \frac{J_0}{k} - \frac{b}{w} \cos \omega t.$$

But we have the trigonometric equality $\cos \omega t = -\sin(\omega t - \pi/2)$. Therefore the system oscillation is delayed by $(\pi/2)$, that is, by a quarter of a period relative to the source oscillation. Moreover, the amplitude is subtracted from a term $J_0/k$, which is very large since $k$ is very small, which greatly damps the signal. Between the two extremes we find intermediate behavior.

Let us examine the consequences of this mathematical result. Suppose first that the source oscillation period is set, say at 100 ka. Chemical elements whose residence time in the oceans is much less than 100 ka, for example neodymium ($R = 1000$ years), will be subjected to fluctuations (if the geochemical processes governing them are involved) in phase with the source oscillations and which may be of large amplitude depending on the corresponding $J_0/b$ ratio (Figure 8.9).

The chemical elements with very long residence times like strontium ($R = 2$–$4$ Ma)) will be subjected to fluctuations with a time lag of half a period compared with the source, but that are greatly damped too. If, for example, the disturbance reflects the glacial–interglacial cycles, the strontium fluctuations will be offset and damped.

Let us examine the effect of the oscillation period. We stay with strontium with its residence time of 2–4 Ma. If the fluctuations are of the order of 100 or 1000 ka (climate, for example) the results will be as already described. If the fluctuations are from some geological source of the order of 20–30 Ma (tectonic), the strontium fluctuations will follow the source fluctuations, in phase and without any attenuation. Of course intermediate cases arise between these two extremes.

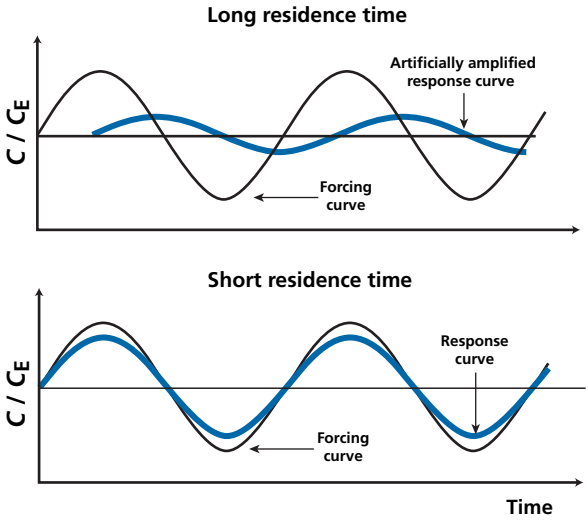


**Figure 8.9** Relationship between residence time and lag in the response curve. The response curve at the top has been greatly amplified vertically so the effect can be seen. $C$, concentration; $C_E$, equilibrium concentration.

The relative importance of the sine and cosine terms depends on the ratio $k/\omega$. We shall see that these properties extend to the fluctuations of isotopic compositions.

## Exercise

We consider sea water and the disturbance to its chemical composition as a result of climatic disruptions introducing different concentrations in rivers. We consider a sinusoidal disturbance with a period of 10 000 years.

We assume the disturbance follows the law: $J = a + b \sin \omega t$.

For four chemical elements Pb, Nd, Os, and Sr whose residence times in sea water are $R_{Pb} = 10^3$ years, $R_{Nd} = 3 \cdot 10^3$ years, $R_{Os} = 3 \cdot 10^4$ years, and $R_{Sr} = 2 \cdot 10^6$ years, respectively, we represent the fluctuations by changing the values of $a$ and $b$ so that $a/R = 1$ and $b = 1$ (this greatly amplifies the Os and Sr fluctuations).

Draw the response curves for the different elements and estimate the phase-shift values. Try to identify any quantitative relationship between residence time and phase shifts. Next try to evaluate damping, taking $a = 1$ and $b = 1$ for all of the elements.

### Answer

The equation describing the response curve is written:

$$\frac{dC}{dt} = a + b \sin \omega t - kC.$$

Integrating gives:

$$C = \frac{a}{k} + \frac{bk}{k^2 + \omega^2} \sin \omega t - \frac{b\omega}{k^2 + \omega^2} \cos \omega t.$$

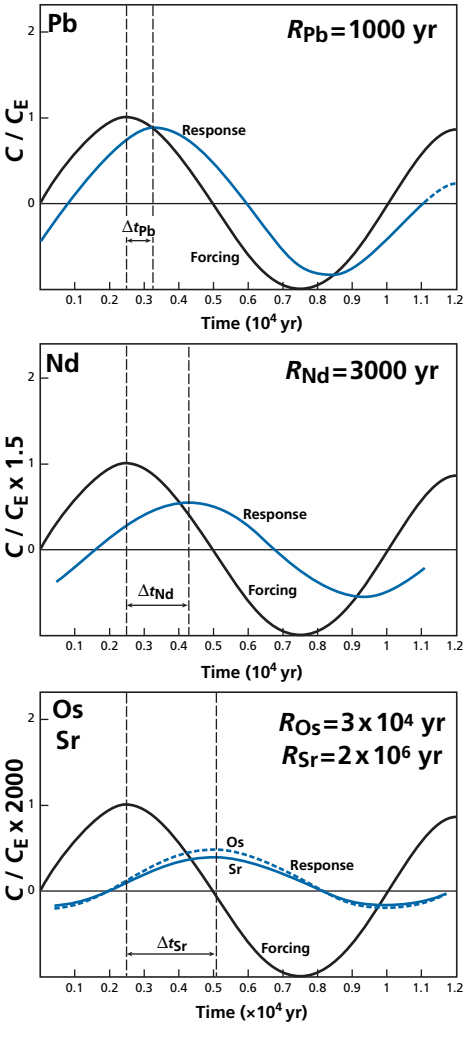


**Figure 8.10** Response curves of Pb, Nd, Os, and Sr concentrations in the ocean, if the sources vary sinusoidally with the characteristics given in the main text. $\Delta C$ = concentration – equilibrium concentration.

We take $10^3$ years as the time unit and $\omega = 2\pi/T = 0.628$.

For Pb, $k = 1$; for Nd, $k = 0.033$; for Os, $k = 0.033$; and for Sr, $k = 5 \cdot 10^{-4}$.

The curves are illustrated in Figure 8.10 ignoring damping. They show the offset in terms of residence time. When the logarithm of $R$ (residence time) is plotted against the phase shift, we get a curve similar to a hyperbola[3] with two asymptotes corresponding to the two limiting cases where $k/\omega$ is very large and $k/\omega$ is very small (Figure 8.11).

To evaluate damping we take $a = 1$ for all the elements, therefore $a/k$ is 1, 3, 30, and 2000 for Pb, Nd, Os, and Sr, respectively. We evaluate the percentage variation:

[3] In fact, it is the curve $tg\ \omega.\Delta t = \omega R$.

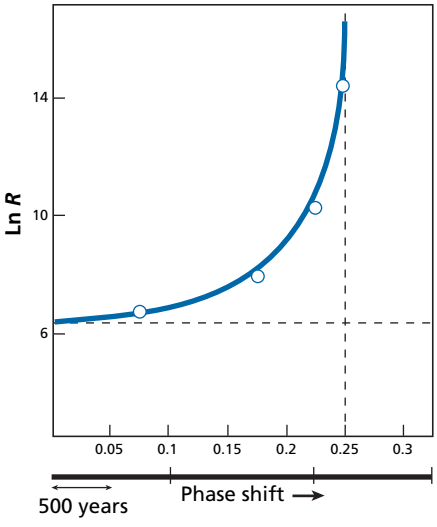


**Figure 8.11** Relationship between residence time as a logarithm and phase shift, expressed in intervals of 10 000 years.

$$\frac{\Delta C}{\bar{C}} = \Delta C / \left(\frac{a}{k}\right).$$

We find 90%, 65%, 0.2%, and 0.15% for the fluctuations of Pb, Nd, Os, and Sr, respectively. We shall see that these properties extend to fluctuations in isotope composition.

## Generalization

### Extension to all forcing functions

The great interest of this study of response to a sinusoidal source is that a response can be obtained for any source function by decomposing it into its Fourier sine functions and then finding the response for each sine function and summing them.

A LITTLE HISTORY

### Joseph Fourier

When he was prefect of France's Isère department under Napoleon, Joseph Fourier (after whom Grenoble's science university is named) proposed one of the most important theorems in mathematics. He showed that any periodic function could be represented by the sum of the sine and cosine functions with appropriate amplitudes and phases. He then showed that when a function was not periodic "by nature," it could be made periodic by truncating it and then repeating the sampled portion. On this basis, any function can be separated into its Fourier components and so represented as a spectrum (frequency, amplitude). Milankovitch cycles are an example that we have already mentioned.

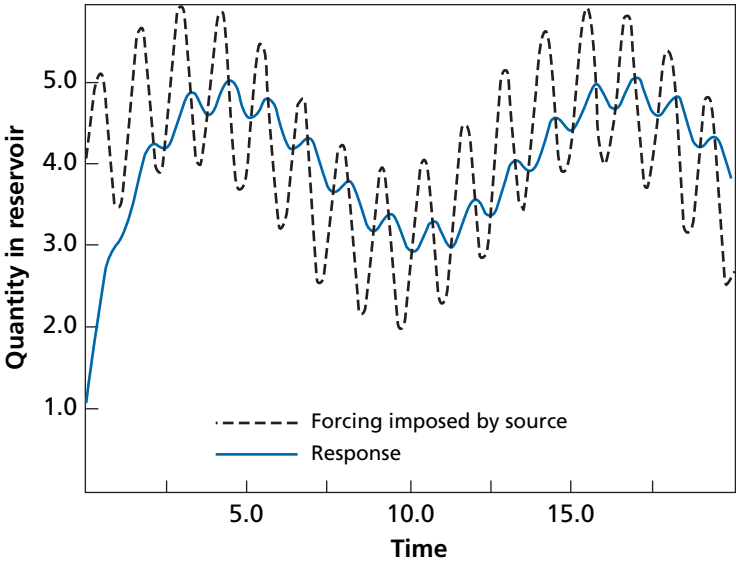


**Figure 8.12** Quantity in the reservoir as a function of time. After Lasaga and Berner (1998).

## Exercise

We take a system (borrowed from Lasaga and Berner) obeying the previous equations with an imposed fluctuation of $F(t) = 4 + \sin(5t) + \sin(t/2)$. The residence time constant is taken as 1 in the arbitrary time units ($t$). Calculate and represent the function at the reservoir outlet.

### Answer

See Figure 8.12. Notice the phase shift, the damping of high frequencies, and the slight alteration of low frequencies.

### The case of radioactive isotopes

We have said that for radioactive systems, the residence time should take account of the mean life of the radioactive element, which is a sort of intrinsic residence time. The dynamic equations we have seen are identical, except for this modification of residence time. In some cases, when the residence time of the reservoir is very large, it is the isotope's lifetime that determines the overall residence time.

The same reasoning applies depending on the value of the $\lambda/\omega$ ratio, where $\omega$ is the frequency of the periodic disturbance and $\lambda$ is the decay constant. The fluctuations imposed by the source shall be taken into account differentially with or without a phase shift and with or without amplitude damping.

EXAMPLE

### Cosmogenic isotopes in the atmosphere

There are three types of cosmogenic isotope in the atmosphere we can look at: $^{10}$Be, $^{3}$H, and $^{14}$C. For $^{3}$H, $\lambda = 5.57 \cdot 10^{-2}$ yr$^{-1}$, for $^{10}$Be, $\lambda = 4.62 \cdot 10^{-7}$ yr$^{-1}$, and for $^{14}$C, $\lambda = 1.209 \cdot 10^{-4}$ yr$^{-1}$.

When we observe fluctuations in the abundance of these isotopes, $^{3}$H reflects rapid fluctuations in the atmosphere whereas $^{14}$C largely damps these variations. However, $^{10}$Be, with a much smaller decay constant, should damp them even more than $^{14}$C. In fact, it reflects rapid oscillations. Why? Because its residence time in the atmosphere of 1–3 years is very short and it is this constant that prevails.

For similar reasons when it comes to deciphering the Earth's early history, the information provided by extinct forms of radioactivity is not the same as that provided by long-lived forms, as we have seen.

## 8.3.5 Non-linear processes

In all the examples examined so far, the basic differential equation has been linear, even if the forcing term was non-linear over time, as in the previous example. Let us now consider a model of growth of the Earth's core. Let the variable $N$ represent the quantity of iron in the core. Then:

$$\frac{dN}{dt} = K(1 - N)$$

where $(1 - N)$ is the mass fraction of iron in the core, the total quantity of iron being normalized to unity. It can be considered that the attraction of this iron dispersed in the form of small minerals is proportionally stronger when the quantity of iron in the core is high (gravitational attraction). To characterize the quantity $N$, we can therefore take $K = QN$.

This gives the equation:

$$\frac{dN}{dt} = QN\,(1 - N).$$

This is a well-known equation, especially in population dynamics. It is the logistic equation (see Haberman, 1997):

$$\frac{dN}{N\,(1 - N)} = Q\,dt.$$

By separating out the simple elements, we can write:

$$\left[\frac{1}{N} + \frac{1}{(1 - N)}\right] dN = Q\,dt.$$

Integrating gives:

$$\ln|N| - \ln|1 - N| = Qt + C,$$

hence:

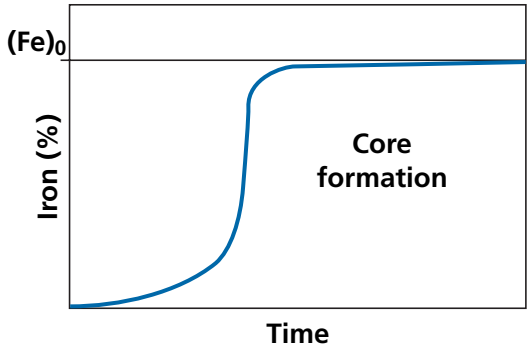


**Figure 8.13** Model curve of core growth. To simplify, it is taken that all the iron is in the core although a fraction (approx. 6%) is in the mantle.

$$N = \frac{N_0}{N_0 + (1 - N_0)\, e^{-Qt}}$$

where $N_0$ is the mass of iron in the core that may be considered as the mass of iron located at the center of the Earth and pooled by melting. This can be shown graphically as an S-shaped curve beginning slowly then accelerating suddenly and ending as an asymptote, with value 1, which is the total quantity of iron (Figure 8.13).

An attempt can then be made to connect time and the constant $Q$. Assuming that $N_0 = 0.1$, the time taken to form 95% of the core is written:

$$t = 5/Q.$$

If this time is estimated at 50 Ma, we get $Q = 1 \cdot 10^{-7}$. (These calculations are to give an order of magnitude of plausible processes.[4])

This logistic law is probably as general in naturally occurring processes as the exponential law is in fundamental physical processes.

## 8.4 The laws of evolution of isotope systems

The various examples we have developed can be used to model the Earth's geodynamic systems using isotope systems as tracers, just as radioactive isotopes can be used to see how the human body or a complex hydrological system behave. This model is made much easier by using general equations describing the evolution of isotope systems in complex dynamic systems. These equations can be used to solve problems directly. But, of course, one of the aims is to obtain a formulation for calculating the system parameters from direct observations.

[4] In actual processes, allowance must be made for oxidation of iron, which allows a fraction of the iron to remain in the mantle.

## 8.4.1 Equation for the evolution of radiogenic systems: Wasserburg's equations

Let us begin with a straightforward case. A reservoir exchanges radioactive and reference isotopes $^{87}Rb$, $^{87}Sr$, $^{86}Sr$, notated $r$, $i$, $j$, with the outside. We notate what enters the reservoir $(\,)_{\downarrow}$ and what exits $(\,)_{\uparrow}$. The decay constant is notated $\lambda$. The fluxes are notated $\dot{r}, \dot{i}, \dot{j}$. We can then write the equations:

$$\frac{dr}{dt} = -\lambda r - (Hr)_{\uparrow} + (\dot{r})_{\downarrow}.$$

$$\frac{di}{dt} = \lambda r - (Gi)_{\uparrow} + (\dot{i})_{\downarrow}.$$

$$\frac{dj}{dt} = -(Gj)_{\uparrow} + (\dot{j})_{\downarrow}.$$

We have written what leaves the reservoir as proportional to what is in the system, assuming the factor is the same for $(i)$ and $(j)$, that is, assuming no isotope fractionation occurs. Let us combine these equations to bring out the ratios $(r/j)$ and $(i/j)$, that is, by our notations ($^{87}Rb/^{86}Sr$) and ($^{87}Sr/^{86}Sr$):

$$\frac{d\left(\frac{r}{j}\right)}{dt} = \left(\frac{r}{j}\right)\left[\frac{dr}{r\,dt} - \frac{dj}{j\,dt}\right] = \left(\frac{r}{j}\right)\left[-\lambda - H + \frac{(\dot{r})_{\downarrow}}{r} + G\,\frac{(\dot{j})_{\downarrow}}{j}\right].$$

We have notated $dr/dt$ and $dj/dt$ as $\dot{r}$ and $\dot{j}$ respectively, as is often done. By bringing out $(r/j)_{\downarrow}$, that is what leaves the system, and by writing:

$$\frac{(\dot{r})_{\downarrow}}{r} = \frac{(\dot{r})_{\downarrow}}{(\dot{j})_{\downarrow}}\,\frac{(\dot{j})_{\downarrow}}{(r)},$$

then by multiplying the bracketed term by $(r/j)$, and noting $r/j = \mu$, as is our standard practice, we get:

$$\frac{d\mu}{dt} = [(G - H) - \lambda]\,\mu + (\mu_{ex} - \mu)\,\frac{(\dot{j})_{\downarrow}}{j}.$$

Doing the same calculations for $(i/j) = \alpha$ gives:

$$\frac{d\alpha}{dt} = \lambda\mu + (\alpha_{ex} - \alpha)\,\frac{(\dot{j})_{\downarrow}}{j}.$$

By noting $(\dot{j})_{\downarrow}/j = L(t)$ and $G - H = F$, we finally obtain:

$$\begin{cases} \dfrac{d\mu}{dt} = [F - \lambda]\,\mu + (\mu_{ex} - \mu)\,L(t) \\ \dfrac{d\alpha}{dt} = \lambda\mu + (\alpha_{ex} - \alpha)\,\mathrm{L(t)}. \end{cases}$$

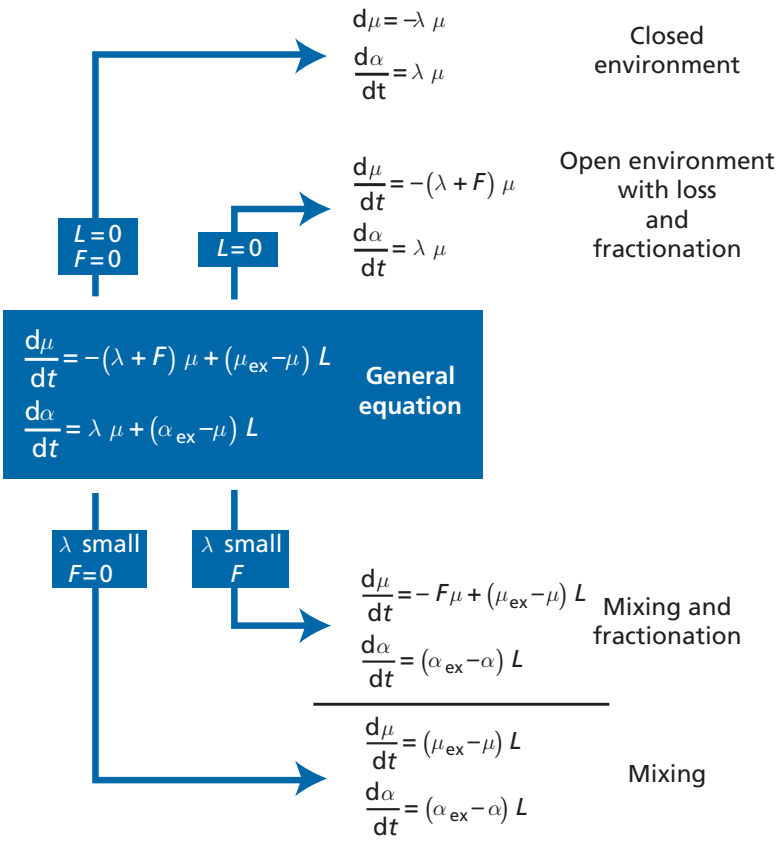


**Figure 8.14** Schema explaining the generality of Wasserburg's equations. Most of the basic equations we have used for radioactive–radiogenic systems can be found in his figure.

These are **Wasserburg's equations** (see Wasserburg, 1964) (Figure 8.14).

Let us make a few remarks about them. Notice that parameter $F$ may be either positive or negative depending on whether the daughter element "leaks" from the reservoir faster ($G > H$) or more slowly ($G < H$) than the parent element. These are two concatenated (and not paired) equations. One ($\mu$) describes the system's chemical evolution. It therefore involves a chemical fractionation factor for the material leaving the reservoir. The other ($\alpha$) involves two terms, one for radioactive decay $\lambda\mu$ and the other for mixing ($\alpha_{ex} - \alpha$). Solving the problem entails integrating the first and then the second. These are very general equations applying to all systems – minerals, rocks, atmosphere, mantle – and thus can be used in both geochronology and isotope geology. Notice that L($t$) is the inverse of residence time ($1/R(t)$).

## 8.4.2 The steady-state box model

This model is developed here through two examples.

## Exercise

Take a reservoir into which flows material from a single external source with a constant chemical and isotopic composition over time ($\mu_{ex}$ and $\alpha_{ex}$) and a constant flow rate. Let us assume that the reservoir attains a steady state.

What is the residence time if we suppose the reservoir is well mixed (that is, having a homogeneous isotope composition $\alpha$)?

### Answer

We find: $-\lambda\mu + (\mu_{ex} - \mu)\, 1/R = 0$ and $\lambda\mu + (\alpha_{ex} - \alpha)\, 1/R = 0$.
This gives:

$$R = \frac{1}{\lambda}\left(\frac{\mu_{ex}}{\mu} - 1\right).$$

We find quite simply the residence time calculated for the $^{14}C/C$ ratio of the deep ocean if $\mu = {}^{14}C/C$ and $\mu_{ex}$ is the $^{14}C/C$ ratio of the surface water in equilibrium with the atmosphere. The time can be computed from the simple radioactive decay $\mu = \mu_{ex}\, e^{-\lambda t}$ or $\mu_{ex} = \mu\, e^{\lambda t}$. If we develop the Taylor series and keep the first two terms:

$$\mu_{ex} = \mu(1 + \lambda t)t = \frac{1}{\lambda}\left(\frac{\mu_{ex}}{\mu} - 1\right).$$

As for the isotope ratio:

$$R = \frac{1}{\lambda}\left(\frac{\alpha - \alpha_{ex}}{\mu}\right) = \tau.$$

This is the expression of the model age of the reservoir, so we are back to the equality:

residence time = model age.

(This is not so for $^{14}C$ because the product $^{14}N$ is drowned in normal $^{14}N$.)

## Exercise

The $^{87}Sr/^{86}Sr$ isotope composition of sea water is the result of erosion of the continents and of exchange at the mid-ocean ridges where Sr from the mantle is injected into sea water, but also of alteration by volcanoes in subduction zones and oceanic islands. We denote the isotope ratios of the continental crust $()_{cc}$ and of the mantle $()_m$: $(\alpha^{Sr})_{cc} = 0.712$, $(\alpha^{Sr})_m = 0.703$, $(\alpha^{Sr})_{sea\ water} = 0.709$.

What are the relative flows $L_{cc}$ and $L_m$, given that the residence time of Sr is $R_{Sr} = 4 \cdot 10^6$ years and that a steady state is attained in the ocean? If we know the ratio of the mass of river water inflow to the mass of the ocean is $3 \cdot 10^{-5}$, calculate the river/ocean Sr concentration ratio.

### Answer

We write the simplified Wasserburg equations, as there is no radioactive decay or growth term:

$$(\alpha^{Sr}_{cc} - \alpha^{Sr}_{water})\, L_{cc} + (\alpha^{Sr}_{m} - \alpha^{Sr}_{water})\, L_m = 0.$$

We obtain:

$$\frac{L_m}{L_{cc}} = \left(\frac{\alpha^{Sr}_{cc} - \alpha^{Sr}_{water}}{\alpha^{Sr}_{water} - \alpha^{Sr}_{m}}\right) = 0.5.$$

We also have:

$$L_m + L_{cc} = 1/R = 2.5 \cdot 10^{-7}\,\text{yr}^{-1},$$

hence $L_{cc} = 1.66 \cdot 10^{-7}\,\text{yr}^{-1}$ and $L_m = 0.83 \cdot 10^{-7}\,\text{yr}^{-1}$.
We then have:

$$L_{cc} = \frac{\text{river water flow} \times \text{Sr concentration in rivers}}{\text{ocean mass} \times \text{Sr concentration in ocean}},$$

hence

$$\frac{\text{Sr concentration in rivers}}{\text{Sr concentration in sea water}} = 0.005.$$

## Exercise

Suppose the variation in continental Sr input into sea water follows the tectonic cycle with a period of 100 Ma. Suppose also that this fluctuation occurs with constant isotope composition for the continental crust and mantle. By how much would the $^{87}Sr/^{86}Sr$ isotope ratio of sea water as indicated by limestone be offset?

**Answer**
It would not be offset. See Section 8.4.

### 8.4.3 The non-steady state

Naturally enough, in the general case, all of the parameters are a function of time: $F(t)$, $\mu_{ex}(t)$, and $L(t)$. It is not generally very easy to integrate these equations when we are unaware a priori of the form of variation of the various parameters. It can easily be seen that if we write $L(t) = 0$, that is, if we are in the case of evolution with no input from outside, without mixing, we come back to the equations developed in Chapter 3 for open geochronological systems with $F(t)$ taking the form of an episodic or continuous loss. Conversely, if we cancel the terms of radioactive decay, we are dealing with pure mixing. The mixing equation we are used to is:

$$\alpha_M = \alpha_1 x + \alpha_2(1 - x).$$

Let us assume that $\alpha_M = \alpha(t+1)$ and $\alpha = \alpha(t)$ are the two values of the reservoir at $(t+1)$ and $(t)$. If we modify the value $\alpha$ of the reservoir by adding a corresponding quantity to $\Delta x$ from the outside, then:

$$\alpha_2(t+1) = (\alpha_1 - \alpha(t))\Delta x + \alpha(t),$$

therefore

$$\alpha(t+1) - \alpha(t) = \Delta\alpha = (\alpha_1 - \alpha)\Delta x.$$

This is the expression for differential mixing already established.

Wasserburg's equations may be extended to several reservoirs exchanging material and with different isotope ratios. For each reservoir, we write:

$$\begin{cases} \dfrac{d\mu}{dt} = \left[\displaystyle\sum_{i=1}^{i=n} Fi \; - \; \lambda\right] \mu \; + \; \sum_{i=1}^{i=n} (\mu_i \; - \; \mu) \; L_i \\ \dfrac{d\alpha}{dt} = \lambda\mu \; + \; \displaystyle\sum_{i=1}^{i=n} (\alpha_i \; - \; \alpha) \; L_i \end{cases}$$

where *Fi* is the total of fractionation factors.

There are as many pairs of equations as there are reservoirs and we switch therefore to a matrix system whose solution is complex and generally difficult to solve because there are many unknown, time-dependent parameters. However, in some cases it can be approximated.

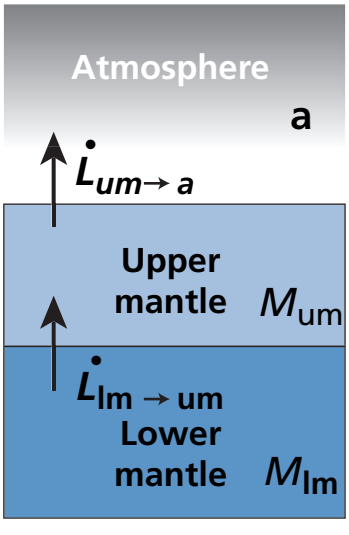


**Figure 8.15** The simplified three-reservoir system.

## Exercise

A simplified three-reservoir system is considered: the lower mantle (lm), upper mantle (um), and atmosphere (a) with transfers of radiogenic rare gases described by the transfer coefficients shown in Figure 8.15, plus a chemical fractionation (*F*) during the transition from the upper mantle to the atmosphere.

Write the matrix equation describing the dynamic evolution of the system. It is assumed there is no reverse transfer either from the atmosphere to the upper mantle or from the upper

to the lower mantle and that transfer from the lower to upper mantle does not involve chemical fractionation.

Keep the $\alpha$ and $\mu$ notations as used in this book.

### Answer

The subscripts to denote the reservoirs are a = atmosphere, um = upper mantle, lm = lower mantle.

$$\mu = \begin{bmatrix} \mu_{a} \\ \mu_{um} \\ \mu_{lm} \end{bmatrix} \text{ and } \alpha = \begin{bmatrix} \alpha_{a} \\ \alpha_{um} \\ \alpha_{lm} \end{bmatrix}.$$

$$\frac{d\mu}{dt} = [T_{\mu}]\mu$$

where $[T_{\mu}]$ is the transfer matrix of $\mu$.

$$\frac{d\alpha}{dt} = [T_{\alpha}]\,\alpha + \lambda\mu$$

where $[T_{\alpha}]$ is the transfer matrix of $\alpha$.

$$[T_{\mu}] = \begin{vmatrix} 0 & 0 & 0 \\ 0 & -(\lambda - F + L_{lm\to um}) & +L_{lm\to um} \\ 0 & 0 & -\lambda \end{vmatrix} \text{ and } [T_{\alpha}] = \begin{vmatrix} -L_{um\to a} & +L_{um\to a} & 0 \\ 0 & -L_{lm\to um} & +L_{lm\to um} \\ 0 & 0 & 0 \end{vmatrix}.$$

This exercise is designed to show how complex the problems are, but also to prepare readers for the mathematical processing used in research work.

The cases of stable isotopes may also be covered by generalizing from these equations somewhat, but in this case, we must consider a combined formula because while there is no radioactive decay to be considered there is isotope fractionation.

By positing $\alpha_s$ = stable isotope ratio, we can write:

$$\frac{d\alpha_s}{dt} = F_i\,\alpha_s + \sum_i \left(F_{ex}\,\alpha_s^i - \alpha_s\right) L^i(t)$$

where $F_i$ is fractionation internal to the system and $F_{ex}$ is fractionation for elements entering the system. This equation shows how worthwhile but how difficult it is to use stable isotopes in balance processes, because it involves an extra parameter – fractionation.

EXAMPLE

## The crust–mantle system

Consider the continental crust-mantle system. Let us take the example of exchange between the continental crust and the mantle. Let us keep our conventional use of $\mu$ and $\alpha$; let us take the $^{87}Rb/^{86}Sr$ system to clarify things. To simplify, we shall assume that the $\mu$ values for the mantle are much lower than those for the continental crust.

The evolution of the crust is written:

$$\frac{d\mu_{cc}}{dt} = -\lambda\mu_{cc} + \left(\mu_{\downarrow m} - \mu_{cc}\right) L$$

$$\frac{d\alpha_{cc}}{dt} = +\lambda\mu_{cc} + (\alpha_{\downarrow m} - \alpha_{cc})\, L$$

where $\mu_{\downarrow m}$ and $\alpha_{\downarrow m}$ indicate the transfer from the mantle to the continental crust.

It is assumed, to simplify matters, that $L$ is constant over time. Integrating the equation in $\mu$ gives:

$$\mu_{cc} = \frac{\mu_{m\downarrow}\, L}{\lambda + L}\left[1 - e^{-(\lambda+L)t}\right] + \mu_{0cc}\, e^{-(\lambda+L)t},$$

$\mu_{0cc}$ being the initial value for continental crust. Notice straight away that since $1 - e^{(\lambda+L)t}\, e^{(\lambda+L)t} = 1$, this is a mixing-type equation whose proportions are time dependent. If $x(t) = e^{(\lambda+L)t}$, we get:

$$\mu_{cc} = \frac{\mu_{m\downarrow}\, L}{\lambda + L}(1 - x(t)) + \mu_{0cc}\, x(t),$$

from which $L$ is of the order of $0.3 \cdot 10^{-9}$ yr$^{-1}$ and $\lambda = 0.0142 \cdot 10^{-9}$ yr$^{-1}$. Therefore $\frac{\mu_{m\downarrow} L}{\lambda + L} \approx \mu_{m\downarrow}$, which is much less than $\mu_{cc}$ and is ignored.

$$\frac{d\alpha_{cc}}{dt} = \lambda\, \mu_{0cc}\, e^{-(\lambda+L)t} + (\alpha_{m\downarrow} - \alpha_{cc})\, L.$$

Integrating gives:

$$\alpha_{cc} = [\alpha_{cc} + \lambda\mu_{0cc}\, t]\, e^{-(\lambda+L)t} + \alpha_{m\downarrow}\left[1 - e^{-(\lambda+L)t}\right].$$

Notice that this is a mixing equation between the evolution of isolated continental crust (whose evolution is written $\alpha_{0cc} + \lambda\mu_{0cc}\, t$) and the $\alpha_{m\downarrow}$ coming from the mantle, which we have taken to be constant, the terms of the mix being weighted by $e^{-Lt}$ (Figure 8.16).

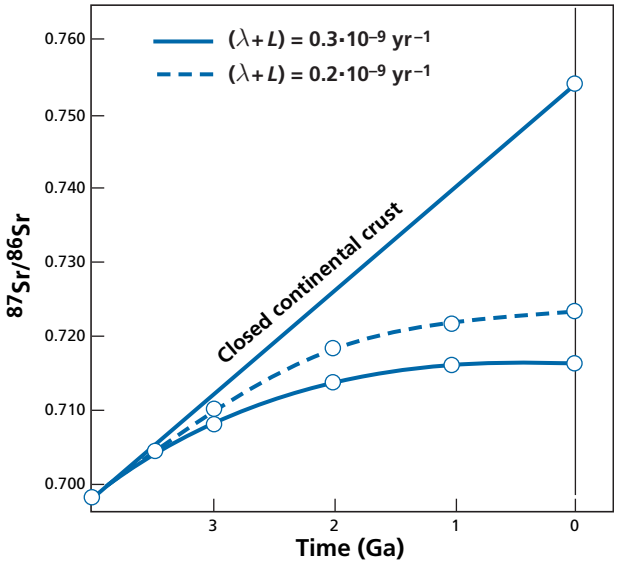


**Figure 8.16** Results of the exercise above with $\mu_{cc} = 0.1$.

## Exercise

Write the Wasserburg equation for stable isotopes (e.g., $^{18}O/^{16}O$) in $\delta$ notation.

### Answer

$$\frac{d\delta}{dt} = (\delta - \Delta_{s\uparrow}) + \sum (\delta_i - \Delta_{i\downarrow})\, L^i(t).$$

The $\Delta_{i\downarrow}$ are isotopic fractionations during transfer from sources to the exterior, and $\Delta_{s\uparrow}$ is the isotopic fractionation towards the reservoir, the $L^i(t)$ are identical to those already defined.

## Exercise

Consider the sea water reservoir. The concentration of elements is determined by the influx of products of erosion from rocks of continental and mantle origin.

We assume the equation governing this composition is written for element $i$:

$$\frac{dC^i}{dt} = J_i(t) - k_i C^i$$

and that $1/k_i = R_i$ is the residence time of element $i$. It is assumed that:
$J_i(t) = J_{0i} + bi \sin \omega t$
where $\omega = 2\pi/10^4$ yr$^{-1}$.
For all elements we take $J_0 = Gi = 1$.

Calculate the curves of variation of $C^i$ for the elements Nd: $R_i = 1000$ years, Os: $R_i = 30\,000$ years, and Sr: $R_i = 2 \cdot 10^6$ years.

### Answer

See Figure 8.10.

## 8.4.4 Statistical evolution of radiogenic systems: mixing times

Here, we shall again take the example of the upper mantle, but our approach is more general and could apply to other convective geochemical reservoirs like the ocean, the atmosphere, or a river. We are now going to look at not just the average values although they are essential, but also the statistical distributions that can be described summarily by their different statistical parameters: a mean, a dispersion, an asymmetry, etc. (Allègre and Lewin, 1995).

As said, the upper mantle is subjected to two types of antagonistic processes. First, **chemical fractionation** (extraction of oceanic crust, extraction of continental crust, reinjection of material via subduction phenomena). These processes result in chemical and isotopic heterogeneity with the help of time. Second, it is also subjected to **mixing processes** related to mantle convection, which stretch the rocks, break them, fold them, and mix them. There are also melting processes which also tend to homogenize the isotope ratios of the source zone.

Thus two types of phenomena are opposed: those producing chemical and isotopic dispersion and those which mix, homogenize, and tend to destroy the heterogeneities (see McKenzie, 1979; Allègre *et al.*, 1980; Allègre and Turcotte, 1986).

## Exercise

Suppose that unaltered oceanic crust, altered oceanic crust, and fine sediments plunge into the mantle in a subduction zone. The extreme compositions for the $^{87}Rb$–$^{86}Sr$ system for unaltered oceanic crust are $\alpha_0^{Sr} = 0.7025$ and $\mu^{Rb/Sr} = 0.1$ and for the sediments $\alpha_S^{Sr} = 0.712$ and $\mu^{Rb/Sr} = 0.4$. The altered crust has intermediate values: $\alpha_{0A}^{Sr} = 0.705$ and $\mu^{Rb/Sr} = 0.2$.

What will be the dispersion of the $\alpha$ isotope ratios if this subducted oceanic crust is in the mantle without mixing for 1 billion years?

### Answer

Dispersion can be evaluated by calculating the two extreme values. We obtain 0.703 92 and 0.717 68 respectively for the pieces of unaltered oceanic crust and for the sediments. The difference $\Delta\alpha$ is 0.0137, while the difference in $\alpha^{Sr}$ values during subduction was 0.0095.

We can also calculate it directly:

$$\Delta\alpha = (\Delta\alpha)_{\text{initial}} + \lambda(\Delta\mu)T.$$

Hence $\Delta$ indicates the dispersion: $\Delta\alpha = 0.0095 + 0.004\,26 = 0.0137$. (Notice that given the value of $\lambda$, the term $-\lambda\mu$ is negligible in the evolution of $\mu$.)

Suppose now that these subduction products are subjected to multiple mixing processes in the mantle. Suppose the result is that $\Delta\mu_i$, which was 0.3 initially, becomes $\Delta\mu = 0.1$, and that $\Delta\alpha$ becomes 0.003.

The effectiveness of this isotopic mixing can be measured by the ratio $30/137 = 0.21$ whereas chemical mixing, measured by $0.1/0.3 = 0.33$, is not quite as effective. (This reasoning probably fails to allow for isotope exchange, but it is a first approximation.)

Let us try to generalize these simple examples. We are looking to write an equation derived from Wasserburg's, but dealing with distributions. So we take as variables not the average values, which has already been done, but the dispersions. Dispersion can be measured by the standard deviation (or by the standard deviation of two extreme values, which, as we know, are about three times the standard deviation) (Allègre and Lewin, 1995).

The following equation can be derived from Wasserburg's equations by noting dispersion $\langle\rangle$. Thus we note the dispersion of isotope ratios $\langle\alpha\rangle$ and the dispersion of chemical ratios $\langle\mu\rangle$ with subscripts $\alpha_{ex}$ (external), $\alpha_i$ (internal), $\mu_{ex}$ (external), and $\mu_i$ (internal).

$$\frac{d\langle\mu_i\rangle}{dt} = [\langle\mu_{ex}\rangle - \langle\mu_i\rangle]\, L - M\langle\mu_i\rangle$$

where the term $-\lambda\langle\mu_i\rangle$ is ignored (Figure 8.17).

The new term that has been introduced is $M\langle\mu_i\rangle$, the term of homogenization of the mixture; $M$ has the dimension of the inverse of a time we shall call **mixing time** ($\tau$). It is the time it takes to reduce the dispersion $\langle\mu\rangle$ by a factor (e) exponential. Suppose a steady state is attained, then:

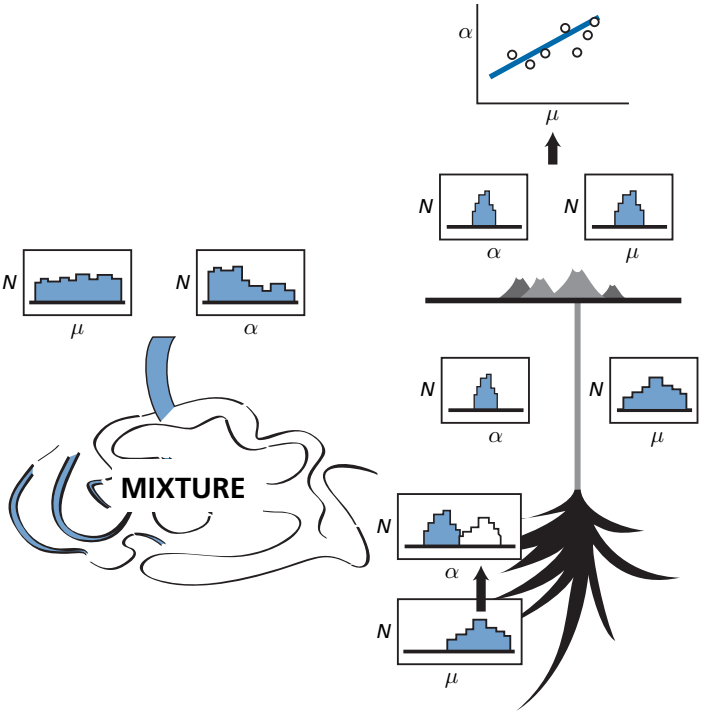


**Figure 8.17** Diagram explaining how the histograms for parameters $\mu$ and $\alpha$ evolve during the geodynamic cycle. Values of $\alpha$ and $\mu$ are represented by histograms. We start on the left with a dispersed histogram for $\alpha$ and $\mu$. In the mantle the spread is reduced by mixing but supplementary $\alpha$ is heated by radioactivity (white in histogram). Then melting reduces the spread of $\alpha$ but not so much as for $\mu$.

$$\langle \mu_i \rangle = \langle \mu_{ex} \rangle \frac{L}{M + L}.$$

Replacing $L$ by its expression $1/\text{residence time} = 1/R$ and $M = 1/\tau$, gives:

$$\langle \mu_i \rangle = \langle \mu_{ex} \rangle \frac{\tau}{R + \tau}.$$

If $\tau \ll R$, mixing is very rapid and $\langle \mu_i \rangle \rightarrow 0$ when $\tau \rightarrow 0$. This is intuitive enough. If mixing time is short, homogenization is vigorous and therefore the standard deviation is zero. If, conversely, $\tau \gg R$, homogenization is poor and $\langle \mu_i \rangle = \langle \mu_{ex} \rangle$: dispersion in the reservoir is the same as that introduced.

For isotope ratios, the equation for standard deviation is written:

$$\frac{d\langle \alpha_i \rangle}{dt} = \frac{\langle \alpha_{ex} \rangle - \langle \alpha \rangle}{2R} + \frac{\lambda}{2} \langle \mu \rangle - \frac{\langle \alpha \rangle}{2\tau}.$$

Let us make two remarks. The first, a purely arithmetical one, is that the factor $^1/_2$ is found everywhere because the calculation made rigorously with variance is $d\langle \alpha \rangle^2 / dt = 2\langle \alpha \rangle \, d\langle \alpha \rangle / dt$. The second and more important remark is that in the terms of creation

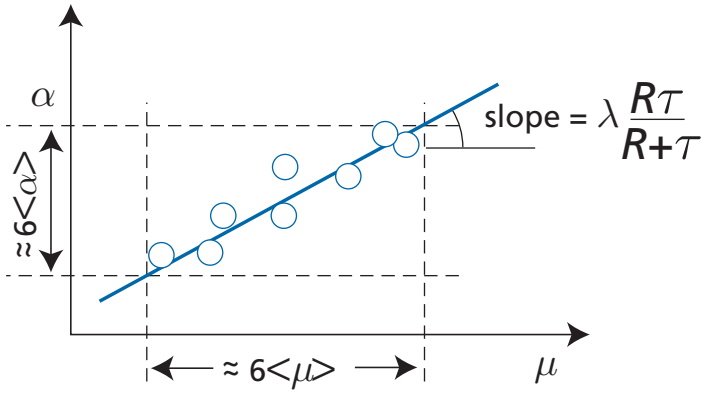


**Figure 8.18** Mantle isochrons constructed from dispersion of ($\mu$) and ($\alpha$). The slope gives a pseudo-age ($R + \tau$).

of heterogeneity, there is the term of external inputs in $\langle \alpha_{ex} \rangle$ but also a term from the dispersion of $\langle \mu \rangle$ values.

If $\lambda$ is small enough for us to speak of a steady state, we get:

$$\langle \alpha_i \rangle = \lambda \langle \mu_i \rangle \left( \frac{R\tau}{R + \tau} \right) + \langle \alpha_{ex} \rangle \left( \frac{\tau}{R + \tau} \right).$$

If $\tau$ is small compared with $R$ (very active mixing):

$$\langle \alpha_i \rangle \approx \lambda \langle \mu_i \rangle \tau + \langle \alpha_{ex} \rangle \left( \frac{\tau}{R} \right).$$

If $\tau$ is very small, $\langle \alpha_i \rangle$ in the mixture is also very small. The mantle is therefore isotopically very homogeneous (small standard deviation).

If $\tau$ is much larger than $R$, mixing is poor, and the standard deviation is equal to the standard deviation of $\mu$ multiplied by residence time, plus the deviation of input from outside.

Let us examine the relationship there may be between the dispersion of $\langle \alpha \rangle$ and that of the $\langle \mu \rangle$ values. We saw when calculating the least squares that in an ($\alpha$, $\mu$) plot, the statistical slope equals $\langle \alpha \rangle / \langle \mu \rangle$ (the ratio of standard deviations multiplied by the correlation coefficient of approximately 1).

If we plot the points representing mantle rock on an ($\alpha$, $\mu$) diagram, e.g., ($^{143}Nd/^{144}Nd$, $^{147}Sm/^{144}Nd$) or ($^{87}Sr/^{86}Sr$, $^{87}Rb/^{86}Sr$), the slope of the straight line yielding an apparent age is equal to the ratios of the standard deviations of the ($\alpha$) and ($\mu$) values.

If it can be considered that $\langle \alpha_{ex} \rangle$ is about constant (this is not the absolute value of $\alpha_{ex}$ but its dispersion!), the slope is equal to $R\tau/(R + \tau)$ (Figure 8.18).

If $\tau$ is small compared with $R$, the slope is about equal to ($\tau$), the mixing time. Unfortunately it is not easy to estimate $\langle \mu \rangle$, the "chemical" dispersion ratio, because chemical fractionation in basalt formation greatly increases $\langle \mu \rangle$ dispersion even if it can be assumed that $\langle \alpha \rangle$ remains the same.

The slope of the correlation diagram obtained for basalts is then written:

$$D \left( \frac{R\tau}{R + \tau} \right)$$

where $D$ is a coefficient greater than unity and rather difficult to estimate.

This difficulty makes the exercise somewhat hazardous. Let us attempt it none the less to get an order of ideas. An isochron has been obtained on oceanic basalt by the $^{147}Sm/^{144}Nd$ method with an age of 350 Ma.

Let us admit a value for $D$ between 2 and 1.5 and a value of $R = 1$ Ga for the residence time of the upper mantle. This gives a mixing time $\tau$ of 530 Ma.

Another way of addressing the issue is to use the $^4He/^3He$ ratios (Allègre *et al.*, 1995). The ratios measured in MORB are the outcome of mixing of OIB ratios which represent an unmixed mantle. As Figure 6.18 shows, the $^4He/^3He$ ratios of MORB seem to be slightly dispersed around the average for OIB.

Suppose, as a first approximation, that the dispersion caused by the decay of uranium is faithfully reflected by the OIB. We can then write:

$$\frac{\langle \alpha_{MORB} \rangle}{\langle \alpha_{OIB} \rangle} = \frac{\tau}{R + \tau}.$$

With $\langle \alpha_{OIB} \rangle = 45 \cdot 10^3$ and $\langle \alpha_{MORB} \rangle = 9$, and still taking $R = 1$ Ga, we find $\tau = 0.25$ Ga. We are still dealing with the same order of magnitude but this time it is for the mantle MORB source alone.

There are two important points to remember from this section. **If we have an $(\alpha, \mu)$ relation for present-day rocks from the mantle, therefore from a convecting reservoir, the slope does not measure the age of some sudden past event but is related to the physical characteristics of the reservoir: mixing time and residence time**. We must henceforth set about describing geochemical reservoirs not by average parameters but by distributions and even by regionalized distributions. Work is under way in this direction.

Notice too that a number of conclusions about the case where external dispersion fluctuates with $\sin \omega t$ can be applied to the dispersion equation. The decisive parameter in this case is $L/(M + L)$, that is: $\tau/(R + \tau)$. Dispersion will be in phase or out of phase, damped or undamped, depending on the value of this parameter. We leave this matter to readers who wish to investigate this area further and who, for this purpose, may transpose the calculations already set out.

## Exercise

It is supposed that the $^4He/^3He$ ratios of the upper mantle vary as a result of dispersion introduced by variable ratios of the OIBs and of mantle convection (see Allègre *et al.*, 1995). The values measured on OIB by $^4He/^3He$ ratios are: mean 93 390, dispersion 45 330.

The values measured for MORB of the North Atlantic ridges are: mean 8938, dispersion 9330.

Calculate the upper mantle mixing time in the North Atlantic, given that the residence time for the Atlantic lithosphere is 1.3 Ga.

The residence time of the North Pacific upper mantle is 582 Ma and the dispersion 3000. Calculate the mixing time of these two zones of the upper mantle.

### Answer

The mixing times for the two upper mantle zones are 300 Ma for the North Atlantic and 40 Ma for the North Pacific.

# Problems

**1** Consider a reservoir whose concentrations evolve in accordance with the equation with standard notation: $dC/dt = J - kC^2$, which is therefore a non-linear evolution equation. What is the residence time of the element in question? Can you imagine a geochemical process for which such a formula might apply? What is the system's response law if a flux $J_0$ is suddenly injected and then left to evolve by itself?

**2** It is assumed that erosion fluctuates with glacial cycles. These cycles are supposedly modeled by the superimposition of three frequencies: 100 ka, 40 ka, and 20 ka, with relative amplitudes of 2, 1, and 1, respectively. Uranium has a residence time in the ocean of 3 Ma. Supposing that the $^{234}U/^{238}U$ ratios injected into rivers vary with climate, draw the $^{234}U/^{238}U$ response curve of the ocean (without calculating).

**3** The residence time of oceanic lithosphere in the primitive upper mantle is 1 Ga. It can be supposed that the corresponding 70 km of mantle are fully degassed when they go through the mid-ocean ridge. The $^4He$ in the upper mantle is the sum of two terms: the radiogenic part formed *in situ* over 1 Ga and the part coming from the lower mantle at the same time as the $^3He$.

(i) Calculate how much $^4He$ accumulated in 1 Ga in the upper mantle with U = 5 ppm and Th/U = 2.5.

(ii) Given that the degassing of $^3He$ from the mid-ocean ridge is $1 \cdot 10^3$ moles $yr^{-1}$ and that $^4He/^3He = 10^5$, calculate the residence time of $^4He$ in the upper mantle.

(iii) What do you conclude about the melting process at the mid-ocean ridges?

**4** Suppose that the dispersion of $^4He/^3He$ ratios in the upper mantle is due to the incorporation of a dispersion through the OIB counterbalanced by mantle convection. Dispersion measured in the MORB of various oceans is given in the table below.

| | Dispersion | Expansion rate (cm $yr^{-1}$) | Residence time (Ma) |
|---|---|---|---|
| North Atlantic | 9 000 | 2.3 | 1400 |
| South Atlantic | 6 000 | 3.5 | 900 |
| South-west Indian Ocean | 11 000 | 1.7 | 1600 |
| North Pacific | 3 000 | 8.0 | 580 |
| Central Indian Ocean | 4 700 | 3.6 | 700 |

Ocean expansion rates are also given in the table along with the residence time of oceanic lithosphere in the corresponding mantle province. Calculate the mixing time of the various portions of the upper mantle, given that the OIB dispersion is 45 000. Is there a relation with the expansion rate? What is the relation? Draw it.

**5** Consider Figure 8.2 showing the hydrological cycle. Construct a system of boxed reservoirs, with four boxes: atmosphere/ocean, atmosphere/landmass, groundwater/runoff, and oceans. Draw the input and output and the corresponding flows for each box. What is the residence time of water in each box? What is the proportion of ocean going through the groundwater/runoff box and that has flowed into the sea as rivers over 1 million years?

# REFERENCES

## Chapter 1


Aldrich, L. T., Doak, J. B., and Davis, G. (1953). The use of ion exchange columns in universal analysis for age determination. *Am. J. Sci.* **251**, 377–80.

Arriens, P. A. and Compston,W. (1968). A method for isotopic ratio measurement by voltage peak switching and its applicaton with digital input. *Int. J. Spectrom. Ion Phys.* **1**, 471–81.

Aston, F. W. (1919). A positive ray spectograph. *Phil. Mag.* (Series 6) **38**, 707–14.

Bainbridge, K. T. and Jordan, E. B. (1936). Mass spectrum analysis. *Harvard Univ., Jefferson Phys. Lab. Contrib.* (Series 2) **3**, No. 2.

Becquerel, H. (1896a). Sur les radiations invisibles émises par phosphorescence. *Comptes Rend. Acad. Sciences Paris* **122**, 420.

Becquerel, H. (1896b). Sur les radiations invisibles émises par les corps phosphorescents. *Comptes Rend. Acad. Sciences Paris* **122**, 501.

Becquerel, H. (1896c). Sur les radiations invisibles émises par les sels d'uranium. *Comptes Rend. Acad. Sciences Paris* **122**, 689.

Beiser, A. (1973). *Concepts of Modern Physics*. New York: McGraw-Hill.

Burchfield, J. D. (1975). *Lord Kelvin and the Age of the Earth*. London: Macmillan.

Curie, P. (1902a). Sur la constante de temps caracteristique de la disparition de la radioactivité induite par le radium dans une enceinte fermée. *Comptes Rend. Acad. Sciences Paris* **135**, 857.

Curie, P. (1902b). Nobel Lecture (6 June 1902). In *Nobel Lectures*, Stockholm: Royal Swedish Academy.

Curie, P. and Laborde, A. (1903). Sur la chaleur dégagée spontanément par les sels de radium. *Comptes Rend. Acad. Sciences Paris* **136**, 673–5.

Ingram, M. G. and Chupka,W. A. (1953). Surface ionisation source using multiple filaments. *Rev. Sci. Instrum.* **24**, 518–20.

Mattauch, R. H. (1934). Über eine neuen Masspektrographen. *Z. Physik* **89**, 786–95.

Nier, A. O. (1940). A mass spectrometer for routine isotope abundance measurements. *Rev. Sci. Instrum.* **11**, 212–16.

Rutherford, E. and Soddy, F. (1902a). The cause and nature of radioactivity. Pt. I. *Phil. Mag.* (Series 6) **4**, 370–96.

Rutherford, E. and Soddy, F. (1902b). The cause and nature of radioactivity. Pt. II. *Phil. Mag.* (Series 6) **4**, 569–85.

Rutherford, E. and Soddy, F. (1902c). The radioactivity of thorium compounds. Pt. II. The cause and nature of radioactivity. *J. Chem. Soc. Lond.* **81**, 837–60.

Rutherford, E. and Soddy, F. (1903). Radioactive change. *Phil. Mag.* (Series 6) **5**, 576–91.

Thomson, J. J. (1914). Rays of positive electricity. *Proc. Roy. Soc. Lond.* (Series 5) **89**, 1–20.

Wasserburg, G. J., Papanastassiou, D., Nerow, E.V., and Bauman, C. A. (1969). A programmable magnetic field spectrometer with online data processing. *Rev. Sci. Instrum.* **40**, 288–95.

## Chapter 2


Aldrich, L. T. and Nier, A. O. (1948a). Argon 40 in potassium minerals. *Phys. Rev.* **74**, 876–7.

Aldrich, L. T. and Nier, A. O. (1948b). The occurrence of $^{3}$He in natural sources of helium. *Phys. Rev.* **74**, 1590–4.

Aldrich, L. T., Herzog, L., Holve, W., Witting, F., and Ahrens, L. (1953). Variation in isotopic abundance of strontium. *Phys. Rev.* **86**, 631–4.

Barbo, L. (2003). *Les Becquerel: Une Dynastie des Scientifiques*. Paris: Belin.

Bateman, H. (1910). Solution of a system of differential equations occurring in the theory of radio-active transformations. *Proc. Cambridge Phil. Soc.* **15**, 423–7.

Birck, J. L. and Allègre, C. J. (1985). Evidence for the presence of $^{53}$Mn in the early solar-system. *Geophys. Res. Lett.* **12**, 745–8.

Harper, C. L. and Jacobsen, S. B. (1994). Investigation of $^{182}$Hf–$^{182}$W systematics. *Lunar Plan. Sci.* **25**, 509–10.

Hirt, B., Tilton, G. R., Herr, W., and Hoffmeister, W. (1963). The half-life of $^{187}$Re. In Geiss, J. and Goldberg, E. D. (eds.) *Earth Science and Meteorites*, Amsterdam: North-Holland, pp. 273–80.

Ivanovich, M. (1982). Uranium series disequilibria application in geochronology. In Ivanovich, M. and Harmon, R. (eds.) *Uranium Series Disequilibrium: Application to Environmental Problems*, Oxford, UK: Oxford University Press, pp. 56–78.

Jeffrey, P. M. and Reynolds, J. H. (1961). Origin of excess $^{129}$Xe in stone meteorites. *J. Geophys. Res.*, **66**, 3582–3.

Kelly, W. R. and Wasserburg, G. J. (1978). Evidence for the existence of $^{107}$Pd in the early Solar System. *Geophys. Res. Lett.* **5**, 1079–82.

Kuroda, P. K. (1960). Nuclear fission in the early history of the Earth. *Nature* **187**, 36–8.

Lee, D.-C. and Halliday, A. N. (1995). Hafnium–tungsten chronometry and the timing of terrestrial core formation. *Nature* **378**, 771–4.

Lee, T., Papanastassiou, D. A., and Wasserburg, G. J. (1977). Aluminium-26 in the early solar-system: fossil or fuel? *Astrophys. J. (Lett.)* **211**, L107–10.

Leighton, R. B. (1959). *Principles of Modern Physics*. New York: McGraw-Hill.

Lin, Y., Guan, Y., Leshin, L. A., Ouyang, Z., and Wang, D. (2005). Short-lived chlorine-36 in a Ca- and Al-rich inclusion from the Ningqiang carbonaceous chondrite. *Proc. Natl Acad. Sci. USA* **102**, 1306–11.

Luck, J. M., Birck, J. L., and Allègre, C. J. (1980). $^{187}$Re–$^{187}$Os systematics in meteorites: early chronology of the solar system and the age of the galaxy. *Nature* **283**, 256–9.

Lugmair, G. W. and Marti, K. (1977). Sm–Nd–Pu timepieces in the Angra dos Reis meteorite. *Earth Planet. Sci. Lett.* **35**, 273–84.

Lugmair, G. W., Scheinin N. B., and Marti, K. (1975). Search for extinct $^{146}$Sm. Pt. I. The isotopic abundance of $^{143}$Nd in the Juvinas meteorite. *Earth Planet. Sci. Lett.* **27**, 9479–84.

McKeegan, K. D., Chaussidon, M., and Robert, F. (2000). Incorporation of short-lived $^{10}$Be in a calcium–aluminium-rich inclusion from the Allende meteorite. *Science* **289**, 1334–7.

Nakaï, S., Shimizu, H., and Masuda, A. (1986). A new geochronometer using lanthanum-138. *Nature* **320**, 433–5.

Nielsen, S. G., Rehkämper, M., and Halliday, A. N. (2006). Large thallium isotopic variation in iron meteorites and evidence for lead-205 in the early solar system. *Geochim. Cosmochim. Acta* **70**, 2643–57.

Notsu, K., Mabuchi, H., Yoshioka, O., Matsuda, J., and Ozima, M. (1973). Evidence of the extinct nuclide $^{146}$Sm in "Juvinas" achondrite. *Earth Planet. Sci. Lett.* **19**, 29–36.

Patchett, P. J. and Tatsumoto, M. (1980a). Lu–Hf total rocks isochron for eucrite meteorites. *Nature* **288**, 263–7.

Patchett, P. J. and Tatsumoto, M. (1980b). A routine high-precision method for Lu–Hf isotope geochemistry and chronology. *Contrib. Mineral. Petrol.* **75**, 263–7.

Price, P. B. and Walker, R. M. (1962). Observation of fossil particle tracks in natural micas. *Nature* **196**, 732–4.
Ramsay, W. and Soddy, F. (1903). Gases occluded in radium bromide, *Nature* **68**, 246.
Reynolds, J. H. (1960). Determination of the age of the elements. *Phys. Rev. Lett.* **4**, 8–10.
Rutherford, E. (1906). *Radioactive Transformations*. New York: Charles Scribner's Sons.
Schonbachler, M., Rehkämper, M., Halliday, A. N., *et al.* (2002). Niobium–zirconium chronometry and early Solar System development. *Science* **295**, 1705–8.
Shukolyukov, A. and Lugmair, G. W. (1993). Live iron-60 in the early solar system. *Science* **259**, 1138–42.
Srinivasan, G., Ulyanov, A. A., and Goswami, J. N. (1994). $^{41}$Ca in the early Solar System. *Astrophys. J. (Lett.)* **431**, L67–70.

## Chapter 3

Ahrens, L. H. (1955). Implications of the Rhodesia age pattern. *Geochim. Cosmochim. Acta* **8**, 1–15.
Aldrich, L. T. and Nier, A. O. (1948a). Argon-40 in potassium minerals. *Phys. Rev.* **74**, 876–7.
Aldrich, L. T. and Nier, A. O. (1948b). The occurrence of $^{3}$He in natural sources of helium. *Phys. Rev.* **74**, 1590–4.
Aldrich, L. T. and Wetherill, G. W. (1958). Geochronology by radioactive decay. *Ann. Rev. Nuclear Sci.* **8**, 257–98.
Allègre, C. J. (1964). Géochronologie: de l'extension de la méthode de calcul graphique concordia aux mesures d'âges absolus effectués à l'aide du déséquilibre radioactif – cas des minéralisations secondaires d'uranium. *Comptes Rend. Acad. Sciences Paris* **259**, 4086–9.
Allègre, C. J. (1967). Méthode de discussion géochronologique concordia généralisée. *Earth Planet. Sci. Lett.* **2**, 57–66.
Allègre, C. J. (1968). $^{230}$Th dating of volcanic rocks: a comment. *Earth Planet. Sci. Lett.* **5**, 209–10.
Allègre, C. J. and Condomines, M. (1976). Fine chronology of volcanic processes using $^{238}$U/$^{230}$Th systematics. *Earth Planet. Sci. Lett.* **28**, 395–406.
Allègre, C. J. and Dars, R. (1966). Chronologie au rubidium–strontium et granitologie. *Geol. Rundschau* **8–55**, 226–37.
Allègre, C. J. and Michard, G. (1964). Sur les discordances des âges obtenus par les méthodes au strontium et à l'argon. *Comptes Rend. Acad. Sciences Paris* **259**, 4313–16.
Allègre, C. J., Albarède, F., Grünenfelder, M., and Köppel, V. (1974). $^{238}$U/$^{206}$Pb–$^{235}$U/$^{207}$Pb–$^{232}$Th/$^{208}$Pb zircon geochronology in Alpine and non-Alpine environments. *Contrib. Mineral. Petrol.* **43**, 163–244.
Allègre, C. J., Birck, J.-L., Capmas, F., and Courtillot, V. (1999). Age of the Deccan Traps using $^{187}$Re–$^{187}$Os systematics. *Earth Planet. Sci. Lett.* **170**, 197–204.
Berger, G. W. and York, D. (1981). Geothermy from $^{40}$Ar/$^{39}$Ar dating experiments. *Geochim. Cosmochim. Acta* **45**, 795–811.
Blichert-Toft, J., Albarède, F., and Kornpolst, J. (1999). Lu–Hf isotope systematics of garnet pyroxenites from Beni-Bousera, Morocco: implication from basalt origin. *Science* **283**, 1303.
Brévart, O., Dupré, B., and Allègre, C. J. (1986). Lead–lead age of the komatiitic lavas and limitations on the structure and evolution of the Precambrian mantle. *Earth Planet. Sci. Lett.* **77**, 293–303.
Castaing, R. and Slodzian, G. (1962). Optique corpusculaire: premiers essais de microanalyse par émission ionique secondaire. *J. Microsp.* **395**, 185–9.
Compston, W. and Jeffrey, P. M. (1959). Anomalous common strontium in granite. *Nature* **184**, 1792–3.
Compston, W., Williams, I. S., and Meyer, C. (1984). U–Pb geochronology of zircons from lunar breccia 73217 using a sensitive high mass-resolution ion microprobe. *J. Geophys. Res.* **89** (Suppl.), B525–34.

Davis, G. and Aldrich, L. T. (1953). Determination of the age of lepidolites by the method of isotope dilution. *Bull. Geol. Soc. Amer.* **64**, 379–80.

De Sigoyer, J., Chavagnac, V., Blichert-Toft, J., *et al.* (2000). Dating the Indian continental subduction and collisional thickening in the north-west Himalaya multichronology of the Morai eclogites. *Geology* **28**, 487–90.

Hamilton, P. J., Evensen, N. M., O'Nions, R. K., and Tarney, J. (1979). Sm–Nd systematics of Lewisian gneisses: implications for the origin of granulites. *Nature* **277**, 25–8.

Hanson, G. N. and Gast, P. W. (1967). Kinetic studies in contact metamorphic zones. *Geochim. Cosmochim. Acta* **31**, 1119–53.

Harrison, T. M. and McDougall, I. (1981). Excess $^{40}$Ar in metamorphic rocks from Broken Hill. *Earth Planet. Sci. Lett.* **55**, 123–49.

Hart, S. R. (1964). The petrology and isotopic–mineral age relations of a contact zone in the Front Range, Colorado. *J. Geol.* **72**, 493–525.

Hirt, B., Tilton, G. R., Herr, W., and Hoffmeister, W. (1963). The half life of $^{187}$Re. In Geiss, J. and Goldberg, E. (eds.) *Earth Science and Meteorites*, Amsterdam: North-Holland, pp. 273–80.

Hohenberg, C. M., Podosek, F., and Reynolds, J. H. (1967). Xenon–iodine: sharp isochronism in chondrites. *Science* **156**, 233–6.

Hohenberg, C. M., Brazzle, R. H., Pravdivtseva, O., and Meshik, A. P. (1998). Iodine–xenon. *Proc. Indian Acad. Sci.* **107** (no. 4), 1–11.

Kober, B. (1986). Whole-grain evaporation for $^{207}$Pb/$^{206}$Pb-age investigations on single zircons using a double-filament thermal ion source. *Contrib. Mineral. Petrol.* **93**, 482–90.

Köppel, V. and Grünnenfelder, M. (1971). A study of inherited and newly formed zircons from paragneisses and granitized sediments of the Strona-Ceneri zone (Southern Alps). *Schweiz. Miner. Petrog. Mitt.* **51**, 387–411.

Koztolanyi, C. (1965). Nouvelle méthode d'analyse isotopique des zircons à l'état naturel. *Comptes Rend. Acad. Sciences Paris* **260**, 5849–51.

Lancelot, J. R. and Allègre, C. J. (1974). Origin of carbonatitic magma in the light of the Pb–U–Th isotope system. *Earth Planet. Sci. Lett.* **22**, 233–8.

Lanphere, M. A., Wasserburg, G. J., Albee, A. L., and Tilton, G. R. (1964). Redistribution of strontium and rubidium isotopes during metamorphism, World Beater complex, Panamint Range, California. In Craig, H., Miller, S. L., and Wasserburg, G. J. (eds.), *Isotopic and Cosmic Chemistry*, Amsterdam: North-Holland, pp. 269–320.

Lee, D.-C. and Halliday, A. N. (2000). Hf–W internal isochron for ordinary chondrites and the initial $^{182}$Hf/$^{180}$Hf of the solar system. *Chem. Geol.* **169**, 35–43.

Luck, J. M., Birck, J. L., and Allègre, C. J. (1980). $^{187}$Re–$^{187}$Os sytematics in meteorites: early chronology of the solar system and the age of the galaxy. *Nature* **283**, 256–9.

Lugmair, G. W. and Marti, K. (1977). Sm–Nd–Pu timepieces in the Angra dos Reis meteorite. *Earth Planet. Sci. Lett.* **35**, 273–84.

Manhès, G., Allègre, C. J., Dupré, B., and Hamelin, B. (1980). Lead isotopic study of basic–ultrabasic layer complexes: speculations about the age of the Earth and primitive mantle characteristics. *Earth Planet. Sci. Lett.* **47**, 370–82.

Merrihue, C. and Turner, G. (1966). Potassium–argon dating by activation with fast neutrons. *J. Geophys. Res.* **71**, 2852–7.

Michard, A. and Allègre, C. J. (1979). A study of the formation and history of a piece of continental crust by the $^{87}$Rb–$^{87}$Sr method: the case of the French oriental Pyrenees: *Contrib. Mineral Petrol.* **50**, 257–85.

Nicolaysen, L. O. (1961). Graphic interpretation of discordant age measurements on metamorphic rocks. *Ann. N. Y. Acad. Sci.* **91**, 198–206.

Nier, A. O. (1939). The isotopic constitution of radiogenic leads and the measurement of geologic time. Pt. II. *Phys. Rev.* **55**, 153–63.

Notsu, K., Mabuchi, H., Yoshioka, O., Matsuda, J., and Ozima, M. (1973). Evidence of the extinct nuclide $^{146}$Sm in "Juvinas" achondrite. *Earth Planet. Sci. Lett.* **19**, 29–36.

Patchett, P. J. (1983). Importance of the Lu–Hf isotopic system in studies of planetary chronology and chemical evolution. *Geochim. Cosmochim. Acta* **47**, 81–91.

Patchett, P. J. and Tatsumoto, M. (1980). A routine high-precision method for Lu–Hf isotope geochemistry and chronology. *Contrib. Mineral. Petrol.* **75**, 263–7.

Reynolds, J. H. (1960). Determination of the age of the elements. *Phys. Rev. Lett.* **4**, 8–10.

Shukolyukov, Y., Ashkinadze, G., and Komarou, A. (1974). A new $X_{es}$–$X_{en}$ neutron induced method of mineral dating. *Dokl. Akad. Nauka USSR* **219**, 952–4. (in Russian)

Shukolyukov, A., Meshik, A., Meshik, D., Krylov, D., and Pravdivtseva, O. (1994). Current status of $X_{es}$–$X_{en}$ dating. In Matsuda, X. (ed.) *Noble Gas Geochemistry and Cosmochemistry*, pp. 125–00.

Steiger, R. H. and Wasserburg, G. J. (1966). Systematics in the $^{208}$Pb–$^{232}$Th, $^{207}$Pb–$^{235}$U, $^{206}$Pb–$^{238}$U systems. *J. Geophys. Res.* **71**, 6065–90.

Teitoma, A. W., Clarke, C. J., and Allègre, C. (1974). Spontaneous fission – neutron fission in xenon: a new technique for dating geological events. *Science* **189**, 878–80.

Tilton, G. R. (1960). Volume diffusion as a mechanism for discordant lead ages. *J. Geophys. Res.* **65**, 2933–45.

Tilton, G. *et al.* (1958). Isotopic composition and distribution of lead, uranium and thorium in a Precambrian granite. *Bull. Geol. Soc. Amer.* **66**, 1131–48.

Turner, G. (1968). The distribution of potassium and argon in chondrites. In Ahrens, L. H. (ed.) *Origin and Distribution of the Elements*, New York: Pergamon, pp. 387–97.

Vervoort, J. D., Patchett, P. J., Gehrels, G. E., and Nutman, A. P. (1996). Constraints on early Earth differentiation from hafnium and neodymium isotopes. *Nature* **379**, 412–14.

Wasserburg, G. J. (1985). Short-lived nuclei in the early solar system. In Black, D. C. and Matthews, M. S. (eds.) *Protostars and Planets II*, Tucson, AZ: University of Arizona Press, pp. 703–37.

Wasserburg, G. J. and Hayden, R. J. (1955). Time interval between nucleogenesis and the formation of meteorites. *Nature* **176**, 130–1.

Wetherill, G. W. (1956). Discordant uranium–lead ages. *Trans. Am. Geophys. Union* **37**, 320–7.

Wetherill, G. W., Tilton, G. R., Davis, G. L., Hart, S. R., and Hopson, C. A. (1966). Age measurements in the Maryland Piedmont. *J. Geophys. Res.* **71**, 2139–55.

Wetherill, G. W., Davis, G. L., and Lee-Hu, C. (1968). Rb–Sr measurements on whole rocks and separated minerals from the Baltimore Gneiss, Maryland. *Bull. Geol. Soc. Amer.* **79**, 757–62.

York, D., Hall, C. M., Yanese, Y., Hanese, J. A., and Kenyon, W. J. (1981). $^{40}$Ar/$^{39}$Ar dating of terrestrial minerals with a continuous laser, *Geophys. Res. Lett.* **8**, 1136–8.

Zinner, E. (1996). Presolar material in meteorites. In Bernatowicz, T. J. and Zinner, E. (eds.) *Astrophysical Implications of the Laboratory Study of Presolar Material*, New York: American Institute of Physics, 59–72.

## Chapter 4

Arnold, J. R. (1956). Beryllium-10 produced by cosmic rays. *Science* **124**, 584–5.

Atkinson, R. and Houtermans, F. G. (1929). Zur Frage der Aufbaumöglichkeit der Elemente in Sternen. *Z. Physik* **54**, 656–65.

Bard, E., Hamelin, B., Fairbanks, R. G., and Zindler, A. (1990). Calibration of the $^{14}$C timescale over the past 30 000 years using mass spectrometric U–Th ages from Barbados corals. *Nature* **345**, 405–10.

Broecker, W. S. and Li, Y. H. (1970). Interchanges of water between the major oceans. *J. Geophys. Res.* **75**, 354–55.

Broecker, W. S., Gerard, R., Ewig, M., and Heezen, B. C. (1960). Natural radiocarbon in the Atlantic Ocean *J. Geophys. Res.* **65**, 2903–31.

Burbidge, E. M., Burbidge, G. R., Fowler,W. A., and Hoyle, F. (1957). Synthesis of the elements in stars. *Rev. Mod. Phys.* **29**, 547–647.

Gamow, G. (1946). Expanding Universe and the origin of elements. *Phys. Rev.* **70**, 572–5.

Harrison, T. M. and McDougall, I. (1981). Excess $^{40}$Ar in metamorphic works from Broken Hill. *Earth Planet. Sci. Lett.* **55**, 123–49.

Honda, M. and Arnold J. R. (1964). Effects of cosmic rays on meteorites. *Science* **143**, 203–212.

Kieser,W. E., Beukens, R. P., Kilius, L. R., Lee, H.W., and Litherland, A. E (1986). Isotrace radiocarbon analysis: equipment and procedures. *Nucl. Instrum. Meth. Phys. Res. B* **15**, 718–21.

Lal, D. (1988). *In situ*-produced cosmogenic isotopes in terrestrial rocks. *Ann. Rev. Earth Planet. Sci.* **16**, 355–88.

Lal, D. and Peters, B. (1967). Cosmic ray-produced radioactivity on the Earth. In *Handbook of Physics*, vol. 46/2, Berlin: Springer-Verlag, pp. 551–612.

Lal, D., Malhotra, K., and Peters, B. (1958). On the production of radioisotopes in the atmosphere by cosmic radiation and their application to meteorology. *J. Atmos. Ten. Phys.* **12**, 306–28.

Lee, D.-C. and Halliday, A. N. (2000). Hf–W internal isochron for ordinary chondrites and the initial $^{182}$Hf/$^{180}$Hf of the solar system. *Chem. Geol.* **169**, 35–43.

Libby, W. F. (1946). Atmospheric helium-3 and radiocarbon from cosmic radiation. *Phys. Rev.* **69**, 671–672.

Libby, W. F. (1970). Ruminations on radiocarbon dating. In Olsson, I. U. (ed.) *Radiocarbon Variations and Absolute Chronology*, New York: John Wiley, pp. 629–40.

Libby, W. F., Anderson, E. C., and Arnold, J. R. (1949). Age determination by radiocarbon content: world-wide assay of natural radiocarbon. *Science* **109**, 227–8.

Lin,Y., Guan,Y., Leshin, L. A., Ouyang, Z., and Wang, D. (2005). Short-lived chlorine-36 in a Ca- and Al-rich inclusion from the Ningqiang carbonaceous chondrite. *Proc. Natl Acad. Sci. USA* **102**, 1306–11.

Marti, K. (1982). Krypton-81 dating by mass spectrometry. In Lloyd, A. (ed.) *Nuclear and Chemical Dating Techniques in Interpreting the Environmental Record*, American Chemical Society, pp. 129–00.

McKeegan, K. D., Chaussidon, M., and Robert, F. (2000). Incorporation of short-lived $^{10}$Be in a calcium–aluminium-rich inclusion from the Allende meteorite. *Science* **289**, 1334–7.

Merrill P. W. (1952). Technetium in the stars. *Science* **115**, 484–5.

Oeschger, H. (1982). The contribution of radioactive and chemical dating to the understanding of the environmental system. In Lloyd, A. (ed.) *Nuclear and Chemical Dating Techniques in Interpreting the Environmental Record*, American Chemical Society, pp. 5–12.

O'Nions, R. K., Franck, M., von Blanckenburg, F., and Ling, H.-F. (1998). Secular variation of Nd and Pb isotopes in ferromanganese crusts from the Atlantic, Indian and Pacific Oceans. *Earth Planet. Sci. Lett.* **155**, 15–28.

Paneth, F., Raesbeck, P. and Mayne, K., (1952). Helium-3 content and age of meteorites. *Geochim. Cosmochim. Acta* **2**, 300–3.

Staudacher, T. and Allègre, C. J. (1993). Ages of the second caldera of Piton de la Fournaise volcano (Réunion) determined by cosmic ray produced $^{3}$He and $^{21}$Ne. *Earth Planet. Sci. Lett.* **119**, 395–404.

Stuiver, M. (1965). Carbon-14 content of 18th- and 19th-century wood: variations correlated with sunspot activity. *Science* **149**, 533–5.

Voshage, H. and Hintenberger, H. (1960). Cosmogenic potassium in iron meteorites and cosmic ray exposure age. In *Summer Course on Nuclear Geology*, Pisa: Laboratorio di Geologica Nucleare, pp. 81–235.

## Chapter 5


Allègre, C. J., Manhès, G., and Göpel, C. (1995). The age of the Earth. *Geochim. Cosmochim. Acta* **59**, 1445–56.

Barbo, L. (1999). *Pierre Curie: Le Rêve Scientifique*. Paris: Belin.

Barrell, J. (1917). Rhythms and the measurement of geologic time. *Bull. Geol. Soc. Amer.* **28**, 745–50.

Berger, G.W. (1975). 40Ar/39Ar step heating of thermally overprinted biotite, hornblende and potassium feldspar from Eldora (Colorado). *Earth Planet. Sci. Lett.* **26**, 387–90.

Bevington, P. R and Robinson, K. (2003). *Data Reduction and Error Analysis for Physical Sciences*. New York: McGraw-Hill.

Boltwood, B. B. (1907). On the ultimate disintegration products of the radioactive elements. Pt. II. The disintegration products of uranium. *Am. J. Sci.* **23**, 78–88.

Brévart, O., Dupré, B., and Allègre, C. J. (1986). Lead–lead age of komatiitic lavas and limitations on the structure and evolution of the Precambrian mantle. *Earth Planet. Sci. Lett.* **77**, 293–303.

Burchfield, H. P. (1975). *Lord Kelvin and the Age of the Earth*. London: Macmillan.

Clayton, D. D. (1968). *Principles of Stellar Evolution and Nucleosynthesis*. New York: McGraw-Hill.

Crumpler, T. B. and Yeo, J. H. (1940). *Chemical Computation and Errors*. New York: John Wiley.

Dalrymple, B. (1991). *The Age of the Earth*. Stanford, CA: Stanford University Press.

Dupré, B. and Arndt, N. T. (1987) Komatiites: témoins précieux pour retracer l'évolution du manteau. *Bull. Soc. Géol. Fr.* **III**, 1125–32.

Eve, A. S (1939). *Rutherford*. New York: Macmillan.

Gerling, E. K. (1942). Age of the Earth according to radioactivity data. *Dokl. Akad. Nauka USSR* **34–9**, 259–72.

Göpel, C., Manhès, G., and Allègre, C. J. (1994). U–Pb systematics of phosphates from equilibrated ordinary chondrites. *Earth Planet. Sci. Lett.* **121**, 153–71.

Hallam, A. (1983). *Great Geological Controversies*. Oxford, UK: Oxford University Press.

Hamilton, P. J., Eversell, N. M., O'Nions, R. K., Smith, H. S., and Erlank, A. J. (1979). Sm–Nd dating on the Ouverwacht group of volcanoes, South Africa. *Nature* **279**, 298.

Hart, S. R., Davis, G. L., Steiger, R. H., and Tilton, G. R. (1968). A comparison of the isotopic mineral age variations and petrological changes induced by contact morphism. In Hamilton, E. I. and Farquhar, R. M. (eds.) *Radiometric Dating for Geologists*, New York: Wiley Interscience, pp. 73–110.

Hohenberg, C. M. (1969). Radioisotopes and the history of nucleosynthesis in the galaxy. *Science* **166**, 212–15.

Holmes, A. (1911). The association of lead with uranium rock minerals and its application to the measurement of geological time. *Proc. Roy. Soc. Lond. A* **85**, 248–50.

Holmes, A. (1927). *The Age of the Earth: An Introduction to Geological Ideas*. London: Ernest Benn.

Holmes, A. (1946). An estimate of the age of the Earth. *Nature* **157**, 680–4.

Houtermans, F. G. (1946). Die Isotopen-Häufigkeiten im natürlichen Blei und das Alter des Urans. *Naturwissenschaften* **33**, 185–7.

Hutchinson, R. (2004). *Meteorites*. Cambridge, UK: Cambridge University Press.

Kanber, B. S. and Moorbath, S. (1998). Initial Pb of the Amitsoq gneiss revisited: Implication for the timing of early Archean crustal evolution in West Greenland. *Chem. Geol.* **15**, 19–41.

Lee, D.-C. and Halliday, A. N. (2000). Hf–W internal isochron for ordinary chondrites and the initial $^{182}Hf/^{180}Hf$ of the solar system. *Chem. Geol.* **169**, 35–43.

Luck, J. M., Birck, J. L., and Allègre, C. J. (1980). $^{187}Re$–$^{187}Os$ sytematics in meteorites: early chronology of the Solar System and the age of the Galaxy. *Nature* **283**, 256–9.

Ludwig, K. R. (1999). *Using Isoplot/Ex Version 2.01: A Geochonological Toolk it for Microsoft Excel*. Berkeley, CA: Geochronological Center.

Michard-Vitrac, A., Lancelot, J., Allègre, C. J., and Moorbath, S. (1977). U–Pb age on single zircons from Early Precambrian rocks of West Greenland and the Minnesota River Valley. *Earth Planet. Sci. Lett*. **35**, 449–53.
Moorbath, S. and Taylor, P. N. (1981). Isotopic evidence from continental growth in the Precambrian. In Kröner, A. (ed.) *Precambrian Plate Tectonics*, Amsterdam: Elsevier, pp. 49–62.
Moorbath, S., Taylor, P. N., and Jones, N.W. (1986). Dating the oldest terrestrial rocks: fact and fiction. *Chem. Geol.* **57** (1–2), 63–86.
Moorbath, S., Whitehouse, M. J., and Kanber, B. S. (1997). Extreme Nd isotope heterogeneity in the early Archean: fact or fiction? Illustrations from northern Canada and West Greenland. *Chem. Geol.* **135**, 213–31.
Nier, A. O. (1938). The isotope constitution of calcium, titanium, sulphur and argon. *Phys. Rev.* **53**, 282–6.
Nier, A. O., Thompson, R.W., and Murphy, B. (1941). The isotopic composition of lead and the measurement of geologic time Pt. III. *Phys. Rev.* **60**, 112–16.
Nutman, A. P., McGregor, V. B., Friend, C. R. L., Benson, V. C., and Kinny, P. D. (1996). The Itsaq gneiss complex of southern West Greenland: the World's most extensive record of early crustal evolution, 3900–3600 Ma. *Precamb. Res.* **78**, 1–39.
Patterson, C. C. (1953). The isotopic composition of meteoritic–basaltic and oceanic lead and the age of the Earth. *Proc. Conf. Nuclear Processes in Geology*, William Bay, 36–40.
Patterson, C. C. (1956). Age of meteorites and the Earth. *Geochim. Cosmochim. Acta* **10**, 230–7.
Reid, M., Coath, C., Harrison, M., and McKeegan, K. (1997). Prolonged residence times for the youngest rhyolites associated with Long Valley Caldera: $^{230}$Th–$^{238}$U ion microprobe dating of young zircons. *Earth Planet. Sci. Lett*. **150**, 27–39.
Strutt, R. J. (1908). On the accumulation of helium in geological time. *Proc. Roy. Soc. Lond. A* **76**, 88–101.
Tatsumoto, M., Knight, R. J., and Allègre, C. J. (1973). Time differences in the formation of meteorites as determined from the ratio of lead-207 to lead-206. *Science* **180**, 1279–83.
Taylor, R. S. (1982). *Planetary Science: A Lunar Perspective*. Houston, TX: Lunar and Planetary Institute.
Wasson, J. (1984). *Meteorites*. New York: W. H. Freeman.
Wasserburg, G. J., Busso, M., Gallino, R., and Nollett, K. M. (2006). Short-lived nuclei in the early solar system: possible AGB sources. *Nucl. Phys A*. **777**, 5–69.
Wendt, J., and Carl, C. (1991). The statistical distribution of the mean squared weighted deviations. *Chem. Geol.* **86**, 275–85.
Wood, J. (1968). *Meteorites and the Origin of the Planets*. New York: McGrow-Hill.
York, D. (1969). Least squares fitting of a straight line with correlated errors. *Earth Planet. Sci. Lett* **5**, 320–4.
Zindler, A. (1982). Nd and Sr isotopic studies of komatiites and selected rocks. In Arndt, N. T. and Nisbet, E. G. (eds.) *Komatiites*, London: George Allen and Unwin, pp. 103–22.

## Chapter 6

Aldrich, L. T. and Nier, A. O. (1948). The occurrence of He-3 in natural sources of helium. *Phys. Rev.* **74**, 1590–4.
Allègre, C. J. (1982). Chemical geodynamics. *Tectonophysics* **81**, 109–32.
Allègre, C. J. (1987). Isotope geodynamics. *Earth Planet. Sci. Lett.* **86**, 175–203.
Allègre, C. J. (1997). Limitation on the mass exchange between the upper and lower mantle: the evolving regime of the Earth. *Earth Planet. Sci. Lett*. **150**, 1–6.
Allègre, C. J. and Ben Othman, D. (1980). Nd–Sr isotopic relationship in granitoid rocks and continental crust development: a chemical approach to orogenesis. *Nature* **286**, 335–342.
Allègre, C. J. and Condomines, M. (1976). Fine chronology of volcanic processes using $^{238}$U–$^{230}$Th systematics. *Earth Planet. Sci. Lett*. **28**, 395–406.
Allègre, C. J. and Condomines, M. (1982). Basalt genesis and mantle structure studied through Th-isotopic geochemistry. *Nature* **299**, 21–4.

Allègre, C. J. and Jaupart, C. (1985). Continental tectonics and continental kinetics. *Earth Planet. Sci. Lett*. **74**, 171–86.

Allègre, C. J. and Luck, J. M. (1980). Osmium isotopes as petrogenetic and geological tracers. *Earth Planet. Sci. Lett*. **48**, 148–54.

Allègre, C. J. and Moreira, M. (2004). Rare gas systematics and the origin of oceanic islands: the key role of entrainment at the 670 km boundary layer. *Earth Planet. Sci. Lett*. **228**, 85–92.

Allègre, C. J. and Rousseau, D. (1984). The growth of the continents through geological time studied by Nd isotope analysis of shales. *Earth Planet. Sci. Lett*. **67**, 19–34.

Allègre, C. J. and Turcotte, D. L. (1985). Geodynamical mixing in the mesosphere boundary layers and the origin of oceanic islands. *Geophys. Res. Lett*. **12**, 207–10.

Allègre, C. J. and Turcotte, D. L. (1986). Implications of a two-component marble-cake mantle. *Nature* **323**, 123–7.

Allègre, C. J., Ben Othman, D., Polvé, M., and Richard, P. (1979). The Nd–Sr isotopic correlation in mantle materials and geodynamic consequences. *Phys. Earth Planet. Int*. **19**, 293–306.

Allègre, C. J., Brévard, O., Dupré, B., and Minster, J. F. (1980). Isotopic and chemical effects produced in a continuously differentiating convecting Earth mantle. *Phil. Trans. Roy. Soc. Lond A* **297**, 447–77.

Allègre, C. J., Hart, S. R., and Minster, J. F. (1983a). The chemical structure of the mantle determined by inversion of isotopic data. I. Theoretical method. *Earth Planet. Sci. Lett*. **66**, 177–90.

Allègre, C. J., Hart, S. R., and Minster, J. F. (1983b). The chemical structure of the mantle determined by inversion of isotopic data. II. Numerical experiments and discussion. *Earth Planet. Sci. Lett*. **66**, 191–213.

Allègre, C. J., Staudacher, T., Sarda, P. and Kurz, M. (1983c). Constraints on evolution of Earth's mantle from rare gas systematics. *Nature* **303**, 762–6.

Allègre, C. J., Manhès, G., and Göpel, C. (1995). The age of the Earth. *Geochim. Cosmochim. Acta* **59**, 1445–56.

Allègre, C. J., Hofmann, A., and O'Nions, R. K. (1996). The argon constraints on mantle structure. *Geophys. Res. Lett*. **23** (24), 3555–7.

Alvarez, L. and Cornog, R. (1939). Helium and hydrogen of mass 3. *Phys. Rev*. **56**, 613–15.

Armstrong, R. L. (1981). Radiogenic isotopes: the case for crustal recycling on a near steady-state continental growth earth. *Phil. Trans. Roy. Soc. Lond. A* **301**, 443–72.

Bennett, V. C. and DePaolo, D. J. (1987). Proterozoic crustal history of the Western United States as determined by neodymium isotopic mapping. *Bull. Geol. Soc. Amer*. **99**, 674–85.

Ben Othman, D., Polvé, M., and Allègre, C. J. (1984). Nd–Sr isotope composition of granulite and constraints on the evolution of the lower continental crust. *Nature* **307**, 510–15.

Blichert-Toft, J. and Albarède, F. (1997). The Lu–Hf isotope geochemistry of chondrites and the evolution of the mantle–crust system. *Earth Planet. Sci. Lett*. **148**, 243–58.

Bowen, N. (1928). *The Evolution of the Igneous Rocks*. Princeton, NJ: Princeton University Press.

Boyet, M. and Carlson, R. (2005). $^{142}$Nd evidence for early (>4.53 Ga) global differentiation of the silicate Earth. *Science* **309**, 576–80.

Caro, G., Bourdon, B., Birck, J.-L., and Moorbath, S. (2003). $^{146}$Sm–$^{142}$Nd evidence from Isua metamorphosed sediments for early differentiation of the Earth's mantle. *Nature* **423**, 428–32.

Clarke, W., Beg, M., and Craig, H. (1969). Excess $^{3}$He in the sea: evidence for terrestrial primoridal helium. *Earth Planet. Sci. Lett*. **6**, 213–30.

Compston, W. and Williams, I. S. (1984). U–Pb geochronology of zircons from lunar brecchia 73217 using a sensitive high mass resolution ion probe. *J. Geophys. Res*. **89** (suppl. B), 525–34.

Condomines, M. and Sigmarson, O. (1993). Why are so many arc magmas close to $^{238}$U–$^{230}$Th radioactive equilibrium? *Geochim. Cosmochim. Acta* **57**, 4491–7.

Condomines, M., Hemond, C., and Allègre, C. J. (1988). U–Th–Ra radioactive disequilibria and magmatic processes. *Earth Planet. Sci. Lett*. **31**, 369–85.

Craig, H. and Lupton, J. (1976). Primordial neon, helium and hydrogen in oceanic basalts. *Earth Planet. Sci. Lett*. **31**, 369–85.

Damon, P. E. (1954). An abundance model for lead isotopes based on the continuous creation of the Earth's sialic crust. *Trans. Am. Geophys. Union.* **35**, 631–42.
Damon, P. E. and Kulp, J. L. (1958). Inert gases and the evolution of the atmosphere. *Geochim. Cosmochim. Acta* **13**, 280–300.
DePaolo, D. J. (1981a). A neodymium and strontium isotopic study of the Mesozoic calcalkaline granitic batholith of the Sierra Nevada and Peninsular range, Calif. *J. Geophys. Res.* **86**, 10470–88.
DePaolo, D. J. (1981b). Neodymium isotopes in the Colorado Front Range and crust–mantle evolution in the Proterozoic. *Nature* **291**, 193–6.
DePaolo, D. J. (1981c). Implication of correlated Nd and Sr isotopic variations for the chemical evolution of the crust and the mantle. *Earth Planet. Sci. Lett.* **43**, 201–11.
DePaolo, D. J. (1988). *Neodymium Isotope Geochemistry.* Heidelberg: Springer-Verlag.
DePaolo, D. J. and Wasserburg, G. J. (1976a). Nd isotopic variations and petrogenetic models. *Geophys. Res. Lett.* **3**, 249–52.
DePaolo, D. J. and Wasserburg, G. J. (1976b). Inferences about magma sources and mantle structure from variations of neodymium-143/neodymium-144. *Geophys. Res. Lett.* **3**, 743–6.
Dietz, R. S. (1963). Continent and ocean evolution by spreading of the sea floor. *Nature* **190**, 854–7.
Doe, B. R. (1970). *Lead Isotopes.* Heidelberg: Springer-Verlag.
Doe, B. R. and Zartman, R. E. (1979). Plumbotectonics I: the Phanerozoic. In Barnes, H. L. (ed.) *Geochemistry of Hydrothermal Ore Deposits*, New York: John Wiley, pp. 22–70.
Dupré, B. and Allègre, C. J. (1980). Pb–Sr–Nd isotopic correlation and the chemistry of the North Atlantic mantle. *Nature* **286**, 17–22.
Dupré, B. and Allègre, C. J. (1983). Pb–Sr isotope variation in Indian Ocean basalts and mixing phenomena. *Nature* **303**, 142–6.
Elliot, T., Plank, T., Zindler, A., White, W., and Bourdon, B. (1997). Element transport from slab to volcanic front at the Mariana arc. *J. Geophys. Res.* **12**, 1491–4.
Farmer, G. L. and DePaolo, D. J. (1983). Origin of Mesozoic and Tertiary granite in the Western United States and implications for pre-Mesozoic crustal structure. I. Nd and Sr isotopic studies in the geocline of the Northern Great Basin. *J. Geophys. Res.* **88**, 3379–402.
Fukao, Y., Obayashi, H., Inoue, H., and Neuberg, M. (1992). Subduction slabs stagnant in the mantle transition zone. *J. Geophys. Res.* **97**, 4809–22.
Gangarz, A. J. and Wasserburg, G. J. (1977). Initial Pb of the Amitsoq gneiss, West Greenland, and implications for the age of the Earth. *Geochim. Cosmochim. Acta* **41**, 1283–301.
Gast, P. W. (1960). Limitations on the composition of the upper mantle. *J. Geophys. Res.* **65**, 1287–90.
Gast, P. W. (1968). Trace element fractionation and the origin of tholeiitic and alkaline magma types. *Geochim. Cosmochim. Acta* **32**, 1057–87.
Gast, P. W., Tilton, G. R., and Hedge, C. E. (1964). Isotopic composition of lead and strontium from Ascension and Gough Island. *Science* **145**, 1181–88.
Gaudette, H., Vitrac-Michard, A., and Allègre, C. J. (1981). North American Precambrian history recorded in a single sample: high resolution U–Pb systematics of the Potsdam sandstone detrital zircons, New York State. *Earth Planet. Sci. Lett.* **54**, 248–60.
Geiss, J. (1954). Isotopic analysis of ordinary lead. *Z. Naturforsch.* **4/9**, 218.
Göpel, C., Allègre, C. J., and Rong Hua Xu. (1984). Lead isotopic study of the Xiagaz ophiolite (Tibet): the problem of the relationship between magmatites (gabbros, dolerites, lavas) and tectonites (harzburgites). *Earth Planet. Sci. Lett.* **69**, 301–10.
Grand, S., van der Hilst, R., and Widiyautaro, S. (1997). Global seismic tomography: a snapshot of convection in the Earth. *GSA Today* **7**, 1–17.
Hamelin, B. and Allégre, C. J. (1985). Large scale regional units in the depleted upper mantle revealed by an isotope study of Southwest Indian Ridge. *Nature* **315**, 52–5.
Hamelin, B., Dupré, B., and Allègre, C. J. (1984). Lead–strontium isotopic variations along the East Pacific Rise and the Mid Atlantic Ridge: a comparative study. *Earth Planet. Sci. Lett.* **67**, 340–50.

Hamelin, B., Dupré, B., and Allègre, C. J. (1986). Pb–Sr–Nd isotopic data of the Indian Ocean Ridge: new evidence of large-scale mapping of mantle heterogeneities. *Earth Planet. Sci. Lett.* **76**, 288–98.

Harper, C. L. and Jacobsen, S. B. (1992). Evidence from coupled $^{147}Sm$–$^{143}Nd$ and $^{146}Sm$–$^{142}Nd$ systematics for very early (4.5 Gyr) differentiation of the Earth's mantle. *Nature* **360**, 728–32.

Harrison, T. M., Blichert-Toft, J., Müller, W., *et al.* (2005). Heterogeneous Hadean hafnium: evidence of continental crust at 4.4 to 4.5 Ga. *Science* **310**, 1950–70.

Hart, S. R. (1984). A large-scale isotope anomaly in the southern hemisphere mantle. *Nature* **309**, 753–7.

Hart, S. R. (1988). Heterogeneous mantle domains: signatures, genesis and mixing chronologies. *Earth Planet. Sci. Lett.* **90**, 273–96.

Hart, S. R. and Zindler, A. (1986). In search of a bulk Earth composition. *Chem. Geol.* **57**, 247–67.

Hart, S. R., Schilling, J. G., and Powell, J. L. (1973). Basalts from Iceland and along the Reykjanes Ridge: strontium isotope geochemistry. *Nature* **246**, 104–7.

Hauri, E. H. and Hart, S. R. (1993). Re–Os isotope systematics of HIMU and EMII oceanic island basalts from the South Pacific Ocean. *Earth Planet. Sci. Lett.* **114**, 353–71.

Hawkesworth, C. J. (1979). $^{143}Nd/^{144}Nd$, $^{87}Sr/^{86}Sr$ and trace element characteristics of magmas along destructive plate margins. In Atherton, M. P. and Tarney, J. (eds.) *Origin of Granite Batholiths*, Sevenoaks, UK: Shiva, pp. 76–89.

Hawkesworth, C. J. and Kemp, A. I. (2006). Using hafnium and oxygen isotopes in zircons to unravel the record of crustal evolution. *Chem. Geol.* **226**, 144–7.

Hofmann, A. (1988). Chemical differentiation of the Earth: the relationship between mantle, continental crust and oceanic crust. *Earth Planet. Sci. Lett.* **90**, 297–304.

Hofmann, A. and Hart, S. R. (1978). An assessment of local and regional isotopic equilibrium in the mantle. *Earth Planet. Sci. Lett.* **38**, 44–62.

Hofmann, A. and White, W. M. (1982). Mantle plumes from ancient oceanic crust. *Earth Planet. Sci. Lett.* **57**, 421–36.

Hofman, A., Jochum, K., Seufert, M., and White, W. M. (1986). Nd and Pb in oceanic basalts: new constraints on mantle evolution. *Earth Planet. Sci. Lett.* **79**, 33–45.

Holmes, A. (1946). An estimate of the age of the Earth. *Nature* **157**, 680–4.

Houtermans, F. G. (1946). Die Isotopenhäufigkeiten im natürlichen Blei und das Alter des Urans. *Naturwissenschaften* **33**, 185–7.

Hurley, P. M. and Rand, R. (1969). Pre-drift continental nuclei. *Science* **164**, 1229–42.

Hurley, P. M., Hughes, H., Faure, G., Fairbairn, H. W., and Pinson, W. H. (1962). Radiogenic strontium-87 model of continent formation. *J. Geophys. Res.* **67**, 5315–34.

Jacobsen, S. (1988). Isotopic constraints on crustal growth and recycling. *Earth Planet. Sci. Lett.* **90**, 315–29.

Jacobsen, S. and Wasserburg, G. J. (1979). The mean age of mantle and crustal reservoirs. *J. Geophys. Res.* **84**, 7411–27.

Jacobsen, S. and Wasserburg, G. J. (1980). Sm–Nd isotopic evolution of chondrites. *Earth Planet. Sci. Lett.* **50**, 139–55.

Kleine, T., Munster, C., Mezger, K., and Palme, H. (2002). Rapid accretion and early core formation on asteroids and the terrestrial planets from Hf–W chronometry. *Nature* **418**, 952–5.

Kuroda, P. K. (1960). Nuclear fission in the early history of the Earth. *Nature* **187**, 36–8.

Kurz, M. and Jenkins, W. J. (1981). The distribution of helium in oceanic basalt glasses. *Earth Planet. Sci. Lett.* **53**, 41–54.

Kurz, M., Jenkins, W. J., and Hart, S. R. (1982). Helium isotopic systematics of oceanic islands and mantle heterogeneity. *Nature* **297**, 43–7.

Lambert, D. D., Morgan, W. J., Walker, R. J., *et al.* (1989). Rhenium–osmium and samarium–neodymium isotopic systematics of the Stillwater Complex. *Science* **244**, 1169–74.

Ledent, D., Patterson, C., and Tilton, G. R. (1964). Ages of zircon and feldspar concentrates from North American beach and river sands. *J. Geol.* **72**, 112–22.

Lupton, J. E. and Craig, H. (1975). Excess $^{3}$He in oceanic basalts: evidence for terrestrial primordial helium. *Earth Planet. Sci. Lett*. **26**, 133–9.
Mamyrin, B. A. and Tolstikhin, I. (1984). *Helium Isotopes in Nature*. Amsterdam: Elsevier.
Mamyrin, B. A., Tolstikhin, I., Anufriev, G. S., and Kamensky, I. L. (1969). Anomalous isotopic composition of helium in volcanic gases. *Dokl. Akad. Nauka USSR* **184**, 1197–9.
McCulloch, M. and Wasserburg, G. J. (1978). Sm–Nd and Rb–Sr chronology of continental crust formation. *Science* **200**, 1003–11.
McKenzie, D. (1979). Finite deformation during fluid flow. *Geophys. J. Roy. Astron. Soc*. **58**, 689–705.
McKenzie, D. (1985). $^{230}$Th–$^{238}$U disequilibrium and the melting process beneath the ridge axis. *Earth Planet. Sci. Lett*. **72**, 149–57.
Montelli, R., Nolet, G., Dahlen, A., *et al*. (2004). Finite frequency tomography reveals a variety of plumes in the mantle. *Science* **303**, 338–43.
Moorbath, S. and Taylor, P. N. (1981). Isotopic evidence from continental growth in the Precambrian. In Kröner, A. (ed.) *Precambrian Plate Tectonics*, Amstendam: Elsevier, pp. 491–525.
Moreira, M. and Allègre, C. J. (1998). Helium–neon systematics and the structure of the mantle. *Chem. Geol*. **147**, 53–9.
Moreira, M., Kunz, M., and Allègre, C. J. (1998). Rare gas systematics in popping rock: isotopic and element compositions in the upper mantle. *Science* **279**, 1178–81.
Morgan, W. J. (1971). Convection plumes in the lower mantle. *Nature* **230**, 42–3.
Nolet, G., Karato, S., and Montelli, R. (2004). Flux estimates from tomographic plume images yield evidence for chemical stratification in the mantle. *EOS (Trans. Am. Geophys. U.)* **85**, 117–26.
O'Nions, R. K. and Oxburgh, E. R. (1983). Heat and helium in the Earth. *Nature* **306**, 429–36.
O'Nions, R. K., Hamilton, P. J., and Evensen, N. M. (1977). Variations in $^{143}$Nd/$^{144}$Nd and $^{87}$Sr/$^{86}$Sr in oceanic basalts. *Earth Planet. Sci. Lett*. **34**, 13–22.
O'Nions, R. K., Hamilton, P. J., and Evensen, N. M. (1980). Differentiation and evolution of the mantle. *Phil. Trans. Roy. Soc. Lond. A* **297**, 479–93.
O'Nions, R. K. and Hamilton, P. J. (1983). A Nd isotope investigation of sediments related to crustal development in the British Isles. *Earth Planet. Sci. Lett*. **63**, 229–40.
Patchett, P. J. (1983). Importance of the Lu–Hf isotopic system in studies of planetary chronology and chemical evolution. *Geochim. Cosmochim. Acta* **47**, 81–91.
Patchett, P. J. and Tatsumoto, M. (1980). Hafnium isotope variations in oceanic basalts. *Geophys. Res. Lett*. **7**, 1077–80.
Patterson, C. (1963). Characteristics of lead isotope evolution on a continental crust. In Craig, H., Miller, S., and Wasserburg, G. J. (eds.) *Isotopic and Cosmic Chemistry*, Amsterdam: North Holland, pp. 244–68.
Patterson, C. and Tatsumoto, M. (1964). The significance of lead isotopes in detrital feldspar with respect to chemical differentiation within the Earth's mantle. *Geochim. Cosmochim. Acta* **28**, 1–22.
Reynolds, J. (1960). Determination of the age of the elements. *Phys. Rev. Lett*. **4**, 5–9.
Richard, P., Shimizu, N., and Allègre, C. J. (1976). $^{143}$Nd/$^{146}$Nd, a natural tracer: an application to oceanic basalts. *Earth Planet. Sci. Lett*. **3**, 269–78.
Roy Barman, M. and Allègre, C. J. (1994). $^{187}$Os/$^{186}$Os ratios of mid-ocean ridge basalts and abyssal peridotites. *Geochim. Cosmochim. Acta* **58**, 53–84.
Russell, R. D. (1972). Evolutionary model for lead isotopes in conformable ore and oceanic volcanoes. *Rev. Geophys. Space Phys*. **10**, 529–36.
Russell, R. D. and Farquhar, R. (1960). *Lead Isotopes in Geology*. New York: Wiley Interscience.
Sarda, P., Staudacher, T., and Allègre, C. J., (1985). $^{40}$Ar/$^{36}$Ar in MORB glasses: constraints on atmosphere and mantle evolution. *Earth Planet. Sci. Lett*. **72**, 357–75.
Sarda, P., Staudacher, T., and Allègre, C. J. (1988). Neon isotopes in submarine basalts. *Earth Planet. Sci. Lett*. **91**, 73–88.

Sarda, P., Moreira, M., Staudacher, T., Schilling, J. G., and Allègre, C. J. (2000). Rare gas systematics on the southernmost Mid-Atlantic Ridge: constraints of the lower mantle and Dupal source. *J. Geophys. Res.* **83**, 5973–96.

Schilling, J. G. (1973). Iceland mantle plume: geochemical study of the Reykjanes Ridge. *Nature* **242**, 565–571.

Schilling, J. G. (1992). In Duthous, X. (ed.) *Les Isotopes Radiogéniques en Géologie*, Paris: Société française de Mineralogie et Cristallographie, pp. 1–34.

Sobolev, A., *et al*. (2007). The amount of recycled crust in sources of mantle-derived melt. *Science* **316**, 412–17.

Staudacher, T. and Allègre, C. J. (1982). Terrestrial xenology. *Earth Planet. Sci. Lett*. **60**, 389–406.

Sun, S. S. (1980). Lead isotopic study of young volcanic rocks from mid-ocean ridges, ocean islands and island arcs. *Phil. Trans. Roy. Soc. Lond. A* **297**, 409–45.

Sun, S. S. and Hanson, G. N. (1975). Evolution of the mantle: geochemical evidence from alkali basalt. *Geology* **3**, 297–302.

Tatsumoto, M. (1966). Genetic relations of oceanic basalts as indicated by lead isotopes. *Science* **153**, 1088–94.

Tatsumoto, M., Hedge, C. E., and Engel, A. E. J. (1965). Potassium, rubidium, strontium, thorium, uranium and the ratio of strontium-87 to strontium-86 in oceanic tholeiitic basalt. *Science* **150**, 886–8.

Tatsumoto, M., Knight, R., and Allègre, C. J. (1973). Time differences in the formation of meteorites as determined from the ratio of lead-207 to lead-206. *Science* **180**, 1278–83.

Tolstikhin, I., Mamyrin, B., Khabarin, L. U., and Erlich, E. N. (1974). Isotope composition of helium in ultrabasic xenoliths from volcanic rocks of Kamchatka. *Earth Planet. Sci. Lett*. **22**, 75–84.

Treuil, M. (1973). Critères petrologiques, géochimiques et structuraux de la génèse et de la différentiation des magmas basaltiques, exemple de l'Afar. Ph.D. thesis, University of Orleans.

Treuil, M. and Joron, J. L. (1975). Utilisation des elements HYB en la simplification de la modelisation quantitative des processus magmatiques. *Soc. Ital. Mineral. Petrol.* **31**, 125–40.

Trieloff, M., Kunz, M., Clague, D., Harrison, D., and Allègre, C. J. (1998). The nature of pristine noble gases in mantle plumes. *Science* **288**, 1036–8.

Turcotte, D. and Schubert, G. (2002). *Geodynamics*. Cambridge, UK: Cambridge University Press.

Turekian, K. K. (1959). The terrestrial economy of helium and argon. *Geochim. Cosmochim. Acta* **17**, 37–43.

Turner, S., Bourdon, B., and Gill, J. (2003). Insights into magma genesis at convergent margins from U-series isotopes. *Rev. Mineral. Geochem*. **52**, 255–315.

van der Hilst, R., Engdahl, W., Spakman, W., and Nolet, G. (1991). Tomographic imaging of subducted lithosphere below the Northwest Pacific Island Arc. *Nature* **353**, 37–43.

Vervoort, J. D. and Blichert-Toft, J. (1999). Evolution of the mantle Hf isotope evidence from juvenile rocks through time. *Geochim. Cosmochim. Acta* **63**, 533–56.

Wasserburg, G. J. (1964). *Geochronology and Isotopic Data Bearing on the Development of the Continental Crust*. Cambridge, MA: MIT Press.

Wetherill, G. W. (1954). Isotopic variations of neon and argon extracted from radioactive materials. *Phys. Rev.* **96**, 679–83.

White, W. (1985). Sources of oceanic basalts: radiogenic isotopic evidence. *Geology* **13**, 115–22.

White, W. and Hoffman, A. (1982). Sr and Nd isotope geochemistry of oceanic basalts and mantle. *Nature* **296**, 821–5.

Winkler, H. (1974). *Petrogenesis of Metamorphic Rocks*. New York: Springer-Verlag.

Zindler, A. and Hart, S. R. (1986). Chemical geodynamics. *Ann. Rev. Earth Planet. Sci*. **14**, 493–510.

## Chapter 7


Berner, R. A., Lasaga, A. C., and Garrels, R. M. (1983). The carbonate–silicate geochemical cycle and its effects on atmospheric carbon dioxide over the past 100 million years. *Am. J. Sci.* **283**, 641–83.

Bigeleisen, J. (1965). Chemistry of isotope science. *J. Chem. Phys.* **147**, 463–71.

Bigeleisen J. and Mayer, M. (1947). Calculation of equilibrium constant for isotope exchange reactions. *J. Chem. Phys.* **15**, 261–7.

Bottinga, Y. and Javoy, M. (1975). Oxygen isotope partitioning among the minerals in igneous and metamorphic rocks. *Rev. Geophys. Space Phys.* **13**, 401–18.

Bowen, N. L. (1928). *The Evolution of Igneous Rocks*. Princeton, NJ: Princeton University Press.

Bradley, R. S. (1999). *Paleoclimatology*. New York: Academic Press.

Burton, K. and Vance, D. (1999). Glacial–interglacial variations in the neodymium isotope composition of seawater in the Bay of Bengal recorded by planktonic foraminifera. *Earth Planet. Sci. Lett.* **76**, 425–46.

Caillon, N., Severinghaus, J., Jouzel, J., *et al.* (2003). Timing of atmospheric $CO_2$ and Antarctic temperature changes across termination. III. *Science* **299**, 172–82.

Clayton, R. N., Grossman, L., and Mayeda, K. (1973). A component of primitive nuclear composition in carbonaceous chondrites. *Science* **182**, 485–7.

Craig, H. (1961). Isotopic variations in meteoric waters. *Science* **133**, 1702–3.

Craig, H. (1963). The isotopic geochemistry of water and carbon in geothermal areas. In: *Proceedings of Conference on Isotopes in Geothermal Waters*, Spoleto, Sept. 9–13, Pisa: Laboratorio di Geologia Nucleare, pp. 53–70.

Craig, H. (1965). The measurement of oxygen isotope paleotemperatures. In: *Stable Isotopes in Oceanographic Studies and Paleotemperature*, Spoleto July 26–27, Pisa: Laboratorio di Geologia Nucleare, pp. 1–24.

Craig, H. and Boato, G. (1955). Isotopes. *Ann. Rev. Chem.* **6**, 403–20.

Craig, H., Boato, G., and White, D. (1956). Isotopic geochemistry of thermal water. *Procs. 2nd Conf. Nuclear Processes in Geology*, pp. 29–42.

Dansgaard, W. (1953). The abundance of $^{18}O$ in atmospheric water and water vapour. *Tellus* **5**, 461–9.

Dansgaard, W. (1964). Stable isotopes in precipitation. *Tellus* **16**, 436–68.

Dansgaard, W. and Tauber, H. (1969). Glacier oxygen-18 content and Pleistocene ocean temperatures. *Science* **166**, 499.

Dansgaard, W., White, J. W., and Johnsen, S. J. (1969). The abrupt termination of the Younger Dryas climatic event. *Nature* **339**, 532–4.

De Niro, M. J. (1987) Stable isotopes in archeology. *Am. Scientist* **75**, 182–8.

Duplessy, J. C., Lalou, C., and Vinot, A. (1970). Differential isotopic fractionation in benthic foraminifera and paleotemperature re-assessed. *Science* **168**, 250–1.

Edmond, J. (1992). Himalayan tectonics, weathering processes and the strontium isotope record in marine limestone. *Science* **258**, 1594.

Emiliani, C. (1955). Pleistocene temperature. *J. Geol.* **63**, 538–78.

Emiliani, C. (1972). Quaternary paleotemperatures. *Science* **154**, 851–78.

EPICA Community (2004). Eight glacial cycles from an Antarctic ice core. *Nature* **429**, 623.

Epstein, S. (1959). The variation of $^{18}O/^{16}O$ ratio in nature and some geological applications. In Abelson, P. (ed.) *Research in Geochemistry*, New York: John Wiley, pp. 1217–40.

Epstein, S. and Mayeda, T. (1953). Variation of $^{18}O$ content of waters from natural sources. *Geochim. Cosmochim. Acta* **4**, 213–24.

Epstein, S. and Sharp, R. (1967). Oxygen and hydrogen isotope variations in a firm core, Eight Station, Western Antarctica. *J. Geophys. Res.* **72**, 5595–618.

Epstein, S. and Taylor, H. P. (1967). Variation of $^{18}O/^{16}O$ in minerals and rocks. In Abelson, P. (ed.) *Research in Geochemistry*, New York: John Wiley, pp. 229–62.

Epstein, S., Buchsbaum, R., Lowenstam, H., and Urey, H. (1953). Revised carbonate–water isotopic temperature scale. *Bull. Geol. Soc. Amer.* **64**, 1315–26.

Epstein, S., Sharp, R., and Gow, A. J. (1965). Six-year record of oxygen and hydrogen isotope variation in South Pole firn. *J. Geophys. Res.* **70**, 1809–14.

Farquhar, J., Bao, H., and Thiemens, M. (2001). Atmospheric influence of Earth's earliest sulphur cycle. *Science* **289**, 757.

Farquhar, J., Peters, H., Johnston, D., *et al.* (2007). Isotopic evidence for mesoarchean anoxia and changing atmospheric sulfur chemistry. *Nature* **449**, 706–9.

Fourcade, S. (1998). Les isotopes : effets isotopiques bases de la radiochimie. In Hageman, J. and Treuil, M. (eds.) *Introduction à la Géochimie*, Paris: CEA.

Galimov, E. (1985). *The Biological Fractionations of Isotopes*, New York: Academic Press.

Gao,Y. Q. and Marcus, R. A (2001). Strange and non-conventional isotope effect in ozone formation. *Science* **293**, 259.

Garlick, G. D. and Epstein, S. (1967). Oxygen isotope ratios in coexisting minerals from regionally metamorphosed rocks. *Geochim. Cosmochim. Acta* **31**, 181–214.

Ghosh, P., Garzione, C., and Eiler, J. (2006a). Rapid uplift of the Altiplano revealed through $^{13}C$–$^{18}O$ bonds in paleosol carbonates. *Science* **311**, 2093–4.

Ghosh, P., Adkins, J., Affek, H., *et al.* (2006b). $^{13}C$–$^{18}O$ bonds in carbonate minerals: a new kind of paleothermometer. *Geochim. Cosmochim. Acta* **70**, 1439–56.

Goldstein, S. L. and Hemming, S. R. (2003). Long-lived isotopic tracers in oceanography, paleo-oceanography and ice-sheet dynamics. In Elderfield, H. (ed.), *Treatise on Geochemistry*, vol. 6, London: Elsevier, pp. 625–000.

Harrison, A. G. and Thode, H. G. (1957). The kinetic isotope effect in the chemical reduction of sulfate. *Trans. Faraday Soc.* **53**, 1–4.

Harrison, A. G. and Thode, H. G. (1958). Mechanism of the bacterial reduction of sulfate from isotope fractionation studies. *Trans. Faraday Soc.* **54**, 84–92.

Heinrich, M. (1988). Origin and consequences of cyclic ice rafting in the northeast Atlantic Ocean during the past 130 000 years. *Quatern. Res.* **29**, 143–52.

Holland, H. (1984). *The Chemical Evolution of the Atmosphere and Oceans*. Princeton, NJ: Princeton University Press.

Ito, E. and Stern, R. J. (1985). Oxygen and strontium isotopic investigation of subduction zone volcanism: the case of the volcano arc and the Marianas island arc. *Earth Planet. Sci. Lett.* **76**, 312–20.

James, D. (1981). The combined use of oxygen and radiogenic isotopes as indicators of crustal contamination. *Ann. Rev. Earth Planet. Sci.* **9**, 311–44.

Javoy, M. (1977). Stable isotopes and geothermometry. *J. Geol. Soc. Lond.* **133**, 609–36.

Javoy, M., Fourcade, S., and Allègre, C. J. (1970). Graphical method for examination of $^{18}O/^{16}O$ fractionation in silicate rocks. *Earth Planet. Sci. Lett.* **10**, 12–16.

Johnsen, S., Dansgaard, W., and White, J. W. (1989). The origin of Arctic precipitation under present-day glacial conditions. *Tellus* **41**, 452–69.

Johnson, C., Beard, B., and Albarède, F. (eds.) (2004). *Reviews in Mineralogy and Geochemistry,* vol. 55, *Geochemistry of Non-Traditional Stable Isotopes*, Mineralogical Society of America.

Jouzel, J. (1986). Isotopes in cloud physics: multistep and multistage processes. In *Handbook of Environmental Isotope Geochemistry*, vol. 2, Amsterdam: Elsevier, pp. 61–112.

Jouzel, J., Lorius, C., and Petit, J. R. (1987). Vostok ice core: a continuous isotopic temperature record over the climatic cycle (160 000 years). *Nature* **329**, 403–8.

Labeyrie, L. (1974). New approaches to surface sea-water paleotemperatures using $^{18}O/^{16}O$ ratios in silica of diatom fructules. *Nature* **248**, 40–2.

Lasaga, A. (1997). *Kinetic Theory.* Princeton, NJ: Princeton University Press.

Longinelli, A. and Nutti, S. (1973). Revised phosphate–water isotopic temperature scale. *Earth Planet. Sci. Lett.* **19**, 373–6.

Lorius, C. and Merlivat, L. (1977). Distribution of mean surface stable isotope values in east Antarctica: observed changes with depth in coastal areas. In *Isotopes and Impurities in Snow and Ice*, IAHS Publ. **118**, pp. 127–37.

Milankovitch, M. M. (1941). *Case of Insolation and the Ice-Age Problem*. Washington, DC: US Department of Commerce and National Scientific Foundation.

Nielsen, H. (1979). Sulfur isotopes. In Jäger, E. and Hunziker, J. C. (eds.) *Lectures in Isotope Geology*, Berlin: Springer-Verlag, pp. 283–312.

Nier, A. O. (1947). A mass spectrometer for isotopes and gas analysis. *Rev. Sci. Instrum.* **18**, 398–411.

Nier, A. O., Ney, E. P., and Inghram, M. (1947). A new method for the comparison of two ion currents in a mass spectrometer. *Rev. Sci. Instrum.* **18**, 294–7.

O'Neil, J. R. (1986). Theoretical and experimental aspects of isotopic fractionation. In Valley, J. M, Taylor, H. P., and O'Neil, J. R. (eds.) *Review of Mineralogy,* vol. 16*, Stable Isotopes*, pp. 1–40.

O'Neil, J. R. and Clayton, R. N (1964). Oxygen isotope geochemistry. In Craig, A., Miller, S., and Wasserburg, G. J. (eds.) *Isotopic and Cosmic Chemistry*, Amsterdam: North-Holland, pp. 157–68.

Oeschger, H. (1982). The contribution of radioactive and chemical dating in the understanding of environmental systems. In Lloyd, A. (ed.) *Nuclear and Chemical Dating Techniques: Interpreting the Environmental Record,* American Chemical Society, pp. 5–18.

Ohmoto, H. and Rye, R. O. (1979). Isotopes of sulfur and carbon. In Barnes, H. L. (ed.) *Geochemistry of Hydrothermal Ore Deposits*, New York: John Wiley, pp. 509–67.

Park, M. and Epstein, S. (1960). Carbon isotope fractionation during photosynthesis. *Geochim. Cosmochim. Acta* **27**, 110–26.

Petit, J. R., Jouzel, J., Raynaud, D., *et al*. (1999). Climate and atmospheric history of the past 420 000 years from the Vostok ice core, Antarctic. *Nature* **399**, 429–36.

Pineau, F. and Javoy, M. (1983). Carbon isotopes and concentrations in mid-oceanic ridge basalts. *Earth Planet. Sci. Lett*. **62**, 239–57.

Raymo, M. and Ruddiman, W. (1992). Tectonic forcing of late Cenozoic climate. *Nature* **259**, 117.

Severinghaus, J. P. and Brook, E. (1999). Abrupt climate change at the end of the glacial period inferred from trapped air in polar ice. *Science* **286**, 930–4.

Severinghaus, J. P., Grachev, A., Luzon, B., and Caillon, N. (2003). A method for precise measurement of argon 40/36 and krypton/argon ratios in trapped air in polar ice. *Geochim. Cosmochim. Acta* **67**, 325–43.

Shackleton, N. J. (1967a). Oxygen isotope analyses and the Pleistocene temperature re-assessed. *Nature* **215**, 15–17.

Shackleton, N. J. (1967b). Oxygen isotopes, ice volume and sea-level Quaternary. *Science Rev.* **6**, 183–90.

Taylor, H. P. (1968). The oxygen isotope geochemistry of igneous rocks. *Contrib. Mineral. Petrol*. **19**, 1–71.

Taylor, H. P. (1974). Oxygen and hydrogen isotope evidence for large-scale circulation and interaction between groundwaters and igneous intrusion with particular reference to the San Juan volcanic field. In Hoffman, A. W., Giletti, B., Yoder, H., and Yund, R. (eds.) *Geochemical Transport and Kinetics*, Washington, DC: Carnegie Institution Press, pp. 299–324.

Taylor, H. P. (1979). Oxygen and hydrogen isotope relationships in hydrothermal mineral deposits. In Barnes, H. L. (ed.) *Geochemistry of Hydrothermal Ore Deposits*, New York: John Wiley, pp. 236–77.

Taylor, H. P. (1980). Oxygen effects of assimilation of country rocks by magmas on $^{18}O/^{16}O$, $^{87}Sr/^{86}Sr$ systematics in igneous rocks. *Earth Planet. Sci. Lett*. **47**, 243–54.

Thiemens, M. H. (1999). Mass-independent isotope effects in planetary atmospheres and the early solar system. *Science* **280**, 341.

Thiemens, M. H. and Heidenreich, J. E. (1983). The mass independent fractionation of oxygen: a novel effect and the possible cosmochemical implication. *Science* **219**, 1073.

Thompson, L. (1991). Ice core records with emphasis on the global record of the last 2000 years. In Bradley, R. S. (ed.) *Global Change of the Past*, Boulder, CO: University Corporation for Atmospheric Research, pp. 201–24.
Tudge, A. P. and Thode, H. G. (1950). Thermodynamic properties of isotopic compounds of sulfur. *Can. J. Res. B* **28**, 567–78.
Urey, H. C. (1947). The thermodynamic properties of istopic substances. *J. Chem. Soc. Lond.*, 562–81.
Urey, H. C., Lowenstam, H., Epstein, S., and McKinney, C. R. (1951). Measurement of paleotemperatures of the Upper Cretaceous of England, Denmark and the south-eastern United States. *Bull. Geol. Soc. Amer.* **62**, 399–426.

## Chapter 8

Albarède, F. (1995). *Introduction to Geochemical Modeling*. Cambridge, UK: Cambridge University Press.
Allègre, C. J. and Jaupart, C. (1985). Continental tectonics and continental kinetics. *Earth Planet. Sci. Lett.* **74**, 171–86.
Allègre, C. J. and Lewin, E. (1995). Isotopic systems and stirring of the Earth's mantle. *Earth Planet. Sci. Lett.* **136**, 629–46.
Allègre, C. J. and Turcotte, D. (1985). Implications of a two-component marble-cake mantle. *Nature* **323**, 123–7.
Allègre, C. J., Brévard, O., Dupré, B., and Minster, J. F. (1980). Isotopic and chemical effects produced in a continuously differentiating convecting Earth mantle. *Phil. Trans. Roy. Soc. Lond. A* **297**, 447–77.
Allègre, C. J., Moreira, M., and Staudacher, T. (1995). $^{4}He/^{3}He$ dispersion and mantle convection. *Geophys. Res. Lett.* **22**, 2325–8.
Beltrani, E. (1987). *Mathematics for Dynamic Modeling*. New York: Academic Press.
Galer, S. and O'Nions, R. K. (1985). Residence time of thorium, uranium and lead in the mantle with implications for mantle convection. *Nature* **316**, 778–82.
Haberman, R. (1977). *Mathematical Models*. New York: Prentice Hall.
Jacobsen, S. (1988). Isotopic constraints on crustal growth and recycling. *Earth Planet. Sci. Lett.* **90**, 315–29.
Jacobsen, S. and Wasserburg, G. J. (1981). Transport models for crust and mantle evolution. *Tectonophysics* **75**, 163–79.
Javoy, M., Pineau, F., and Allègre, C. J. (1982). Carbon geodynamic cycle. *Nature* **300**, 171–3.
Lasaga, A. and Berner, R. (1998). Fundamental aspects of quantitative models for geochemistry cycles. *Chem. Geol.* **145**, 161–74.
McKenzie, D. (1979). Finite deformation during fluid flow. *Geophys. J. Roy. Astron. Soc.* **58**, 689–705.
Richter, F. and Turekian, K. K. (1993). Simple models for the geochemical response of the ocean to climatic and tectonic forcing. *Earth Planet. Sci. Lett.* **119**, 121–8.
Rodhe, H. (2000). Modelling biogeochemical cycles. In Jacobson, M., Charlson, R. Rodhe, H. and Orians, G. (eds.) *Earth System Science*, New York: Academic Press, pp. 62–92.
Wasserburg, G. J. (1964). Pb – U – Th evolution models for homogeneous systems with transport. *EOS (Trans. Am. Geophys. U.)* **45**, 111–18.

# APPENDIX

**Table A.1** Symbols and orders of magnitude

| Prefix | Factor |
|---|---|
| exa (E) | $10^{18}$ |
| peta (P) | $10^{15}$ |
| tera (T) | $10^{12}$ |
| giga (G) | $10^{9}$ |
| mega (M) | $10^{6}$ |
| kilo (k) | $10^{3}$ |
| hecto (h) | $10^{2}$ |
| deca (da) | $10^{1}$ |
| deci (d) | $10^{-1}$ |
| centi (c) | $10^{-2}$ |
| milli (m) | $10^{-3}$ |
| micro ($\mu$) | $10^{-6}$ |
| nano (n) | $10^{-9}$ |
| pico (p) | $10^{-12}$ |
| femto (f) | $10^{-15}$ |
| atto (a) | $10^{-18}$ |

**Table A.2** Constants

| | Symbol | Value |
|---|---|---|
| Speed of light | $c$ | $2.997\,924\,58 \cdot 10^{8}\,\mathrm{m\,s^{-1}}$ |
| Electron charge | $e$ | $-1.602\,177\,33 \cdot 10^{-19}\,\mathrm{C}$ |
| Planck constant | $h$ | $6.620\,607\,55 \cdot 10^{-34}\,\mathrm{J\,s}$ |
| Boltzmann constant | $k$ | $1.380\,658 \cdot 10^{-23}\,\mathrm{J\,K^{-1}}$ |
| Gravitational constant | $G$ | $6.6726 \cdot 10^{-11}\,\mathrm{N\,m^{2}\,kg^{-2}}$ |
| Electron rest mass | $m_e$ | $0.910\,938\,97 \cdot 10^{-30}\,\mathrm{kg}$ |
| Atomic mass unit | $u$ | $1.660\,540\,2 \cdot 10^{-27}\,\mathrm{kg}$ |
| Avogadro constant | $N_A$ | $6.022\,136\,7 \cdot 10^{23}\,\mathrm{mole^{-1}}$ |
| Ideal gas constant | $R$ | $8.314\,510\,\mathrm{J\,mole^{-1}K^{-1}}$ |
| | | $1.989\,\mathrm{cal\,mole^{-1}K^{-1}}$ |

**Table A.3** Geological data

| | |
|---|---|
| Mass of the Earth | $5.9737 \cdot 10^{24}$ kg |
| Volume | $1.083\,20 \cdot 10^{21}$ m$^3$ |
| Mean radius assuming spherical Earth | 6 371 000 m |
| Mean density of Earth | 5515 kg m$^{-3}$ |
| Mass of atmosphere | $5.1 \cdot 10^{18}$ kg |
| Mass of oceans | $1.37 \cdot 10^{21}$ kg |
| Mass of ice caps | $2.9 \cdot 10^{19}$ kg |
| Mass of fresh water (rivers and lakes) | $3 \cdot 10^{16}$ kg |
| Mass of continental crust | $2.36 \cdot 10^{22}$ kg |
| Mass of whole mantle | $4 \cdot 10^{24}$ kg |
| Mass of upper mantle (above 670 km) | $1 \cdot 10^{24}$ kg |
| Mass of core | $1.950 \cdot 10^{24}$ kg |
| Mass of outer core | $1.85 \cdot 10^{24}$ kg |
| Mass of inner core | $9.7 \cdot 10^{22}$ kg |
| Area of Earth | $5.100\,655 \cdot 10^{8}$ km$^2$ |
| Area of oceans | $3.62 \cdot 10^{8}$ km$^2$ |
| Area of continents (and continental margins) | $2 \cdot 10^{8}$ km$^2$ |
| Area of exposed continents | $1.48 \cdot 10^{8}$ km$^2$ |
| Area of Atlantic Ocean | $9.8 \cdot 10^{7}$ km$^2$ |
| Area of Indian Ocean | $7.7 \cdot 10^{7}$ km$^2$ |
| Area of Pacific Ocean | $1.7 \cdot 10^{8}$ km$^2$ |
| Hydrothermal flux at ocean ridges | $1-2.3 \cdot 10^{14}$ kg yr$^{-1}$ |
| Flux of rivers to ocean | $4.24 \cdot 10^{4}$ km$^3$ yr$^{-1}$ $= 4.24 \cdot 10^{16}$ kg yr$^{-1}$ |
| Flux of river sediment load | $1.56 \cdot 10^{13}$ kg yr$^{-1}$ |
| Flux of oceanic crust formed | $8.4 \cdot 10^{13}$ kg yr$^{-1}$ |
| Flux of oceanic lithosphere created | $8.4 \cdot 10^{14}$ kg yr$^{-1}$ |
| Length of ocean ridges | 50 000 km |
| Flux from hot spots | $2.5 \cdot 10^{14}$ kg yr$^{-1}$ |
| Average sea-floor spreading rate | 3 cm yr$^{-1}$ |
| Flux of lithospheric subduction | $8.4 \cdot 10^{14}$ kg yr$^{-1}$ |
| Average altitude of landmasses | 875 m |
| Average depth of oceans | 3794 m |
| Average thickness of continents | 35 km |
| Average thickness of oceanic crust | 6.0 km |
| Average heat flow | 87 mW m$^{-2}$ |
| Total geothermal flow | 44.3 TW |
| Average continental heat flow | 65 mW m$^{-2}$ |
| Average oceanic heat flow | 101 mW m$^{-2}$ |
| Solar flux | 1373 W m$^{-2}$ |

**Table A.4** Long-lived radioactivity

| Percentage of element | Decay constant, $\lambda\,(\mathrm{yr}^{-1})$ | Mean life, $T\,(\mathrm{yr})$ | Half-life, $T_{1/2}\,(\mathrm{yr})$ | Product |
|---|---|---|---|---|
| $^{40}\mathrm{K}$ | $\beta^{-}4.962 \cdot 10^{-10}$ | $2.015 \cdot 10^{9}$ | $1.397 \cdot 10^{9}$ | $^{40}\mathrm{Ca}$ |
| $1.167 \cdot 10^{-4}\,\mathrm{K}_{\mathrm{total}}$ | $\mathrm{e}^{-}\,\mathrm{cap}\,0.581 \cdot 10^{-10}$ | $17.21 \cdot 10^{9}$ | $11.93 \cdot 10^{9}$ | $^{40}\mathrm{Ar}$ |
| | Total $5.543 \cdot 10^{-10}$ | $1.80 \cdot 10^{9}$ | $1.25 \cdot 10^{9}$ | |
| $^{87}\mathrm{Rb}\,\beta^{-}\,0.25$ | $1.42 \cdot 10^{-11}$ | $70.42 \cdot 10^{9}$ | $48.8 \cdot 10^{9}$ | $^{87}\mathrm{Sr}$ |
| $^{138}\mathrm{La}\begin{bmatrix}\beta^{-}\\ 0.089\\ \mathrm{e}^{-}\mathrm{cap}\end{bmatrix}$ | $\beta^{-}2.25.10^{-12}$ | $4.44 \cdot 10^{11}$ | $3.08 \cdot 10^{11}$ | $\begin{bmatrix}^{138}\mathrm{Ce}\\ ^{138}\mathrm{Ba}\end{bmatrix}$ |
| $\mathrm{La}_{\mathrm{total}}$ | $\mathrm{e}^{-}\,\mathrm{cap}\,4.4 \cdot 10^{-12}$ | $2.2 \cdot 10^{11}$ | $1.57 \cdot 10^{11}$ | |
| | Total $6.65 \cdot 10^{-12}$ | $1.5 \cdot 10^{11}$ | $1.04 \cdot 10^{11}$ | |
| $^{147}\mathrm{Sm}\,\alpha(15.07)$ | $6.54 \cdot 10^{-12}$ | $152.88 \cdot 10^{9}$ | $1.06 \cdot 10^{11}$ | $^{143}\mathrm{Nd}$ |
| $^{176}\mathrm{Lu}\,\beta^{-}(2.6)$ | $2 \cdot 10^{-11}$ | $50 \cdot 10^{9}$ | $3.5 \cdot 10^{10}$ | $^{176}\mathrm{Hf}$ |
| $^{187}\mathrm{Re}\,\beta^{-}\,(63.93)$ | $1.5 \cdot 10^{-11}$ | $66.66 \cdot 10^{9}$ | $4.6 \cdot 10^{10}$ | $^{187}\mathrm{Os}$ |
| $^{190}\mathrm{Pt}\,\alpha\,(0.0127)$ | $1.16 \cdot 10^{-12}$ | $862 \cdot 10^{9}$ | $6 \cdot 10^{11}$ | $^{186}\mathrm{Os}$ |
| $^{232}\mathrm{Th}\,(100)\,(6\alpha, 4\beta^{-})$ | $4.9475 \cdot 10^{-11}$ | $20.21 \cdot 10^{9}$ | $1.4010 \cdot 10^{10}$ | $^{208}\mathrm{Pb}$ |
| $^{235}\mathrm{U}\,(0.73)\,(7\alpha, 5\beta^{-})$ | $9.8485 \cdot 10^{-10}$ | $1.015\,38 \cdot 10^{9}$ | $0.703\,809\,9 \cdot 10^{9}$ | $^{207}\mathrm{Pb}$ |
| $^{238}\mathrm{U}\,(99.27)\,(8\alpha, 6\beta^{-})$ | $1.551\,25 \cdot 10^{-10}$ | $6.44 \cdot 10^{9}$ | $4.4683 \cdot 10^{9}$ | $^{206}\mathrm{Pb}$ |

**Table A.5** Extinct radioactivity

| Percentage of element | Decay constant, $\lambda$ $(\mathrm{yr}^{-1})$ | Mean life, $T$ (Ma) | Half-life, $T_{1/2}$ (Ma) | Product |
|---|---|---|---|---|
| $^{26}\mathrm{Al}\,\beta^{+}$ | $9.7 \cdot 10^{-7}$ | 1.03 | 0.714 58 | $^{26}\mathrm{Mg}$ |
| $^{10}\mathrm{Be}\,\beta^{-}$ | $4.6 \cdot 10^{-8}$ | $2.16 \cdot 10^{7}$ | $1.5 \cdot 10^{7}$ | $^{10}\mathrm{B}$ |
| $^{36}\mathrm{Cl}\,\beta^{+}$ | $2.25 \cdot 10^{6}$ | 0.44 | 0.308 | $^{36}\mathrm{Ar}\,(98.1\%)$ |
| $^{36}\mathrm{Cl}\,\beta^{-}$ | | | | $^{36}\mathrm{S}\,(1.9\%)$ |
| $^{41}\mathrm{Ca}\,\beta^{+}$ | $6.7 \cdot 10^{-6}$ | 0.15 | 0.1 | $^{41}\mathrm{K}$ |
| $^{53}\mathrm{Mn}\,\beta^{+}$ | $1.886 \cdot 10^{-7}$ | 5.3 | 3.3867 | $^{53}\mathrm{Cr}$ |
| $^{60}\mathrm{Fe}\,2\beta^{-}$ | $4.761 \cdot 10^{-7}$ | 2.2 | 1.456 | $^{60}\mathrm{Ni}$ |
| $^{92}\mathrm{Nb}\,\beta^{+}$ | $2.777 \cdot 10^{-8}$ | 36 | 25.67 | $^{92}\mathrm{Zr}$ |
| $^{107}\mathrm{Pd}\,\beta^{-}$ | $1.063 \cdot 10^{-7}$ | 9.4 | 6.538 | $^{107}\mathrm{Ag}$ |
| $^{129}\mathrm{I}\,\beta^{-}$ | $4 \cdot 10^{-8}$ | 25 | 17.327 | $^{129}\mathrm{Xe}$ |
| $^{146}\mathrm{Sm}\,\alpha$ | $6.849 \cdot 10^{-9}$ | 146 | 101.19 | $^{142}\mathrm{Nd}$ |
| $^{182}\mathrm{Hf}\,2\,\beta^{-}$ | $7.692 \cdot 10^{-8}$ | 13 | 9.01 | $^{182}\mathrm{W}$ |
| $^{205}\mathrm{Pb}\,\beta^{+}$ | $4.62 \cdot 10^{-8}$ | 21.64 | 15 | $^{205}\mathrm{Tl}$ |
| $^{244}\mathrm{Pu}$ fission | $8.264 \cdot 10^{-9}$ | 121 | 83.91 | $\mathrm{Xe}_{\mathrm{fission}}$ |
| $^{247}\mathrm{Cm}\,2\alpha, 3\beta^{+}$ | $4.4 \cdot 10^{-8}$ | 22.5 | 15.6 | $^{235}\mathrm{U}$ |

**Table A.6** Half-lives of radium isotopes used in geology

| Parent | Ra isotope | Half-life |
|---|---|---|
| $^{238}U$ | $^{226}Ra$ | 1622 years |
| $^{235}U$ | $^{223}Ra$ | 11.435 days |
| $^{232}Th$ | $^{228}Ra$ | 6.7 years |
| $^{232}Th$ | $^{224}Ra$ | 3.64 days |

**Table A.7** Half-lives and decay constants of disintegration reactions for radioactive chains used in geology

| Nuclide | Half-life (years) | Decay constant $\lambda$ ($yr^{-1}$) |
|---|---|---|
| $^{234}_{92}U$ | $2.48 \cdot 10^5$ | $2.794 \cdot 10^{-6}$ |
| $^{230}_{90}Th$ | $7.52 \cdot 10^4$ | $9.217 \cdot 10^{-6}$ |
| $^{226}_{88}Ra$ | $1.622 \cdot 10^3$ | $4.272 \cdot 10^{-4}$ |
| $^{210}_{82}Pb$ | 22.26 | $3.11 \cdot 10^{-2}$ |
| $^{231}_{91}Pa$ | $3.248 \cdot 10^4$ | $2.134 \cdot 10^{-5}$ |

**Table A.8** Mass ratios of selected elements

| Chemical mass ratio | Isotope ratio |
|---|---|
| (Rb/Sr) | 0.341 ($^{87}Rb/^{86}Sr$) |
| (Sm/Nd) | 1.645 ($^{147}Sm/^{144}Nd$) |
| (Lu/Hf) | 1.992 ($^{176}Lu/^{177}Hf$) |
| (Re/Os) | 0.212 ($^{187}Re/^{188}Os$) |
| (Re/Os) | 0.0252($^{187}Re/^{186}Os$) |
| (U/Pb) | $\approx 70$ ($^{238}U/^{204}Pb$)[a] |

[a] This is indicative only because the figure varies with the lead isotope composition. Care must be taken with chemical values in the literature for rocks when compared with, say, carbonaceous meteorites, which have primitive isotopic compositions.

**Table A.9** Values of selected isotope ratios

| | Bulk silicate earth | Initial values |
|---|---|---|
| $^{143}Nd/^{144}Nd$ | 0.512 638 | 0.505 83 |
| $^{147}Sm/^{144}Nd$ | 0.1966 | |
| $^{176}Hf/^{177}Hf$ | 0.282 95 | 0.279 78 |
| $^{176}Lu/^{177}Hf$ | 0.036 | |
| $^{87}Sr/^{86}Sr$ | 0.7047 | 0.698 998 |
| $^{87}Rb/^{86}Sr$ | 0.031 | |
| $^{187}Os/^{186}Os$ | 1.06 | 0.805 |
| $^{187}Os/^{188}Os$ | 0.130 | 0.0987 |
| $^{187}Re/^{186}Os$ | 3.3 | |
| $^{187}Re/^{188}Os$ | 0.412 | |
| $^{206}Pb/^{204}Pb$ | 18.426 | 9.307 |
| $^{207}Pb/^{204}Pb$ | 15.518 | 10.294 |
| $^{208}Pb/^{204}Pb$ | 39.081 | 29.476 |
| $^{238}U/^{204}Pb$ | 9.2 | |
| $^{232}Th/^{238}U$ | 4.25 | |

**Table A.10** Atomic number (Z), chemical symbol, and atomic mass (A) of the natural elements

| Atomic number | Element | Atomic mass |
|---|---|---|
| 1 | Hydrogen (H) | 1.0079 |
| 2 | Helium (He) | 4.002 60 |
| 3 | Lithium (Li) | 6.941 |
| 4 | Beryllium (Be) | 9.012 18 |
| 5 | Boron (B) | 10.81 |
| 6 | Carbon (C) | 12.011 |
| 7 | Nitrogen (N) | 14.0067 |
| 8 | Oxygen (O) | 15.9994 |
| 9 | Fluorine (F) | 18.998 40 |
| 10 | Neon (Ne) | 20.179 |
| 11 | Sodium (Na) | 22.9898 |
| 12 | Magnesium (Mg) | 24.305 |
| 13 | Aluminum (Al) | 26.981 54 |
| 14 | Silicon (Si) | 28.086 |
| 15 | Phosphorus (P) | 30.973 76 |
| 16 | Sulfur (S) | 32.06 |
| 17 | Chlorine (Cl) | 35.453 |
| 18 | Argon (Ar) | 39.948 |
| 19 | Potassium (K) | 39.098 |
| 20 | Calcium (Ca) | 40.08 |
| 21 | Scandium (Sc) | 44.9559 |
| 22 | Titanium (Ti) | 47.90 |
| 23 | Vanadium (V) | 50.9414 |
| 24 | Chromium (Cr) | 51.996 |
| 25 | Manganese (Mn) | 54.9380 |
| 26 | Iron (Fe) | 55.847 |
| 27 | Cobalt (Co) | 58.9332 |
| 28 | Nickel (Ni) | 58.71 |
| 29 | Copper (Cu) | 63.545 |
| 30 | Zinc (Zn) | 65.38 |
| 31 | Gallium (Ga) | 69.72 |
| 32 | Germanium (Ge) | 72.59 |
| 33 | Arsenic (As) | 74.9216 |
| 34 | Selenium (Se) | 78.96 |
| 35 | Bromine (Br) | 79.904 |
| 36 | Krypton (Kr) | 83.80 |
| 37 | Rubidium (Rb) | 85.468 |
| 38 | Strontium (Sr) | 87.63 |
| 39 | Yttrium (Y) | 88.9059 |
| 40 | Zirconium (Zr) | 91.22 |
| 41 | Niobium (Nb) | 92.9064 |
| 42 | Molybdenum (Mo) | 95.94 |
| 43 | Technetium (Tc) | (97) |
| 44 | Ruthenium (Ru) | 101.07 |
| 45 | Rhodium (Rh) | 102.9055 |
| 46 | Palladium (Pd) | 106.4 |
| 47 | Silver (Ag) | 107.868 |
| 48 | Cadmium (Cd) | 112.40 |
| 49 | Indium (In) | 114.82 |

**Table A.10** (cont.)

| Atomic number | Element | Atomic mass |
|---|---|---|
| 50 | Tin (Sn) | 118.69 |
| 51 | Antimony (Sb) | 121.75 |
| 52 | Tellurium (Te) | 127.60 |
| 53 | Iodine (I) | 126.9045 |
| 54 | Xenon (Xe) | 131.30 |
| 55 | Cesium (Cs) | 132.9054 |
| 56 | Barium (Ba) | 137.34 |
| 57 | Lanthanum (La) | 138.9055 |
| 58 | Cerium (Ce) | 140.12 |
| 59 | Praseodymium (Pr) | 140.9077 |
| 60 | Neodymium (Nd) | 144.24 |
| 61 | Promethium (Pm) | (145) |
| 62 | Samarium (Sm) | 150.4 |
| 63 | Europium (Eu) | 151.96 |
| 64 | Gadolinium (Gd) | 157.25 |
| 65 | Terbium (Tb) | 158.9524 |
| 66 | Dysprosium (Dy) | 162.50 |
| 67 | Holmium (Ho) | 164.9304 |
| 68 | Erbium (Er) | 167.26 |
| 69 | Thulium (Tm) | 168.9342 |
| 70 | Ytterbium (Yb) | 173.04 |
| 71 | Lutetium (Lu) | 174.97 |
| 72 | Hafnium (Hf) | 178.49 |
| 73 | Tantalum (Ta) | 180.9479 |
| 74 | Tungsten (W) | 183.85 |
| 75 | Rhenium (Re) | 186.2 |
| 76 | Osmium (Os) | 190.2 |
| 77 | Iridium (Ir) | 192.2 |
| 78 | Platinum (Pt) | 195.09 |
| 79 | Gold (Au) | 196.9665 |
| 80 | Mercury (Hg) | 200.61 |
| 81 | Thallium (Tl) | 204.37 |
| 82 | Lead (Pb) | 207.2 (variable) |
| 83 | Bismuth (Bi) | 208.9804 |
| 84 | Polonium (Po) | (209) |
| 85 | Astatine (At) | (210) |
| 86 | Radon (Rn) | (222) |
| 87 | Francium (Fr) | (223) |
| 88 | Radium (Ra) | 226.0254 |
| 89 | Actinium (Ac) | 227.0278 |
| 90 | Thorium (Th) | 232.0381 |
| 91 | Protactinium (Pa) | 231.0359 |
| 92 | Uranium (U) | 238.029 |
| 93 | Neptunium (Np) | 237.048 |
| 94 | Plutonium (Pu) | (244) |
| 95 | Americium (Am) | (243) |
| 96 | Curium (Cm) | (247) |

# FURTHER READING


Albarède, F., *Introduction to Geochemical Modeling*, Cambridge University Press, 1995. A fine book on modeling although a little hard going for those not keyed up in mathematics.

Bourdon, B., Turner, S., Henderson, G., and Lundstrom, C. C., *Introduction to U-Series Geochemistry*, Reviews in Mineralogy and Geochemistry vol. 52, Washington, DC, Geochemical Society and Mineralogical Society of America, 2003. A very good book for the different applications of radioactives series.

Bradley, R., *Paleoclimatology*, New York, Academic Press, 1999. An excellent clarification of isotopic methods and problems in climatology.

Broecker, W. S. and Peng, T.-H., *Tracers in the Sea*, New York, Eldigio Press of Columbia University, 1982. The reference book for students and anyone interested in marine isotope geochemistry.

Clayton, D. D., *Principles of Stellar Evolution and Nucleosynthesis*, University of Chicago Press, 1968. A clear and well-written book for anyone wanting to go into the nitty-gritty of nuclear astrophysics and nucleosynthesis.

Dalrymple, B., *The Age of the Earth*, Stanford University Press, 1991. An outstanding book on the age of the Earth and a good introduction to isotope geology.

De Paolo, D., *Neodymium Isotope Geochemistry*, Heidelberg, Springer-Verlag, 1988. The reference book for neodymium isotope geochemistry.

Dickin, A., *Radiogenic Isotope Geology*, 2nd edn, Cambridge University Press, 2005. The book for advanced students to move on to after this one. Excellent.

*Encyclopedia of Earth Systems Science*, London, Academic Press, 2005. An exhaustive introduction to studying external geodynamic systems.

Faure, G., *Principles of Isotope Geology*, New York, John Wiley, 1986. A primer for a generation now.

Muséum national d'histoire naturelle, *Les Météorites*, Paris, Bordas, 1996. A clear and simple review of meteorites accessible to all. (In French.)

Roth, E. and Poty, B., *Nuclear Methods of Dating*, New York, Springer-Verlag, 1989. A collection of papers reviewing the main methods of nuclear dating.

Rowlinson, H., *Using Geochemical Data*, Harlow, UK, Longman, 1993. A book to initiate students in the use of geochemical data.

Turcotte, D. and Schubert, G., *Geodynamics*, Cambridge University Press, 2002. A reference book for geophysics.

Valley, J. M., Taylor, H. P., and O'Neil, J. R., *Stable Isotopes in High Temperature Geological Processes*, Reviews in Mineralogy vol. 16, Washington, DC, Mineralogical Society of America. A good round-up of research on high-temperature stable isotope geochemistry, for advanced students.

Walker, J., *Numerical Adventures with Geochemical Cycles*, Oxford University Press, 1990. An excellent introduction to geochemical cycles using simple computer technology.

# SOLUTIONS TO PROBLEMS

## Chapter 1

(1) The mass of one atom of $^{17}O$ is $28.455\,75 \cdot 10^{-27}$ kg. Since the atomic mass unit is $1.660\,540\,2 \cdot 10^{-27}$ kg, the mass of $^{17}O$ in mass unit is 17.136 4415.

The mass of each of the two molecules $^{12}CDH_3$ and $^{13}CH_4$ is 17.133 367 132 in mass units. The difference is 0.002 77, which in relative mass is about $1.610^{-4}$ which corresponds to a resolution power of 6100 for the interference of separation.

(2) There are 31.7 ppm of lithium in the rock

(3) The measured isotopic ration $\frac{^{87}Sr}{^{86}Sr} = R_{mes}$ is equal to the real ratios + the pollution (estimated by the blank). The supposed isotopic ratio of the blank is $R_{bl}$. The real isotopic ratio of the sample is $R_s$. So:

$$R_{mes} = R_s(1 - x) + R_{bl}(X),$$

where $(X)$ is the mass fraction of the blank in the mixture (this is the same formula as isotope dilution).
If the precision is measured at $1.10^{-4}$, $R_{mes} - R_s$ should be greater than 10 times this value:

$$R_{mes} - R_s < 1.10^{-5}$$

which translates to

$$(R_{bl} - R_s)X < 10^{-5},$$

since $R_{bl} - R_s \sim 0.006$ and

$$x < 1.6\,10^{-3} \qquad x \simeq \frac{\text{blank}}{\text{sample}}.$$

So if the sample is $10^{-6}$g of Sr, $x < 1.6\,10^{-9}$g. If we increase the accuracy by 10 times the blank should be $0.16\,10^{-9}$g.

(4) The radius must be 63 meters if the angle of incidence is at 90° to the electromagnet's input faces, 31 meters if the angle is 27%.

(5) Present day: 13.59 dps; $4.5 \cdot 10^9$ years ago: 77.15 dps.

(6) Production of radioactive heat for a mantle of primitive composition: $19.9 \cdot 10^{12}$ W. For a mantle analogous to the upper mantle: $2.6 \cdot 10^{12}$ W.

Urey ratios: (i) 47%, (ii) 6%. The second ratio makes the production of radioactive heat virtually negligible. All the internal heat would therefore be related to the Earth's early history.

## Chapter 2

(1) Answers on pp. 288 and following.

(2) Apparent ages in Ma

| $^{206}Pb/^{238}U$ | $^{207}Pb/^{235}U$ | $^{207}Pb/^{206}Pb$ | $^{208}Pb/^{232}Th$ |
|---|---|---|---|
| 473 | 510 | 677 | 502 |
| 472 | 489 | 572 | 469 |
| 442 | 460 | 548 | 471 |
| 439 | 457 | 547 | 492 |

(3) 5.14 Ma; 4.2 Ma. They correspond to lava from different eruptions.

(4) In activity:

$$\left(\frac{^{234}U}{^{238}U}\right) = \left(\frac{^{234}U}{^{238}U}\right)_0 e^{-\lambda_4 t} + (1 - {}^{-\lambda_4 t})$$

$$\left(\frac{^{230}Th}{^{238}U}\right) = \frac{\lambda_{230}}{\lambda_{230} - \lambda_{234}}\left(\frac{^{234}U}{^{238}U} - 1\right)(1 - {}^{e-(\lambda_{230}-\lambda_{234})t}) + [1 - e^{\lambda_{230} t}].$$

(5) (i) $$\left(\frac{^{230}Th}{^{231}Pa}\right)_{excess} = \left(\frac{^{230}Th}{^{231}Pa}\right)_{\substack{initial \\ excess}} e^{-(\lambda_{230}-\lambda_{231})t}$$

(ii) About 300 000 years.

## Chapter 3

(1) 0.75 Ga.

(2) With $T$ being the temperature, we have:

$$^{40}Ar = (^{40}AR)_0 \exp\left[-\left(\frac{aT^2}{2} + GT\right)\right]$$

(3) (i) The ages are: Pyke Hill: 2.75 Ga; Fred's Flow: 2.58 Ga; Theo's Flow: 2.46 Ga.
(ii) The sulfides not containing uranium lie on the isochrons and give roughly the initial values of the lead isotope compositions.

(4) Lu–Hf ages: M 101 = 24.7 ± 1.2 Ma, M 214 = 30.6 ± 2 Ma.
Sm–Nd ages: M 101 = 23.6 ± 4.3 Ma, M 214 = 20.0 ± 7 Ma.
The Sm–Nd ages seem younger than the Lu–Hf ages, but the pyroxenite beds are probably 24 Ma years old.

(5) *Ages of three populations of zircons*

| | | | |
|---|---|---|---|
| Little Belt Mountains | 1935–2000 Ma | and | 2630–2650 Ma |
| Finland | 2700–2800 Ma | and | 2000 Ma |
| Maryland | | | $600 \pm 60$ Ma |

It can be seen that two of the zircon populations are double.

(6) A straight line.

## Chapter 4

(1) C/N = 14.4 million! Plants have C/N ratios of 100–200. Draw your own conclusions!

(2) About 1350 years! It is therefore not the shroud in which Christ was wrapped.

(3) $$\left(\frac{^{41}K}{^{40}K}\right)_{cosm} = \left(\frac{^{41}K}{^{39}K}\right)_{cosm} \cdot \left(\frac{^{39}K}{^{40}K}\right)_{measured} \left[\frac{\left(\frac{^{41}K}{^{39}K}\right)_{measured} - \left(\frac{^{41}K}{^{39}K}\right)_{normal}}{\left(\frac{^{41}K}{^{39}K}\right)_{cosm} - \left(\frac{^{41}K}{^{39}K}\right)_{normal}}\right].$$

(4) $8.9 \cdot 10^5$ years.

(5) $a = 1.62 \pm 0.1$ mm Ma$^{-1}$.

## Chapter 5

(1) (i) Basalt >1.6 mg, granite >3 mg.
(ii) Yes: basalt (2 Ga) = 0.7072; basalt (0.5 Ga) = 0.700 98; granite (2 Ga) = 0.7829; granite (0.5 Ga) = 0.7197.
(iii) 3‰ for Sr, 2% for the Rb/Sr ratio.
(iv) Five 200-g pieces are better than one 1-kg piece. The result is cross-referenced and there is a hope of constructing an isochron.

(2) $110 \pm 16$ ka.

(3) $277 \pm 5$ Ma.

(4) (i) (a) 1.12 ions per minute.
(b) The uncertainty is ±11 540 years, or 20%, compared with 0.7% uncertainty on the present-day measurement.
(c) Minimum age: $311 \pm 50$ years.
(d) Counting for 8 days, 300 mg of carbon would have to be extracted.
(ii) The error by the $^{230}Th$–$^{234}U$ method is 420 years for an age of 55 000 years, which corresponds to 0.76%. It is therefore an excellent method for this half-life, far superior to $^{14}C$ in theory. Geochemical conditions must hold for it to apply, that is: closed system and sufficient abundance levels.

(5) (i) The $^{87}Rb/^{87}Sr$ age of the gneisses is 1.05 Ga.
(ii) The age of the granite determined by the concordia diagram is 2.11 Ga with an intercept less than about 1 Ga (see figure). The apparent ages and the geometric relations established by geology are therefore contradictory. A granite that cross-cuts a gneiss cannot be older than the gneiss! Either of two hypotheses may hold. The first (A) is that both gneiss and granite are about 1 Ga old (given by the concordia intercept and the Rb–Sr isochron). The second (B) is to accept that the gneiss is 2 Ga old and

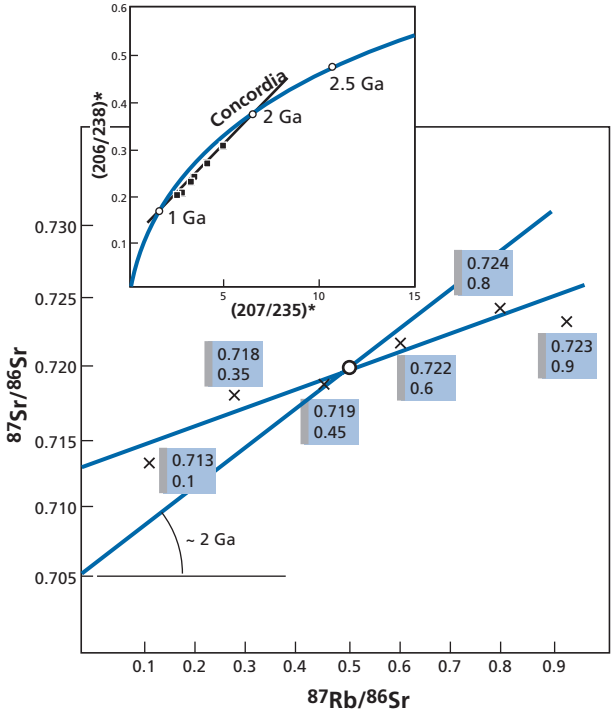


the granite a little younger, but that the whole was subjected to a large tectonic crisis 1 Ga ago, making the zircons discordant and partially re-homogenizing the $^{87}Rb$–$^{87}Sr$ system.

How do we choose between A and B? Hypothesis B is the more likely for two reasons. First, it is the concordia diagram that gives two ages of 2 Ga and about 1 Ga. Now, the 1 Ga corresponds to the $^{87}Rb$–$^{87}Sr$ age of the gneiss which has a poor alignment and above all a $(^{87}Sr/^{86}Sr)_{initial}$ ratio of about 0.713, which is very clear and indicates isotope re-homogenization. If we take the average of the $^{87}Sr/^{86}Sr$ and $^{87}Rb/^{86}Sr$ ratios, we get an average point. Taking an initial ratio of 0.705, we find an age of 1.95 Ga. Everything seems to be coherent therefore. However, of course, a series of U–Pb measurements on the zircon of the granite would be needed to confirm this.

(6) Initial age: 2.7 Ga, Grenville orogeny 1.1 Ga. The zircon ages of 2.8 Ga show that some of the zircon is inherited.

(7) $235 \pm 5$ Ma.

(8) (i) All the time intervals are mathematically possible. Allowing for diffusion $T < 30$ Ma.

(ii) Rock of interest would contain zircon, apatite, and sphene.

(9) The rhyolite is the result of partial melting (whether followed by differentiation or not) of the ancient basalt crust. This buried hydrated crust is heated and melts a little to give rise to the rhyolite.

(10) See Figure 5.11 for how to construct the diagram.

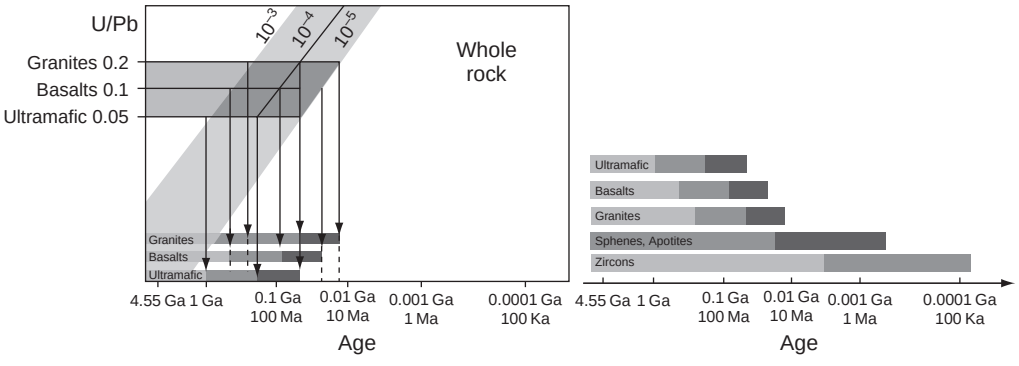


## Chapter 6

(1) (i) The initial two proportions in the two volcanogenic sediments are 0.576 and 0.423, respectively, giving:

$$(^{87}Sr/^{86}Sr)_{J.Sedian} = 0.709\,46 \text{ and } (^{87}Rb/^{86}Sr)_{Sedian} = 0.1239.$$

(ii) Initial ratios: $(^{87}Sr/^{86}Sr)_{granite} = 0.718\,65$, $(^{87}Rb/^{86}Sr)_{granite} = 3.885$.
Final ratio: $(^{87}Sr/^{86}Sr)_{granite} = 0.7738$.

(2) (i) Mass of $^{40}Ar$ assumed to be contained in the core approx. $20 \cdot 10^{18}$ g, mass of $^{40}Ar$ in the lower mantle $60 \cdot 10^{18}$ g. This putative evaluation does not alter the general idea behind the $^{40}Ar$ balance, a missing part of which must be in the mantle.

(ii) Concentration of non-radiogenic lead in the core $C_N^{Pb} = 1.81$ ppm.

(iii) For $T = 3$ Ga, $(^{206}Pb/^{204}Pb)_{\text{lower mantle}} = 17.40$, $(^{207}Pb/^{204}Pb)_{\text{lower mantle}} = 14.74$. The values for the closed system are 17.35 and 14.53, respectively. The point is slightly to the right of the geochron at 4.5 Ga.

(iv) Taking $T = 4$ Ga, we have $(^{206}Pb/^{204}Pb)_{\text{lower mantle}} = 17.90$ and $(^{207}Pb/^{204}Pb)_{\text{lower mantle}} = 16.10$.

(v) This phenomenon places the representative points in the J domain but is insufficient to give lead values with an isotope signature like the island of St. Helena. For this, 50% of the lead in the mantle would have had to pass into the core after 4.4 Ga, which seems a lot. The idea of explaining OIBs with high $\mu$ values by this mechanism does not seem to be corroborated by the data.

(3) (i) For the mantle, the reinjection of continental crust plays virtually no part. This is because of the mass difference. Only the initial differentiation is seen.

For the continental crust, it does play a role, but its evolution does not correspond to observation. The concavity observed with time is the opposite of what is observed, which seems on the contrary to involve increasing recycling of continental crust.

(ii) Neither the Nd nor Sr curves of mantle evolution show the evolution really observed, which see a progressive onset of primitive mantle evolution.

(iii) Overall, with the simplifying assumptions made here, this model does not account for the observations very well (see figure).

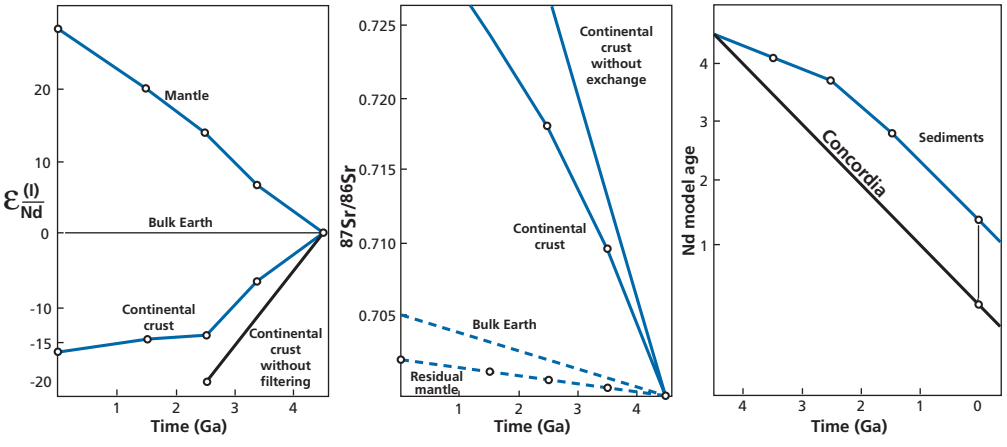


Armstrong's model of continent growth.

(4) (i) The upper mantle has a mass of $1 \cdot 10^{27}$g with 5 ppb uranium, corresponding to $2 \cdot 10^{16}$ moles.

(ii) Production of $^4$He in 1 Ga is 2.12 times that of uranium in moles, therefore $4.45 \cdot 10^{16}$ moles. The quantity of $^4$He outgassed is about $10^8$ moles yr$^{-1}$. Therefore, the residence time $^4\text{He} = 440$ Ma is equal to half the residence time of the lithosphere, which means that when the oceanic lithosphere forms at the mid-ocean ridges, there is enrichment in $^4$He towards the melting zone.

(5) (i) Values of $W^{Nd}$ are calculated in both hypotheses $\alpha_{cc}^{Nd} = 0.5110$ and $\alpha_{cc}^{Nd} = 0.5120$, which are the extremes using the balance equation $\mu$. Next the $T^{Nd}$ model ages are calculated using the two extreme data by the age formula deduced from continental crust data. This gives a pair of values ($W^{Nd}$, $T^{Nd}$) which are (0.2465; 2.84 Ga) and (0.4608; 1.08 Ga). Values of $W^{Nd}$ are calculated with the $\mu$ balance equation under both extreme conditions $\mu_{dm}^{Sm/Nd} = 0.227$ and $\mu_{dm}^{Sm/Nd} = 0.28$.

Then $T^{Nd}$ is calculated using the formula for the depleted mantle. We get a pair of values ($W^{Nd}$, $T^{Nd}$) of (0.256; 2.6 Ga) and (0.4882; 0.964 Ga). We then take a ($W^{Nd}$, $T$) plane and draw the two straight lines corresponding to the pair of values ($W$, $T$)

taken two by two (see figure). Their point of intersection gives $W^{Nd} = 0.335$, $T^{Nd} = 2.05 \cdot 10^9$ years.

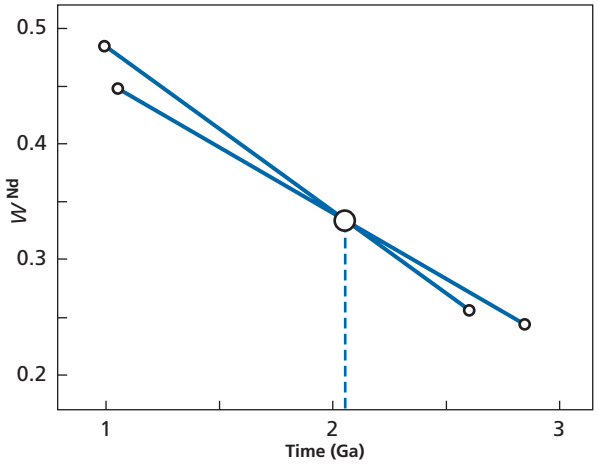


Returning then to the balance equations, we get: $\alpha_{cc}^{Nd} = 0.511\,567$ and $\mu_{dm}^{Sm/Nd} = 0.241$.

(ii) Using $W^{Nd}$, $W^{Sr}$ is calculated as 0.22. From the balance equation for $\mu$ values we deduce $\mu_{cc} = 0.409$. From the balance equation for the $\alpha$ values, we deduce $\alpha_{cc}^{Sr} = 0.713\,28$. We check by calculating the $T^{Sr}$ model age on the depleted mantle values $T^{Sr} = 2.1$ Ga; with continental crust values $T^{Sr} = 1.90$ Ga, for an average of 2 Ga. The overall picture is fairly coherent.

## Chapter 7

(1) The first job is to estimate the fractionation factors at the missing temperatures $+10\,^{\circ}$C and $-30\,^{\circ}$C.

(i) We plot the two curves $\alpha_D$, $\delta_{18_O}$ against temperature and interpolate and extrapolate linearly, which is warranted because they seem to vary linearly. The complete table is given below.

| | $\alpha_D$ | $\alpha_{18_O}$ |
|---|---|---|
| +20 | 1.085 | 1.0098 |
| +10 | 1.10 | 1.0106 |
| 0 | 1.1123 | 1.0117 |
| –20 | 1.1492 | 1.0141 |
| –30 | 1.175 | 1.0155 |

(ii) The results are as given below.

| | $\delta^{D}_{vapor}$ | $\delta^{D}_{rain}$ | $\delta^{18}O_{vap}$ | $\delta^{18}O_{rain}$ |
|---|---|---|---|---|
| 1 | –133 | –33 | –16.3 | –6.5 |
| 2 | –208 | –96 | –24.13 | –12.4 |
| 3 | –307 | –158 | –33.57 | –19.47 |
| 4 | –424 | –249 | –43.95 | –28.38 |

(iii) See figure.

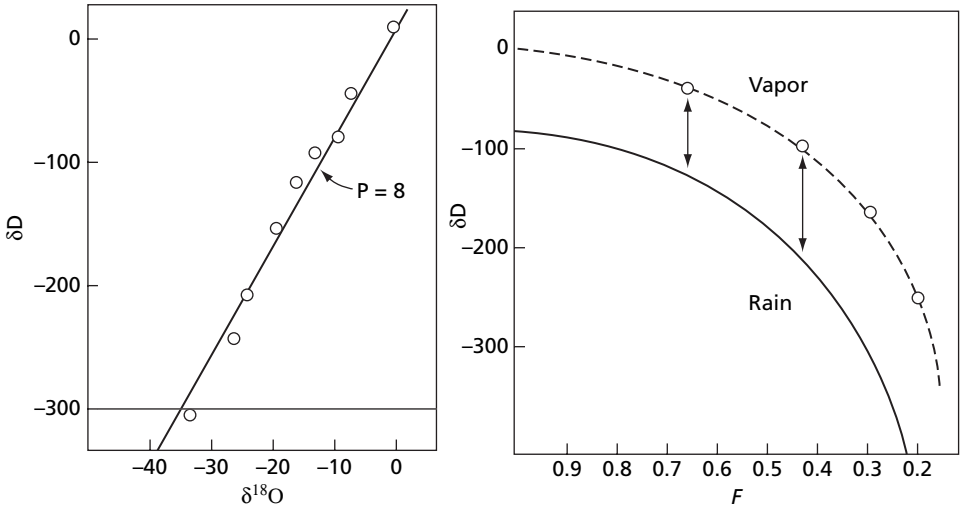


(2) The equation is:

$$\delta = \delta_0 + 10^3(\alpha - 1)\ln f.$$

For the first phase, $f$ varies from 1 to 0.7. The results are given in the table and figure below.

| | $\alpha_{-1} = 0.0002$ | | $\alpha_{-1} = 0.00025$ | | $\alpha_{-1} = 0.00035$ |
|---|---|---|---|---|---|
| | $f = 0.9$ | $f = 0.7$ | $f = 59, \Delta f = 0.84$ | $f = 0.49, \Delta f = 0.7$ | $f = 0.388, \Delta f = 0.79$ |
| Melt | 5.52 | 5.571 | 5.614 | 5.66 | 5.74 |
| Olivine | 5.32 | 5.37 | 5.414 | 5.46 | 5.54 |
| Pyroxene | | | 5.31 | 5.36 | 5.44 |
| Plagioclase | | | | | 5.14 |

As can be seen, great precision is required to bring out these variations.

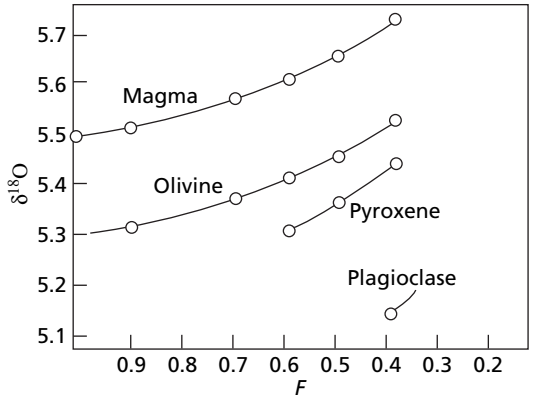


(3) With $\delta_D = 70\%$ and Craig's straight line of precipitation, we deduce $\delta_O = 10\%$. We calculate the partition coefficient at 550 °C.

$\Delta_{A-B} = A \cdot 10^6 T^{-2} + B$

| | $A$ | $B$ | $\Delta_{\text{mineral-water}}$ |
|---|---|---|---|
| Quartz | 4.10 | −3.7 | 2.35 |
| Magnetite | −1.47 | −3.7 | −5.8 |
| Muscovite | 1.9 | −3.10 | −0.41 |
| Feldspar | 3.13 | −3.41 | 1.20 |
| Calcite | 2.78 | −2.89 | 1.21 |
| Plagioclase | 2.15 | −2.0 | 1.149 |

The balance equation is written:

$$(\delta_Q - \delta_{H_2O})\, x_1 + (\delta_{Mg} - \delta_{H_2O})x_2 + (\delta_{Mg} - \delta_{H_2O}) - x_3 + (\delta_{feld} - \delta_{H_2O})x_4 + (\delta_{cal} - \delta_{H_2O})x_5 + (\delta_{plag} - \delta_{H_2O})x_6 = Q.$$

From this we get:

$$\delta_{silicate} - \delta_{H_2O} = 0.99\ (2),$$

but we also know the initial balance:

$$\delta_{\text{initial silicate}} \times y_1 + \delta_{\text{initial water}} y_2 = \delta_{\text{initial}}$$

where $y_1$ and $y_2$ are calculated allowing for the fact that by mass:

$H_2O = 15\%$ and silicate $= 85\%$.

In the silicates, oxygen = 54%; in the water, oxygen = 88.8%. Therefore the initial overall value of the system, if assumed closed, is:

$$\delta_{initial} = 7 \times 0.77 \pm (-10) \times 0.23 = 5.39 - 2.3 = 3.09.$$

This is preserved, so we have:

$$\delta_{\text{silicate}} + \delta_{H_2O} = 3.09\ (2).$$

We then deduce $\delta_{H_2O}$ by eliminating $\delta_{\text{silicate}}$ between (1) and (2):

$$\delta_{H_2O} = 1.05$$

All that is left is to calculate the mineral $\delta$ values:

$$\delta_{\text{quartz}} = +3.4$$

$$\delta_{\text{magnetite}} = -4.7$$

$$\delta_{\text{muscovite}} = 0.68$$

$$\delta_{\text{feldspar}} = +2.29$$

$$\delta_{\text{calcite}} = +2.28$$

$$\delta_{\text{plagioclase}} = +2.39.$$

(4) (i) The quantity of carbon burnt is $5.9 \cdot 10^{16}$ g, which corresponds to 410 ppm of $CO_2$.
(ii) Now, the content is 330 ppm. The remainder has been dissolved in the ocean after homogenization.
(iii) The $\delta^{13}C_{\text{calcite}}$ has gone from +3 to 0.
(iv) If $\delta$ can be measured with a precision of 0.1 $\delta$ or 0.05 $\delta$, this criterion can be used as a pollution control.

(5) $$\Delta_{g-m} = \delta_g - \delta_{\text{maj}} = \delta_{SO_2} - \left[x\delta_{S^{2-}} + (1-x)\delta_{SO_4^{2-}}\right]$$

$$x = \frac{S^{2-}}{S^{2-} + SO_4^{2-}}$$

$$x = \frac{K(T)}{(\alpha^2 + K(T))}$$

$$\Delta_{g-m} = 7.5x - 4.5.$$

Therefore if $x < 0.6$ $\Delta_{g-m}$ it is negative, otherwise it is positive.

(6) (i) $\delta = 0.344$ and 1.386, respectively.
(ii) $\delta = -1.05$.
(iii) 0.0081 $\delta$ $m^{-1}$ and 0.011 08 $\delta$ $m^{-1}$ for the two snowball scenarios and for the scorched Earth scenario 0.0148 $\delta$ $m^{-1}$.
(iv) No.

## Chapter 8

(1) We find:

$$R = \frac{1}{\sqrt{Jk}}.$$

A decay reaction, for example, decay of organic matter, obeys a second-order kinetic equation:

$$x = \frac{J_0}{J_0\, kt + 1}.$$

(2) The frequency 100 ka will be continued unchanged. The 40 ka and 20 ka frequencies will be phase-shifted and damped and therefore the 100 ka frequency will predominate.

(3) (i) The upper mantle $1 \cdot 10^{27}$ g with 5 ppm of U, corresponding to $2 \cdot 10^{16}$ moles. Production of $^4$He in 1 Ga is 2.2 times that of uranium in moles, therefore $4.4 \cdot 10^8$ yr. The quantity of $^4$He degassed is about $10^8$ moles per year.

(ii) Therefore the residence time of $^4$He of 440 Ma is twice the residence time in the lithosphere.

(iii) This means that when the oceanic lithosphere forms at the ocean ridges, there is enrichment of $^4$He towards the melting zones.

(4) Mixing times in the upper mantle

| | Mixing time (Ma) |
|---|---|
| North Atlantic | 350 |
| South Atlantic | 138 |
| South-west Indian Ocean | 533 |
| North Pacific | 42 |
| Central Indian Ocean | 77 |

Yes, there is a relation with the expansion rate (see figure).

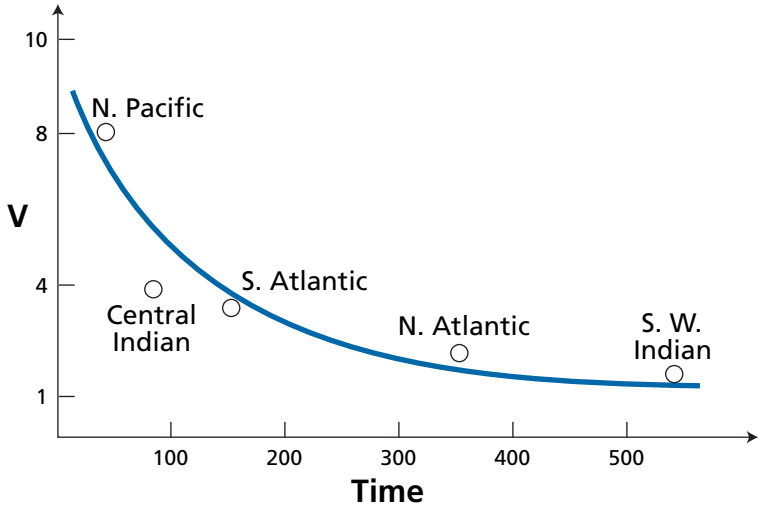

# INDEX OF NAMES

# SUBJECT INDEX